VOLUME 27 (1961) No. 4

NUCLEAR PHYSICS

JOURNAL DEVOTED TO THE EXPERIMENTAL AND
THEORETICAL STUDY OF THE FUNDAMENTAL
CONSTITUENTS OF MATTER AND THEIR INTERACTIONS

EDITOR: L. ROSENFELD · COPENHAGEN

LAST NUMBER OF THIS VOLUME

R. G. ALBRIDGE, J. M. HOLLANDER, C. J. GALLAGHER and J. H. HAMILTON, The energy levels of U^{233} 529
R. G. ALBRIDGE and J. M. HOLLANDER, The K- and L-auger spectrum of uranium 554
MICHEL FABRE DE LA RIPELLE, Le mouvement collectif dans la résonance géante photonucléaire. (I) Énergie de résonance pour les noyaux sphériques et dédoublement pour les noyaux déformés 561
N. A. BONCH-OSMOLOVSKAYA, B. S. DZELEPOV, O. E. KRAFT and WANG YOUNG-YU, Decay chain $Er^{158} \xrightarrow[E]{2.5\,h} Ho^{158} \xrightarrow[E,\,\beta^+]{27\,min} Dy^{158}_{stab}$ 581
L. BIRD, P. CHRISTMAS, A. E. TAYLOR and E. WOOD, De-polarization parameter in p-p scatttering at 143 MeV 586
R. A. PECK, Jr., Gross structure in reactions of deformed nuclei 596
J. R. ROOK, Polarisation of protons elastically scattered by Li^7 near the 441 keV resonance 606
F. R. METZGER, Lifetime and *g*-factor of the first excited state in Fe^{56}. . . . 612
P. SWAN, Distorted wave expansion for scattering problems 620
U. HAUSER, K. RUNGE and G. KNISSEL, Measurements of E1 transition probabilities in several deformed odd-mass nuclei as a study of single particle motion . . 632
V. I. GOLDANSKY, Two-proton radioactivity 648
JACOB BENVENISTE, REX BOOTH and ARTHUR C. MITCHELL, Level structure of A^{40} 665
TORKILD ANDERSEN, K. MAACK BISGÅRD and P. GREGERS HANSEN, Low lying states of Th^{229} 673
W. H. G. LEWIN, B. VAN NOOIJEN and A. H. WAPSTRA, The K-conversion coefficient of the 368 keV E2 transition in ^{200}Hg 681
News Items 688
Book Reviews 690
Author Index 694
Subject Index 699

November 1961

NORTH-HOLLAND PUBLISHING COMPANY-AMSTERDAM

EDITORIAL BOARD

AUSTRALIA & NEW ZEALAND:	H. Messel (Sydney), M. L. Oliphant (Canberra)
AUSTRIA:	B. Karlik (Vienna), H. Thirring (Vienna)
BELGIUM:	M. de Hemptinne (Louvain), J. Verhaeghe (Ghent)
CANADA:	G. Volkoff (Vancouver)
DENMARK:	C. Møller (Copenhagen), S. Rozental (Copenhagen), G. E. Brown (Copenhagen)
FINLAND:	L. Simons (Helsinki)
FRANCE:	A. Berthelot (Saclay), S. Gorodetzky (Strasbourg)
GERMANY (DEM. REP.):	G. Hertz (Leipzig)
GERMANY (FED. REP.):	W. Gentner (Freiburg i. B.), J. H. D. Jensen (Heidelberg)
GREAT BRITAIN:	W. E. Burcham (Birmingham), R. J. Blin-Stoyle (Brighton)
HUNGARY:	L. Janossy (Budapest)
INDIA:	H. Bhabha (Bombay), R. Ramanna (Trombay)
IRISH REPUBLIC:	J. McConnell (Maynooth)
ISRAEL:	G. Racah (Jerusalem)
ITALY:	E. Amaldi (Rome)
JAPAN:	S. Kikuchi (Tokay), S. Tomonaga (Tokyo)
MEXICO:	M. Moshinsky (Mexico)
NETHERLANDS:	H. Brinkman (Groningen), S. R. de Groot (Leiden)
NORWAY:	E. Hylleraas (Oslo), A. Lundby (Oslo), H. Wergeland (Trondheim)
POLAND:	L. Infeld (Warsaw), J. Werle (Warsaw)
PORTUGAL:	J. M. Araújo (Porto), J. R. de Almeida Santos (Coimbra)
SOUTH AMERICA:	G. Beck (Rio de Janeiro), J. Leite Lopes (Rio de Janeiro)
SOUTH-EAST ASIA:	T. H. R. Skyrme (Kuala Lumpur)
SPAIN:	J. M. Otero (Madrid), C. Sanchez del Rio (Madrid)
SWEDEN:	O. Klein (Stockholm), K. Siegbahn (Uppsala), I. Waller (Uppsala)
SWITZERLAND:	P. Huber (Basel), P. Scherrer (Zürich)
U.A.R. & ARAB COUNTRIES:	F. El Bedewi (Cairo), M. G. Nooh (Cairo)
U.S.A.:	H. H. Barschall (Madison, Wisconsin), S. Devons (New York), G. C. Wick (Brookhaven), D. Inglis (Argonne)
U.S.S.R.:	M. A. Markov (Moscow), I. S. Shapiro (Moscow), D. V. Skobeltzyn (Moscow)
YUGOSLAVIA:	I. Supek (Zagreb)

CONTRIBUTIONS may be sent to the Editor, Professor L. Rosenfeld, NORDITA, Blegdamsvej 17, Copenhagen Ø, either directly, or preferably through the intermediary of one of the members of the Editorial Board of the country or region in which the author is working. They may be written in English, French or German.

NUCLEAR PHYSICS is published in fortnightly issues. The subscription price per volume of 700 pages is fl 57.00; 114s; $ 15.00. Post-free.

SUBSCRIPTIONS should be sent to the publishers, NORTH-HOLLAND PUBLISHING COMPANY P.O. Box 103, Amsterdam or to any subscription-agent.

BOOKS FOR REVIEW should be sent to Professor Rosenfeld.

No part of this issue may be reproduced in any form, by print, photoprint, microfilm or any other means without permission from the publisher.

Printed in the Netherlands

NUCLEAR PHYSICS 1962

Personal subscription scheme

Only to be used for new personal subscriptions, not for renewals

When Nuclear Physics was started at the end of 1955, the intention was to publish one or two volumes a year of 700 pages each. Neither the publisher nor the editor could envisage that the influx of papers would make it necessary to publish eight such volumes a year, as were in 1961.

Although since 1955 the guilder has been revaluated with 4 %, the production costs of mathematical composition have risen by approximately 25% and the number of words per page has been increased by 20% since the first volume, the subscription price per volume has been maintained at $ 15.00 (108s.).

Moreover Nuclear Physics does not impose any page charge, in order to make it easier for scientists from countries with a weak currency to contribute to the journal.

It is difficult to compare subscription prices, but per page Nuclear Physics is undoubtedly one of the less expensive journals in the field of physics.

However, we realize that a total subscription price per year of $ 120.00 for eight volumes is prohibitive for a private subscriber and the suggestion has been made that Nuclear Physics could fix a special price for personal subscriptions.

Indeed, there are a number of scientific journals which give a certain discount to private subscribers. In the case of Nuclear Physics a discount of 30% or even 50% would not be sufficient to attract private subscriptions.

→ *personal subscription scheme*

Now it is known that for technical publications the composition of the type is the most expensive part of the production and that as soon as the break-even point is reached, the run-on costs are comparatively low.

Accordingly, we decided early 1961 to make Nuclear Physics available to personal subscribers at the run-on costs. This meant that starting with 1961 individual physicists could subscribe for their own use to the eight volumes (approx. 5600 pages) of Nuclear Physics scheduled for 1961 at a total price of $ 20.00 or the equivalent in other currency (postage included).

Should you want to join this personal subscription scheme for 1962, please return the order-form.

It has to be understood that the publisher has the right to refuse a personal subscription or its renewal. In case of refusal, the publisher will return the cheque.

We were glad to see that this new arrangement appealed to many nuclear physicists and that it did not lead to any misunderstanding about the extremely complicated way of fixing subscription prices for learned journals.

THE EDITOR
L. Rosenfeld

THE PUBLISHER
M. D. Frank

How to act:

Write a letter to the Subscription Department of North-Holland Publishing Company, P.O. Box 103, Amsterdam, Netherlands, asking for a personal subscription.

This letter should contain:

- **a cheque or banknotes for $ 20.00**
  (£ 7.4.0-; DM 80; N.Frs. 100)
- **a statement running as follows:**

"This subscription is for personal use only and will not replace an existing library subscription, nor will it be put at the disposal of any library now or in the future.

My position is: ______________________________"

(Mention should be made of the institution to which you are attached.)

Any enquiry or communication concerning the personal subscription scheme should be addressed to the publisher, North-Holland Publishing Company, P.O. Box 103, Amsterdam, Netherlands.

Only to be used for NEW personal subscriptions, not for renewals

SUBSCRIPTION FORM

NORTH-HOLLAND PUBLISHING COMPANY
P.O. BOX 103
AMSTERDAM - NETHERLANDS

Date ______________________

(tear off here)

Please enter my personal subscription to

NUCLEAR PHYSICS 1962

(VOLUMES 29—36)

at the **total** subscription price of $ 20.00

(£ 7.4.0.; DM. 80; N. Frs. 100)

I declare that this subscription is for my personal use only and that it will not replace an existing library subscription, nor will it be put at the disposal of any library now or in the future.

I enclose ☐ banknotes

☐ cheque

My position is ______________________

(mention should be made of the institution to which you are attached)

Name (please print) ______________________

____

Address ______________________

____

City, Zone, State ______________________

Signature

____

NUCLEAR PHYSICS

EDITORIAL BOARD

AUSTRALIA & NEW ZEALAND:	H. Messel (Sydney), M. L. Oliphant (Canberra)
AUSTRIA:	B. Karlik (Vienna), H. Thirring (Vienna)
BELGIUM:	M. de Hemptinne (Louvain), J. Verhaeghe (Ghent)
CANADA:	G. Volkoff (Vancouver)
DENMARK:	C. Møller (Copenhagen), S. Rozental (Copenhagen), G. E. Brown (Copenhagen)
FINLAND:	L. Simons (Helsinki)
FRANCE:	A. Berthelot (Saclay), S. Gorodetzky (Strasbourg)
GERMANY (DEM. REP.):	G. Hertz (Leipzig)
GERMANY (FED. REP.):	W. Gentner (Freiburg i. B.), J. H. D. Jensen (Heidelberg)
GREAT BRITAIN:	W. E. Burcham (Birmingham), R. J. Blin-Stoyle (Brighton)
HUNGARY:	L. Janossy (Budapest)
INDIA:	H. Bhabha (Bombay), R. Ramanna (Trombay)
IRISH REPUBLIC:	J. McConnell (Maynooth)
ISRAEL:	G. Racah (Jerusalem)
ITALY:	E. Amaldi (Rome)
JAPAN:	S. Kikuchi (Tokai), S. Tomonaga (Tokyo)
MEXICO:	M. Moshinsky (Mexico)
NETHERLANDS:	H. Brinkman (Groningen), S. R. de Groot (Leiden)
NORWAY:	E. Hylleraas (Oslo), A. Lundby (Oslo), H. Wergeland (Trondheim)
POLAND:	L. Infeld (Warsaw), J. Werle (Warsaw)
PORTUGAL:	J. M. Araújo (Porto), J. R. de Almeida Santos (Coimbra)
SOUTH AMERICA:	G. Beck (Rio de Janeiro), J. Leite Lopes (Rio de Janeiro)
SOUTH-EAST ASIA:	T. H. R. Skyrme (Kuala Lumpur)
SPAIN:	J. M. Otero (Madrid), C. Sanchez del Rio (Madrid)
SWEDEN:	O. Klein (Stockholm), K. Siegbahn (Uppsala), I. Waller (Uppsala)
SWITZERLAND:	P. Huber (Basel), P. Scherrer (Zürich)
U.A.R. & ARAB COUNTRIES:	F. El Bedewi (Cairo), M. G. Nooh (Cairo)
U.S.A.:	H. H. Barschall (Madison, Wisconsin), S. Devons (New York), G. C. Wick (Brookhaven), D. Inglis (Argonne)
U.S.S.R.:	M. A. Markov (Moscow), I. S. Shapiro (Moscow), D. V. Skobeltzyn (Moscow)
YUGOSLAVIA:	I. Supek (Zagreb)

NUCLEAR PHYSICS

JOURNAL DEVOTED TO THE EXPERIMENTAL AND THEORETICAL STUDY OF THE FUNDAMENTAL CONSTITUENTS OF MATTER AND THEIR INTERACTIONS

EDITOR: L. ROSENFELD - COPENHAGEN

VOLUME XXVII

SEPTEMBER 1961 — NOVEMBER 1961

NORTH-HOLLAND PUBLISHING COMPANY - AMSTERDAM

PRINTED IN THE NETHERLANDS

EDITORIAL NOTE

To contributors from the United States

The Editor is glad to welcome to the Editorial Board Prof. G. C. Wick, Brookhaven National Laboratory, Upton (New York) and Prof. D. Inglis, Argonne National Laboratory, 9700 South Cass Avenue, Argonne (Illinois). It will considerably help the editorial work if theoretical papers by authors working in the United States are submitted to one of these new members of the editorial board, while experimental papers are submitted either to Prof. H. H. Barschall, Dept. of Physics, The University of Wisconsin, Madison 6 (Wisconsin) or to Prof. S. Devons, Dept. of Physics, Columbia University, New York (New York).

To contributors from the United Kingdom

Dr. R. Blin-Stoyle, Clarendon Laboratory, Oxford, has kindly accepted to join the Editorial Board. Authors of theoretical papers working in the United Kingdom are requested to send their manuscripts to him. Experimental papers are dealt with, as hitherto, by Prof. W. E. Burcham, Physical Laboratory, University of Birmingham, Edgbaston, Birmingham.

To all contributors

Contributors are again urgently requested to prepare their manuscripts in conformity with the Instructions published at the end of vol. **26**, copies of which are available on request from the publishers or the Editor.

1.E.1:
4.E

Nuclear Physics **27** (1961) 529—553; © *North-Holland Publishing Co., Amsterdam*

Not to be reproduced by photoprint or microfilm without written permission from the publisher

THE ENERGY LEVELS OF U^{233}

R. G. ALBRIDGE, J. M. HOLLANDER [†]
University of California Lawrence Radiation Laboratory, Berkeley, California

C. J. GALLAGHER [††]
California Institute of Technology, Pasadena, California

and

J. H. HAMILTON [†††]
Vanderbilt University, Nashville, Tennessee [‡]

Received 17 april 1961

Abstract: The beta decay of Pa^{233} was studied by means of high resolution permanent-magnet electron spectrographs, an iron free double-focussing beta spectrometer and a curved-crystal gamma ray spectrometer. Measured values of relative conversion electron and photon intensities are used to determine conversion coefficients and to assign multipolarities and multipole mixing ratios for the transitions in U^{233}. The quantum assignments of the levels in U^{233} are considered, by comparisons of observed beta and photon branching ratios to those predicted by theory. Several new transitions were observed and some of these are used to postulate new levels in U^{233}.

1. Introduction

The energy levels of U^{233} have been studied by a number of workers, and the general features of the level scheme are well known. In their comprehensive review of the single particle levels of spheroidally deformed nuclei, Mottelson and Nilsson ¹) have discussed these levels in terms of four intrinsic states, excited either by Coulomb excitation of U^{233}, alpha decay of Pu^{237} or beta decay of Pa^{233}. The scheme as summarized by Mottelson and Nilsson is shown in fig. 1.

The electron and photon spectra of Pa^{233} were first seriously investigated by Hok *et al.* ²), Keller and Cork ³) and Brodie ⁴). A discussion of the U^{233} levels has been given by Newton ⁵), who observed the Coulomb excitation of two rotational levels in U^{233}. More recently, and concurrently with this study, two other investigations of Pa^{233} decay have been reported by Albouy and Valadares ⁶) and by Bisgård, Dahl and Olesen ⁷). The results of all these studies form a generally consistent picture of Pa^{233} decay.

[†] 1958—1959 Guggenheim Fellow at University of Uppsala, Uppsala, Sweden
[††] Present address: Institute for Theoretical Physics, Copenhagen, Denmark
[†††] 1958—1959 N.S.F. Post Doctoral Fellow at University of Uppsala, Uppsala, Sweden
[‡] This work was performed under the auspices of the U.S. Atomic Energy Commission

November (1961)

A primary aim of this work was to obtain accurate measurements with high-resolution equipment of both the energies and intensities of the conversion electron and photon lines, in order that multipolarities, mixing ratios and transition intensities could be obtained. We hoped that the correlation of these data with the transition intensities predicted by the theory of Bohr and Mottelson [8]) would serve as a test of the quantum assignments of the nuclear energy levels of U^{233}. In addition, the ability to produce very intense sources of Pa^{233} by the neutron irradiation of Th^{232} which could be studied with high-resolution equipment offered the hope of discovering weak, previously unobserved, transitions.

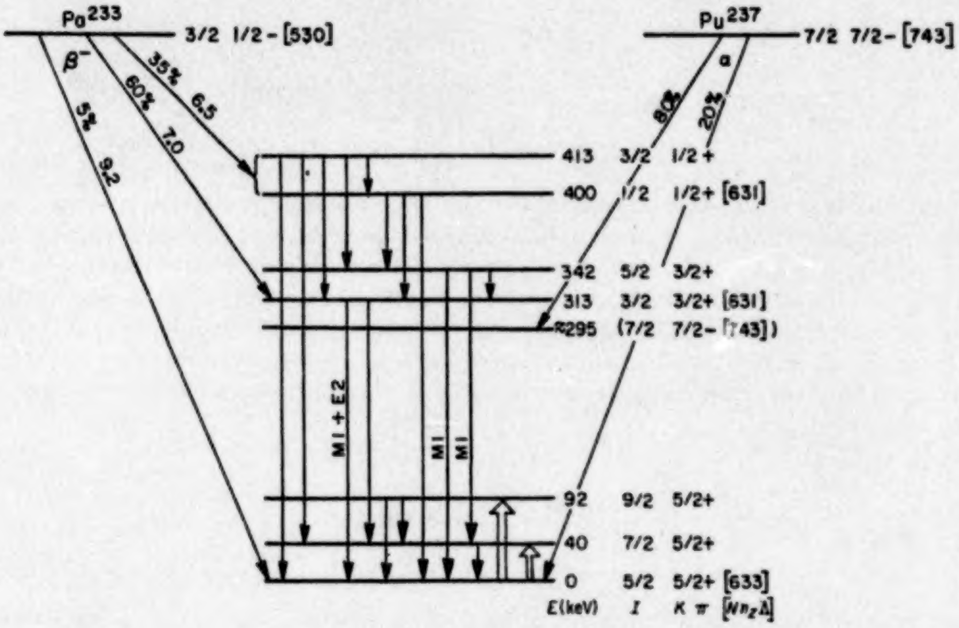

Fig. 1. Basic level scheme of U^{233} as summarized by Mottelson and Nilsson [1]).

2. Experimental Equipment

2.1. ELECTRON MEASUREMENTS

The internal conversion spectrum was measured with several types of instruments.

(a) Permanent-magnet 180° spectrographs with field strengths 50, 100, 215 and 340 G. The resolution obtained with these spectrographs is $\Delta\rho/\rho \approx 0.1$ %.

The relative intensities of the conversion lines recorded photographically by the permanent-magnet spectrographs on Eastman no-screen X-ray emulsion were determined by two different means, i.e. densitometer tracings and visual estimates. The densitometer tracings were analyzed by the method of Mladjenović and Slätis [9]).

In some instances the ratio of background to line intensity was too high to permit an accurate analysis by means of densitometry. In these cases relative intensities were obtained from visual comparisons of plates exposed for different periods of time. Two photographic plates differing in exposure by a known factor were placed one on-top-of the other with emulsions touching, and were viewed over a diffuse source of light. Two lines that were to be analyzed were lined up beside each other and their relative intensities compared. If, under these conditions, the intensities of the lines appeared to be equal, the absolute intensities of the lines were assumed to differ by the same factor as the exposures. By superimposing the plates in this manner differences in the backgrounds of the plates tend to cancel because both lines are viewed through the same background. In those cases in which comparison could be made the deviation between intensities obtained by densitometry and visual estimates was $\approx 10\%$. In all cases corrections were made for instrument geometry (by multiplying by the radius of curvature of the electron path [9]), for film efficiency, and for decay during exposure.

(b) A permanent-magnet pre-accelerating spectrograph, used to measure the low-energy conversion and Auger electron spectrum. The field strength of this instrument is 50 G; it has been described by Albridge [10]).

(c) The 30-cm iron-free double-focussing spectrometer located at the Physics Institute, University of Uppsala, Sweden [11]). A resolution equal to or better than 0.14 % was obtained with conversion lines of energy > 65 keV, but because of source thickness, the resolution became poorer at lower energies (e.g. 0.24 % at 23 keV). This instrument was used primarily for determinations of the relative intensities of the stronger internal conversion lines. The electron line intensities were assumed to be proportional to the product of peak height times line width. Recording was by a G-M counter with a 2-keV window cutoff.

2.2. PHOTON MEASUREMENTS

The DuMond bent-crystal spectrometer Mark I, located at the California Institute of Technology, Pasadena, was used for precision measurements of the energies and intensities of the X-ray and gamma-ray lines. Two different detector arrangements were used. The initial experiment employed a 7.6 cm diameter by 5.1 cm cylindrical sodium iodide crystal connected to a single-channel pulse-height analyzer with chart recorder. Later, a 12.7 cm diameter by 7.6 cm cylindrical sodium iodide crystal was used with the single-channel analyzer for energy determinations and with a 100-channel Penco gamma analyzer for intensity measurements.

The instrument is such that the width at half maximum of the recorded peak ($\Delta\lambda$) is constant over the wave length range; $\Delta\lambda$ is of the order of 0.28 x-unit. The resolution, ($\Delta\lambda/\lambda$) varies with λ. The resolution is of order 0.2 % at 100 keV and 0.9 % at 400 keV. The transmission is determined almost completely by the product of the solid angle subtended by the bent crystal at 2 m from a 0.020 cm diameter $\times$ 2.5 cm high source and the $1/E^2$ dependence of the reflectivity of the bent quartz crystal.

The gamma ray spectrum was also examined by use of a 100-channel Penco pulse-height analyzer with a 7.6×7.6 cm NaI(Tl) crystal. The resolution was 8 % at 560 keV and 10 % at 280 keV.

3. Preparation of Sources

For the measurements performed in Berkeley, the Pa^{233} was prepared by neutron irradiation of 0.5—to 1.0 g quantities of Th^{232} metal foil in the Materials Testing Reactor at Arco, Idaho. The Uppsala sample was irradiated at the reactor in Kjeller, Norway.

The purification procedure for carrier-free protactinium was typically the following. The thorium was dissolved in a 10 *M* HCl-0.1 *M*HF solution and the sample was passed through a Dowex A-1 column after the fluoride had been complexed with H_3BO_3. The protactinium was eluted with 3 *M* HCl, extracted from 6.9 *M* HCl into di-isopropyl ketone and back-extracted into 2*M* HCl. The HCl concentration was increased to 10 *M*, and the protactinium was again adsorbed onto a Dowex A-l column. Possible zirconium impurities were then eluted with 6.0 *M* HCl. The protactinium was finally eluted with a 9.0 *M*HCl-0.1*M*HF solution.

Sources used in the permanent magnet spectrographs were prepared by electrodeposition onto 0.25 mm-diameter platinum wires; the Uppsala sample was electrodeposited onto a 0.2 mm nickel wire. An ammonium fluoride electrolyte (pH 6.3) was used with a plating current of 100 to 150 mA. These sources varied in strength from 0.02 to 50 R/h as measured by a beta-gamma survey meter at a distance of approximately 7 cm. A 0.5 mm wide flat source (on Pt-coated Mylar) was also used in Uppsala as a check on some of the intensities.

Two sources were prepared for the Pasadena bent-crystal spectrometer. The first was electroplated onto a 0.12 mm-diameter platinum wire in the manner described above. This wire was threaded into a 0.2 mm in diam quartz capillary which was then sealed with a torch. The source was measured as greater than 100 R/h of gamma activity at a distance of approximately 10 cm. Because X-ray emission of the platinum wire (induced by the intense beta source) proved troublesome, a second source was prepared without the wire. Approximately 3.5 mg of ThO_2 in a 0.020 cm diameter quartz capillary was neutron-irradiated for two months in the Materials Testing Reactor at a flux of $\approx 3\times10^{14}$ neutrons/cm^2 sec. The irradiated ThO_2 in the capillary was itself used as the spectrometer source without chemical treatment.

4. Experimental Data

4.1. CONVERSION ELECTRONS

The Pa^{233} conversion-electron data, taken with the Berkeley permanent-magnet spectrographs and the Uppsala iron-free spectrometer, are summarized in table 1. The unassigned lines, listed in table 7, are discussed separately. The lines of the 17-keV transition and the L lines of the 28-keV transition were detected with the pre-accelerator spectrograph [10]). The relative precision of measurement of the energies of lines taken on a single spectrograph is within 0.1 % except for extremely weak or extremely strong lines. The transition energies listed in table 1 are weighted averages of several determinations.

Only *relative* conversion-electron intensities were determined directly in this work. The absolute intensities listed in table 1 were obtained by a normalization procedure described in sect. 7. The intensities listed from permanent-magnet spectrograph plates are averages of from 2—7 visual estimates and, when possible, 2 or 3 densitometer traces.

The intensities of the stronger conversion lines were measured with the Uppsala iron-free double-focussing spectrometer. Because of the very thin G-M counter window used, there was no need to make window-absorption corrections. However, the intensities of the low-energy lines are subject to uncertainties arising from source absorption effects; these are manifested by the observed line widths of the 40-keV L_{II} and L_{III} lines, which are $\approx$ 0.4 % and 0.24 %, respectively, as compared with widths of 0.11 % to 0.15% for the higher energy lines. It was not possible to measure accurately the full area of each conversion line because of the presence of large "tails", so the area was approximated by multiplying the observed peak-height of each line by its half-width.

In most cases where relative intensities were measured with both the photographic and the double-focussing instruments, the Uppsala values were selected, though for the low-energy lines, where the Uppsala values are also uncertain, an average value is used. A large number of conversion lines observed in the Berkeley spectrographs were, for lack of time, not measured in the iron-free spectrometer; for example the weaker members of L and M subshell groups. In these cases the relative subshell intensities obtained from the photographic plates were taken as "final" with a normalization of the intensity of the strongest subshell line to the iron-free spectrometer value. In a few cases two conversion lines of different transitions overlap. In these cases the intensities of the two lines were estimated from the assigned multipolarities of the transitions. Estimated values are so indicated in table 1. The electron intensities reported there are probably accurate within $\approx$ 20 % for the strong and medium lines, and within a factor of two for the weak lines.

The interpretation of the two highest energy levels in U^{233} depends strongly on the assignments of multipolarities to the 375, 398 and 416 keV transitions. The multipole assignments of these transitions in turn depend upon the measured intensities of their conversion lines. Because of the importance of these intensity values and of the difficulty in obtaining them, the following special comments are made:

TABLE 1

Pa^{233} conversion-electron data

Electron energy (keV)	Conversion shell	Transition energy [a]) (keV)	Selected transition energy [b]) (keV)	Conversion-electron intensities [c]) (percent beta decay)			Remarks
				Berkeley P.M.	Uppsala iron-free	Selected value	
11.72	M_I	17.27					
12.07	M_{II}	17.25					
12.96	M_{III}	17.26					
15.78	N_I	17.22					
15.97	N_{II}	17.24					
			17.26				
6.76	L_I	28.52					
7.57	L_{II}	28.51					
11.37	L_{III}	28.53					
23.01	M_I	28.56		1.7	2.7	2.2	
23.37	M_{II}	28.55		0.84	0.75	0.8	
24.26	M_{III}	28.56		0.90		0.85	
27.06	N_I	28.50					
27.22	N_{II}	28.49					
27.50	N_{III}	28.54					
28.25	O_I	28.57					
			28.54				
18.62	L_I	40.38		1.0		1.3	
19.42	L_{II}	40.36		3.7	5.0	4.4	
23.15	L_{III}	40.31		2.7	4.3	3.5	
34.73	M_I	40.28					
35.10	M_{II}	40.28		0.62	1.4	1.1	
35.96	M_{III}	40.26		0.69	1.3	1.0	
38.99	N_{II}	40.26					
39.24	N_{III}	40.28					
40.06	O_{II}	40.31					
			40.29				
36.92	L_{II}	57.86					L_I line masked by 40-M_{III}
40.74	L_{III}	57.90					M_{III} line masked by 75-L_I
			57.90				
53.37	L_I	75.13		7.2	8.6	8.6	masks 58-M_{III}
54.14	L_{II}	75.08		1.0	1.2	1.2	
58.01	L_{III}	75.17		0.11			
69.57	M_I	75.12		2.2	2.1	2.1	
69.90	M_{II}	75.08					
70.81	M_{III}	75.11					
73.65	N_I	75.09		0.69		0.69	
73.82	N_{II}	75.09					
74.77	O_I	75.09		0.27		0.27	
75.06	P_I	$\approx$75.1					
			75.13				
64.75	L_I	86.51		8.5	9.4	9.4	
65.50	L_{II}	86.44		1.1	1.3	1.3	

TABLE 1
(continued)

Electron energy (keV)	Conversion shell	Transition energy a) (keV)	Selected transition energy b) (keV)	Conversion-electron intensities c) (percent beta decay)			Remarks
				Berkeley P.M.	Uppsala iron-free	Selected value	
69.4	L_{III}				0.26	0.26	
80.85	M_I	86.40		2.5	2.6	2.6	
81.14	M_{II}	86.32		0.42	0.58	0.58	
82.2	M_{III}				0.13	0.13	masked by 103-L_I
84.93	N_I	86.37		0.65		0.65	
86.05	O_I	86.37		0.16		0.16	
			86.45				
81.91	L_I	103.7		2.4	2.4	2.4	masks 86-M_{III}
82.68	L_{II}	103.6		0.35	0.44	0.44	
86.37	L_{III}	103.5		0.10	0.10	0.10	
98.11	M_I	103.7		0.72		0.72	
98.39	M_{II}	103.6					
99.36	M_{III}	103.7					
102.2	N_I	103.7		0.32		0.32	
103.3	O_I	103.7					
			103.6				
155.8	K	271.4		0.050		0.050	
250.6	L_I, L_{II}	271.5		0.049		0.049	
254.4	L_{III}	271.5		$\leqq$0.037		$\leqq$0.037	
266.0	M_I, M_{II}	271.6					
269.9	N_I, N_{II}	271.3					
			271.5				
184.4	K	300.0		4.9	5.2	5.2	
278.1	L_I	299.9		1.1	0.81	0.81	
278.5	L_{II}	299.4		0.12	0.12	0.12	
	L_{III}			(est. 0.012)			masked by 398-K
294.4	M_I	299.9		0.27	0.23	0.23	masks 312 L_{III}
298.3	N_I	299.7		0.073		0.073	
300.0	O_I	300.3		(est. 0.021)			masked by 416-K
			299.8				
196.2	K	311.8		(very strong)	27	27	
289.7	L_I	311.4		4.2	4.6	4.6	
290.7	L_{II}	311.6		0.50	0.43	0.43	
	L_{III}			(est. 0.019)			masked by 300-M_I
306.3	M_I	311.9		1.3	1.0	1.0	
306.9	M_{II}	312.1					
310.0	N_I	311.4		0.46		0.46	
311.4	O_I	311.8		0.11		0.11	
			311.7				
224.9	K	340.5		(2.3) d)	2.3	2.3	
318.5	L_I	340.3		0.50		0.50	

TABLE 1
(continued)

Electron energy (keV)	Conversion shell	Transition energy [a] (keV)	Selected transition energy [b] (keV)	Conversion-electron intensities [c] (percent beta decay)			Remarks
				Berkeley P.M.	Uppsala iron-free	Selected value	
319.5	L_{II}	340.5		0.065		0.065	
323.0	L_{III}	340.1					
334.8	M_I	340.3		0.16		0.16	
339.5	N_I	340.9		0.064		0.064	
340.1	O_I	340.4					
			340.3				
259.9	K	375.5		(0.049) [e]	0.038	0.038	
353.6	L_I	375.3		[0.020] [f]		[0.010]	
354.2	L_{II}	375.2		[0.043]		[0.021]	
358.4	L_{III}	375.5		[0.021]		[0.011]	
369.8	M_I	375.4					
			375.5				
282.7	K	398.3		(0.065) [e]		0.065	masks 300-L_{III}
376.6	L_I	398.3		[0.039] [f]		[0.020]	M_{III} line masked by 416-L_I, L_{II}
377.3	L_{II}	398.3		[0.067]		[0.035]	
381.3	L_{III}	398.4		[0.021]		[0.011]	
			398.3				
300.0	K	415.6		(0.16) [e]	0.16	0.16	masks 300-O_I
393.7	L_I	415.5		[0.070] [f]		[0.035]	masks 398-M_{III}
394.4	L_{II}	415.3		[0.049]		[0.025]	masks 398M_{III}
398.3	L_{III}	415.4		[0.013]		[0.006]	
410.0	M_I	415.5					
413.8	N_I	415.3					
			415.6				

[a] Electron binding energies were taken from Hill *et al.* [13]).

[b] Selected values are weighted averages of the experimental values.

[c] Measured relative intensities have been converted to absolute values by a method described in sect. 7.

[d] Photographic intensities normalized to K (340) = 2.3

[e] Normalized to K (416) = 0.16. See subsect. 4.1.

[f] Square brackets indicate an uncertainty in the normalization factor used for these values. See subsect. 4.1.

The intensities of the K-lines of the 375, 398 and 416 keV transitions relative to each other were carefully measured from the photographic plates, but they could not be measured in this way with any accuracy relative to the K-line of the 312 keV transition, which is very much stronger. However, the intensity of the 416-keV K line relative to the 312-keV K line was established with the Uppsala iron-free spectrometer and also by an independent measurement with a 25-cm (iron) double-focussing spectrometer in Berkeley, so this determination was used to fix the intensities of these three K-lines.

The intensities of the L lines of the **375**, **398** and **416** keV transitions were determined only from the photographic spectrographs. A problem arose in normalizing these values to the intensity scale used for reporting the data, both because the lines are quite weak and because the lower-energy portion of the photographic plate on which the lines were seen is so dark that it was difficult to observe a line of known intensity to which the unknown lines could be normalized. Fortunately, it was possible to bring about this normalization in an indirect manner. The values of the total intensities of the L lines of the **375**- and **416**-keV transitions were carefully measured with the Berkely 25-cm double-focussing spectrometer. This measurement indicated that the intensity values of these lines determined from the photographic plates were too large by a factor of approximately two; hence the spectrographically determined intensity values for these L lines have been corrected by dividing by the factor two. These corrected values are listed as the selected values in table 1. Because of these uncertainties the intensities of these lines are enclosed in square brackets. The L-subshell ratios of these transitions are of course not affected by this normalization uncertainty.

4.2. PHOTONS

The gamma-ray and X-ray data taken on the Pasadena bent-crystal spectrometer are listed in table 2. The method of determining the energy of an observed photon is described fully by DuMond [12]). The limits of error quoted are based upon estimates of the precision with which the centre positions of the line profiles were determined. The agreement between the measured and accepted energies of the uranium and platinum K X-rays [17]) indicates that the accuracy of the energy measurements is good.

The photon relative-intensity values were obtained by positioning the source at the angular position determined during the energy measurements as the profile centre and recording the pulse height spectrum from the NaI crystal with a pulse-height analyzer, in order to differentiate the background counting rate from the monochromatic gamma rays. The values obtained by means of the wire source and the single-channel analyzer, and those obtained with the ThO_2 source and the 100-channel analyzer are listed in table 2.

These intensities have been corrected for detector efficiency and the photopeak-to-total ratio [19]). Corrections were made for absorption in the source, SiO_2 capsule, air between source and detector, and the aluminium cover of the detector crystal. With the exception of the source absorption these corrections were made by the direct use of the exponential attenuation equation and the attenuation coefficients of Grodstein [20]). A graphical integration method was used to calculate the source absorption [10]).

The largest correction applied to the gamma-intensity data arises from the energy dependence of the reflectivity of the quartz crystal. Lind *et al.* [21]) have reported that for a bent quartz crystal the ratio of the diffracted beam to the incident beam (the reflection coefficient) is proportional to $1/E^2$. The intensity data in table 2 were normalized to the 340-keV transition, which was chosen because it is near the middle of the energy range investigated and because the majority of the gamma rays observed have energies close to 340 keV.

TABLE 2

Pa^{233} photons measured with the Pasadena bent-crystal spctrometer

	Energy (keV)		Intensity (percent beta decay)			
	This work	Browne [16])	Pt wire source	ThO_2 source	Average	Browne [16])
Gamma rays		28.67±0.02				0.060
	40.35±0.01	40.47±0.1	0.015		0.015	0.048
	41.65±0.02		(weak)			
	75.28±0.01	75.4±0.2		0.82	0.82	1.3
	86.59±0.01	87.0±0.3	2.0	1.5	1.7	[1.7]
	103.86±0.02		0.62	0.70	0.66	
	145.42±0.05			0.44	0.44	
	271.62±0.23		0.33	0.25	0.29	
	300.20±0.24		6.0	6.5	6.3	
	311.91±0.13		[34]	[34]	[34]	
	340.51±0.18		3.9	3.8	3.9	
	375.35±0.32		0.51	0.61	0.56	
	398.57±0.40		1.1	1.0	1.1	
	415.87±0.42		1.4	1.6	1.5	

	Energy (keV)		Intensity (percent beta decay)					Transition
	This work	Accepted (ref. [17]))	Pt wire source	ThO_2 source	Average	Browne [11])	Beckman [18])	
X-rays	**Uranium**							
	94.655	94.664	9.5	8.3	[8.8]	[8.8]	8.8	$K\text{-}L_{II}(K\alpha_2)$
	98.441	98.442	18	14	16	17	16	$K\text{-}L_{III}(K\alpha_1)$
	110.421	110.428	2.3	1.1	1.7		2.3	$K\text{-}M_{II}(K\beta_3)$
	111.297	111.307	4.1	3.4	3.8		4.4	$K\text{-}M_{III}(K\beta_1)$
	114.502	114.568	1.5	2.0	1.7		2.0	$K\text{-}N_{II}, N_{III}$ $(K\beta_2)$
	115.405	115.412	0.42	0.42	0.42		0.48	$K\text{-}O_{II}, O_{III}$
	Platinum							
	65.127	65.122						$K\text{-}L_{II}(K\alpha_2)$
	66.861	66.831						$K\text{-}L_{III}(K\alpha_1)$
	75.292							$75\text{-keV}\gamma + K\beta_3$
	75.754	75.749						$K\text{-}M_{III}(K\beta_1)$

The magnitude of the correction factor varies from 0.014 for the 40 keV transition to 1.49 for the 416-keV transition. The averages of two intensity determinations have been chosen as the final values.

Gamma-ray data published by Browne [16]) are also presented in table 2. The energy data of Browne are in reasonably good agreement with the data of this work; however, the relative intensities of the low-energy gamma rays are not in agreement. For the purpose of comparison the intensity data of Browne were normalized to the 87-keV photon intensity. The values of this work and of Browne, so normalized, deviate considerably at lower energies. This deviation is such that the ratio of Browne's intensities to those of this work, for photons of lower energy than 87 keV, varies linearly with energy, suggesting a systematic error in one of the sets of data. The cause of the deviation is unknown.

In table 2 uranium K-X-ray relative-intensity data of Beckman [18]) and of Browne [16]) are also listed, normalized to a value of 8.8 for the K α_2 line. The relative intensities of this work are seen to be in close agreement with those of the previous workers.

Since the intrinsic line widths of X-rays are not narrow relative to the instrumental window width of the crystal spectrometer, whereas those of gamma rays are, it is necessary to normalize differently X-ray and gamma ray intensities determined by peak heights. The normalisation of the K X-ray intensities was done by setting the total intensity equal to 34 % of the beta disintegrations. This value for the total X-ray intensity was determined indirectly, as follows:

(a) The total K-conversion line intensity is 35.1 % of the total number of decays. Correcting for the fluorescence yield (0.963), the total KX-ray intensity† is calculated to be 34 %.

(b) The total intensities of the KLL Auger lines were determined [10]) as 0.68 % per beta disintegration (including estimates of 0.02 % and 0.08 % for the unobserved $KL_{II}L_{II}$ and KL_{III} L_{III} lines). From the tables of Wapstra *et al.* [17]) we take the ratio KLY/KLL and KXY/KLL to be 0.7 and 0.05, respectively, for $Z = 90$, and calculate the total K-Auger intensity to be 1.2 %. The K X-ray intensity is therefore $1.2\ \%/(1-0.963) = 32\ \%$.

5. The 312-keV Magnetic Dipole Transition

From a measurement of L-subshell conversion ratios and K-conversion coefficient, the multipolarity of the 312-keV transition is determined to be essentially pure magnetic dipole. These data are as follows: The L_I/L_{II} ratio, determined with the iron-free spectrometer, is 10.5 ± 1. The theoretical value [22]) (table 3) for M1 radiation is 10. E2 admixture would lower the observed L_I/L_{II} ratio markedly, because E2 radiation favours L_{II} conversion. The error limit as given would indicate a maximum of 2 % E2 admixture in this transition.

A more sensitive indication of the extent of E2 admixture should be given by the L_I/L_{III} ratio, but here unfortunately the L_{III} line is unresolved from the much stronger 300-keV M_I line. Our measured intensity ratio of (300 L_I)/

---

† The "accepted" X-ray energies were deduced from electron binding energies listed in ref. [17]).

TABLE 3. Experimentally determined conversion coefficients of transitions in U^{233}

	Energy (keV)	α_K	α_{L_I}	$\alpha_{L_{II}}$	$\alpha_{L_{III}}$	α_{M_I}	$\alpha_{M_{II}}$	$\alpha_{M_{III}}$	α_{N_I}	α_{O_I}	$\alpha\sum L_i$ a)	$\frac{\alpha_K}{\alpha\sum L_i}$ a)	Multipole assignment
Experimental values	28					$M_I : M_{II} : M_{III} =$ 1.0 : 0.36 : 0.39							97% M1 3% E2
	40		87	293	234		73	67			614		70% M1 30% E2
	75		11	1.5	0.16	2.6			0.84	0.33	13		99% M1 1% E2
	87		5.5	0.76	0.15	1.5	0.34	0.076	0.38	0.09	6.4		98% M1 2% E2
	104		3.6	0.67	0.15	1.1			0.48		4.5		96% M1 4% E2
	272	0.17	0.17		≦0.13						≦0.30	≧0.56	E2
	300	0.83	0.13	0.019		0.036			0.012		0.15	5.5	88% M1 12% E2
	312	0.79 b)	0.136	0.013		0.029			0.014	0.003	0.15	5.2	M1
	340	0.59	0.13	0.017		0.041			0.02		0.14	4.0	90% M1 10% E2
	375	0.068	0.018	0.037	0.020						0.075	0.90	E2
	399	0.059	0.018	0.032	0.010						0.060	1.0	E2
	416	0.11	0.023	0.017	0.004						0.044	2.5	18% M1 82% E2

	M1						E2					
	α_K	α_{L_I}	$\alpha_{L_{II}}$	$\alpha_{L_{III}}$	$\alpha\sum L_I$ a)	$\frac{\alpha_K}{\alpha\sum L_i}$ a)	α_K	α_{L_I}	$\alpha_{L_{II}}$	$\alpha_{L_{III}}$	$\alpha\sum L_i$ a)	$\frac{\alpha_K}{\alpha\sum L_i}$ a)
Theoretical values [22])		$M_I : M_{II} : M_{III} = 1.0 : 0.1 : 0.0047$						$M_I : M_{II} : M_{III} = 1.0 : 28 : 28$				
		50	4.2	0.29	54			16	400	390	806	
		8.9	0.75	0.043	9.7			1.2	23	17	41	
		5.8	0.49	0.027	6.3			0.60	11	8.0	20	
		3.5	0.30	0.016	3.8			0.30	4.9	3.2	8.0	
	1.2	0.23	0.023	0.00093	0.25	4.7	0.089	0.023	0.082	0.033	0.138	0.65
	0.86	0.17	0.017	0.00068	0.19	4.6	0.075	0.018	0.055	0.020	0.073	1.0
	0.79	0.16	0.016	0.00062	0.18	4.5	0.070	0.017	0.048	0.017	0.065	1.1
	0.60	0.12	0.012	0.00046	0.13	4.5	0.059	0.014	0.033	0.011	0.047	1.3
	0.48	0.098	0.0099	0.00036	0.11	4.4	0.051	0.012	0.024	0.0076	0.044	1.2
	0.40	0.081	0.0082	0.00030	0.089	4.5	0.045	0.010	0.018	0.0055	0.034	1.3
	0.36	0.074	0.0076	0.00027	0.082	4.4	0.043	0.0094	0.016	0.0047	0.030	1.4

a) $\alpha\sum L_i$ refers to the sum of the L-conversion coefficients determined in this work. α_{L_i} differs from α_L (total L-conversion coefficient) in those cases in which not all of the L-subshell electron intensities were measured.

b) Relative photon intensities were normalized to relative electron intensities by means of the theoretical α_K^{312}, which is 0.79 (sect. 6).

(300 M_I+312 L_{III}) lies between 3.5 and 4.0. Since 3.5 is approximately the value expected for the L_I/M_I ratio of the 300 keV transition alone, the contribution of the 312-keV L_{III} line to the composite line must be quite small. A quantitative estimate of the amount of 312-L_{III} in the composite line indicates that the E2 admixture in the 312-keV transition lies between zero and 5 %.

An experimental measurement of the K-conversion coefficient of this transition was also made, with four samples of varying strengths, by use of a thick-lens spectrometer and a 100-channel scintillation spectrometer. The photon spectrum is shown in fig. 2. Normalization between the two instruments was effected with the 570-keV transition of Bi^{207}, whose conversion coefficient [23]) is known ($\alpha_K = 0.015 \pm 0.002$). Our experimental value 0.8 ± 0.3 is consistent with the interpretation of this transition as pure M1, but is not accurate enough for use in any quantitative way. The theoretical M1 conversion coefficient for a 312-keV transition in $Z = 92$ is given as 0.79 by Rose [22]) and as 0.72 by Sliv and Band [24]).

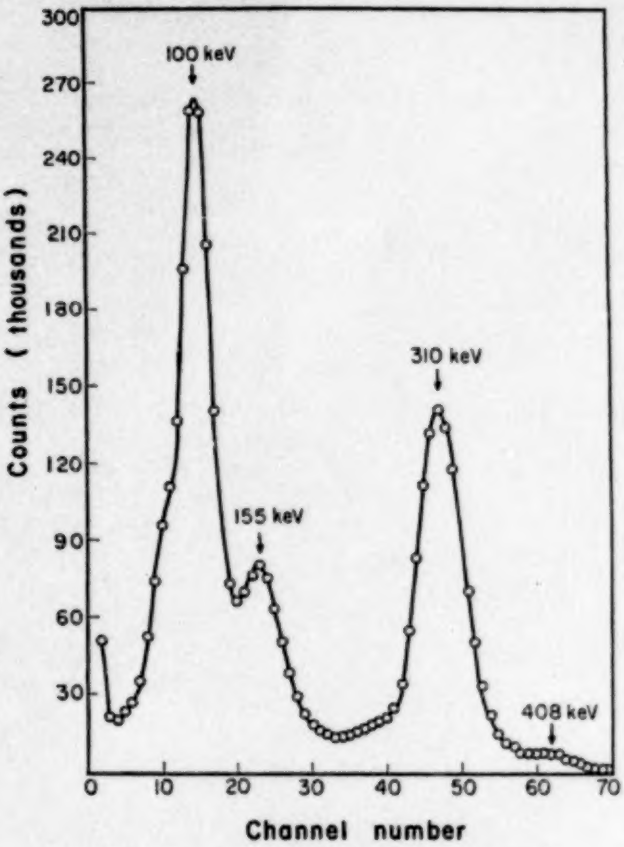

Fig. 2. Gamma-ray spectrum of Pa^{233}.

6. Conversion Coefficients and Multipole Assignments

In order to calculate conversion coefficients from the relative electron and gamma intensities, the gamma intensities were normalized to the electron intensities by means of Rose's theoretical K-conversion coefficient for the 312-keV M1 transition 22)). This normalization was chosen because the large limits of error on the experimental value of α_K^{312} made this value undesirable as a normalization factor although it does serve as a check against a gross error in the interpretation. If the 312-keV transition should have the 2 % E2 admixture which we have set as an upper limit, then the use of the theoretical α_K^{312} for a pure M1 transition would introduce a 2 % error in the normalization and in the calculated conversion coefficients.

TABLE 4

Pa^{233} transition intensities and multipolarities

Transition energy keV	Transition intensity (% β decay)	M1-E2 mixing (% E2 photons)		
		Bisgård *et al.* 7)	Albouy and Valadares 6)	This work
17.26				
28.54	≈19	M1+E2	4 % E2	(3 ±0.5)% E2
40.35	12	M1+E2	60% E2	(30±10)% E2
75.28	14	M1	M1(<1% E2)	(1±0.1)% E2
86.59	17	M1	M1(<1% E2)	(2±0.5)% E2
103.86	4.8	M1	M1(<1% E2)	(4±1)% E2
271.62	0.5	E2	E3, E4, E5 or M1+E2	≈ 100% E2
300.20	13	M1	M1	(12±10)% E2
311.91	68	M1	M1	M1(<2% E2)
340.51	7.0	M1	M1	10±10% E2
375.35	0.7	E2		≈ 100% E2
398.57	1.2	E2		≈100% E2
415.87	1.7	M1		(82±7)% E2

The conversion coefficients so calculated are listed in table 4. From the limits of error placed on the electron and gamma intensities, we estimate limits of error of about 35 % for most of the experimental conversion coefficients listed in table 4. The values for the weak transitions may be in error by as much as a factor of two.

The experimental L-subshell ratios, $\alpha_K/\alpha_{\Sigma L_i}$ ratios † and absolute conversion coefficients are compared with the theoretical values of Rose 22)) in order to assign transition multipolarities. Rose's theoretical values for M1 and E2 transitions are listed in table 3 along with the experimental values and the assigned multipolarities. In calculating the percentages of mixed multipoles, most weight has been given to the L-subshell ratio data.

Some general observations can be made about the data and assignments presented in table 3. In most cases the major multipole component of each transition is clearly indicated. Especially evident in the pure E2 assignments is the fact that the experimental absolute conversion coefficients are somewhat larger than the theoretical conversion coefficients. These differences are probably due to experimental errors in the electron- and photon-intensity data and to the means of normalizing the photon intensities to the electron intensities. Note that if the theoretical $\alpha_K{}^{312}$ of Sliv had been used for normalization, all experimental values would be lowered by ≈ 9 %, but this difference would not be sufficient to bring our values into line. It would be desirable to determine these conversion coefficients with higher precision in order to check the absolute values of the conversion coefficients.

---

† ΣL_i refers to the sum of the measured L-subshell intensities. It differs from the total L intensity when one or more of the subshells were not measured.

In table 4 a comparison is given of the multipolarity assignments made by Bisgård *et al.* [7]), Albouy and Valadares [6]) and in this study. Although the previous assignments have been largely qualitative, there is agreement with regard to the major component of all transitions except the 416 keV. Bisgård *et al.* assign this transition as magnetic dipole, whereas we interpret it as an M1–E2 mixture with 82±7 % E2. In the case of the 40-keV transition, Albouy and Valadares report an M1–E2 mixture with approximately 40 % M1, whereas our data indicate an approximately 70 % M1 admixture.

7. Absolute Transition Intensities and log *ft* Values

From the data of previous investigators [2,4,14]), it is apparent that approximately 95 % of the beta decay populates the upper four levels in U^{233}. We have therefore attempted to make an absolute estimate of the measured relative intensities in tables 1, 2 and 3 by assuming that the sum of the intensities of the transitions depopulating the upper four levels is equal to 95 % of the total beta decay. The transition intensities (the sums of the electron and gamma-ray intensities) calculated under this assumption are listed in table 4.

Since no gamma-ray data and only limited electron-intensity data are available for the 28-keV transition, its total intensity was estimated in the following manner: The multipolarity of the 28-keV transition was deduced from the relative M-subshell ratios by comparing the experimental values to Rose's theoretical values [22]). The transition was found to be M1 with approximately 3 % E2 admixture. The total L-electron intensity was approximated as 3.6 times the total M electron intensity (average of the ratio of total L to total M intensities for other M1 transitions observed here) and the N and O electron intensities were estimated respectively as $\frac{1}{3}$ and $\frac{1}{9}$ of the M-electron intensity. This latter assumption was made also in estimating the total intensities of other transitions whose N and O intensities had not been measured. Because of the high conversion coefficients, the photon intensity of this transition is a very small fraction (≈ 0.2 %) of the total intensity.

The percent beta populations to the levels in U^{233} were deduced from the absolute transition intensities and are listed in table 5. Hok's measured intensity values for the low- and medium-energy beta components are 37 % and 58 %, respectively [2]). The corresponding values deduced from the values in table 5 are 40 % and 53 %; thus the intensities of these beta-decay branches determined in two independent ways are equal within experimental error.

TABLE 5

Beta-component intensities and log *ft* values in the decay of Pa^{233}

Final state (keV)	Beta-group intensity (percent)	log *ft*
415.80	$\lesssim 21$	$\gtrsim 6.7$
398.55	$\gtrsim 19$	$\lesssim 6.9$
340.52	25	7.2
311.93	28	7.3
40.35 0.00	≈ 5	9.2

The value of 5 % decay to the ground-state band listed in table 5 is that measured by previous workers [2, 4, 14]). The log *ft* values in table 5 were calculated from the curves of Moszkowski [26]) by use of the beta intensities listed.

8. Discussion of Decay Scheme

The above data have been used to construct the decay scheme shown in fig. 3. The general features of the scheme are the same as proposed by Brodie [4]) and supported by Hok and Kramer [2]) .The quantum assignments of the U^{233} levels suggested by Newton [5]) are confirmed. Some Coulomb-excitation data of Newton are included in the scheme for completeness. The energies assigned the levels are a best fit to the sums and differences of the energies of the gamma rays connecting the levels. In all cases the difference in the possible energy values of a level as computed by different sums and differences is within 0.04 %.

The ground state spin of U^{233} has been measured as $\frac{5}{2}$ by a number of investigators [27–31]). As pointed out by Newton [5]), the ground state is most probably the $\frac{5}{2}+[633]$ Nilsson level. The ground state spin of Pa^{233} was measured as $\frac{3}{2}$ by Hubbs and Winocur [32]). Evidence that the ground state of Pa^{233} has odd parity was obtained by a beta-gamma angular correlation experiment performed at Uppsala by Hamilton, Hollander, Pettersson and Subba Rao [33]). An anisotropy observed between the 250-keV beta group and the 312-keV photon establishes that the beta transition to the 312-keV level cannot be purely allowed. Thus, the parity of Pa^{233} is odd if that of the 312-keV level is even. The Pa^{233} ground state has been interpreted [34]) as the $\frac{3}{2}$ member of a $K = \frac{1}{2}$ band based on the Nilsson level $\frac{1}{2}-[530]$. With this basic information and the data at hand it is possible to analyze the scheme with respect to beta branchings, photon branchings and log *ft* values. It is convenient to discuss each of the rotational bands separately.

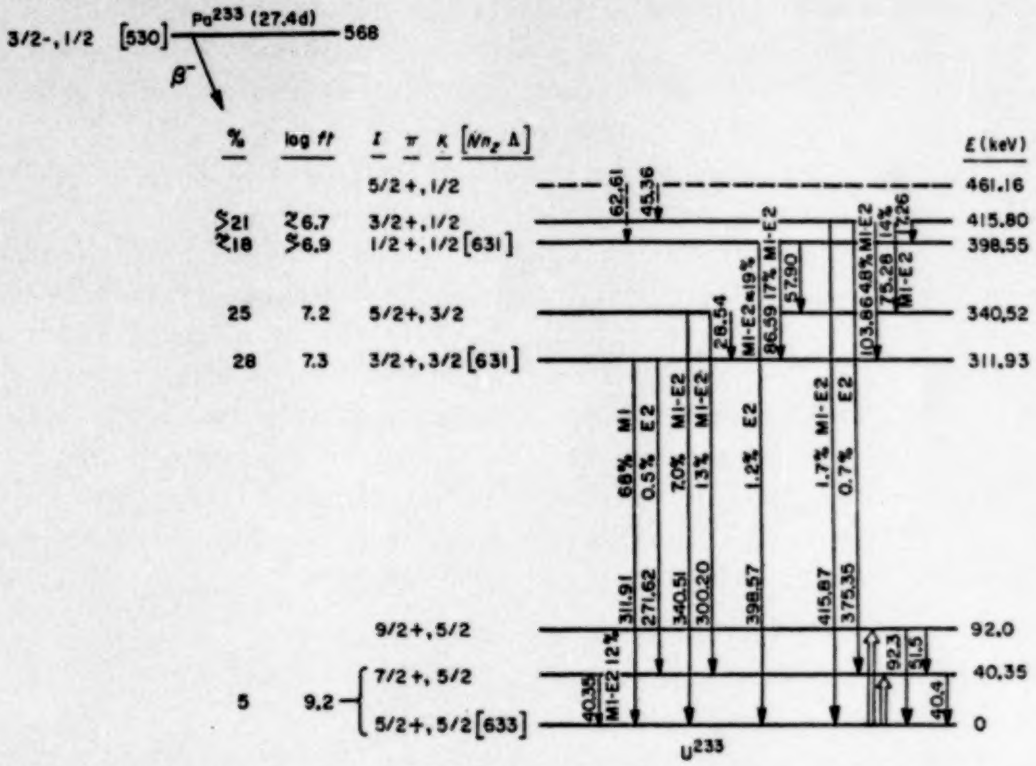
3/2-, 1/2 [530]
Pa233 (27.4d)
568
β-
%
log ft
I π K [Nnz Λ]
E (keV)
5/2+, 1/2
461.16
≲21 ≳6.7 3/2+, 1/2
415.80
≳18 ≲6.9 1/2+, 1/2 [631]
398.55
25 7.2 5/2+, 3/2
340.52
28 7.3 3/2+, 3/2 [631]
311.93
9/2+, 5/2
92.0
7/2+, 5/2
40.35
5 9.2
5/2+, 5/2 [633]
0
U233
62.61
45.36
28.54
M1-E2≈19%
86.59 17% M1-E2
57.90
103.86 48% M1-E2
75.28 14% M1-E2
17.26
311.91 68% M1
271.62 0.5% E2
340.51 7.0% M1-E2
300.20 13% M1-E2
398.57 1.2% E2
415.87 1.7% M1-E2
375.35 0.7% E2
40.35 M1-E2 12%
92.3
51.5
40.4

Fig. 3. The energy levels of U^{233} populated by the decay of Pa^{233}.

8.1. GROUND-STATE BAND

The assigned quantum states indicate that the beta transitions to the ground-state band proceed largely by the "unique" $\Delta I = 2$, yes, type of decay, since $\Delta I = 1$ transitions are K-forbidden ($\Delta K = 2$). In addition, the first-forbidden transition to the ground state is "hindered", in the notation of Alaga [35]), since a selection rule on the asymptotic quantum number Λ is violated. The experimental log *ft* of 9.2 for transitions to the ground — and first — excited states (unresolved) is consistent with "unique' 1st forbidden decay and hence with the assigned quantum states [36]).

The rotational constant ($\hbar^2/2\mathscr{I}$) for the ground-state band was calculated from the energy of the first excited state (40.35 keV) by means of the equation [8])

$$E_{\text{rot}} = \hbar^2/2\mathscr{I}[I(I+1)-I_0(I_0+1)].$$

The result is $\hbar^2/2\mathscr{I} = 5.76$ keV. With this constant the energy of the second excited state is calculated to be 92.22 keV. Newton's measured value [5]) is 92.0 keV.

The recent results of Albouy and Valaderes [6]) indicated a possible discrepancy in the Pa^{233} decay scheme: they reported that the total feeding of the 40-keV level is stronger than the measured intensity of the 40-keV transition by a factor of 3 or 4. We find, however, that the 40-keV transition is too weak by only 15 %. The predominant decay to the 40-keV state occurs via the 300, 270 and 375-keV transitions (total intensity 14 %) whereas our measured intensity of the 40-keV transition is 12 %. This unbalance of ≈ 15 % is within the combined sources of error of the transitions involved, thus we feel that there is no inconsistency with the proposed scheme.

We have assigned the 40-keV transition as 70 % M1 and 30 % E2; Albouy and Valadares [6]) report this mixture as 40 % M1 and 60 % E2. In addition, these workers [6]) have calculated a value of 20 % M1 and 80 % E2 based upon the data of Newton [5]). The mixing ratio of this transition is important because it can be used along with the experimental values of the magnetic and quadrupole moments to calculate the gyromagnetic ratios for the particle (g_Ω) and core (g_R) for the ground state rotational band. The calculation is based on the fact that the reduced transition probability for collective M1 transitions is proportional to $(g_\Omega - g_R)^2$, and that of collective E2 transitions [8]) is proportional to Q_0^2, where Q_0 is the intrinsic quadrupole moment. Also, the magnetic moment is related to g_Ω and g_R by the equation [8])

$$\mu = \frac{I^2}{I+1} g_\Omega + \frac{I}{I+1} g_R \text{ for } I = K = \Omega \geqq \tfrac{3}{2}.$$

The values of g_Ω and g_R cannot be determined uniquely unless the signs as well as the values of Q_0 and μ are known. Newton [5]) discusses this calculation in more detail.

For U^{233}, μ has been measured as ± 0.51 nuclear magnetons [36]) and q, the measured quadrupole moment, is ± 3.4 b. From the latter we deduce a value [8]) of ± 9.5 b for Q_0. Using the mixing ratio of 70 % M1 and 30 % E2 for the 40-keV transition, and assuming that Q_0 and g_R are both positive we calculate the following choices:

$$g_\Omega = 0.16, g_R = 0.32, \qquad \text{or} \qquad g_\Omega = 0.25, g_R = 0.09.$$

The second choice is not acceptable since g_R is expected to have a value of approximately [8]) $+Z/A = 0.4$.

The mixing ratio of 40 % M1 and 60 % E2 reported by the French [6]) workers leads to values of

$$g_\Omega = 0.23, g_R = 0.14, \qquad \text{or} \qquad g_\Omega = 0.18, g_R = 0.27.$$

Newton [5]) has previously reported calculated values of

$$g_\Omega = 0.25, g_R = 0.17, \qquad \text{or} \qquad g_\Omega = 0.20, g_R = 0.28.$$

In Newton's calculation, however, a value of Q_0 of ≈ 14 b was used.

8.2. THE K = $\frac{3}{2}$ BAND

The levels at 312 keV and 340 keV have been interpreted [5]) as the $\frac{3}{2}$ and $\frac{5}{2}$ members of rotational band based on the Nilsson level $\frac{3}{2}+[631]$.

The calculated log *ft* values listed in table 5 for beta decay to these levels are consistent [37]) with first-forbidden nonunique decay ($\Delta I = 0$ or 1, yes) and hence support the assigned spins and parities. The experimental beta branching to these two levels is also in reasonably good agreement with the theoretical value predicted from vector-addition coefficients. The theoretical value for $L = 1$ decay is $B(\frac{3}{2} \to \frac{5}{2})/B(\frac{3}{2} \to \frac{3}{2}) = 1.5$, and the experimental value (inverse ratio of *ft* values) is ≈ 1.3. We here compare only $L = 1$ beta decay because $L = 0$ decay to the $\frac{3}{2}$ level is K forbidden.

TABLE 6

The decay of Pa^{233}-experimental and theoretical relative reduced photon transition probabilities

E_γ/E'_γ	K_i K_f	$\frac{L:\ B(I_i \to I_f)}{L:\ B(I_i \to I'_f)}$	Theoretical values	Experimental values	
				Albouy and Valadares [a])	This work
$\frac{75}{103}$	$\frac{1}{2}$ $\frac{3}{2}$	$\frac{M1:\ B(\frac{3}{2} \to \frac{5}{2})}{M1:\ B(\frac{3}{2} \to \frac{3}{2})}$	1.5	1.3 → 1.7	3.2
$\frac{416}{375}$	$\frac{1}{2}$ $\frac{5}{2}$	$\frac{E2:\ B(\frac{3}{2} \to \frac{5}{2})}{E2:\ B(\frac{3}{2} \to \frac{7}{2})}$	1.3	>2.4	1.3
$\frac{300}{340}$	$\frac{3}{2}$ $\frac{5}{2}$	$\frac{M1:\ B(\frac{5}{2} \to \frac{7}{2})}{M1:\ B(\frac{5}{2} \to \frac{5}{2})}$	2.5	1.3	2.3
$\frac{300}{340}$	$\frac{5}{2}$ $\frac{5}{2}$	$\frac{M1:\ B(\frac{5}{2} \to \frac{7}{2})}{M1:\ B(\frac{5}{2} \to \frac{5}{2})}$	0.4		
$\frac{300}{340}$	$\frac{3}{2}$ $\frac{5}{2}$	$\frac{E2:\ B(\frac{5}{2} \to \frac{7}{2})}{E2:\ B(\frac{5}{2} \to \frac{5}{2})}$	0.037		≈3.6

[a]) These values were deduced from data presented in ref. [6])

It is possible to test the K-quantum assignment of the 340-keV level by a comparison of the relative reduced photon transition probabilities of both the M1 and E2 components of the 300- and 340-keV transitions with those predicted theoretically for states of definite K. The experimental and theoretical values are listed in table 6. The theoretical values are as discussed above; the experimental ones were calculated from the ratios of the measured gamma-ray relative intensities corrected for the E^{2l+1} energy dependence and for multipole admixtures. Also listed are experimental values deduced from the data of Albouy and Valadares [6]).

A comparison of the experimental and theoretical ratios for the M1 radiation should best indicate the major K-component of the 340- keV level, since the amount of E2 mixing in the 300 and 340 keV transitions is small and inaccurately known. For the M1 components our experimental values agree well with the theoretical value for $K = \frac{3}{2}$, and support the assignment of the 340 keV state as the first rotational member of the band based on the $\frac{3}{2}+[631]$ intrinsic state. From the energy difference between $\frac{3}{2}+$ and $\frac{5}{2}+$ members of this band (28.59 keV) one calculates a rotational constant of 5.72 keV. The calculated energy of the $\frac{7}{2}+$ member is, then, 380.6 keV. No evidence for a state of this energy was found in this work.

There appears to be a large discrepancy between our experimental and theoretical ratios for the weak E2 components of the 300 and 340 keV radiation. This disagreement may be due to the large errors in the experimental determination of the mixing ratios and perhaps in part is due to an admixture of $K = \frac{1}{2}$ in the 340-keV level. Such an admixture would not affect the branching ratio of the M1 components since for $K = \frac{1}{2} \rightarrow K = \frac{5}{2}$ dipole radiation is K-forbidden.

8.3. THE $K = \frac{1}{2}$ BAND

According to the multipole assignments listed in tables 3 and 4 the levels at 398 and 416 keV must have spins and parities of $\frac{1}{2}+$ and $\frac{3}{2}+$, respectively. These assignments support the interpretation that these levels are the first two members of a $K = \frac{1}{2}$ rotational band with the Nilsson level $\frac{1}{2}+[631]$ as the base state [5]). The division of the primary beta population between these two levels cannot be estimated accurately because the intensity of the 17-keV transition is not known. In table 5 the log *ft* values listed for these two levels were calculated with the assumption of an intensity of 0 % for the 17-keV transition, and the uncertainties indicated by (<) and (>) signs. These approximate log *ft* values support the postulated spin and parity assignments.

The theoretical branching ratio for beta decay to these levels cannot be calculated from vector-addition coefficients without knowledge of the relative amounts of $L = 0$ and $L = 1$ types of decay to the 416-keV level; however, if the quantum assignments of the 399- and 416-keV levels are assumed to be correct it is possible to make an indirect test of the assignment $K = \frac{1}{2}$ to the ground state of Pa^{233}. The only other K value consistent with the measured spin for Pa^{233} is $K = \frac{3}{2}$. If this value is assumed, it is possible to make branching-ratio comparisons for decay to the 416- and 399-keV levels because $L = 0$ transitions are then K-forbidden. With this assumption the theoretical ratio for $L = 1$ decay to the two highest levels is $B(\frac{3}{2} \rightarrow \frac{1}{2})/(B\frac{3}{2} \rightarrow \frac{3}{2}) = 1.25$; the experimental value is 0.62, calculated by assuming the intensity of the 17-keV transition to be negligible. (The experimental ratio would be smaller if a finite value were assumed for the intensity of the 17-keV transition). Thus, the theoretical and experimental values differ by at least a factor of two. This in itself is not conclusive evidence against an assignment of $K = \frac{3}{2}$ for the ground state of Pa^{233} because such deviations can be caused by admixtures of K values in the initial or final states. However, additional evidence that the ground state of Pa^{233} has $K = \frac{1}{2}$ comes from the work of Stephens, Asaro and Perlman [38]) on the alpha decay of Np^{237}, which populates several excited states in Pa^{233} whose spacings appear to be characteristic of a $K = \frac{1}{2}$ band.

The theoretical and experimental values of the reduced photon branching ratio (416—E2)/(375—E2) are compared in table 6. The theoretical value and our experimental value are within experimental error. The data thus support the quantum assignment of $(\frac{3}{2}+, \frac{1}{2})$ for the 416-keV level. Note that M1 transitions from the $K = \frac{1}{2}$ band to the ground-state band are K-forbidden. This accounts for the predominantly E2 character of the 416-keV transition.

The theoretical and experimental reduced photon branching ratios (75—M1)/(103—M1) also are compared in table 6. Our experimental value is more than a factor of two larger than the theoretical value, a discrepancy outside the assigned limits of error. If the multipolarities of the gamma rays depopulating the 416-keV level have been correctly deduced, the only choice of spin for this level is $\frac{3}{2}$; and thus the only possible K values are $\frac{1}{2}$ and $\frac{3}{2}$. The alternative choice of $K = \frac{3}{2}$ leads to a theoretical value of $[\mathrm{M1}: B(\frac{3}{2} \rightarrow \frac{5}{2})]/[\mathrm{M1}: B(\frac{3}{2} \rightarrow \frac{3}{2})] = 0.67$, which differs from the experimental value by a factor of 4.8, in worse disagreement than the results for $K = \frac{1}{2}$.

The difference between the experimental and theoretical values may be due to admixtures in the initial or final states of K values differing from the principal one by ± 1. Approximate calculations show that although interaction between the observed $K = \frac{3}{2}$ and $K = \frac{1}{2}$ band is probably not large enough to explain the discrepancy, the Nilsson state $\frac{1}{2}+[640]$ may mix with the $K = \frac{1}{2}$ and/or $K = \frac{3}{2}$ band to a degree large enough to affect the relative reduced transition probabilities appreciably. Thus, the evidence indicates that the major component of the 399- and 416-keV states is $K = \frac{1}{2}$.

9. Other Transitions and New States

There is weak evidence that transitions from the previously unobserved $\frac{5}{2}$ member of the $K = \frac{1}{2}$ band were seen in this study. These transitions, of 62.61 and 45.36 keV, are shown in fig. 3 depopulating a level at 461.16 keV. The evidence for these transitions is two weak electron lines of energies 41.67 and 23.60 keV listed in table 7.

It was assumed that the first of these lines is the L_{II} line of a 63-keV E2 transition, and that the second is the L_I line of a 45-keV M1-E2 transition. The fact that no other electron lines of these transitions were observed is consistent with the very weak intensities of the observed lines and the multipole assignments of the transitions. This evidence is tenuous, since in the energy region of these lines there are many unassigned lines among which one might expect some coincidental agreement. Some support is given the postulate by the very close agreement between the differences of the postulated transitions (17.25 keV) and the measured energy (17.26) of the $\frac{3}{2}+ \rightarrow \frac{1}{2}+$ transition.

With the assignment of the $\frac{5}{2}$ member, it is possible to calculate the rotational constant $\hbar^2/2\mathscr{I}$ and the decoupling parameter a for this $K = \frac{1}{2}$ band. These constants are defined by the equation [8])

$$E_{\text{rot}} = \hbar^2/2\mathscr{I}[I(I+1)+a(-)^{I+\frac{1}{2}}(I+\tfrac{1}{2})].$$

Substitution of the measured energies gives $\hbar^2/2\mathscr{I} = 7.41$ keV and $a = -0.22$.

TABLE 7

Unassigned electron lines in the decay of Pa^{233}

E_{e^-} (keV)	Possible assignments	E_{e^-} (keV)	Possible assignments
1.90	[a])	232.1	250-L_{III}
2.83	[a])	232.3	
4.08	[a])	232.5	
108.3	130-L_{I}	262.7	
112.7	130-L_{III}	281.1	
166.5		292.0	314-L_{I}
172.4	[a])	293.0	314-L_{II}
226.6		445.4	
229.5	250-L_{II}		

Questionable lines: 6.84, 9.31, 9.44, 19.86, 20.25, 20.49, 21.30, 21.75, 22.08, 23.60, 23.84, 24.68, 25.70, 28.52, 30.64, 35.53, 37.77, 41.67, 47.59, 53.86, 54.16, 63.91, 65.15, 65.83, 67.23, 69.42, 72.21, 74.46, 81.73, 105.6, 217.7, 219.5, 221.5, 227.2, 396.7.

[a]) Much stronger than others listed in tbis table.

These values may be compared with those of the same rotational band occurring in other nuclei. In U^{235} the $\frac{1}{2}+[631]$ level is a low-lying isomeric state. Albridge and Hollander [39]), using permanent-magnet spectrographs, have determined the energies of the $\frac{3}{2}+$ and $\frac{5}{2}+$ members of this band in U^{235} by measuring the $\frac{5}{2} \rightarrow \frac{1}{2}$ and $\frac{5}{2} \rightarrow \frac{3}{2}$ transition energies from the alpha decay of Pu^{239}. The energies of the $\frac{5}{2}+$ and $\frac{3}{2}+$ levels were found to be 51.67 keV and 13.00 keV, respectively. These energies lead to values of $\hbar^2/2\mathscr{I} = 6.04$ keV and $a = -0.28$. The $\frac{1}{2}+$ [631] level is also the ground state of Pu^{239}. In studies of the decay of Np^{239}, Hollander *et al.* [40, 41]) and Ewan *et al.* [42]) determined values of $\hbar^2/2\mathscr{I}$ and a for the $K = \frac{1}{2}$ band in Pu^{239} as 6.28 keV and -0.58, respectively.

In table 1 are listed two lines assigned as the L_{II} and L_{III} lines of a 57.90-keV E2 transition. In fig. 3 this transition is placed between the 399- and 341-keV levels. The 57.9-keV L lines assigned in this work were too weak to be given a numerical intensity. This weakness, in addition to the fact that the transition is thought to be E2 and, therefore, highly converted, is consistent with the fact that Browne [16]) failed to detect the gamma ray of this transition. That a 58-keV photon was not detected with the Pasadena spectrometer may not be significant since it is possible that during the sweep of this energy region the discriminator of the detector was not properly adjusted. This fact was not discovered until the source had been returned from Pasadena to Berkeley.

There is evidence for the existence of other gamma transitions in the Pa^{233} decay. This evidence is a number of unassigned electron lines (table 7) detected with the permanent-magnet spectrographs and two photon lines (table 2) of energies 41.65 and 145.42 keV detected with the Pasadena bent-crystal spectrometer. The electron lines listed in table 7 are divided into two groups. In the first group are lines whose existence is considered relatively certain because of their intensities or because of their detection on more than one photographic plate. The second group contains lines whose existence is questionable or doubtful.

Bisgård *et al.* [7]) have reported weak electron lines of energies approximately 5 keV less than those of the 300-, 312- and 341-keV K lines (i.e., at $\approx$180, $\approx$185 and $\approx$ 220 keV). With the exception of a questionable line at approximately 220 keV, lines of these energies were not observed in this work, although they would most likely have been visible had they been present in the intensities reported by the Danish workers.

It is of interest to discuss the 42- and 145- keV photons seen in the bent-crystal spectrometer. Fairly large error limits have been placed on the measured energies of these photons (table 2) because in the spectrum the lines were not well defined. The 41.65-keV gamma was observed only with the platinum wire source because the line was of too low intensity to be seen with the weaker ThO_2 source. The 145-keV line was observed only with the ThO_2 source because this region of the energy spectrum was not scanned with the platinum wire source. In table 7 there is no definite evidence of the conversion electrons corresponding to transitions of 42 or 145 keV. One extremely weak line, seen at an energy of 19.86 keV, could be the L_I line of a 41.62-keV transition, but this line is of doubtful existence. The fact there is no definite evidence of conversion electrons of these two transitions raises the question whether the recorded gamma rays have arisen from impurities in the particular sources used for gamma spectroscopy. The source with which the 41-keV gamma was detected underwent the same chemistry as used for the permanent-magnet spectrograph sources; and although the source used for the detection of the 145-keV gamma underwent no chemistry, it is likely that very few fission products were formed, owing to the low thermal-neutron fission cross section of Th^{232}. Besides, no gamma ray of 145 keV has been reported as being associated with a fission product. Thus we may tentatively consider these photons to arise in Pa^{233} decay. The most probable reason for the failure to observe conversion electrons from these transitions is that they have small conversion coefficients. For example, if the transitions were electric dipole the conversion-electron intensities would have been too small to be detected.

The difference between the energies of the 42- and 145-keV photons is 103.77±0.05 keV. This difference agrees with the energy of the 103.86±0.02-keV transition to within 0.1 %. Although this deviation is not within the assigned limits of errors, possibly the error limits have been underestimated. With the assumption that this energy difference is significant, the two new photons can be used to define a level at either 270.3 keV or 457.4 keV, as shown in fig. 4. Thomas *et al.* [25]) have reported a level in U^{233} of approximately 290±28-keV populated by the alpha decay of Pu^{237}, and this may possibly be identified with our 270.3 keV alternative.

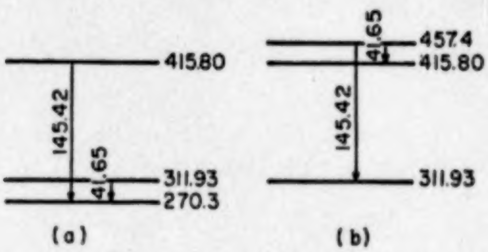

Fig. 4. (a) and (b) Possible assignments of two new transitions in the decay of Pa^{23} .

Stephens *et al.* [34]) and Mottelson and Nilsson [1]) have discussed the possible Nilsson assignment of the ≈ 290 keV level. The former workers favour the assignment $\frac{5}{2}-[752]$, the latter, $\frac{7}{2}-[743]$. Of the two possibilities, our data allow only the $\frac{5}{2}-$assignment to be made to the new state, regardless of its energy. The $\frac{7}{2}-$assignment would demand that the 42- and 145-keV transitions be M2, which would be inconsistent with our failure to see conversion lines. On the other hand, with the $\frac{5}{2}$-assignment the transitions would be electric dipoles with small conversion coefficients. (The 145-keV transition would, however, be *K*-forbidden.) Because of its high resolution, the bent-crystal spectrometer was not used to sweep the entire energy spectrum; thus it is not known whether photons associated with this level other than the two reported here are observable. The existence of a 270.3-keV state would of course pose the additional demand that there be an E1 transition to ground. It would be of value to search for the 270.3 keV photon, which would have to be at least as intense as the 145-keV photon (0.44 %), with which it would be in coincidence.

10. Auger Transitions

An investigation of the K- and L-Auger spectrum of uranium, which results from the decay of Pa^{233}, was also made. The results are discussed in a following paper [43]).

We are indebted to Professor J. O. Rasmussen, Dr. S. G. Nilsson and Dr. R. Stockendal for helpful discussions. We are also grateful to Professor J. W. M. DuMond for his kind cooperation in making the bent-crystal spectrometer available to us for the present study.

References

1) B. R. Mottelson and S. G. Nilsson, Mat. Fys. Skr. Dan. Vid. Selsk. **1**, No 8 (1959)
2) Ong Ping Hok and G. J. Sizoo, Physica **20** (1954) 77;
Ong Ping Hok and P. Kramer, Physica **21** (1955) 676
3) H. B. Keller and J. M. Cork, Phys. Rev. **79** (1950) 1030
4) W. A. Brodie, Proc. Phys. Soc. **67** (1954) 397
5) J. O. Newton, Nuclear Physics **5** (1958) 218
6) G. Albouy and M. Valadares, J. Phys. Radium **20** (1959) 816, Comp. Rend. **250** (1960) 2877
7) Bisgård, Dahl and Olesen, Nuclear Physics **12** (1959) 612
8) A. Bohr and B. R. Mottelson Mat. Fys. Medd. Dan. Vid. Selsk. **27**, No. 16 (ed. 2 (1957));
Beta and gamma ray spectroscopy, ed. by K. Siegbahn (Interscience Publishers, Inc., New York, 1955), chapt. 17, p. 468
9) M. Mladjenović and H. Slätis, Ark. Fys. **8** (1954) 65
10) R. G. Albridge, Jr., UCRL-8642, Thesis (1960)
11) K. Siegbahn and K. Edvarson, Nuclear Physics **1** (1956) 137
12) J. W. M. Du Mond in Beta and gamma ray spectroscopy, ed. by K. Siegbahn (Interscience Publishers, Inc., New York, 1955) chapt. 4, p. 100
13) Hill, Church and Mihelich, Revs. Sci. Instr. **23** (1952) 523
14) L. G. Elliott and A. B. Underhill, Harwell Report HAR 761 (1952)
15) D. Saxon, Phys. Rev. **81** (1951) 639
16) C. I. Browne, Jr., UCRL-1764, Thesis (1952)
17) Wapstra, Nijgh and van Lieshout, Nuclear spectroscopic tables (North-Holland Publ. Co., Amsterdam, 1959)
18) O. Beckman, Ark. Fys. **9** (1955) 495
19) R. L. Heath, AEC report IDO-16408 (July, 1957)
20) G. W. Grodstein, National Bureau of Standards research paper no. 583
21) Lind, West and DuMond, Phys. Rev. **77** (1950) 475
22) M. E. Rose, Internal conversion coefficients (North-Holland Publishing Co., Amsterdam, 1958)
23) F. K. McGowan and E. C. Campbell, Phys. Rev. **92** (1953) 523
24) L. A. Sliv and I. M. Band, Internal conversion coefficients of gamma rays — Part I, K-Shell (issued in U.S.A. as University of Illinois Report 57lccK1)
25) Thomas, Vandenbosch, Glass and Seaborg, Phys. Rev. **106** (1957) 1228
26) S. A. Moszkowski, Phys. Rev. **82** (1951) 35
27) K. L. Van der Sluis and J. R. McNally, Jr., J. Opt. Soc. Am. **45** (1955) 65
28) K. L. Van der Sluis and P. M. Griffin, J. Opt. Soc. Am. **45** (1955) 1087
29) N. I. Kaliteevskii and M. P. Chaika, Doklady Akad. Nauk S.S.S.R. **103** (1955) 49;
Optika i Spectroskopiya **1** (1956) 809
30) L. A. Korostyleva, A. R. Stringanov, and N. M. Yashin, JETP **28** (1955) 471 [translation JETP (Soviet Physics) **1** (1955) 310], Izvest. Akad. Nauk S.S.S.R. Ser. Fiz. **19** (1955) 31
31) A. G. Zimin and N. M. Yashin, Doklady Akad. Nauk. S.S.S.R. **109** (1956) 283 [translation: Soviet Phys. Doklady **1** (1957) 419]
32) J. C. Hubbs and J. Winocur, Bull. Am. Phys. Soc. **3** (1958) 319
33) Hamilton, Hollander, Pettersson and Subba Rao, unpublished results (1959)
34) Stephens, Asaro and Perlman, Phys. Rev. **113** (1959) 212
35) G. Alaga, Phys. Rev. **100** (1955) 432, Nuclear Physics **4** (1957) 625
36) P. B. Dorain, C. A. Hutchinson, Jr. and E. Wong, Phys. Rev. **105** (1957) 1307
37) R. W. King and D. C. Peaslee, Phys. Rev. **94** (1954) 1284
38) Stephens, Asaro and Perlman, unpublished data (1957)
39) Albridge and Hollander, unpublished data (1956)
40) Hollander, Smith and Mihelich, Phys. Rev. **102** (1956) 740
41) J. M. Hollander, Phys. Rev. **105** (1957) 1518
42) Ewan, Geiger, Graham and MacKenzie, Phys. Rev. **116** (1959) 950
43) R. G. Albridge and J. M. Hollander, Nuclear Physics **27** (1961) 554

3.C *Nuclear Physics* **27** (1961) 554—560; © *North-Holland Publishing Co., Amsterdam*

Not to be reproduced by photoprint or microfilm without written permission from the publisher

THE K- AND L-AUGER SPECTRUM OF URANIUM

R. G. ALBRIDGE [†] and J. M. HOLLANDER

Lawrence Radiation Laboratory, University of California, Berkeley, California [††]

Received 17 April 1961

Abstract: Measurements have been made of the K- and L-Auger electron spectrum of uranium, which results from the beta decay of Pa^{233}. These data are presented and compared with previously known information on the Auger transitions in heavy elements. Low energy lines, including Coster-Kronig transitions in the energy range 0.9- to 4-keV, were observed by means of a permanent-field electron spectrograph with source pre-acceleration.

1. Introduction

In a preceding paper [1]) (referred to hereafter as I) an investigation [†††] of the beta decay of Pa^{233} is described. In the course of part of this work, information was obtained about the K- and L-Auger electron transitions in uranium. Because little information has been available concerning the Auger spectra of elements with atomic number greater than 80, it was thought worthwhile to report these data. Tables 1 and 2 summarize the results of this and of previous investigations.

2. Experimental Methods

Details of the experimental techniques are given in I. In brief, Pa^{233} sources were prepared by neutron irradiations of thorium metal followed by chemical purification and electrodeposition of the activity on to 0.25 mm platinum wires. The K-Auger spectra were recorded in 180° permanent-field electron spectrographs with field strengths 50 and 100 G. A 50 G spectrograph which employs 10 kV pre-acceleration between source and aperture [2]) was used to record the L-Auger spectrum. The Pa^{233} source used in the pre-accelerator spectrograph, made by dipping a 0.25 mm platinum wire into a solution of very high specific activity, was essentially mass-free and showed little line broadening even for electrons whose initial energies were less than 1 keV.

3. K-Auger Spectrum

Table 1 summarizes our measurements on the K-Auger spectrum. The energies listed are the mean averages of several determinations, and the error limits are standard deviations from the mean values. Where only a single energy measurement was made the estimated error is given in brackets.

[†] Present address: Vanderbilt University, Nashville, Tennessee

[††] Work performed under the auspices of the U. S. Atomic Energy Commission.

[†††] Parts of this work are discussed more fully in ref. [3]).

In the initial state of a KLL-Auger process there is a "hole" in the K shell, and the final state has two holes in the same or different L-subshells. The energy of the emitted electron is written as $E_{KL_pL_q} = E_K - E_{L_p} - E_{L_q}$, where the quantities on the right hand side are the individual electron binding energies. Because during the Auger process the emitted electron feels the potential of an ionized atom, the electron binding energies are not expected to be equal to those obtained from critical absorption tables (e.g. Hill, Church and Mihelich [3]) but should be somewhat higher. Following a careful study of the Auger spectrum of mercury, Bergström and Hill [4]) analyzed the electron energies by introducing empirically an effective nuclear charge increment ΔZ with which to correct the tabulated [3]) binding energy of the last-written shell in the formula (L_q). ΔZ is defined as

$$\frac{E^*_{L_q} - (E_{L_q})_Z}{(E_{L_q})_{Z+1} - (E_{L_q})_Z}$$

where $E^*_{L_q}$ is the empirically adjusted value. They find for mercury that $\Delta Z = 0.6$ when $L_p = L_I$, L_{II} or L_{III} and $L_q = L_I$ or L_{II} and that $\Delta Z' = 0.8$ when $L_p = L_I$, L_{II} or L_{III} and $L_q = L_{III}$.

However, ΔZ and $\Delta Z'$ are not entirely independent parameters, because it is equivalent to write KL_pL_q or KL_qL_p, and it is arbitrary whether L_p or L_q is adjusted. If $L_p = L_{II}$ and $L_q = L_{III}$, for example,

$$\frac{\Delta Z'}{\Delta Z} = \frac{(E_{L_{II}})_{Z+1} - (E_{L_{II}})_Z}{(E_{L_{III}})_{Z+1} - (E_{L_{III}})_Z}.$$

For Hg, the ratio $\Delta Z'/\Delta Z$ is computed from the binding energy tables to be 1.3; this is about equal to 0.8/0.6, which is the quotient of the individual values reported by Bergström and Hill. We find for uranium (column 3) that an average value of ΔZ for the L_I and L_{II} shells is 0.56 and for the L_{III} shell is 0.82. The ratio 0.82/0.56 is 1.46, which is close to 1.5, the value calculated from the above equation for $Z = 92$.

A single ΔZ correction factor is sufficient to correlate the observed Auger energies of uranium to about 1 part in 10^3 if the correction is applied to the *average* of both L subshell binding energies. That is, the Auger electron energy may be defined as

$$E_{KL_pL_q} = E_K - E_{L_p} - E_{L_q} - \tfrac{1}{2}\Delta Z_{av}[(E_{L_p})_{Z+1} - (E_{L_p})_Z + (E_{L_q})_{Z+1} - (E_{L_q})_Z].$$

The measured K-Auger energies of uranium, plutonium [5]) and protactinium [6]) are given in table 1, together with values calculated with $\Delta Z_{av} = 0.6$.

The relative intensities were measured by a visual comparison method described in I. These intensities are equal, within our experimental error of

. TABLE 1

Uranium K-Auger spectrum

Auger transition	Expt. energy (keV) This work $Z = 92$	E(calc.) $\Delta Z_{av} = 0.6$ $Z = 92$	ΔZ Bergström[4])	Expt. energy (keV) Ewan *et al.* [5]) $Z = 94$	E(calc.) (keV) $\Delta Z_{av} = 0.6$ $Z = 94$	Expt. energy (keV) Hollander *et al.* [6]) $Z = 91$	E(calc.) (keV) $\Delta Z_{av} = 0.6$ $Z = 91$	Relative intensity		
								This work [a]) $Z = 92$	Ewan *et al.*[5]) $Z = 94$	Hollander *et al.* [6]) $Z = 91$
$KL_I L_I$	71.69 ± 0.10	71.68	0.58	75.18 ± 0.015	75.13	70.05	69.98	0.10	0.13	0.13
$KL_I L_{II}$	72.54 ± 0.10	72.50	0.54	76.05 ± 0.015	75.98	70.87	70.79	0.25	0.23	0.27
$KL_{II} L_{II}$		73.32		76.78 ± 0.04	76.84		71.60		0.01	
$KL_I L_{III}$	76.29 ± 0.16	76.34	0.84	80.24 ± 0.015	80.24	74.45	74.43	0.09	0.08	0.11
$KL_{II} L_{III}$	77.13 ± 0.13	77.16	0.80	81.06 ± 0.015	81.09	75.21	75.24	[0.14] [b])	[0.14] [b])	[0.14] [b])
$KL_{III} L_{III}$		81.00		85.30 ± 0.015	85.35		78.88		0.07	
$KL_I M_I$	87.96 ± [0.2]		1.7							
$KL_I M_{II}$	88.33 ± [0.2]		1.8							
$KL_I M_{IV,V}$	90.02 ± [0.2]									
$KL_{III} M_{I,II}$	92.95 ± [0.2]									
$KM_I M_{III}$?	105.6 ± [0.2]									

[a]) Error limits are estimated to be ±25 %.

[b]) Normalized to 0.14.

about ±25 %, to the more accurate values for $Z = 94$ measured by Ewan *et al.* [5]). The measured intensities are normalized to "percent beta decay" as discussed in I.

4. The L-Auger Spectrum

The uranium L-Auger spectrum, recorded with the 50-G pre-accelerator spectrograph, is shown in table 2. The spectrum was recorded both with and without the 10 kV acclerating voltage, and in most cases the deviation between the two energy determinations was less than 0.04 keV. If a line was seen in both measurements, the average value is given in table 2.

Assignments of lines to particular L-Auger transitions were made solely on the basis of energy agreement with values calculated from electron binding energies. An effective charge increment (ΔZ) of unity was assumed for the binding energy of the last written subshell in the formula LXY; the validity of this assumption has been discussed by Burhop [7]) and it has been used with good results by Sujkowski and Slätis [8]) for calculation of the bismuth L-Auger transition energies. Because of the large number of possible Auger transitions per energy interval, these assignments are, of course, not certain.

Visual estimates of the strengths of the lines (uncorrected for geometry or efficiency) are also given in table 2, and the intensities reported by Sujkowski and Slätis for bismuth and by Nall *et al.* [9]) for mercury are also given, as well as data on six L-Auger lines of uranium reported by Albouy and Valadares [10]). There is a definite correspondence between the intensities of the four sets of data listed in only a few cases were lines of reasonable intensity not observed by all three groups (Albouy and Valadares observed only the 6 most intense lines). It should be noted that lines which are close lying or unresolved in the spectrum of one element may not be near one another in the spectrum of a different element; this, of course, depends on how the binding energies vary with Z. For this reason, in table 2 some of the lines are displaced from a strict order of increasing energy in order to compare the uranium spectrum with those of mercury and bismuth.

Eight of the electron lines listed in table 2 have been assigned as Coster-Kronig transitions. In these transitions, which are designated by L_pL_qY, an initial L-subshell vacancy is transferred to another L-subshell with the emission of an electron from a higher (Y) shell. As discussed by Burhop, only those transitions are possible for which $(E_{L_p} - E_{L_q}) > E_Y$. In uranium, transitions of the type $L_IL_{II}M$ and $L_{II}L_{III}M$ (except M_V) are energetically forbidden. $L_IL_{III}M_I$ and $L_IL_{III}M_{II}$ are forbidden also, but $L_IL_{III}M_{III,IV,V}$ are allowed, and a transition which corresponds in energy to $L_IL_{III}M_V$ is seen in the Pa^{233} Auger spectrum.

TABLE 2

Uranium L-Auger spectrum

Auger transition	Relative intensity a)			Energy (keV) $Z = 92$		
	$Z = 80$ Nall *et al.* b)	$Z = 83$ Sujkowski and Slätis 8)	$Z = 92$ This work	Observed (Albouy and Valadares) 10)	Observed (This work)	Calculated
$L_1L_3M_5$			vw(b)		0.96	0.94
$L_2L_3N_1$			w		2.24	2.28
$L_2L_3N_3$			wm		2.64	2.70
$L_2L_3O_1$			w		3.48	3.44
$L_1L_3N_3$						3.52
$L_2L_3O_3$						3.52
$L_2L_3O_4$			w(b)		3.71	3.68
$L_1L_3N_4$						3.78
$L_3M_1M_2$	1(?)					6.25
$L_3M_2M_2$						6.62
$L_3M_1M_3$	1.5	vw	vw(b)		7.17	7.18
$L_3M_2M_3$	4.0	w	(?)		7.47	7.55
$L_3M_1M_4$		vw	(?)		7.71	7.76
$L_3M_1M_5$		vw				7.95
$L_3M_2M_5$	0.76	vw	(?)		8.22	8.32
$L_3M_3M_3$	6.45	w	w(b)		8.42	8.43
$L_3M_2M_4$						8.13
$L_3M_3M_4$	5.6	m	w(b)	8.86	8.98	9.01
$L_3M_3M_5$	5.7	m	w(b)	9.08	9.12	9.20
$L_3M_4M_4$	2.1	vw				9.59
$L_3M_4M_5$	11.0	vs	m	9.66	9.72	9.78
$L_3M_5M_5$	(8.6)	s	wm	9.85	9.93	9.95
$L_2M_1M_2$			(?)		10.02	10.03
$L_2M_2M_2$	(0.5)					10.40
$L_1M_1M_1$			vw(b)		10.47	10.47
$L_3M_2N_1$						10.48
$L_3M_2N_2$	0.33					10.66
$L_3M_1N_5$		vw	vw(b)		10.88	10.83
$L_1M_1M_2$						10.85
$L_3M_2N_3$	(0.66)					10.90
$L_2M_1M_3$		vw				10.96
$L_3M_2N_{4,5}$	(1.6)					11.16 c)
$L_2M_2M_3$	5.0	w	(masked by 28-L_{III})			11.33
$L_3M_1O_4$			vw		11.54	11.51
$L_3M_3N_2$	0.59					11.54
$L_2M_1M_4$						11.54
$L_3M_2N_{6,7}$	(1.7)	w				11.57
$L_3M_3N_3$						11.78
$L_1M_1M_3$	(0.3)					11.78
$L_2M_2M_4$	1.7	w				11.91
$L_2M_3M_3$						12.21
$L_3M_{4,5}N_{1,2}$	(0.4)					11.94 c)
$L_3M_3N_{4,5}$	(1.4)					12.04
$L_2M_2M_5$	(2.4)	w	(masked by 17-M_{II})			12.10
$L_1M_1M_4$	(0.4)		vvw		12.39	12.36
$L_3M_4N_3$	(1.5)					12.36
$L_3M_3N_6$						12.45
$L_1M_1M_5$	(0.4)					12.55
$L_3M_3O_2$			vvw		12.59	12.60

TABLE 2
(continued)

Auger transition	Relative intensity a)			Energy (keV) $Z = 92$		
	$Z = 80$ Nall *et al.* b)	$Z = 83$ Sujkowski and Slätis 8)	$Z = 92$ This work	Observed (Albouy and Valadares) 10)	Observed (This work)	Calculated
$L_1M_2M_4$	(0.2)	vw				12.73
$L_2M_3M_4$	(2.2)	m	wm(b)	12.64	12.80	12.79
$L_3M_5N_4$	(4.3)					12.70
$L_1M_2M_5$	(0.2)	vw	(masked by 17-M_{III})			12.92
$L_2M_3M_5$	(1.0)					12.98
$L_3M_4N_{6,7}$	0.26	vw				13.03
$L_3M_4O_3$			vw		13.16	13.18
$L_3M_5N_{6,7}$	1.3	m				13.20
$L_3M_4O_4$			vw		13.34	13.34
$L_2M_4M_4$	(4.4)	m				13.37
$L_2M_4M_5$	7.2	vs	wm	13.43	13.56	13.56
$L_1M_3M_{4,5}$	(0.5)					13.61 c)
$L_2M_5M_5$	(1.5)	vw				13.73
$L_1M_4M_4$	0.62					14.19
$L_2M_1N_3$			w		14.32	14.31
$L_1M_4M_5$	0.81	w				14.38
$L_2M_2N_2$	(0.3)					14.44
$L_1M_5M_5$	(0.2)					14.55
$L_2M_1N_5$		w	vvw		14.67	14.61
$L_2M_2N_3$	0.78					14.68
$L_2M_1N_{6,7}$	1.0	w	(?)		14.98	14.98
$L_2M_2N_5$						14.98
$L_2M_3N_1$						15.14
$L_3N_1N_{6,7}$		w	vw		15.34	15.31
$L_1M_1N_4$		vw				15.39
$L_2M_3N_2$	0.67	vw				15.32
$L_2M_3N_3$						15.56
$L_3N_4N_5$	(0.4)		vvvw		15.60	15.60
$L_2M_4N_1$	1.1					15.72
$L_2M_3N_4$		vw	(masked by 17-N_1)			15.82
$L_2M_5N_1$	(0.5)	w				15.89
$L_2N_2N_5$						15.11
$L_3N_3N_3$	(0.2)					15.04
$L_3N_{4,5}N_{6,7}$	(0.2)					15.97 c)
$L_2M_{4,5}N_3$	0.95					16.14 c)
$L_3N_6N_6$	0.14		vvw		16.35	16.36
$L_1M_2O_4$			(??)		16.48	16.48
$L_2M_5N_4$	(3.4)	w				16.57
$L_2M_4N_{6,7}$	(1.2)	w				16.81
$L_3N_5N_{6,7}$						16.01
$L_1M_3N_{6,7}$		vw				17.05
$L_2N_4N_{4,5}$	0.27	w	(masked by 40-L_{II})			19.34
$L_2N_5N_5$						19.42
$L_2N_{4,5}N_{6,7}$	0.1					19.75 10)

a) Symbols are: w = weak, m = medium, s = strong, v = very, (b) = broad, ? = questionable.

b) ref. 9). Parentheses around intensity values indicate uncertainty due to incomplete resolution of the lines.

c) Of the choices given by Nall *et al.*, only that of lowest energy is listed here.

References

1) Albridge, Hollander, Gallagher, and Hamilton, Nuclear Physics **27** (1961) 529
2) R. G. Albridge, UCRL-8642, thesis (1960)
3) Hill, Church and Mihelich, Rev. Sci. Instr. **23** (1952) 523
4) I. Bergström and R. D. Hill, Ark. Fys. **8** (1954) 21
5) Ewan, Geiger, Graham and MacKenzie, Can. J. Phys. **37** (1959) 174
6) Hollander, Stephens, Asaro and Perlman, to be published
7) E. H. S. Burhop, The auger effect and other radiationless transitions (University Press, Cambridge, 1952)
8) Z. Sujkowski and H. Slätis, Ark. Fys. **14** (1958) 101
9) Nall, Baird and Haynes, Phys. Rev. **118** (1960) 1278
10) G. Albouy and M. Valadares, Compt. Rend. **250** (1960) 2877

I.D.4:
2.I

Nuclear Physics **27** (1961) 561—580; © *North-Holland Publishing Co., Amsterdam*

Not to be reproduced by photoprint or microfilm without written permission from the publisher

LE MOUVEMENT COLLECTIF DANS LA RÉSONANCE GÉANTE PHOTONUCLÉAIRE

(I) Énergie de Résonance pour les noyaux sphériques et dédoublement pour les noyaux déformés

MICHEL FABRE DE LA RIPELLE

Laboratoire de Physique Nucléaire, Orsay, France [†]

Reçu le 27 fevrier 1961

Abstract: In the framework of a quantal treatment of the collective model analogous to the Fujita model, the resonance energy of the collective motion and the splitting for deformed nuclei are obtained. It is pointed out that the resonance energy depends on the nuclear density but very weakly on the potential shape, the mainly significant parameters being the r.m.s. radius and the Fourier transforms of the n-p potentials for very small momentum transfers. For the comparison with experiment the Gammel-Thaler exchange potential with hard core is used with a Fermi distribution of the nuclear states and the nuclear density parameters of Hofstadter.

1. Introduction

L'étude des réactions photonucléaires dans un domaine d'énergie situé au dessus de 10 MeV a montré l'existence d'une résonance géante; l'énergie du maximum de cette résonance diminuant continuement de 22 MeV à 14 MeV lorsque l'on passe des noyaux légers aux noyaux lourds. La première explication de ce phénomène a été donné par Goldhaber et Teller [1a]) à l'aide d'un modèle faisant appel à des propriétés collectives de vibration de l'ensemble des protons par rapport à l'ensemble des neutrons, chaque ensemble étant considéré comme une sphère rigide.

La justification de ce modèle réside dans les faits suivants:

1°) La longueur d'onde des photons est plus grande que les dimensions nucléaires, l'ensemble des protons est donc sollicité, tantôt d'un côté, tantot de l'autre, le mouvement vibratoire collectif autour du centre de masse étant réalisé par l'inertie des neutrons et la force de couplage neutron-proton.

2°) Le mouvement collectif a une amplitude très petite devant les dimensions nucléaires, on peut alors utiliser une approximation de petits mouvements autour de la position d'équilibre (centre de masse du noyau).

[†] Un rapport préliminaire de ce travail a été présenté dans les références [1]).

L'approximation des petits mouvements conduit à un potentiel collectif du type oscillateur $\frac{1}{2}M\omega^2x^2$, où x désigne la variable collective, distance entre les centres de masse des protons et des neutrons, $M = (NZ/A)m$ la masse réduite dans le mouvement collectif.

L'excitation de la résonance géante consiste alors en une transition dipolaire qui conduit le mouvement collectif de son état fondamental à son premier état excité 1^-. L'énergie E_m du maximum de la résonance étant donnée par $E_\mathrm{m} = h\omega$, on obtient l'amplitude maximum du mouvement collectif en écrivant que l'énergie totale E est égale à l'énergie potentielle

$$\tfrac{1}{2}M\omega^2{x_0}^2 = E.$$

Dans l'état fondamental $E = \frac{3}{2}h\omega$ et

$$x_0 = 11.1 \left[\frac{NZ}{A}\, E_\mathrm{m}\,(\mathrm{MeV})\right]^{-\frac{1}{2}}.$$

Dans la fig. 1 on donne la courbe x_0/R en fonction de A, utilisant pour R les valeurs données par Hofstadter 2) et pour E_m les valeurs expérimentales.

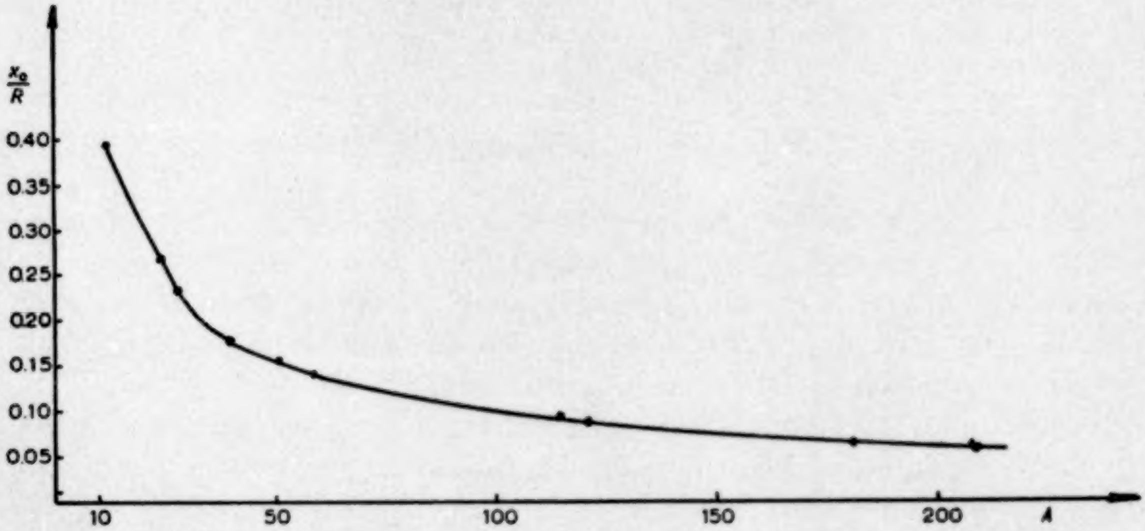

Fig. 1. Rapport en fonction de A, de l'amplitude maximum du mouvement collectif au rayon nucléaire, dans l'état fondamental.

Pour obtenir une description quantique, on désigne par x_i et y_j les coordonnées des protons et des neutrons, par $T(x_i)$ et $T(y_j)$ leur énergie cinétique, par V_pp, V_nn et V_np les potentiels d'interaction proton-proton, neutron-neutron et neutron-proton. L'hamiltonien nucléaire s'écrit alors

$$H_\mathrm{T} = \sum_1^Z T(x_i) + \sum_1^N T(y_j) + \sum_{i,\,k>i} V_\mathrm{pp}(\mathbf{x}_i - \mathbf{x}_k) + \sum_{j,\,k>j} V_\mathrm{nn}(\mathbf{y}_j - \mathbf{y}_k) + \sum_{i,\,j} V_\mathrm{np}(\mathbf{x}_i - \mathbf{y}_j).$$

Pour faire apparaître le mouvement collectif, on effectue un changement de variables rapportant les coordonnées des protons et des neutrons à leurs centres de masse respectifs $\mathbf{X}_\mathrm{P}$ et $\mathbf{X}_\mathrm{N}$:

$$\text{(I)}\qquad \begin{aligned} \mathbf{x}_i &= \mathbf{X}_\mathrm{P}+\xi_i = \mathbf{X}_\mathrm{G}+\frac{N}{A}\mathbf{x}+\xi_i, & \mathbf{X}_\mathrm{P} &= \frac{1}{Z}\sum_1^Z \mathbf{x}_i, \\ \mathbf{y}_j &= \mathbf{X}_\mathrm{N}+\eta_j = \mathbf{X}_\mathrm{G}-\frac{Z}{A}\mathbf{x}+\eta_j, & \mathbf{X}_\mathrm{N} &= \frac{1}{N}\sum_1^N \mathbf{y}_j. \end{aligned}$$

Dans ces formules, $\mathbf{X}_\mathrm{G}$ est le centre de masse du noyau, et $\mathbf{x} = \mathbf{X}_\mathrm{P}-\mathbf{X}_\mathrm{N}$, les coordonnées intrinsèques ξ_i et η_j des protons et neutrons vérifiant le relation

$$\sum_1^Z \xi_i = \sum_1^N \eta_j = 0.$$

L'hamiltonien nucléaire prend alors la forme

$$\begin{aligned} H_\mathrm{T} = T(X_\mathrm{G})+\sum T(\xi_i)+\sum T(\eta_j)+T(x)+\sum_{i,\,k>i} V_\mathrm{pp}(\xi_i-\xi_k) \\ +\sum_{j,\,k>j} V_\mathrm{nn}(\eta_j-\eta_k)+\sum_{i,\,j} V_\mathrm{np}(\mathbf{x}+\xi_i-\eta_j). \end{aligned} \tag{1}$$

Afin de séparer le mouvement collectif ne dépendant que de $\mathbf{x}$ des mouvements intrinsèques ne dépendant que des (ξ, η), on décompose l'hamiltonien H_T en trois parties:

$$\begin{aligned} H_0 &= \sum T(\xi_i)+\sum T(\eta_j)+\sum V_\mathrm{pp}(\xi_i-\xi_k)+\sum V_\mathrm{nn}(\eta_j-\eta_k)+\sum \bar{V}_\mathrm{np}(\xi_i-\eta_j), \\ H_\mathrm{c} &= T(x)+W(\mathbf{x}), \\ H &= \sum_{i,\,j}[V_\mathrm{np}(\mathbf{x}+\xi_i-\eta_j)-\bar{V}_\mathrm{np}(\xi_i-\eta_j)]-W(\mathbf{x}), \end{aligned} \tag{2}$$

la partie H étant l'interaction résiduelle couplant les mouvements collectifs et intrinsèques.

On doit définir $\bar{V}_\mathrm{np}$ et $W(\mathbf{x})$ de manière à rendre l'interaction résiduelle la plus petite possible. Développant la fonction d'onde nucléaire Φ en fonctions propres de H_c et H_0 d'énergies propres ε_a et E_b on a

$$\Phi(\mathbf{x}, \xi, \eta) = \sum_{a,\,b} a_{a,\,b}\varphi_a(\mathbf{x})\psi_b(\xi, \eta) \qquad \text{où} \begin{cases} H_\mathrm{c}\varphi_a = \varepsilon_a\varphi_a, \\ H_0\psi_b = E_b\psi_b. \end{cases} \tag{3}$$

Pour un mélange se rapprochant le plus possible d'un état pur $\varphi_\alpha(\mathbf{x})\,\psi_\beta(\xi, \eta)$, on choisira $W(\mathbf{x})$ et $\bar{V}_\mathrm{np}(\xi_i-\eta_j)$ de manière à ce que

$$\langle\psi_\beta(\xi, \eta)|H|\psi_\beta(\xi, \eta)\rangle = 0, \qquad \langle\varphi_\alpha(\mathbf{x})|H|\varphi_\alpha(\mathbf{x})\rangle = 0. \tag{4}$$

On obtient alors

$$W(x) = \langle \psi_\beta(\xi, \eta)| \sum_{i,j} [V_{\mathrm{np}}(\mathbf{x}+\xi_i-\eta_j)-\bar{V}_{\mathrm{np}}(\xi_i-\eta_j)]|\psi_\beta(\xi, \eta)\rangle,$$

$$\bar{V}_{\mathrm{np}}(\xi_i-\eta_j) = \langle \varphi_\alpha(\mathbf{x})|V_{\mathrm{np}}(\mathbf{x}+\xi_i-\eta_j)|\varphi_\alpha(\mathbf{x})\rangle.$$

Il en résulte d'ailleurs que

$$\langle \varphi_\alpha(\mathbf{x})|W(\mathbf{x})|\varphi_\alpha(\mathbf{x})\rangle = 0. \tag{5}$$

Le potentiel collectif $W(\mathbf{x})$ et le potentiel intrinsèque moyen neutron-proton $\bar{V}_{\mathrm{np}}(\xi_i-\eta_j)$ dépendent des états collectifs et intrinsèques φ_α et ψ_β. Avec une telle définition (4) le développement (3) s'écrit

$$\Phi_{\alpha,\beta}(\mathbf{x}, \xi, \eta) = a_{\alpha\beta}\varphi_\alpha\psi_\beta + \sum_{a\neq\alpha,\ b\neq\beta} a_{ab}\varphi_a\psi_b, \tag{6}$$

la sommation ne portant que sur des états différant de φ_α et de ψ_β. Dans l'état fondamental, la fonction Φ_{00} est paire, the fonction fondamentale $\varphi_0(x)$ de l'oscillateur est paire, et il en est de même pour la fonction fondamentale intrinsèque $\psi_0(\xi, \eta)$. Le produit $\varphi_0\psi_0$ correspond à une énergie ε_0+E_0; dans les termes du mélange, le produit $\varphi_a\psi_b$ qui a l'énergie la plus proche de ε_0+E_0 correspond au produit du premier état excité 1^- du mouvement collectif avec un état 1^- du mouvement intrinsèque; comme les états 1^- intrinsèques se situent eux aussi dans un domaine d'énergie voisin de la résonance géante, le produit correspond à une énergie d'excitation de l'ordre de $2\hbar\omega$ au dessus de celle de l'état fondamental. L'état fondamental étant celui ayant l'énergie la plus basse, on est donc conduit à penser que les valeurs des a_{ab} sont petites et que l'on a une bonne représentation de l'état fondamental en ne gardant qu'un seul terme:

$$\Phi_{00} = \varphi_0(\mathbf{x})\psi_0(\xi, \eta). \tag{6}$$

Le même raisonnement ne serait plus valable pour un état excite 1^- de la résonance géante, l'énergie de l'état $\varphi_1(\mathbf{x})$ correspondant à l'excitation de la partie collective étant du même ordre de grandeur que celle des états 1^- de la partie intrinsèque. On doit donc s'attendre à une description des états 1^- de la résonance géante contenant des mélanges d'états collectifs et intrinsèques et conduisant ainsi à une structure en raies du spectre d'absorption, cette structure étant par ailleurs fortement atténuée par la largeur des raies qui les amène à se chevaucher et à se fondre en un ensemble moyen ayant en gros l'aspect d'une résonance unique, sauf, peut-être, pour les noyaux légers, et dans le cas des noyaux non déformés.

2. Potentiel Collectif

Si l'on néglige le terme constant qui a pour effet d'annuler la moyenne de $W(x)$ prise sur l'état $\varphi_\alpha(x)$ on peut écrire (négligeant dans la suite l'indice β)

$$W(\mathbf{x}) = \text{const.} + V_{\mathrm{NP}}(\mathbf{x}),$$
$$V_{\mathrm{NP}}(\mathbf{x}) = \langle \psi(\xi, \eta) | \sum_{ij} V_{\mathrm{np}}(\mathbf{x} + \xi_i - \eta_j) | \psi(\xi, \eta) \rangle.$$

Utilisant un développement en intégrale de Fourier du potentiel, on a

$$V_{\mathrm{NP}}(\mathbf{x}) = \int \mathrm{d}^3 k \mathrm{e}^{i\mathbf{k}\cdot\mathbf{x}} \sum_{ij} \langle \psi(\xi, \eta) | \mathrm{e}^{i\mathbf{k}\cdot(\xi_i - \eta_j)} v_{\mathrm{np}}(\mathbf{k}) | \psi(\xi, \eta) \rangle.$$

Lorsque le potentiel ne contient pas de termes d'échange et qu'on le pondère en $\frac{3}{4}$ pour le potentiel triplet et $\frac{1}{4}$ pour le potentiel singulet, on peut érire, si l'on admet que l'état intrinsèque est le produit d'un état $\psi_{\mathrm{P}}(\xi)$ des protons un état $\psi_{\mathrm{N}}(\eta)$ des neutrons,

$$\sum_{ij} \langle \psi(\xi, \eta) | \mathrm{e}^{i\mathbf{k}\cdot(\xi_i - \eta_j)} | \psi(\xi, \eta) \rangle = NZ F_{\mathrm{P}}(\mathbf{k}) F_{\mathrm{N}}(\mathbf{k}), \tag{8}$$

où $F_{\mathrm{P}}(\mathbf{k})$ et $F_{\mathrm{N}}(\mathbf{k})$ désignent les facteurs de forme intrinsèque pour les protons et les neutrons. Le potentiel collectif se réduit alors à

$$V_{\mathrm{NP}}(\mathbf{x}) = NZ \int \mathrm{e}^{i\mathbf{k}\cdot\mathbf{x}} v_{\mathrm{np}}(\mathbf{k}) F_{\mathrm{P}}(\mathbf{k}) F_{\mathrm{N}}(\mathbf{k}) \mathrm{d}^3\mathbf{k}. \tag{9}$$

La portée du potentiel étant petite devant les dimensions nucléaires, il en résulte que le domaine d'extension du facteur de forme est faible devant celui de $v_{\mathrm{np}}(\mathbf{k})$. Le produit $F_{\mathrm{P}} F_{\mathrm{N}}$ a donc une variation prépondérante devant $v_{\mathrm{np}}(\mathbf{k})$ dont il suffit de connaître la valeur pour $k = 0$ et, à titre de correction, la dérivée seconde par rapport à k, puisque dans le cas d'un potentiel central la dérivée première par rapport à k est nulle pour $k = 0$. Ceci indique physiquement que seuls les petits transferts de quantité de mouvement contribuent au mouvement collectif. On vérifie facilement le bien-fondé de l'approximation en effectuant un calcul exact avec un potentiel n-p du type gaussien $V_0\ \mathrm{e}^{-\alpha r^2}$ et un facteur de forme $\mathrm{e}^{-\frac{1}{6}a^2k^2}$ du même type, et en utilisant l'approximation $F_{\mathrm{N}} = F_{\mathrm{P}}$ justifiée par le fait que la densité de présence des protons et des neutrons se recouvre. On obtient alors

$$V_{\mathrm{NP}}(\mathbf{x}) = \frac{NZ\pi^{\frac{3}{2}} v_{\mathrm{np}}(0)}{\left(\dfrac{a^2}{3} + \dfrac{1}{4\alpha}\right)^{\frac{3}{2}}} \mathrm{e}^{-\frac{1}{4}x^2/\left(\frac{a^2}{3} + \frac{1}{4\alpha}\right)}. \tag{10}$$

Le terme $1/2\alpha = |v''_{\mathrm{np}}(0)/v_{\mathrm{np}}(0)|$, rapport de la dérivée seconde de $v_{\mathrm{np}}(k)$ à sa valeur pour $k = 0$, est pour les potentiels nucléaires usuels de l'ordre de 1; le rayon carré moyen a^2 est relié au rayon nucléaire par $a = 0.775\ R$; l' approximation consistant à se limiter à $v_{\mathrm{np}}(0)$ est donc vérifiée. Comme pour l'amplitude maximum x_0, on a

$$\tfrac{3}{4}\left(\frac{x_0}{a}\right)^2 = 1.25 \left(\frac{x_0}{R}\right)^2 \ll 1,$$

l'approximation des petits mouvements, dans laquelle on se limite à un potentiel d'oscillateur

$$V_{\mathrm{NP}}(\mathbf{x}) = \frac{NZ\pi^{\frac{3}{2}}v_{\mathrm{np}}(0)}{\left(\dfrac{a^2}{3}+\dfrac{1}{4\alpha}\right)^{\frac{3}{2}}}\left[1-\tfrac{3}{4}\frac{x^2}{a^2+\dfrac{3}{4\alpha}}\right],$$

est également justifiée.

Négligeant le calcul du terme constant et n'utilisant que le terme en x^2 on peut mettre $V_{\mathrm{NP}}(x)$ sous la forme

$$\begin{aligned} V_{\mathrm{NP}}(x) &= \text{const.} -\tfrac{1}{2}NZ\int(\mathbf{k}\cdot\mathbf{x})^2 v_{\mathrm{np}}(\mathbf{k})F_{\mathrm{N}}(\mathbf{k})F_{\mathrm{P}}(\mathbf{k})\mathrm{d}^3k \\ &= \text{const.} -\tfrac{1}{2}NZ\int \mathrm{d}^3k v_{\mathrm{np}}(\mathbf{k})\left[\int\sum_i \mathrm{e}^{i\mathbf{k}\cdot\mathbf{x}_i}\mathbf{x}\cdot\boldsymbol{\nabla}_{\xi_i}|\psi_{\mathrm{P}}(\xi)|^2\mathrm{d}^3\xi\right] \qquad (11) \\ &\quad\times\left[\int\sum_j \mathrm{e}^{-i\mathbf{k}\cdot\boldsymbol{\eta}_i}\mathbf{x}\cdot\boldsymbol{\nabla}_{\eta_j}|\psi_{\mathrm{N}}(\eta)|^2\mathrm{d}^3\eta\right], \end{aligned}$$

avec la condition supplémentaire $\sum\boldsymbol{\nabla}_{\xi_i}\psi_{\mathrm{P}} = \sum\boldsymbol{\nabla}_{\eta_j}\psi_{\mathrm{N}} = 0$.
On voit ainsi que le coefficient du terme en x^2 dépend de la dérivée de la densité de présence des nucléons, c'est-à-dire des conditions à la surface nucléaire.

Nous étudierons maintenant un modèle plus réaliste dans lequel la densité des nucléons est constante à l'intérieur d'une sphère de rayon $R = r_0A^{\frac{1}{3}}$ pour chaque ensemble intrinsèque de neutrons et de protons, le potentiel n-p étant du type de Yukawa $[(V/\mu)\,\mathrm{e}^{-\mu r}/r]$. Il en résulte, avec l'identité des facteurs de forme $F_{\mathrm{P}} = F_{\mathrm{N}} = F_0$,

$$F_0(kR) = \frac{3}{kR}j_1(kR), \qquad v_{\mathrm{np}}(\mathbf{k}) = \frac{V}{2\pi^2\mu}\,\frac{1}{k^2+\mu^2},$$

$$\begin{aligned} V_{\mathrm{NP}}(\mathbf{x}) &= \frac{9}{\pi}\,\frac{V}{\mu}\,\frac{NZ}{R^2}\int_{-\infty}^{+\infty} j_1{}^2(kR)j_0(kx)\frac{\mathrm{d}k}{k^2+\mu^2} \\ &= \tfrac{9}{2}NZ\frac{V}{\beta\alpha^7}\left\{(1-\alpha^2)(1-\mathrm{e}^{-\alpha\beta})+\tfrac{1}{2}\alpha^2\beta^2\left(1-\alpha^2+\frac{\alpha^2\beta^2}{12}\right)\right. \qquad (12) \\ &\qquad\left.+\tfrac{2}{3}\beta\alpha^4+(1+\alpha)^2\mathrm{e}^{-2\alpha}\,\mathrm{Sh}\,\alpha\beta\right\}, \end{aligned}$$

$$\alpha = \mu R, \qquad \beta = x/R.$$

Pour $\alpha \gg 1$ et $\alpha\beta \ll 1$ on obtient l'approximation des petits mouvements. Développant alors $V_{\mathrm{NP}}(x)$ pour β petit et négligeant le terme contenant $\mathrm{e}^{-2\alpha}$, on a

$$V_{\mathrm{NP}}(\mathbf{x}) = \text{const.} -\tfrac{3}{4}NZ\frac{V}{\mu^2}\times\frac{1}{R^4}\left\{\left[1-\frac{1}{(\mu R)^2}\right]x^2+\tfrac{1}{4}\mu x^3+\ldots\right\}. \qquad (13)$$

On peut considérer le terme en x^3 comme une perturbation et calculer la correction d'énergie au premier ordre. Nous le laisserons de côté pour l'instant, les forces d'échange introduisant aussi un terme en x^3 qui compense en grande partie celui-là.

On obtient la pulsation ω et l'énergie correspondante $E_{\mathrm{m}} = \hbar\omega$ en égalant le coefficient de x^2 à $\frac{1}{2}M\omega^2$. Pour un noyau sphérique et un potentiel gaussien $V_0 \,\mathrm{e}^{-\alpha r^2}$ on a

$$E_{\mathrm{m}}{}^2 = \tfrac{1}{2} 3^{\frac{1}{2}} \pi^{\frac{3}{2}} \frac{\hbar^2}{m} v_{\mathrm{np}}(0) \frac{A}{\left(a^2 + \dfrac{3}{4\alpha}\right)^{\frac{5}{2}}},$$

$$\frac{1}{2\alpha} = \left|\frac{v''_{\mathrm{np}}(0)}{v_{\mathrm{np}}(0)}\right|, \qquad v_{\mathrm{np}}(0) = \frac{V_0}{8\pi^{\frac{3}{2}}} \frac{1}{\alpha^{\frac{3}{2}}}.$$

Négligeant $3/4\alpha$ devant a^2, on voit que E_{m} varie en gros comme $A^{-\frac{1}{3}}$. On donne dans le tableau 1 les valeurs de E_{m} obtenues en prenant $1/2\alpha = 1$ et en ajustant $v_{\mathrm{np}}(0)$ de manière à ce que $E_{\mathrm{m}}(\mathrm{Pb}^{208}) = 13.8$ MeV. On utilise pour a les valeurs données par Hofstadter [2]). La valeur de r_0 est celle d'un modèle uniforme de rayon $R = r_0 A^{\frac{1}{3}}$ ayant a^2 pour rayon carré moyen. On obtient dans ces conditions

$$E_{\mathrm{m}} = \frac{70A^{\frac{1}{2}}}{(a^2 + 1.5)^{5/4}},$$

où E_{m} est exprimé en MeV et a en fm.

TABLEAU 1

Valeurs experimentales et théoriques de E_{m}

	a (fm)	r_0 (fm)	E_{m} (théor) (MeV)	E_{m} (exp) (MeV)
$_{6}\mathrm{C}^{12}$	2.37	1.33	20.8	22.0 [b])
$_{12}\mathrm{Mg}^{24}$	2.98	1.33	18.4	18.8 [a])
$_{14}\mathrm{Si}^{28}$	3.04	1.29	19.0	20.9 [a])
$_{16}\mathrm{S}^{32}$	3.19	1.30	18.3	20.1 [a])
$_{20}\mathrm{Ca}^{40}$	3.52	1.32	16.5	19.3 [a])
$_{23}\mathrm{V}^{51}$	3.59	1.25	17.8	18.7 [b])
$_{27}\mathrm{Co}^{59}$	3.83	1.27	16.5	16.9 [a])
$_{49}\mathrm{In}^{115}$	4.50	1.19	15.9	15.0 [a])
$_{51}\mathrm{Sb}^{122}$	4.63	1.20	15.4	14.8 [a])
$_{73}\mathrm{Ta}^{181}$	5.50	1.25	12.3	13.9 [a])
$_{79}\mathrm{Au}^{197}$	5.32	1.18	14.1	14.2 [a])
$_{82}\mathrm{Pb}^{208}$	5.42	1.18	13.8	13.7 [a])
$_{83}\mathrm{Bi}^{209}$	5.52	1.20	13.3	13.2 [b])

[a]) Montalbetti *et al.*, Phys. Rev. **91** (1953) 659

[b]) Nathan et Halpern, Phys. Rev. **93** (1954) 437

Les valeurs expérimentales de a sont exactes à 2 % près (sauf peut être pour le Ta^{181}), ce qui correspond à une erreur possible sur la valeur théorique de E_{m} de l'ordre de 5 %. Les valeurs expérimentales de E_{m} peuvent d'autre part présenter des erreurs de l'ordre du MeV.

Pour un potentiel de Yukawa et un modèle uniforme de rayon $R = r_0 A^{\frac{1}{3}}$, négligeant la correction due au terme x^3, on a

$$E_{\mathrm{m}}{}^2 = \frac{3\hbar^2}{2mr_0{}^4} A^{-\frac{1}{3}} \frac{V}{\mu^2} \left[1 - \frac{1}{(\mu R)^2}\right]. \tag{14}$$

L'énergie E_{m} varie alors en gros comme $A^{-\frac{1}{6}}$. La différence de variation entre $A^{-\frac{1}{3}}$ et $A^{-\frac{1}{6}}$ n'est pas très sensible pour les noyaux lourds. Le terme en $1/(\mu R)^2$ étant négligeable devant 1 pour les noyaux lourds, le seul paramètre ajustable est V/μ^2, la valeur de r_0 étant donnée. La valeur $V/\mu^2 = 40$ MeV · fm^2 rend bien compte des valeurs expérimentales pour une valeur de $r_0 = 1.2$ fm. Pour les noyaux lourds, elle correspond à

$$E_{\mathrm{m}} = \frac{50}{r_0{}^2} \left\{1 - \tfrac{1}{2} \frac{1}{(\mu r_0)^2 A^{\frac{2}{3}}}\right\} A^{-\frac{1}{6}},$$

où E_{m} est exprimé en MeV et r_0 en fm.

3. Forces d'Échange

Le potentiel utilisé jusqu'à présent était un potentiel central sans échange, mais qui pouvait dépendre des spins; c'est-à-dire que l'on pouvait utiliser un potentiel différent pour les états singulet et triplet, les résultats étant pris, en moyenne, avec $\frac{3}{4}$ d'états triplet et $\frac{1}{4}$ de singulet.

Introduire un potentiel d'échange conduit à séparer les états pairs et impairs, de diffusion nucléon-nucléon, les potentiels triplet et singulet pairs étant différents des potentiels triplet et singulet impairs. On utilise alors un potentiel neutron-proton de la forme

$$V(r_{ij}) = \tfrac{1}{2} V_+(r_{ij})(1 + P_{\mathrm{M}}(i, j)) + \tfrac{1}{2} V_-(r_{ij})(1 - P_{\mathrm{M}}(i, j)), \tag{15}$$

où $r_{ij} = |\mathbf{x}_i - \mathbf{y}_j|$. Les potentiels centraux $V_\pm(r_{ij})$ peuvent dépendre des spins, et l'opérateur de Majorana $P_{\mathrm{M}}(i, j)$, qui échange les positions $\mathbf{x}_i$ et $\mathbf{y}_j$ du proton i et du neutron j, agit sur les coordonnées collectives et intrinsèques de la manière suivante:

$$\begin{aligned}
&P_{\mathrm{M}}(i, j)\mathbf{x} = \mathbf{x} - \frac{A}{NZ}(\mathbf{x}_i - \mathbf{y}_j), && P_{\mathrm{M}}(i, j)\boldsymbol{\xi}_i = \boldsymbol{\eta}_j - \mathbf{x} + \frac{1}{Z}(\mathbf{x}_i - \mathbf{y}_j),\\
&P_{\mathrm{M}}(i, j)\boldsymbol{\xi}_k = \boldsymbol{\xi}_k + \frac{1}{Z}(\mathbf{x}_i - \mathbf{y}_j), && P_{\mathrm{M}}(i, j)\boldsymbol{\eta}_j = \boldsymbol{\xi}_i + \mathbf{x} - \frac{1}{N}(\mathbf{x}_i - \mathbf{y}_j),\\
&P_{\mathrm{M}}(i, j)\boldsymbol{\eta}_k = \boldsymbol{\eta}_k - \frac{1}{N}(\mathbf{x}_i - \mathbf{y}_j).
\end{aligned} \tag{16}$$

On voit ainsi que si la fonction d'onde nucléaire est séparée en parties collective et intrinsèque, l'opérateur $P_{\mathrm{M}}(i, j)$ a pour effet de mélanger ces deux parties.

Les fonctions d'onde collectives étant des fonctions d'oscillateur, on a pour l'état fondamental et le premier état excité

$$\varphi_0(x) = \left[\frac{4\nu^{\frac{3}{2}}}{\sqrt{\pi}}\right]^{\frac{1}{2}} \mathrm{e}^{-\frac{1}{2}\nu x^2} Y_0^{\,0}(\omega_x), \qquad \frac{\hbar\nu}{M} = \omega,$$

$$\varphi_1(x) = \left[\frac{8\nu^{\frac{3}{2}}}{3\sqrt{\pi}}\right]^{\frac{1}{2}} x\mathrm{e}^{-\frac{1}{2}\nu x^2} Y_1^{\,m}(\omega_x),$$

$$P_{\mathrm{M}}(i,j)\varphi_0(x) = \mathrm{e}^{\frac{\nu A}{NZ}\mathbf{x}\cdot(\mathbf{x}_i-\mathbf{y}_j)}\, \mathrm{e}^{-\frac{1}{2}\nu\left(\frac{A}{NZ}\right)^2(\mathbf{x}_i-\mathbf{y}_j)^2}\, \varphi_0(x),$$

$$\begin{aligned} P_{\mathrm{M}}(i,j)xY_1^{\,m}(\omega_x) &= xY_1^{\,m}(\omega_x) - \frac{A}{NZ}\,[x_i Y_1^{\,m}(\omega_{x_i}) - y_j Y_1^{\,m}(\omega_{y_j})] \\ &= \left(1 - \frac{A}{NZ}\right) xY_1^{\,m}(\omega_x) - \frac{A}{NZ}\,[\xi_i Y_1^{\,m}(\omega_{\xi_i}) - \eta_j Y_1^{\,m}(\omega_{\eta_j})]. \end{aligned}$$

Le potentiel collectif se décompose en deux termes, un terme provenant de la partie directe sans échange

$$V_{\mathrm{NP}}^{(\mathrm{d})}(\mathbf{x}) = \tfrac{1}{2}\langle\psi(\xi,\eta)|\sum_{ij}[V_+(r_{ij})+V_-(r_{ij})]|\psi(\xi,\eta)\rangle,$$

et un terme provenant de la partie avec échange

$$V_{\mathrm{NP}}^{(\mathrm{e})}(\mathbf{x}) = \tfrac{1}{2}\frac{1}{\varphi(\mathbf{x})}\,\langle\psi(\xi,\eta)|\sum_{ij}[V_+(r_{ij})-V_-(r_{ij})]P_{\mathrm{M}}(i,j)\varphi(\mathbf{x})|\psi(\xi,\eta)\rangle,$$

où la moyenne ne porte que sur les (ξ, η).

4. Modèle de Fermi

Comme fonctions d'onde intrinsèque, nous utiliserons pour des noyaux lourds un modèle à particules indépendantes avec une distribution de Fermi,

$$\psi_{\mathrm{p}}(\xi_i) = \psi_0(\xi_i)\mathrm{e}^{i\mathbf{k}_{\mathrm{p}}\cdot\xi_i}, \qquad \psi_{\mathrm{n}}(\eta_j) = \psi_0(\eta_j)\mathrm{e}^{i\mathbf{k}_{\mathrm{n}}\cdot\eta_j}, \qquad \langle\psi_0|\psi_0\rangle = 1, \quad (17)$$

où les états diffèrent par le vecteur $\mathbf{k}_{\mathrm{p}}$ pour les protons et $\mathbf{k}_{\mathrm{n}}$ pour les neutrons, avec

$$0 \leqq |\mathbf{k}_{\mathrm{p}}| \leqq K_{\mathrm{P}}, \qquad 0 \leqq |\mathbf{k}_{\mathrm{n}}| \leqq K_{\mathrm{N}}.$$

La sommation sur les états se réduit à une intégrale

$$\sum_{\mathrm{p}} f(\mathbf{k}_{\mathrm{p}}) = \frac{2V}{(2\pi)^3}\int f(\mathbf{k}_{\mathrm{p}})\mathrm{d}^3k_{\mathrm{p}}.$$

L'intégration est étendue à l'intérieur d'une sphère, de rayon K_{P} pour les protons et K_N pour les neutrons, de sorte que le nombre d'états est

$$\sum_{p} \langle \psi_p | \psi_p \rangle = Z \qquad \text{pour les protons,}$$

$$\sum_{n} \langle \psi_n | \psi_n \rangle = N \qquad \text{pour les neutrons,}$$

ce qui impose

$$K_P = \left(\frac{Z}{A}\right)^{\frac{1}{3}} \left(\frac{9\pi}{4}\right)^{\frac{1}{3}} \frac{1}{r_0}, \qquad K_N = \left(\frac{N}{A}\right)^{\frac{1}{3}} \left(\frac{9\pi}{4}\right)^{\frac{1}{3}} \frac{1}{r_0} \tag{18}$$

pour un volume nucléaire $V = \frac{4}{3}\pi r_0^3 A$.

Pour un modèle intrinsèque de Fermi à particules indépendantes, les conditions supplémentaires

$$\sum_i \nabla_{\xi_i} \psi_P(\xi) = \sum_j \nabla_{\eta_j} \psi_N(\eta) = 0,$$

qui expriment que la résultante des quantités de mouvements dans les mouvements relatifs aux centres de masse respectifs des protons et des neutrons est nulle impliquent que

$$\sum \mathbf{k}_p = \sum \mathbf{k}_n = 0.$$

Utilisant

$$P_M(i,j)\left[\sum_1^Z \xi_k{}^2 + \sum_1^N \eta_k{}^2\right] = \sum_1^Z \xi_k{}^2 + \sum_1^N \eta_k{}^2 + 2\mathbf{x}\cdot(\mathbf{x}_i - \mathbf{y}_j) - \frac{A}{NZ}(\mathbf{x}_i - \mathbf{y}_j)^2,$$

on voit que, si l'on prend pour $\psi_0(\xi)$ une fonction gaussienne proportionnelle à $\exp(-\frac{3}{4}\xi^2/a^2)$,

$$\begin{aligned} P_M(i,j)\varphi_0(\mathbf{x})\psi_p(\xi)\psi_n(\eta) &= \varphi_0(\mathbf{x})\psi_p(\xi)\psi_n(\eta)\mathrm{e}^{i(\mathbf{k}_n - \mathbf{k}_p)\cdot(\mathbf{x}_i - \mathbf{y}_j)} \\ &\quad \times \mathrm{e}^{\left(\frac{\nu A}{NZ} - \frac{3}{2a^2}\right)\mathbf{x}\cdot(\mathbf{x}_i - \mathbf{y}_j)} \mathrm{e}^{-\frac{A}{2NZ}\left(\frac{\nu A}{NZ} - \frac{3}{2a^2}\right)(\mathbf{x}_i - \mathbf{y}_j)^2}. \end{aligned} \tag{19}$$

La quantité a^2 désignant le rayon carré moyen, $3/2a^2$ est très petit devant $\nu A/NZ$ qui, pour les valeurs expérimentales des énergies de résonance, est de l'ordre de 0.4. De même la variation de la dernière exponentielle est négligeable dans un domaine de l'ordre de la portée des forces nucléaires. On justifie ains l'approximation

$$P_M(i,j)\varphi_0(\mathbf{x})\psi_p(\xi)\psi_n(\eta) = \varphi_0(\mathbf{x})\psi_p(\xi)\psi_n(\eta)\mathrm{e}^{i(\mathbf{k}_n - \mathbf{k}_p)\cdot(\mathbf{x}_i - \mathbf{y}_j)}\,\mathrm{e}^{\frac{\nu A}{NZ}\mathbf{x}\cdot(\mathbf{x}_i - \mathbf{y}_j)}. \tag{20}$$

La partie du potentiel collectif dû aux termes d'échange est

$$V_{NP}^{(e)}(x) = \tfrac{1}{2}\langle \psi_0(\xi)\psi_0(\eta) | [V_+(r) - V_-(r)] \mathrm{e}^{\frac{\nu A}{NZ}\mathbf{x}\cdot\mathbf{r}} \sum_{p,n} \mathrm{e}^{i(\mathbf{k}_n - \mathbf{k}_p)\cdot\mathbf{r}} | \psi_0(\xi)\psi_0(\eta)\rangle,$$

où $\mathbf{r} = \mathbf{x} + \xi - \eta$. La somme porte sur les états occupés des neutrons et des protons; on a

$$\sum_{\mathrm{p,n}} \mathrm{e}^{i(\mathbf{k}_\mathrm{n}-\mathbf{k}_\mathrm{p})\cdot \mathbf{r}} = NZF_0(K_\mathrm{N}r)F_0(K_\mathrm{P}r).$$

Tout se passe donc comme si l'introduction d'un terme d'échange avait pour effet de transformer le potentiel d'interaction n-p en un potentiel effectif dépendant de **x**:

$$[V_+(r)-V_-(r)]\, F_0(K_\mathrm{N}r)F_0(K_\mathrm{P}r)\mathrm{e}^{\frac{\nu A}{NZ}\mathbf{x}\cdot\mathbf{r}}.$$

Désignant par $v_\mathrm{M}(\mathbf{k}, \mathbf{x})$ la transformée de Fourier, on a

$$V^{(\mathrm{e})}_{\mathrm{NP}}(x) = \tfrac{1}{2}NZ \int v_\mathrm{M}(\mathbf{k}, \mathbf{x})\mathrm{e}^{i\mathbf{k}\cdot\mathbf{x}} F^2(\mathbf{k})\mathrm{d}^3k, \tag{21}$$

ou $F(\mathbf{k})$ est le facteur de forme de la censité nucléaire $|\psi_0|^2$. Pour montrer l'effet de l'opérateur d'échange, nous avons porté sur la fig. 2 la fonction $v_\mathrm{M}(k, 0)$ pour un potentiel de Yukawa et nous l'avons comparée au potentiel sans échange (12), en utilisant l'approximation $K_\mathrm{N} = K_\mathrm{P} = K = (9\pi)^{\frac{1}{3}}/2r_0$, pour des valeurs $\mu = 1$, $r_0 = 1.22$ fm qui correspondent à $\mu/K = 0.8$, et aussi pour $\mu/K = 0.6$.

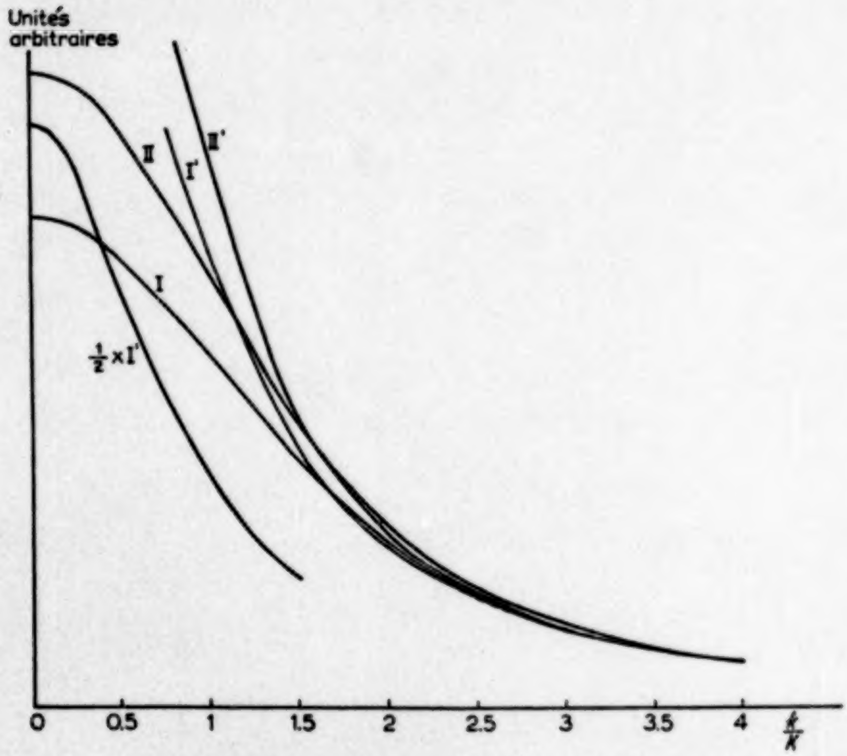

Fig. 2. Les courbes I' et II' sont les transformés de Fourier $[(k/K)^2+(\mu/K)^2]^{-1}$ des potentiels de Yukawa; I et II celles des potentiels d'échange effectifs pour une distribution de Fermi pour $(\mu/K) = 0.8$ et 0.6.

Pour des valeurs de $k/K > 1.5$ la différence entre les deux potentiels est très faible, mais en dessous de cette valeur $v_M(k, 0)$ croît beaucoup moins vite que $v(k)$. Pour $k = 0$ le rapport $v_M(0, 0)/v(0)$ est donné par le tableau suivant:

$\frac{\mu}{K}$	0.6	0.7	0.8	0.9	1	1.1	1.2
$\frac{v_M(0.\ 0)}{v(0)}$	0.3067	0.3653	0.4196	0.4692	0.5148	0.5561	0.5934

Ce rapport croît à peu près linéairement avec μ/K. L'opérateur d'échange a donc pour effet:

1°) de réduire considérablement l'intensité du potentiel effectif pour les petits transferts de quantité de mouvement;

2°) de ne pas changer l'interaction pour les grands transferts ($k/K > 1.5$).

Le mouvement collectif n'étant tributaire que des faibles transferts sera donc très sensible au pourcentage de force d'échange.

Posant $\boldsymbol{\lambda} = (\nu A/NZ)\mathbf{x}$ et $V_+(r) - V_-(r) = V(r)$, l'éq. (21) s'écrit

$$V_{\mathrm{NP}}^{(\mathrm{e})}(x) = \tfrac{1}{2}\frac{NZ}{(2\pi)^3}\int \mathrm{d}^3 r V(r) F_0^2(Kr) \mathrm{e}^{\boldsymbol{\lambda}\cdot\mathbf{r}} \int \mathrm{d}^3 k \mathrm{e}^{i\mathbf{k}\cdot(\mathbf{x}-\mathbf{r})} F^2(\mathbf{k}). \tag{22}$$

Pour le modèle uniforme à symétrie sphérique $F(\mathbf{k}) = F_0(\mathbf{k}R)$, on a

$$V_{\mathrm{NP}}^{(\mathrm{e})}(x) = \frac{3}{8\pi}\frac{NZ}{(KR)^3}\int \mathrm{d}^3 v V\left(\frac{v}{K}\right) F_0^2(v) \mathrm{e}^{\boldsymbol{\lambda}\cdot\mathbf{v}/K}\left[1 - \tfrac{3}{4}\frac{|K\mathbf{x}-\mathbf{v}|}{KR} + \tfrac{1}{16}\frac{|K\mathbf{x}-\mathbf{v}|^3}{(KR)^3}\right].$$

On peut négliger le dernier terme de l'accolade ($KR \gg 1$).

Pour le potentiel de Yukawa, en se limitant à un terme en x^3, on a

$$\begin{aligned} V_{\mathrm{NP}}^{(\mathrm{e})}(x) &= \tfrac{3}{32} NZ \frac{V}{\mu R}\left(\frac{x}{R}\right)^3 + \tfrac{3}{2}\frac{NZ}{(KR)^3}\left(\frac{K}{\mu}\right) V \\ &\quad \times \left\{ J_0\left(\frac{\mu}{K}\right) - \tfrac{1}{4} KR J_1\left(\frac{\mu}{K}\right)\left(\frac{x}{R}\right)^2 + \tfrac{1}{6} J_2\left(\frac{\mu}{K}\right)\left(\frac{\lambda}{K}\right)^2 + \frac{1}{4KR} J_3\left(\frac{\mu}{K}\right)\lambda x \right\}, \\ J_0(y) &= I_1(y) - \frac{3}{4KR} I_2(y), \qquad J_1(y) = I_0(y) - \tfrac{1}{2}\frac{1}{(KR)^2} I_2(y), \\ J_2(y) &= I_3(y) - \frac{3}{4KR} I_4(y), \qquad J_3(y) = I_2(y), \\ I_n(y) &= 9\int_0^{+\infty}\left[\frac{\sin u - u\cos u}{u^3}\right]^2 \mathrm{e}^{-yu} u^n \mathrm{d}u. \end{aligned} \tag{23}$$

Le tableau 2 donne les valeurs de I_n pour les valeurs usuelles de $y = \mu/K$. On remarquera que $yI_1(y)$ est à peu près constant pour $0.6 \leqq y \leqq 1.2$. Pour des valeurs intermédiaires de I_n on utilisera la relation

$$I_n(y+h) = I_n(y) + \sum_{1}^{+\infty} (-1)^p I_{n+p}(y) \frac{h^p}{p!}.$$

TABLEAU 2

Valeurs calculées de I_n

y	I_0	I_1	I_2	I_3	I_4	I_5
0.6	1.035	0.8525	1.167	2.114	4.742	13.09
0.7	0.9558	0.7454	0.9774	1.702	3.637	9.370
0.8	0.8861	0.6555	0.8246	1.382	2.825	6.900
0.9	0.8245	0.5792	0.6994	1.130	2.230	5.197
1.0	0.7698	0.5148	0.5966	0.9315	1.776	3.966
1.1	0.7212	0.4595	0.5117	0.7722	1.426	3.080
1.2	0.6778	0.4121	0.4412	0.6437	1.154	2.414

5. Force Tensorvielle et Potentiel Spin-Orbite

La force tensorielle ne donne pas de contribution au potentiel collectif de la résonance géante; en effet, la somme $S_{ij}+S_{ik}$ de l'opérateur du potentiel tensoriel agissant entre un proton i et deux neutrons j et k de spins opposés et situés en un même point est nulle. Il en résulte que la moyenne du potentiel tensoriel prise entre un proton i et une paire de neutrons de spins opposés situés sur la même orbite est nulle.

L'opérateur du potentiel de spin-orbite entre un proton et un neutron

$$(\boldsymbol{\sigma}_i+\boldsymbol{\sigma}_j) \cdot [\mathbf{x}_i-\mathbf{y}_j) \wedge (\boldsymbol{\nabla}_{x_i}-\boldsymbol{\nabla}_{y_j})]$$

se décompose dans le formalisme du mouvement collectif en

$$(\boldsymbol{\sigma}_i+\boldsymbol{\sigma}_j) \cdot \left[(\mathbf{x}+\boldsymbol{\xi}_i-\boldsymbol{\eta}_j) \wedge \left(\frac{A}{NZ}\boldsymbol{\nabla}_x+\boldsymbol{\nabla}_{\xi_i}-\boldsymbol{\nabla}_{\eta_j}\right)\right].$$

On voit tout de suite apparaître une partie intrinsèque

$$(\boldsymbol{\sigma}_i+\boldsymbol{\sigma}_j) \cdot [(\boldsymbol{\xi}_i-\boldsymbol{\eta}_j) \wedge (\boldsymbol{\nabla}_{\xi_i}-\boldsymbol{\nabla}_{\eta_j})].$$

La partie restante donne une contribution que l'on peut négliger du fait qu'elle est nulle pour deux nucléons de spin opposés sur une même orbite.

6. Énergie de la Résonance Géante

Identifiant le coefficient de x^2 de

$$V_{\mathrm{NP}}(\mathbf{x}) = V_{\mathrm{NP}}^{(\mathrm{d})}(\mathbf{x})+V_{\mathrm{NP}}^{(\mathrm{e})}(\mathbf{x})$$

à $\frac{1}{2}M\omega^2$ et utilisant le terme correctif en $3/2a^2$ dans la définition de λ avec la relation $\nu A/NZ = (m/\hbar^2)E_{\mathrm{m}}$ où $E_{\mathrm{m}} = \hbar\omega$, on trouve que l'énergie E_{m} est la solution positive d'une équation du second degré

$$a_0 E_{\mathrm{m}}^2 + 2b_0 E_{\mathrm{m}} + c_0 = 0, \tag{24}$$

dans laquelle

$$a_0 = 1 - \frac{4}{9\pi}\,\frac{m}{\hbar^2 K^2}\,\frac{V_{\mathrm{e}}}{y_{\mathrm{e}}}\,J_2(y_{\mathrm{e}}),$$

$$b_0 = -\tfrac{3}{8}\,\frac{A}{(KR)^4}\,\frac{V_{\mathrm{e}}}{y_{\mathrm{e}}}\left[J_3(y_{\mathrm{e}}) - \frac{2R}{Ka^2}\,J_2(y_{\mathrm{e}})\right],$$

$$c_0 = \tfrac{3}{4}\,\frac{\hbar^2}{m}\,\frac{A}{R^4}\left\{\frac{V_{\mathrm{d}}}{\mu_{\mathrm{d}}^2}\left(1 - \frac{1}{(\mu_{\mathrm{d}} R)^2}\right) + \frac{1}{K^2}\,\frac{V_{\mathrm{e}}}{y_{\mathrm{e}}}\left[J_1(y_{\mathrm{e}}) + \tfrac{3}{2}\,\frac{J_3(y_{\mathrm{e}})}{(Ka)^2} - \frac{3aR}{(Ka)^5}\,J_2(y_{\mathrm{e}})\right]\right\};$$

$$y_{\mathrm{e}} = \frac{\mu_{\mathrm{e}}}{K}, \qquad K = \frac{(9\pi)^{\frac{1}{3}}}{2r_0}, \qquad R = r_0 A^{\frac{1}{3}}, \qquad a = 0.775\,R,$$

$(V_{\mathrm{e}}/y_{\mathrm{e}})J_i(y_{\mathrm{e}})$ et $V_{\mathrm{d}}/\mu_{\mathrm{d}}^2$ désignent les valeurs pondérées $\frac{3}{4}$ triplet et $\frac{1}{4}$ singulet des paramètres des potentiels $V_+ - V_-$ et $V_+ + V_-$. Pour les valeurs usuelles des potentiels (exprimées en MeV), a_0 et b_0 sont de l'ordre de l'unité et c_0 de quelques centaines; b_0^2 est donc négligeable devant $-a_0 c_0$ et on a

$$E_{\mathrm{m}} \approx \sqrt{-\frac{c_0}{a_0}} - \frac{b_0}{a_0},$$

le dernier terme étant une petite correction. La quantité c_0 variant comme $A^{-\frac{1}{3}}$ et a_0 variant peu on retrouve une variation en $A^{-\frac{1}{3}}$.

7. Utilisation d'un Potentiel avec Cœur Dur

Un potentiel avec cœur dur empêche les nucléons de se rapporcher à une distance inférieure au rayon ρ du cœur dur. Il en résulte que si $\varepsilon(r_{ij})$ désigne une fonction de la distance r_{ij} de deux nucléons égale à 1 pour $r_{ij} > \rho$ et nulle pour $r_{ij} < \rho$, la fonction d'onde exacte est invariante pour une multiplication par

$$\prod_{ij} \varepsilon(r_{ij}).$$

Il en est évidemment de même pour la densité de présence nucléaire $|\psi|^2$. On est donc conduit à remplacer, dans le calcul du potentiel collectif, $|\psi|^2$ par la densité de présence multipliée par $\prod_{ij}\varepsilon(r_{ij})$ qui interdit la région intérieure au cœur dur, ce qui revient à calculer la moyenne pour $r_{ij} > \rho$.

Le calcul du potentiel $V_{\mathrm{NP}}(\mathbf{x})$ se fait alors aisément, et on obtient pour la partie sans échange une expression analogue à (13), obtenue en changeant V en $V\,\mathrm{e}^{-\mu\rho}$ et le terme correctif $1/(\mu R)^2$ en $(1+\mu\rho+\frac{1}{2}(\mu\rho)^2)/(\mu R)^2$. Dans la partie avec échange, la limite inférieure d'intégration devient $K\rho$, elle dépend donc de la valeur de r_0.

Une autre manière de voir consiste à remarquer que pour des diffusions à basse énergie et pour un cœur dur de faible portée ρ, on peut remplacer le cœur dur par un puits carré fortement attractif ayant pour portée celle du cœur dur et pour profondeur

$$V_0 = \frac{\hbar^2}{2m} k_0^2, \qquad k_0 = \frac{\pi}{\rho}.$$

On peut alors calculer la fonction d'onde de la manière habituelle et la fonction d'onde avec cœur dur s'obtiendra en multipliant par $\prod_{ij} \varepsilon(r_{ij})$ et en normalisant la fonction d'onde ainsi obtenue. Pour un cœur dur de portée 0.4 fm, on a $V_0 = 1290$ MeV.

8. COMPARAISON AVEC L'EXPÉRIENCE

Pour comparer avec les résultats expérimentaux, on utilise la partie du potentiel de Gammel et Thaler [5]) qui correspond aux diffusions à basse énergie, c'est-à-dire les potentiels centraux triplet et singulet pairs ${}^3V_c{}^+$ et ${}^1V_c{}^+$.

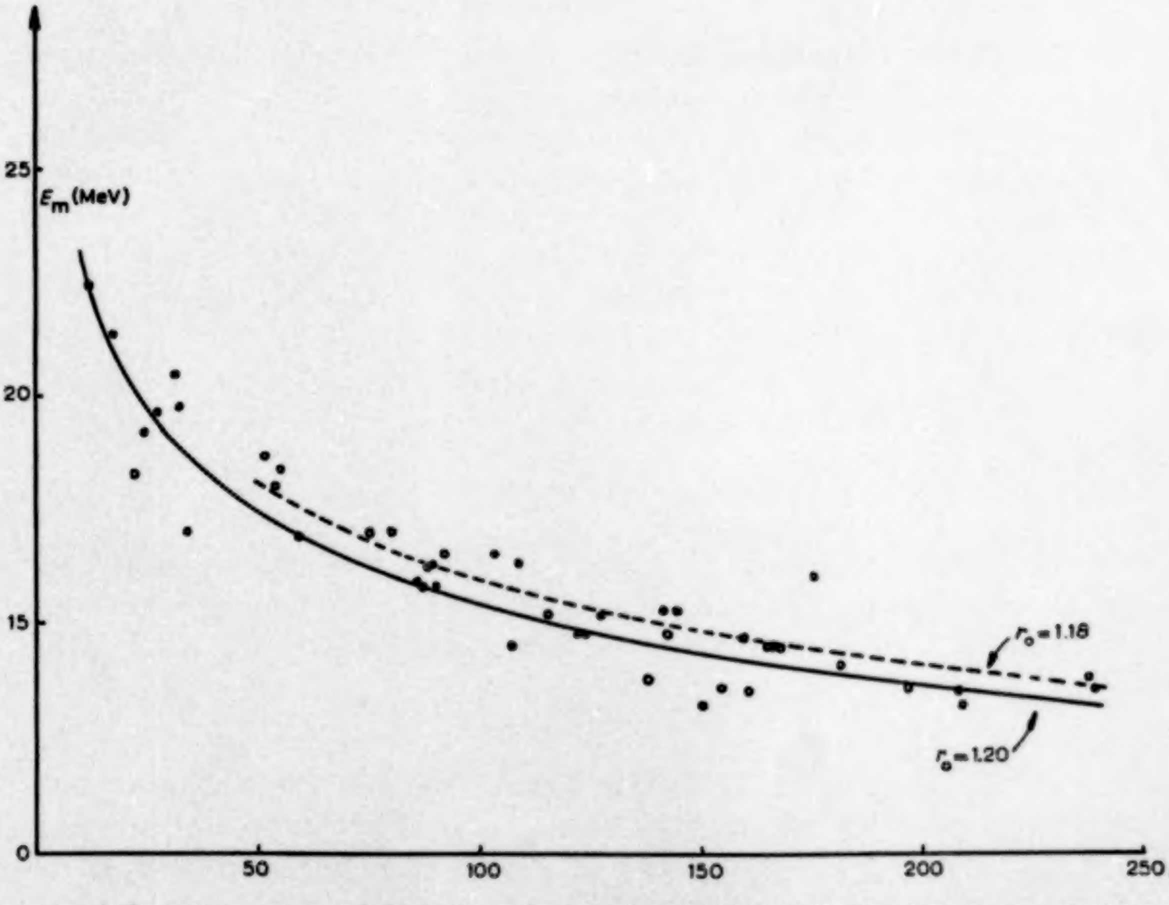

Fig. 3. Énergie du maximum de la résonance géante en fonction de A pour les valeurs $r_0 = 1.18$ et 1.20 fm.

On doit remarquer en effet que la force singulet impaire provenant des expériences de diffusion proton-neutron à grande énergie est relativement mal connue: elle est donnée comme répulsive, mais son poids statistique étant de $\frac{1}{4}$, elle est contrebalancée par une faible force attractive triplet impaire qui semble exister dans les diffusions à faible énergie (voir la note à la fin de la référence [5])). Ce choix revient à utiliser un potentiel de Serber avec cœur dur mais dépendant des spins.

La figure 3 donne les courbes théoriques pour les valeurs $r_0 = 1.2$ et 1.18 fm; pour les valeurs expérimentales on a utilisé les références [3]). Les valeurs des coefficients de l'éqn. (24) sont, pour $r_0 = 1.2$ fm,

$$a_0 = 1.3002 - 0.2806\, A^{-\frac{1}{3}},$$

$$b_0 = 6.179\, A^{-\frac{1}{3}} - 21.62\, A^{-\frac{2}{3}} + 20.2\, A^{-1},$$

$$-c_0 = 1451\, A^{-\frac{1}{3}} + 114.6\, A^{-1} - 1543\, A^{-\frac{4}{3}} + 1442\, A^{-\frac{5}{3}},$$

les énergies étant exprimées en MeV.

9. NOYAUX DÉFORMÉS

Lorsque le noyau est déformé, le facteur de forme, et par suite, le potentiel collectif ne possède plus la symétrie sphérique. Il en résulte, pour une déformation quelconque, un potentiel collectif d'oscillateur ayant des pulsations différentes ω_0, ω_1 et ω_2 suivant chacun des 3 axes. A chacun de ces axes correspond une énergie d'excitation $\hbar\omega_i$. Pour un noyau de forme ellipsoïdale, ayant son axe de symétrie dans la direction de z, on a $\omega_0 = \omega_1$ et les énergies d'excitation se réduisent à deux.

La déformation produit un élargissement de la résonance géante et son dédoublement pour des noyaux très déformés, l'énergie de séparation étant de l'ordre de $\hbar\Delta\omega$ où $\Delta\omega = \omega_1 - \omega_2$ dans le cas d'un noyau à symmétrie axiale.

Nous allons calculer l'énergie de séparation pour un noyau de forme ellipsoïdale

$$x^2 + y^2 + (1+\varepsilon)z^2 = R^2,$$

ayant pour rayons principaux R et $R/\sqrt{1+\varepsilon}$. La déformation ε est positive ou négative suivant que l'ellipsoïde est aplati ou allongé. Pour simplifier les calculs, nous utiliserons un facteur de forme gaussien avec l'approximation

$$F_{\mathrm{P}}(\mathbf{k}) = F_{\mathrm{N}}(\mathbf{k}) = \mathrm{e}^{-\frac{1}{4}a_1^2(k_x^2+k_y^2)}\, \mathrm{e}^{-\frac{1}{4}a_2^2 k_z^2},$$

où $a_1 = 0.775\, R$, $a_2 = 0.775\, R(1+\varepsilon)^{-\frac{1}{2}}$ et $R = r_0 A^{\frac{1}{3}}(1+\varepsilon)^{\frac{1}{6}}$ pour un volume nucléaire $\frac{4}{3}\pi r_0^3 A$. Les calculs s'effectuent facilement avec un potentiel n-p de type gaussien $V_0 \mathrm{e}^{-\alpha r^2}$, on obtient alors les deux énergies de résonance E_1 et E_2 correspondant au plan de symétrie et à l'axe de révolution du noyau ellipsoïdal ainsi que la relation déterminant le paramètre de déformation ε en fonction des énergies E_1 et E_2,

$$E_1{}^2 = \tfrac{1}{2}3^{\frac{1}{2}}\pi^{\frac{3}{2}}\frac{\hbar^2}{m}v_{\mathrm{np}}(0)\frac{A}{\left(a_1{}^2+\dfrac{3}{4\alpha}\right)^2\left(a_2{}^2+\dfrac{3}{4\alpha}\right)^{\frac{1}{2}}},$$

$$E_2{}^2 = \tfrac{1}{2}3^{\frac{1}{2}}\pi^{\frac{3}{2}}\frac{\hbar^2}{m}v_{\mathrm{np}}(0)\frac{A}{\left(a_1{}^2+\dfrac{3}{4\alpha}\right)\left(a_2{}^2+\dfrac{3}{4\alpha}\right)^{\frac{3}{2}}}, \tag{26}$$

$$(1+\varepsilon)+\frac{3}{4\alpha a_0{}^2}\left[1-\left(\frac{E_2}{E_1}\right)^2\right](1+\varepsilon)^{\frac{2}{3}}-\left(\frac{E_2}{E_1}\right)^2 = 0, \qquad a_0 = 0.775\, r_0 A^{\frac{1}{3}}.$$

Négligeant pour les noyaux lourds le terme correctif en $3/4\alpha$ qui provient du facteur de forme du potentiel n-p, le rapport des énergies de résonance est égal à l'inverse du rapport des rayons principaux de l'ellipsoïde nucléaire:

$$E_1/E_2 = a_2/a_1.$$

À la même approximation on a

$$E_1 = E_{\mathrm{m}}(1+\varepsilon)^{-\frac{1}{3}}, \qquad E_2 = E_{\mathrm{m}}(1+\varepsilon)^{\frac{2}{3}},$$

où E_{m} désigne l'énergie du maximum de la résonance en l'absence de déformation ($\varepsilon = 0$); effectuant un développement pour ε petit on en tire

$$\frac{E_1-E_{\mathrm{m}}}{E_{\mathrm{m}}-E_2} = \tfrac{1}{2}(1-\tfrac{1}{4}\varepsilon).$$

Les énergies E_1 et E_2 se répartissent de part et d'autre de E_{m}, à une distance respective $\frac{1}{3}$ et $\frac{2}{3}$ de l'énergie de séparation E_1-E_2.

Un noyau déformé possède un moment quadrupolaire qui est donné en fonction du facteur de forme nucléaire par la relation

$$Q_0 = \lim_{\mathbf{k}\to 0} Z\left[\frac{\partial^2}{\partial k_x{}^2}+\frac{\partial^2}{\partial k_y{}^2}-2\frac{\partial^2}{\partial k_z{}^2}\right]F_{\mathrm{P}}(\mathbf{k}).$$

Le moment Q_0 ne dépend donc que des rayons carrés moyens du noyau déformé, c'est-à-diré des trois rayons principaux d'un ellipsoïde pour la déformation la plus générale. Pour un noyau possédant la symétrie de révolution, on retrouve ainsi la valeur connue

$$Q_0 = \tfrac{2}{3}Z(a_2{}^2-a_1{}^2) = \tfrac{2}{5}Z(R_2{}^2-R_1{}^2) = -\frac{0.4\varepsilon}{(1+\varepsilon)^{\frac{2}{3}}}r_0{}^2ZA^{\frac{2}{3}},$$

qui est indépendante de l'expression raffinée du facteur de forme lorsque les rayons carrées moyens sont donnés.

Si l'on admet [4]) que la largeur Γ de la résonance géante peut se décomposer en deux parties:

1) une largeur intrinsèque Γ_0 qui varie peu d'un noyau à l'autre dès que A est assez grand,

2) une largeur $\Delta\Gamma \approx E_1 - E_2$ qui provient de la déformation et qui est nulle pour les noyaux sphériques.

il existe une relation entre le moment quadrupolaire Q_0 et la largeur totale $\Gamma = \Gamma_0 + \Delta\Gamma$. Pour les noyaux lourds, à l'approximation où $\frac{3}{4}\alpha$ est négligeable devant a_0^2, on obtient

$$\Delta\Gamma = \frac{1-\sqrt{1+\varepsilon}}{(1+\varepsilon)^{\frac{1}{6}}}\, E_{\mathrm{m}},$$

et lorsque le paramètre de déformation ε est petit on retrouve la relation

$$\Delta\Gamma = +\tfrac{5}{4}\frac{Q_0}{r_0{}^2 Z A^{\frac{2}{3}}}, \qquad \varepsilon \ll 1.$$

Lorsque la déformation n'est plus petite, on doit revenir aux expressions (26).

Pour un certain nombre de noyaux très déformés, on a pu observer les énergies E_1 et E_2 des deux maxima. On déduit immédiatement de ces valeurs le coefficient de déformation ε et le moment quadrupolaire Q_0 en utilisant pour r_0 la valeur 1.2 fm, qui concorde d'une part avec les mesures expérimentales du facteur de forme données par Hofstadter et d'autre part avec les valeurs théoriques de E_{m}.

TABLEAU 3

Valeurs expérimentales de E_1, E_2 et Q_0 et valeurs calculées de ε et Q_0

corps	E_1	E_2	ε	Q_0 (théorique)	Q_0 (exp)	Références
$_{79}\mathrm{Au}^{197}$	13.90	13.15	−0.110	1.83	2.2	[6, 11])
$_{73}\mathrm{Ta}^{181}$	15.45	12.45	−0.365	6.65	6.8	[6, 11])
	15.5	12.5	−0.364	6.62	6.8	[7, 11])
$_{65}\mathrm{Tb}^{159}$	16.2	12.5	−0.429	6.85	6.9	[6, 11])
$_{67}\mathrm{Ho}^{165}$	16.0	12.2	−0.435	7.40	7.8	[8, 11])
$_{68}\mathrm{Er}^{166}$	16.0	12.2	−0.435	7.54	7.5	[8, 11])
$_{27}\mathrm{Co}^{59}$	19.0	16.5	−0.267	0.841	1.07±0.43	[9, 11])
$_{25}\mathrm{Mn}^{55}$	19.75	16.8	−0.301	0.863	1.12±0.56	[9, 13])
	19.5	16.5	−0.309	0.894	1.12±0.56	[10])
$_{45}\mathrm{Rh}^{103}$	17	14.5	−0.290	2.07	2.2	[10, 12])

Pour ε on a utilisé l'expression approchée

$$\varepsilon = \left[\left(\frac{E_2}{E_1}\right)^2 - 1\right]\left[1 + \frac{3}{4\alpha a_0{}^2}\left(\frac{E_2}{E_1}\right)^2\right] \text{ avec } \frac{1}{2\alpha} = 1.$$

Le tableau 3 donne les valeurs expérimentales de E_1 et de E_2, celles du coefficient de déformation ε que l'on en déduit à partir de (26) en utilisant

$r_0 = 1.2$ fm pour les noyaux lourds et $r_0 = 1.25$ fm pour les noyaux dans la région du Cobalt (suivant le tableau 1), enfin les valeurs expérimentales de Q_0 obtenues par excitation coulombienne.

10. Conclusions

La précision de l'accord entre les résultats expérimentaux et théoriques semble indiquer que la base d'explication des phénomènes de résonance géante photonucléaire réside bien dans un mouvement collectif des protons par rapport aux neutrons.

Ceci n'exclut d'ailleurs pas une explication par un modèle à particules indépendantes; en effet dans ce cas l'état d'une particle peut être décomposé en une partie collective, possédant un certain poids statistique $|a_0|^2$, et une partie intrinsèque, la probabilité de photo-excitation étant proportionnelle à $|a_0|^2$, puisque dans une telle décomposition seul le mode collectif (si l'on fait abstraction des forces d'échange) peut être excité. L'existence d'une structure dans la résonance géante provient de ce que les états 1^- sont des mélanges d'une partie intrinsèque possédant des niveaux distincts et d'une partie collective.

Dans le tableau 1 la valeur de E_{m} obtenue pour le C^{12} semble trop faible: cela s'explique par le fait que la valeur de r_0 que l'on doit utiliser correspond à l'extension de la partie intrinsèque et que le facteur de forme $F_{\mathrm{d}}(\mathbf{k})$ mesuré dans les expériences de diffusion électron-noyau est relié aux facteurs de forme collectif $F_{\mathrm{c}}(\mathbf{k})$ et intrinsèque $F_{\mathrm{P}}(\mathbf{k})$ par la relation

$$F_{\mathrm{d}}(\mathbf{k}) = F_{\mathrm{c}}\left(\frac{N}{A}\,\mathbf{k}\right) F_{\mathrm{P}}(\mathbf{k}).$$

La différence donnée par

$$r_0^2 = r_{\mathrm{d}}^2 - \tfrac{5}{2}\,\frac{N}{Z}\,\frac{1}{A^{\frac{1}{3}}}\,\frac{\hbar^2}{m}\,\frac{1}{E_{\mathrm{m}}}$$

n'est d'ailleurs significative que pour les noyaux légers. Pour le C^{12} la valeur corrigée $r_0 = 1.3$ fm conduit à une énergie $E_{\mathrm{m}} = 22.4$ MeV conforme aux résultats expérimentaux.

Le calcul montre d'autre part, que l'énergie de résonance n'est pas sensible à la forme du potentiel n-p mais seulement aux deux premiers termes de sa transformée de Fourier pour **k** voisin de zéro;

$$v_{\mathrm{np}}(k) = v_{\mathrm{np}}(0) - \tfrac{1}{2}v''_{\mathrm{np}}(0)k^2,$$

le second terme n'intervenant qu'à titre de correction et ne prenant d'importance que pour les noyaux légers. Notamment pour les noyaux lourds, une interaction ponctuelle $V\delta(\mathbf{x}_i - \mathbf{y}_j)$ dont l'intensité est déterminée par $v_{\mathrm{np}}(0) = V/(2\pi)^3$ donnera de bons résultats.

Dans l'utilisation du facteur de forme nucléaire le paramètre le plus important est évidemment le rayon carré moyen a^2 ou ce qui revient au même, la valeur de r_0. Cependant l'effet dû à l'épaisseur de la surface nucléaire se fait sentir d'une façon importante pour les noyaux légers. Un calcul a notamment été entrepris en utilisant les facteurs de forme [14]) obtenus par diffusion électron-noyau à 410 MeV sur C^{12} et O^{16}, et le potentiel phénoménologique de Gammel-Thaler: les résultats expérimentaux et théoriques concordent. La précision obtenue dans la détermination du paramètre de déformation ε conduit à penser que dans la limite des erreurs expérimentales, la mesure du dédoublement ou de l'élargissement de la résonance donnerait de précieuses indications sur les déformations nucléaires. On doit cependant faire attention au fait que pour les corps légers et pour de fortes déformations, la résonance la plus basse peut se trouver dans le voisinage du seuil de la réaction (γ, n). La différence d'énergie entre les deux maxima peut alors apparaître expérimentalement plus petite que la valeur réelle; c'est d'ailleurs ce qui semble se passer [15]) pour Mg^{24}.

Nous étudierons dans un prochain article les phénomènes d'excitation de la résonance géante qui sont plus sensibles que l'énergie de résonance à un modèle détaillé.

Références

1) M. Fabre de la Ripelle, C. R. Acad. Sc. **247** (1958) 926, 1568; Jour. Phys. et Rad. **21** (1960) 302
1a) Goldhaber et Teller, Phys. Rev. **74** (1948) 1046
2) Hofstadter, Rev. Mod. Phys. **28** (1956) 214;
J. Fujita, Progr. Theor. Phys. **16** (1956) 112
3) Montalbetti, Katz *et al.*, Phys. Rev. **91** (1953) 659;
Nathan et Halpern, Phys. Rev. **93** (1954) 437;
De Sonza Santos, Goldemberg *et al.*, Acad. Brasil **27** (1955) 437;
Fuller, Petree et Weiss, Phys. Rev. **112** (1958) 554;
Carver et Turchinetz, Proc. Phys. Soc. **73** (1959) 69;
Mutsuro, J. Phys. Soc. Japan **14** (1959) 1649
4) M. Danos, Bull. Phys. Soc. **1** (1956) 135;
K. Okamoto, Prog. Theor. Phys. (Japan) **15** (1956) 75; Phys Rev. **110** (1958) 143
5) Gammel et Thaler, Phys. Rev. **107** (1957) 1337
6) Fuller et Weiss, Phys. Rev. **112** (1958) 560
7) Parson et Katz, Canad. J. Phys. **37** (1959) 809
8) Fuller et Hayward, Karlsruhe Photonuclear Conf. 1960
9) Flournoy *et al.*, Karlsruhe Photonuclear Conf. 1960
10) Parson, Canad. J. Phys. **37** (1959) 1344
11) C. H. Townes, Hand. Phys. (Springer Verlag, Berlin) Vol. **38**, Bd. 1, p. 443
12) Heydenburg et Temmer, Phys. Rev. **95** (1954) 861
13) K. Murakawa, J. Phys. Soc. Japan **10** (1955) 336
14) Ehrenberg *et al.*, Phys. Rev. **113** (1959) 666
15) King et Mc. Donald, Nuclear Physics **19** (1960) 94

4.E

Nuclear Physics **27** (1961) 581—585; © *North-Holland Publishing Co., Amsterdam*

Not to be reproduced by photoprint or microfilm without written permission from the publisher

DECAY CHAIN $Er^{158} \xrightarrow[E]{2.5\,h} Ho^{158} \xrightarrow[E,\,\beta^+]{27\,min} Dy^{158}_{stab}$

N. A. BONCH-OSMOLOVSKAYA, B. S. DZELEPOV, O. E. KRAFT
and WANG YOUNG-YU

Physics Faculty, Leningrad University, Leningrad, USSR
Joint Institute for Nuclear Research, Dubna, USSR

Received 6 February 1961

Abstract: The existence of the radiactive chain $Er^{158} \xrightarrow{2.5\,h} Ho^{158} \xrightarrow{27\,min} Dy^{158}_{stab}$ is established. The change in intensity of 330 keV and 715 keV positons was observed. An analysis of the accumulation and disintegration curves at these positon energies and of positon spectra in Er and Ho isolated from Er warrants the conclusion that the β^+-spectrum with $E_{e.p.} = 1320$ keV belongs to the daughter Ho^{158}, while the β^+-spectrum with $E_{e.p.} = 780$ keV belongs to the decay of Er^{158} itself.

1. Introduction

In 1954 Handley and Olson ¹) for the first time observed that in the chemically isolated Er fraction there is an activity with a half-life of 3.6 h following the bombardment of Er_2O_3 by protons of $E_p = 24$ MeV. This activity also occurred with 17 MeV protons and the reaction threshold (p, 3n) in this region was found > 19 MeV, and was ascribed to Er^{161} which might have come from the reactions Er^{162} (p, pn) Er^{161} or Er^{162} (p, 2n) $Tu^{161} \rightarrow Er^{161}$. Somewhat later Mitchel and Templeton ²) established with a mass spectrometer that the 3.5 h Er actually had the mass number $A = 161$. They failed, however, to notice the growth of the daughter holmium.

Using a scintillation spectrometer, Handley and Olson noticed 65, 195, 824 and 1120 keV γ-rays, but no annihilation line. In the low spectrum energy region Handley and Olson observed the growth of the daughter holmium Ho^{161}. The holmium isolated from Er fraction had a half-life of 2.5 h, emitted $h\nu = 90$ keV γ-rays and yielded no annihilation radiation. Thus Handley and Olson established the existence of the chain

$$Er^{161} \xrightarrow[E]{3.6\,h} Ho^{161} \xrightarrow[E]{2.5\,h} Dy^{161}.$$

Later Nervik and Seaborg ³) who studied the products of the bombardment of tantalum by protons of $E_p = 340$ MeV also detected in the Er fraction a β^+-activity which had a half-life of 183 min and an end point energy of the

β^+-spectrum of some 1200 keV (measurements were carried out with a rough β-spectrometer). Basing themselves on the similarity of the half-lives of the activity observed by them and described in ref. [1]), Nervik and Seaborg ascribed this β^+-spectrum to Er^{161} or the daughter Ho^{161} (the authors made no attempt to separate the daughter holmium from erbium).

While investigating the Er fraction isolated from tantalum bombarded by protons of $E_p = 660$ MeV, Dneprovsky [4]) observed for the first time (in 1959) conversion lines with 2.5 h half-life.

The investigation of the daughter holmium isolated from erbium described in ref. [4]) as well as the investigation by Gromov *et al* [5]) of the conversion spectrum of the holmium fraction pointed to the existence of the spallation chain

$$\mathrm{Er} \xrightarrow[\mathrm{E}]{2.5\,\mathrm{h}} \mathrm{Ho} \xrightarrow[\mathrm{E}]{27\,\mathrm{min}} \mathrm{Dy}.$$

The mass number 158 was ascribed to this chain on the strength of the considerations given in ref. [4]).

2. Our Measurements

We measured the positon radiation of the Er fraction isolated from a tantalum target after 15 min bombardment by 660 MeV protons. The measurement was performed with a β-spectrometer with beam triple focussing 1.5 h after the isolation of erbium. We noticed an intense positon spectrum with

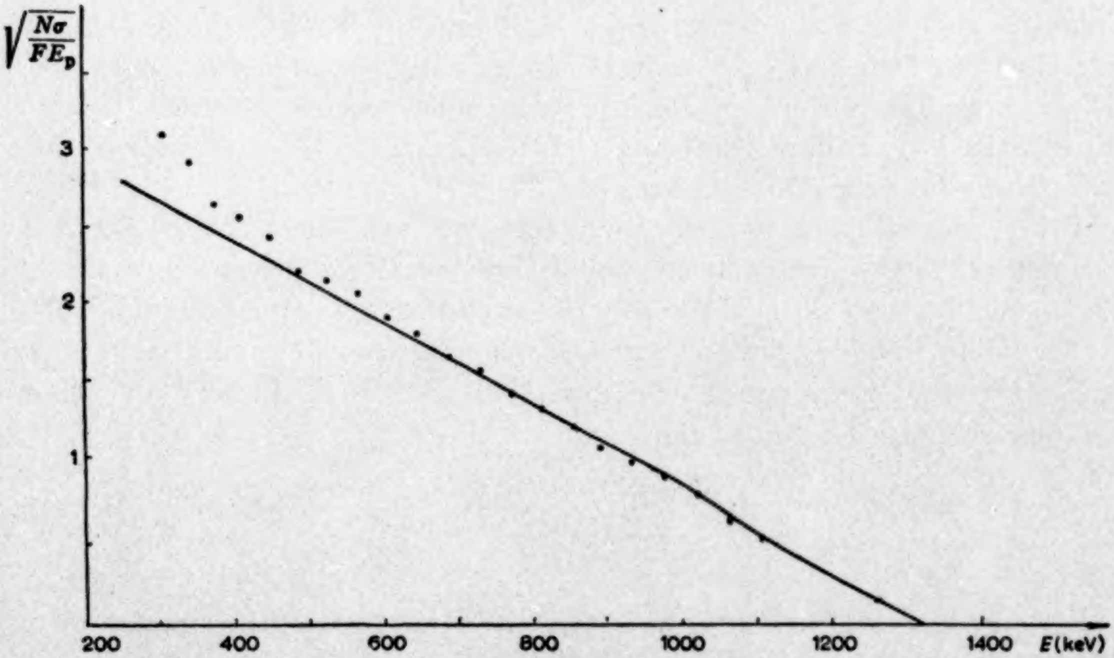

Fig. 1. Curie graph of the β^+-spectrum with $T_{\frac{1}{2}} = 2.5$ h in the Er fraction.

$T_{\frac{1}{2}} = 150 \pm 10$ min (evidently these were the same positons which were observed by Nervik and Seaborg).

Fig. 1 represents the Curie graph of this spectrum. From the graph it is clear that the β^+-spectrum consists of two components with end-point energies 1320 ± 50 and 780 ± 80 keV and relative intensities 10 : 1.

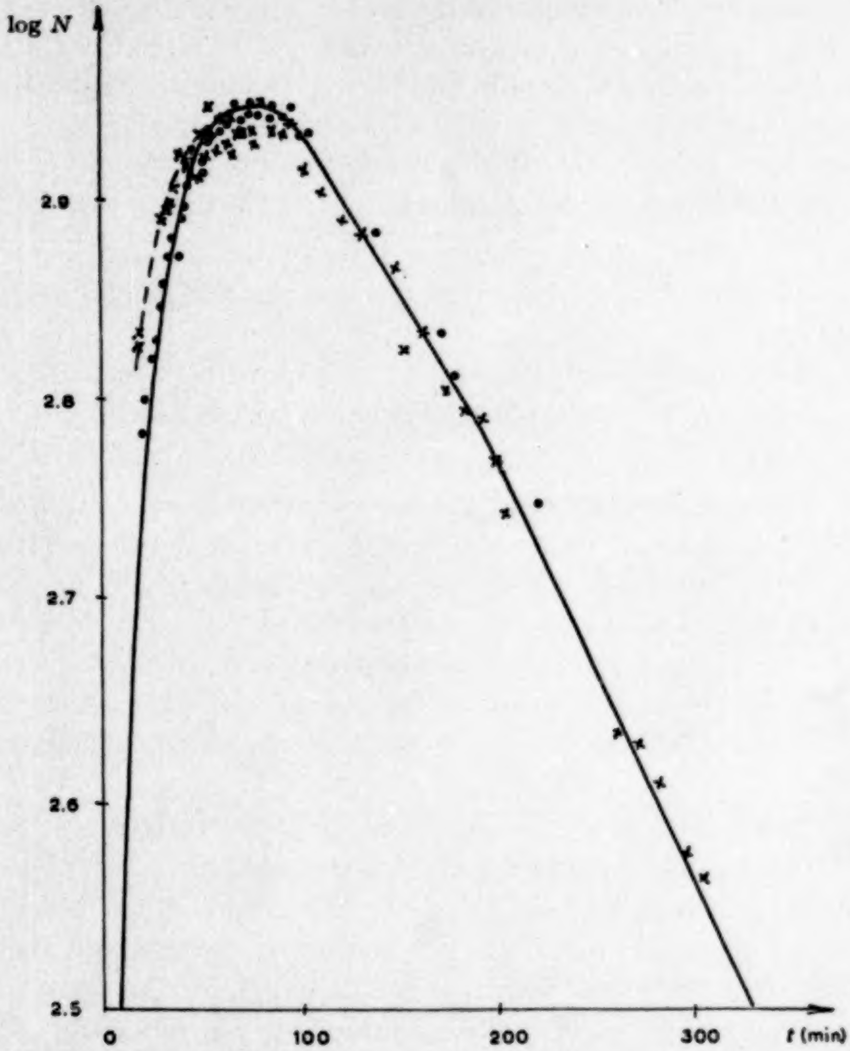

Fig. 2. The dependence of the counting rate

- ● with a positon energy of 715 keV in the Er fraction
- × with a positon energy of 330 keV in the Er fraction
- – – The calculated curve of the accumulation and disintegration of the substance B in the chain $A \xrightarrow{2.5\ h} B \xrightarrow{27\ min} C$ in observing the positons B → C and under the assumption that there are no positons of the given energy in the mother nucleus A.

Our next step was the measurement of positon activity in holmium isolated from erbium. We detected a simple β^+-spectrum with $T_{\frac{1}{2}} = 30 \pm 5$ min and $E_{e.p.} = 1350 \pm 50$ keV; there was no soft component of the spectrum in the holmium fraction. The similarity of the β^+-spectrum of erbium (2.5 h) and of Ho isolated from Er (30 min) suggested the idea that the β^+-spectrum with $E_{\text{e.p.}} = 1350$ keV belongs to the daughter Ho in the chain

$$\text{Er}^{158} \rightarrow \text{Ho}^{158} \rightarrow \text{Dy}^{158}.$$

To check this supposition we observed the change in the intensity of 715 keV-particles in the Er fraction. The measurements began 22 min after the isolation of the fraction and continued for 4 h. Dots in fig. 2 show the time dependence of the counting rate at 750 keV (on a semi-logarithmic scale).

The graph shows quite distinctly the increase of intensity of β^+-particles for $\approx$ 80 min and then its decrease. A solid line in fig. 2 sums up the calculation of the time dependence of the counting rate for the chain $\text{A} \xrightarrow{2.5\ \text{h}} \text{B} \xrightarrow{27\ \text{min}} \text{C}$ under the assumption that there are no positons of the given energy in the mother nucleus A.

It can be seen that the points coincide fairly well with the calculated curve. Thus the experiment is conclusive evidence that positons of $E_{\text{e.p.}} = 1350$ keV belong to the daughter Ho in the chain $\text{Er}^{158} \xrightarrow{2.5\ \text{h}} \text{Ho}^{158} \xrightarrow{27\ \text{min}} \text{Dy}^{158}$ and the existence of the chain itself can be regarded as proved beyond argument.

We have indicated above that the soft component of the β^+-spectrum with $E_{\text{e.p.}} = 780 \pm 80$ keV was observed only in the Er fraction which suggested that the positons of this end-point energy correspond to the decay of Er^{158} itself.

If this is the case, the curve of the accumulation and spallation of the chain $\text{Er}^{158} \rightarrow \text{Ho}^{158} \rightarrow \text{Dy}^{158}$ in the region of low energies in which Er^{158} accounts for an appreciable portion of positons must differ from the calculated curve of fig. 2.

We made observations of the β^+ -spectrum intensity variation with time at 330 keV positon energy. Judging by the Curie graph the positons belonging to Er^{158} account for about 20 % in this case. The results of the measurements are indicated by crosses in fig. 2. It is clear from the graph that the experimental points actually deviate from the calculated curve. An analysis of the experimental time dependence of the counting rate warrants the conclusion that with an energy of β^+-particles = 330 keV a fraction of $(15 \pm 10)\%$ of the positons belong to Er^{158} itself.

To determine this magnitude with higher accuracy does not seem possible at present because of our approximate information on the half-lives of Er^{158} and Ho^{158} and an inevitable allowance ($\approx$ 2 to 3 min) for the moment in the yield of the fraction.

It will be noted that the mass differences $\text{Er}^{158}-\text{Ho}^{158}$ and $\text{Ho}^{158}-\text{Dy}^{158}$ amount to 1.59 and 3.8 MeV, respectively, according to the Cameron tables. According to our measurements these values $\geqq$ 1.8 MeV for $\text{Er}^{158}-\text{Ho}^{158}$ and $\geqq$ 2.35 MeV for $\text{Ho}^{158}-\text{Dy}^{158}$.

References

1) T. Handley and E. Olson, Phys. Rev. **93** (1954) 524
2) M. Mitchel and D. Templeton, Phys. Rev. **93** (1954) 1442
3) E. Nervik and G. Seaborg, Phys. Rev. **97** (1955) 1092
4) I. S. Dneprovsky, preprint of the JINR **483** (1959) 5
5) K. Ya. Gromov *et al.*, preprint of the JINR **483** (1959) 37

1.B
Nuclear Physics **27** (1961) 586—595; © *North-Holland Publishing Co., Amsterdam*

Not to be reproduced by photoprint or microfilm without written permission from the publisher

DE-POLARIZATION PARAMETER IN p-p SCATTERING AT 143 MeV

L. BIRD, P. CHRISTMAS [†], A. E. TAYLOR and E. WOOD
Atomic Energy Research Establishment, Harwell, Nr. Didcot, Berks

Received 17 April 1961

Abstract: Measurements are reported of the Wolfenstein D parameter in p–p scattering at 143 MeV in the angular range $30^\circ-90^\circ$ (centre-of-mass). A longitudinal magnetic field has been used to precess the polarization vector of the incident beam, thus largely eliminating similar sources of systematic error to those possible in the method used for measuring the asymmetries in the previous Harwell and Harvard determinations of D. The results of this remeasurement agree with the previous ones at small angles and are intermediate between the Harvard and previous Harwell values at large angles. However, since the method used is less subject to systematic error, the present results should be regarded as superseding the previous Harwell values.

1. Introduction

Earlier work had shown that F waves are present in proton-proton scattering at 142 MeV [1]) and that in order to carry out a phase shift analysis other data than the differential cross section and polarization would be needed. In particular it seems that measurements of the Wolfenstein triple scattering parameters [2]) D, R and A would be sufficient to enable a unique phase shift solution to be obtained.

The most recent and successful attempts at interpreting the nucleon-nucleon interaction have been those by Gammel and Thaler [3]) (GT) and Signell, Zinn and Marshak [4]) (SZM). The former have proposed a phenomenological model based on energy independent potentials giving a weak long range central force with a repulsive core together with a long range tensor force and a short range spin-orbit force. This model fits nucleon-nucleon scattering data reasonably well up to about 300 MeV. The SZM model although based upon a meson-theoretic combination of central and tensor forces (Gartenhaus) together with a phenomenological force, is broadly similar to the GT model and is successful up to 150 MeV. Later modifications (Saylor, Bryan and Marshak [5])) have improved the fit to the data.

Work in this laboratory on the measurement of the D parameter was briefly reported at the 1958 Annual International Conference on High Energy Physics and shortly afterwards measurements at Harvard gave results in disagreement with these values. By that time much of the apparatus was being used for the measurement of the *R* parameter and it was not possible to return immediately to the *D* experiment. After careful checks no major errors were found in the Harvard results and so the disagreement remained. It was therefore essential that the earlier experiment should be repeated.

[†] Clarendon Laboratory, Oxford

The GT and SZM models differ notably in the prediction for the angular dependence of the *D* parameter at 140 MeV. The Harvard results are closer to the GT prediction whereas the early Harwell results favoured the SZM prediction. Further, phase shift analyses have shown that the $^3P_0$ phase shift is particularly sensitive to this type of disagreement.

The acquisition of a solenoid with which to rotate the polarization vector of the proton beam through 180° offered an alternative method of measuring *D* in which the systematic errors would be much smaller than in the previous measurements. The opportunity has also been taken to improve the angular resolution and to extend the measurements to larger angles.

2. Method

2.1. PRINCIPLE

The measurement of the *D* parameter requires a triple scattering experiment in which the first scattering produces a polarized beam and the third scattering measures the polarization of the beam after it has been scattered at the second scatterer, all scatterings taking place in the same plane. The *D* parameter is a measure of the change in polarization of the beam, perpendicular to the scattering plane, due to the scattering at the second target.

As can be seen (fig. 1) there are four possible scattering directions, LL, LR, RL and RR, respectively. The counts in each of the four directions per unit monitor count is given by

$$\begin{aligned}
\mathrm{LL} &= [1+P_1A_2+A_3(P_2+DP_1)]\,\sigma(\theta_2)^{\mathrm{L}}\mathrm{d}\Omega^{\mathrm{L}}\sigma(\theta_3)^{\mathrm{LL}}\,\mathrm{d}\Omega^{\mathrm{LL}}\,\eta^{\mathrm{LL}}\,M,\\
\mathrm{LR} &= [1+P_1A_2-A_3(P_2+DP_1)]\,\sigma(\theta_2)^{\mathrm{L}}\mathrm{d}\Omega^{\mathrm{L}}\,\sigma(\theta_3)^{\mathrm{LR}}\,\mathrm{d}\Omega^{\mathrm{LR}}\eta^{\mathrm{LR}}\,M,\\
\mathrm{RL} &= [1-P_1A_2-A_3(P_2-DP_1)]\,\sigma(\theta_2)^{\mathrm{R}}\mathrm{d}\Omega^{\mathrm{R}}\sigma(\theta_3)^{\mathrm{RL}}\,\mathrm{d}\Omega^{\mathrm{RL}}\eta^{\mathrm{RL}}\,M,\\
\mathrm{RR} &= [1-P_1A_2+A_3(P_2-DP_1)]\,\sigma(\theta_2)^{\mathrm{R}}\mathrm{d}\Omega^{\mathrm{R}}\sigma(\theta_3)^{\mathrm{RR}}\mathrm{d}\Omega^{\mathrm{RR}}\eta^{\mathrm{RR}}M,
\end{aligned}$$

where P_1 is the polarization of the incident beam, A_2 and A_3 the asymmetry in pp scattering at angle θ_2 and in p-Be scattering at angle θ_3 for a 100 % polarized beam, P_2 is the polarization produced in pp scattering at angle θ_2, *D* is the Wolfenstein depolarization parameter, $\sigma(\theta_2)$ and $\sigma(\theta_3)$ are the cross sections for scattering at the Hydrogen second and Berillium third scatterers and $\mathrm{d}\Omega$ and η are the solid angle and efficiency of detection in the scatterings designated by the superscripts. Similar superscripts applicable to A_2, A_3 and P_2 have been omitted.

M is a normalizing term related to the target thickness and the number of incident protons required to give a monitor count. This latter monitor calibration may be sensitive to beam intensity.

If the invariance of pp scattering under time reversal is a valid concept, we have $P_2 = A_2$.

In this experiment the presence of the solenoid permits the use of the two possible spin directions designated Up and Down, for which P_1 has a positive or negative value, $\pm P_1$, respectively. Using the convention that LLU represents two left scatterings with spin up while LLD represents two left scatterings with spin down and so on the following ratios can be formed:

$$r_1 = \left(\frac{\text{LLU}}{\text{LLD}}\,\frac{\text{RRD}}{\text{RRU}}\right)^{\frac{1}{2}} = \frac{1+P_1A_2+A_3(P_2+DP_1)}{1-P_1A_2+A_3(P_2-DP_1)},$$

$$r_2 = \left(\frac{\text{LRU}}{\text{LRD}}\,\frac{\text{RLD}}{\text{RLU}}\right)^{\frac{1}{2}} = \frac{1+P_1A_2-A_3(P_2+DP_1)}{1-P_1A_2-A_3(P_2-DP_1)}.$$

It is to be noted that the $\sigma(\theta_2)$, $\sigma(\theta_3)$, $d\Omega$, η and M terms cancel, and therefore measurements based on these ratios are self monitoring and independent of the efficiency of detection. The values of A_2, A_3 and P_2 are now the values at the mean values of θ_2 and θ_3 for left and right scattering.

We may now form quantities ε_1 and ε_2 such that

$$\varepsilon_1 = (1+P_2A_3)\,\frac{(r_1-1)}{(r_1+1)} = P_1A_2+DP_1A_3,$$

$$\varepsilon_2 = (1-P_2A_3)\,\frac{(r_2-1)}{(r_2+1)} = P_1A_2-DP_1A_3,$$

and hence

$$\varepsilon_1-\varepsilon_2 = 2DP_1A_3, \qquad \varepsilon_1+\varepsilon_2 = 2P_1A_2$$

So that, knowing the polarization of the initial beam, a value for A_2 can be obtained directly and substitution of interpolated values for A_3 together with P_1 enables a value for D to be obtained.

Target full measurements were made in repeated cycles, interspersed with background measurements, in the following sequence: spin up, spin down (precession+180°), spin down (precession+180°), spin up, spin up, spin down (precession−180°), spin down (precession−180°) and spin up. This tended to reduce the effects of any drifts or movements of the beam at the target.

3. Apparatus and Layout

A schematic diagram of the apparatus is shown (fig. 1). The first scattering was inside the cyclotron and the protons scattered to the left from carbon at about 8° were extracted from the machine. For this experiment, a slightly lower energy beam than is normally used was extracted in order to maintain the mean energy of scattering in the hydrogen target close to that for the previous measurements of cross section, polarization and rotation parameter. This external primary beam of polarization 46 % ±1 %, which was determined in a separate double scattering experiment, has a mean energy of 146 MeV with a spread of 8 MeV full width at half height. The sign of polarization, conventionally upwards, was determined by a p-He scattering 6)). For the second scattering a liquid hydrogen target was used which was 6 cm long (i.e. 0.432 $g \cdot cm^{-2}$ thick) and about 3 cm wide with walls of 0.005 cm Mellinex. This shape was chosen so that the scattered protons would have as high an energy as possible in order to obtain a high analysing efficiency. The third scattering was at a 2 $g \cdot cm^{-2}$ thick Be analyser, the scattered protons being detected with counter telescopes set at 12° on either side.

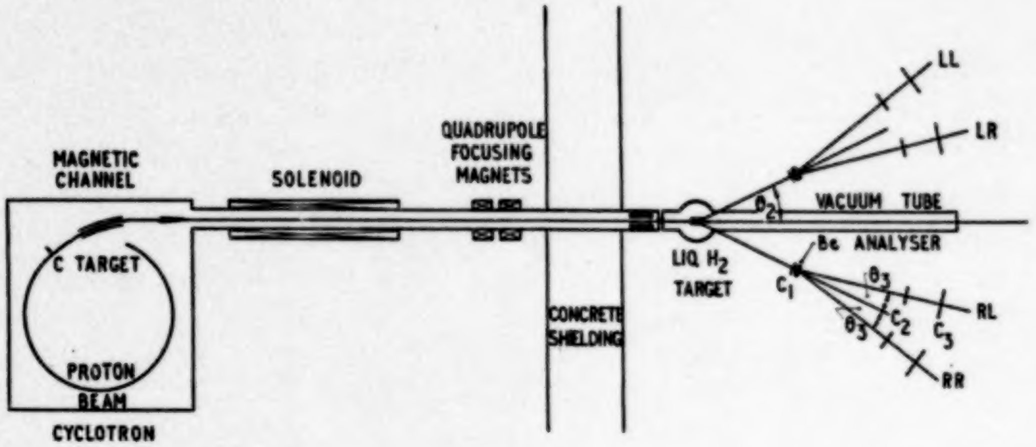

NOT TO SCALE

Fig. 1. Schematic diagram of the experimental set-up.

The counters were positioned on movable plates by means of a micrometer theodolite set up over the table pivot and a trammel. Distances from the pivot of the scattering table were laid off with the trammel and calculated angular positions were fixed accurately by the theodolite. Estimated errors for the measurements are 0.040 cm and 1′ of arc.

Different angular settings for the movable plates were found using the theodolite and a sine bar technique was adopted to fix their positions. When the pivot of the table had been carefully aligned by means of X-ray film in the primary polarized beam, the zero line of the beam was found also by film and the sine bar pinned to the zero line.

Accuracy of alignment of the hydrogen target with the beam was accomplished by X-ray film taken behind the target and using double exposures. One exposure was taken with the normal primary beam and the other with some lead in the beam in order to obtain a shadow photograph of the target (fig. 2). This procedure not only allowed the hydrogen target to be accurately positioned but also enabled the beam size and shape to be adjusted by varying the currents of the quadrupole magnets so that it was well clear of the target body. Since the measurements would be most sensitive to movements of the beam centre of gravity in a horizontal plane, the beam shape adopted was tall and thin and small bending magnets were employed to place all beams accurately through the target.

Although the counter geometry was such that the triple coincidence telescopes could not directly see the liquid hydrogen target it was inevitable that they should look at some part of the primary beam, and the last two counters considered as a doubles telescope would see much more of the beam. In order to avoid the possibility of air scattering which would lead to an awkward background and high random counting rates, the primary beam was contained in a vacuum pipe to a position well behind the counters and the scattered beam was brought out through a long 0.013 cm Mellinex window.

Front plastic scintillators were made 0.254 cm thick, 3 cm wide × 5 cm high, and placed 1 cm in front of the Be analyser centre, which was positioned 80 cm from the table pivot. The analysing telescopes to left and right were at 12° with a 0.127 cm thick scintillator, 2.75×5 cm, at 50 cm from the Be and a 0.127 cm thick scintillator, 5.2×8.8 cm, a further 17 cm away.

Pulses from the front counter, defining the second scattering angle, were split and fed into two transistorized coincidence circuits designed by Chaplin and Candy [7]). One circuit measured triple coincidences between the first and the two left counters whereas the other measured triples between the first and right counters. Three sets of analysing telescopes were set up on either side of the second scatterer on movable plates so that D could be measured simultaneously at a number of angles. Counters were set up on voltage and delay plateaux in the usual way and these were checked at the beginning of each run.

Although the experiment is self-monitoring, the primary beam was monitored by an ionization chamber placed behind the apparatus. This chamber output was used as the input to a count down circuit for stopping the scalers automatically. It also allowed a continuous check of beam level and enabled the cyclotron to be kept always "on tune". It also made possible a proper subtraction of the backgrounds although, since these were very small, the asymmetries were rather insensitive to the exact ratio of proton flux per monitor count for the two conditions target full and empty.

4. Analysing Power for D

The earlier D and R determinations here [8]) and at Harvard [9,10]) had shown that there were no significant differences between separate measurements of

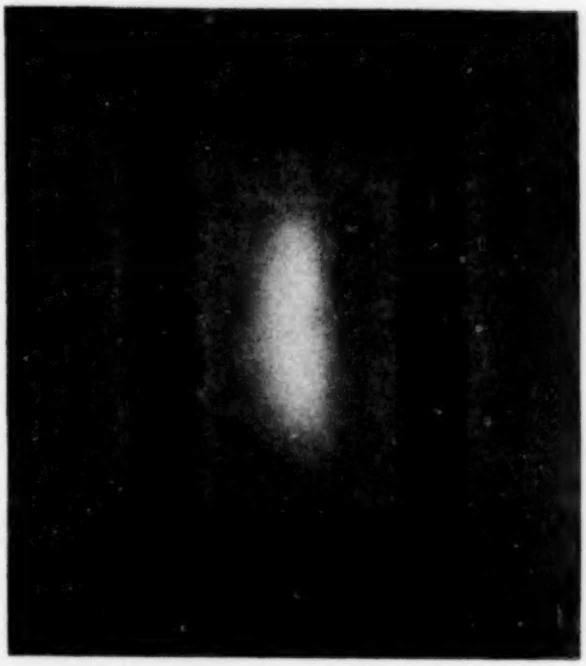

Fig. 2. Shadow photograph of beam through hydrogen target.

L. BIRD *et al.*
Facing p. 590

A_3 with the triple scattering apparatus and other published values. Hence, for the present experiment where the separate measurement of A_3 was not possible without removing the H target, interpolated mean values were used. Since the analysing power P_1A_3 decreases rapidly with increase of scattering angle, because of the decrease in the effective energy of the scattered protons, the target was made as small as possible, taking into account counting rates and beam size, so that energy loss through the target should be as low as possible. Even so at 40° the effective energy of the scattered protons at the centre of the Be analyser was 68 MeV and the value adopted for P_1A_3 was 0.075. Consequently the statistical error on D for a given number of counts progressively increases with increasing θ_2.

5. Background

The earlier D experiment had been subject to troublesome background scattering from the thin Be-Cu and Ni windows on target and vacuum container and from the air path immediately after the target assembly. This air scattering was shielded off in that experiment whereas in the present one it was thought advisable to contain the proton beam in a vacuum tube to a point behind the counting set up. Also Melinex windows were used, 0.005 cm on the liquid hydrogen target and 0.013 cm on the long slit windows bringing the beam out of the vacuum chamber. By this means the background was kept down to 2 % for all angles except 15° where it was 10 %. A range-energy measurement at each angle was made in order to decide upon the aluminium absorber needed in the analysing telescopes. Background measurements were made by emptying the liquid hydrogen target and increasing the analysing telescope absorbers an equivalent amount. Tests were made to see where the background was coming from and the counts obtained indicated that there was less than 0.25 % neutron contamination in the beam and that nearly all the background came from the target except at 45° where only about half of the background came from the target.

6. Systematic Errors

The use of a solenoid to rotate the proton spin instead of swinging the analysing telescope from side to side removes the geometrical systematic errors, provided that the centre of gravity of the incident beam does not change as the solenoid current is changed. Exhaustive tests during the measurement [8]) of R had shown that the changes of counting rate and asymmetry for changes of beam position were those to be expected. However, various checks were made in this experiment to determine the magnitude of any systematic error brought about by these changes.

Beam photographs immediately behind the target were taken for all conditions at the start and finish of every run and the centre of gravity was found ro change by less than 0.05 cm. Measurements were also made of the scattered beam profile by scanning across it with a small counter in coincidence with the first counter in the telescope. This small counter was placed in the position of the second counter in the telescope in order to obtain the angular variation of the scattered beam. The shape obtained corresponded to that expected from the known geometry and angular variation of cross section and polarization and showed that the variation of intensity across the beam, which differed slightly for the different spin direction, was about 10 %. This variation would correspond to a difference between the optical alignment and scattered beam directions of less than 0.02°. These measurements determined directly the change in θ_3 brought about not only by the change in beam position at the target but also by the reversal of the spin and indicated that the change in θ_3 was less than 0.014° between the different spin directions.

In order to estimate the correction to be made to the measured asymmetries arising from the changes in θ_3, it was necesssary to know the counting rates as a function of θ_3. For this purpose the analysing angles were changed either to 11° or 13°. The measured variation of counting rate was 10 % per degree at $\theta_2 = 15°$ falling to 4 % per degree at $\theta_2 = 45°$ in agreement with published values of the differential cross section. The calculated corrections based upon these values are shown in table 1.

In addition, various experimental ratios may be formed from the results which would reveal different sources of the systematic errors. For instance the spin down counting rates can be compared for +180° and −180 ° precession designated N and R. Under these two conditions there is a known beam shift at the target of about 4 times the magnitude of that between the mean spin down and spin up conditions and the beam intensities differed by 12 %. This larger beam shift arises from the fact that positive and negative directions of precession produce beam shifts in opposite directions, whereas the mean position of the beam for 180° precession is close to the unprecessed position. The mean of the ratios

$$\frac{\mathrm{LL^N}}{\mathrm{LL^R}}\,\frac{\mathrm{RR^R}}{\mathrm{RR^N}} \quad \text{and} \quad \frac{\mathrm{LR^R}}{\mathrm{LR^N}}\,\frac{\mathrm{RL^N}}{\mathrm{RL^R}}$$

should be sensitive to beam movement only. For all the angles the mean value is 1.002 ± 0.025, compared with the value of 1.002 expected from the known movement of beam and variation of counting rate. Since the beam shift at the target between spin up and the mean of the two spin down conditions was less than that between the two spin down conditions, the very small and calculable correction to D will be smaller than indicated by these values. The alternative ratios taken,

$$\frac{\mathrm{LL^N}}{\mathrm{LL^R}}\,\frac{\mathrm{RR^N}}{\mathrm{RR^R}} \quad \text{and} \quad \frac{\mathrm{LR^N}}{\mathrm{LR^R}}\,\frac{\mathrm{RL^N}}{\mathrm{RL^R}},$$

are largely independent of beam movement but sensitive to the different beam intensities. The mean value obtained 1.015±0.025 is consistent with that to be expected from the known non-linearity of the monitor. However, the measured values of asymmetry used in calculating D are independent of the monitor.

As a final check one measurement was made using an unpolarized beam for the laboratory angels 15°, 20° and 35°. The measured asymmetries were sensibly zero with a weighted mean value of 0.0052±0.007.

Since these checks showed that the small systematic errors were not greater than could be accounted for, the corrections to D have been based upon these measurements, and they are given by the expression

$$\frac{1}{P_1A_3}\frac{1}{C}\frac{\mathrm{d}C}{\mathrm{d}\theta_3}\Delta\theta_3,$$

where $(1/C)\ (\mathrm{d}C/\mathrm{d}\theta_3)$ is the fractional variation of counting rate with θ_3 and $2\Delta\theta_3$ is the difference between θ_3 for spin up and spin down. As P_1A_3 decreases with θ_2 at about the same rate as $(1/C)\ (\mathrm{d}C/\mathrm{d}\theta_3)$ does, the correction is nearly constant and in fact less than 0.01. This is considerably smaller than the statistical errors.

7. Results

The values of D obtained in this experiment are given in table 1 together with the Harvard [10]) and previous Harwell [8]) values. Also included are the measured asymmetries, the values used for the analysing power P_1A_3 and the calculated corrections to the asymmetries. The values of A_2 determined from the triple scattering data are also included and for comparison the values obtained earlier in a double scattering experiment [1]).

There was no significant difference in the asymmetries obtained between the spin up conditions and either of the spin down conditions i.e. precession by ±180°, the experimental difference being 0.0015±0.007. This was again confirmation that systematic errors were small and probably considerably smaller than the statistical counting errors, which are those given in table 1. The results for $\theta_2 = 20°$ and 25° were obtained with two different sets of telescopes and again no significant differences were noticed.

8. Discussion

From table 1 it is seen that there is no great discrepancy between the three measurements of D up to $\theta_2 = 30°$. Beyond this angle the early Harwell results gave values more negative and the Harvard results gave values more positive than in the present experiment. Perhaps too much emphasis should not be laid on the last points of the previous determinations in which, because of the low analysing power, systematic errors are the most serious. In the lastest determination it is believed that such systematic errors as could arise in the earlier

TABLE 1

Values of D

θ_2 (lab.)	θ_2 (c.m.)	Measured DP_1A_2	Correction to DP_1A_2	Analysing power P_1A_2	D	D (previous Harwell data)	D (Harvard)	A_2 (this experiment)	A_2 (double scattering data)
15	31	+0.0176 ±0.0166	0.0010	0.215	+0.082 ±0.077	+0.215 ±0.080	+0.137 ±0.033	+0.217 ±0.036	+0.241 ±0.010
20	41	+0.0324 ±0.0080	0.0006	0.200	+0.162 ±0.040	+0.065 ±0.070	+0.156 ±0.031	0.280 ±0.020	+0.239 ±0.010
25	51½	+0.0193 ±0.0088	0.0006	0.175	+0.110 ±0.050	−0.015 ±0.085	+0.178 ±0.033	0.223 ±0.020	0.230 ±0.006
30	62	+0.0054 ±0.0072	0.0006	0.120	+0.045 ±0.060	−0.145 ±0.110	+0.076 ±0.031	0.165 ±0.024	0.180 ±0.005
35	72	+0.0019 ±0.010	0.0007	0.100	+0.019 ±0.100	−0.340 ±0.150	+0.147 ±0.070	0.127 ±0.022	0.119 ±0.006
40	82	−0.00275 ±0.010	0.0004	0.075	−0.037 ±0.133		+0.286 ±0.099	0.046 ±0.022	0.051 ±0.015
45	92	−0.00135 ±0.0085	0.0003	0.050	−0.027 ±0.170			−0.0078 ±0.020	−0.008

measurements are not now present and that any others are negligible. For this reason this determination should be regarded as superseding the previous measurement.

The values of D obtained in this experiment have been used [11]) together with the $d\sigma/d\Omega$, P and R data at the same energy [1, 8]) for a phase shift analysis.

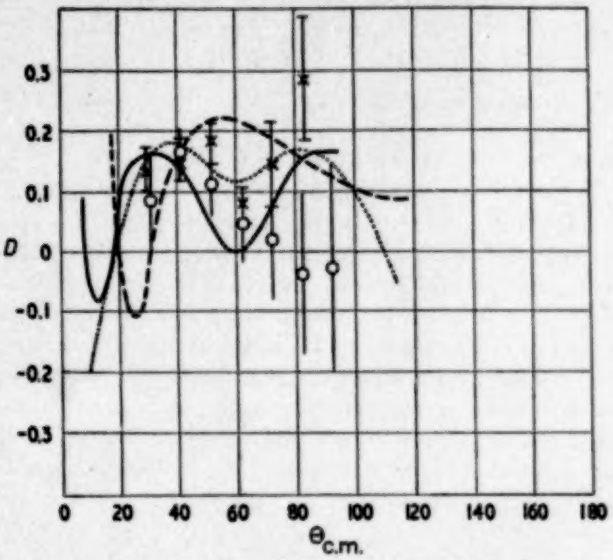

Fig. 3. The depolarization parameter D in p-p scattering as a function of $\theta_{c.m.}$ at 143 MeV. ɸ Harwell. ⌶ Harvard. ——— Gammel and Thaler. ...... Saylor, Bryan and Marshak. - - - - - Perring.

Two solutions were found, corresponding to the Stapp no. 1 and no. 2 solutions [12]) at 310 MeV. Analysis of lower energy data would tend to eliminate the type no. 2 solution by the unrealistic value of the S phase shift. The results [13]) of an analysis at 210 MeV tend to suggest that a smooth extrapolation to the no. 1 solution at 310 MeV is obtained with the remaining solution at 142 MeV.

In fig. 3 these latest values of D are compared with the prediction of the GT potential [3]) and the Saylor, Bryan and Marshak model [5]). Also included is the fit obtained by Perring [11]) in a phase shift analysis using this information together with the $d\sigma/d\Omega$, P and R data at the same energy.

References

1) Taylor, Wood and Bird, Nuclear Physics **16** (1960) 320
2) L. Wolfenstein, Ann. Rev. Nuc. Sci **6** (1956) 43
3) Gammel and Thaler, Phys. Rev. **107** (1957) 291
4) Signell, Zinn and Marshak, Phys. Rev. Lett. **1** (1958) 416
5) Saylor, Bryan and Marshak, Phys. Rev. Lett. **5** (1960) 266
6) Brinkworth and Rose, Nuovo Cim. **3** 1956) 195
7) Chaplin and Candy, Nuc. Inst. and Methods **5** (1959) 242
8) Bird, Edwards, Rose, Taylor and Wood, to be submitted to Nuclear Physics
9) Thorndike, Lefrancais and Wilson, Phys. Rev. **120** (1960) 1819
10) Hwang, Opel, Thorndike and Wilson, Phys. Rev. **119** (1960) 352
11) J. Perring, Nuclear Physics **23** (1961) 153
12) Cziffa, Moravscik, MacGregory and Stapp, Phys. Rev. **114** (1959) 880
13) MacGregor and Moravcsik. Phys. Rev. Lett. **4** (1960) 524

2.F

Nuclear Physics **27** (1961) 596—605; © *North-Holland Publishing Co., Amsterdam*

Not to be reproduced by photoprint or microfilm without written permission from the publisher

GROSS STRUCTURE IN REACTIONS OF DEFORMED NUCLEI

R. A. PECK, Jr.
Brown University, Providence, Rhode Island †

Received 19 May 1961

Abstract: The Nilsson model is applied to determine the effect of nuclear deformation on gross structure in direct reaction spectra among intermediate nuclei. While the gross structure known for spherical nuclei is obscured to low resolution observations, it is replaced by an equally distinctive pattern whose major features are fixed relative to single nucleon levels in the *undeformed* well. Definite minima in the spectrum persist at magic number gaps even for fairly large deformations. Location of the gross structure pattern on a nuclear excitation scale is determined by deformation and nucleon population numbers, so that shifts of the structure among spectra of neighbouring nuclei are definite and predictable. The angular distribution in each part of the spectrum should be dominated by a few specific $l_{\min}$ values even though the single particle l is not a quantum number and parities are mixed. The effects are illustrated numerically with respect to the (n, p) reaction on target isotopes of Rh, In and Sb.

1. Introduction

In an attempt to study gross structure in (n, p) spectra, an experimental survey has been made of charged particle distributions resulting from the neutron bombardment of six nuclei in the mass range 100–120. The distributions (published elsewhere [1])) fail in this purpose because of strong (n, d) groups which obscure the (n, p) yield over most of the accessible energy range ††. However, preliminary consideration of the influence of the finite core deformation which obtains in the intermediate mass region has suggested a number of qualitative modifications in the anticipated character of (n, p) gross structure. These effects, some of which are sufficiently interesting to warrant experimental attention, will be described and illustrated by numerical application to the (n, p) reactions leading to Ru^{103}, Cd^{115} and Sn^{121}.

For intermediate coupling between nucleon and core, the strength function is characterized by broad resonances in excitation ranges dominated by single nucleon excitations [2]). These maxima in the envelope of reduced widths for individual levels may be seen in reaction spectra so displayed as to combine at every data point contributions from a number of true levels, as in low resolution experiments. Each maximum is attributed to the predominance of

---

† Work supported in part by the U. S. Atomic Energy Commission.

†† The (n, d) data have no relevance to gross structure since they lead to resolved levels in the cases studied.

a particular single nucleon excitation, for levels near to it in excitation, in the expansion of the nuclear wave function in a complete set of single particle eigenfunctions. Since each such dominating term is associated with a particular particle orbital quantum number (l), that value should influence the angular distribution within the gross structure peak to the same extent as the energy of the single particle excitation shapes the local intensity pattern in forming that peak.

The gross structure to be expected in a survey of reactions on neighbouring nuclei thus reflects properties of the accessible single nucleon levels, which will be very similar for the different nuclei in the absence of deformation. Specifically, for neutron-addition reactions such as (n, p) and (d, p), all the spectra should display the same gross pattern with peaks at energies corresponding to single neutron levels in the common well. The patterns should be aligned on a residual excitation scale for those nuclei having the same neutron configuration in the ground state and otherwise be displaced by the energy difference of the ground state neutron configurations. The angular distribution of each gross structure group should have the direct interaction form [†] appropriate to l_n of the neutron level to which it corresponds, the same for each reaction in which the group appears. These features have been exploited in detail for (d, p) gross structure among near-spherical nuclei [3]). No detailed studies of (n, p) gross structure have yet been published.

2. Effects of Core Deformation

In a deformed core single nucleon levels [††] lose most of their spherical-well degeneracy and are displaced rapidly with increasing deformation. For even the most nearly spherical nuclei of intermediate mass, the separation of component levels is comparable to that between major shells in the undeformed well, and substantially larger than that between single particle levels within a shell. It may therefore be supposed that all reference to the spherical well positions is lost. In fact, the proliferation of single nucleon levels by the reduction of degeneracy produces so many "gross structure" peaks that very good energy resolution is required to distinguish them at all [5]). Further, while the direct interaction type of angular distribution should persists, it is not to be expected that l_n will be a relevant parameter since it is not a quantum number in a non-spherical well.

[†] In the intermediate coupling situation the bulk of the reaction yield, falling within one or another of the gross structure groups, is dominated by some configuration of single neutron excitation. Insofar as such a configuration dominates in formation of the product nucleus, the core configuration is unaltered and the process is describable as a direct interaction.

[††] All information on single nucleon states in a deformed well utilized in this paper has been taken from ref. [4]). Nilsson's deformation parameter δ is used.

We now inquire about the systematic characteristics of the distributions from deformed nuclei to be seen with the same low resolution that reveals the ordinary gross structure from undeformed nuclei. The following effects are found. (1) The spectrum so obtained is modulated by a new form of gross structure, related to the level pattern in a spherical well. Hence, as in the spherical case, the structure should be essentially the same in reactions on neighbouring nuclei. (2) The yield is concentrated in broad bands of the spectrum extending over regions of excitation occupied, in the sperical well, by single nucleon levels of one oscillator shell, and separated by marked gaps at excitations corresponding to the intervals between shells. (3) The structure is almost everywhere independent of the population number of the active nucleon, and relatively insensitive to δ. In particular, the major gaps persist up to deformations at which they have been crossed by many single particle levels. (4) In contrast, the location of the nuclear ground state relative to the gross structure changes rapidly with δ, and hence from one nucleus to a neighbour. However, the relative position of the ground state fluctuates within a fairly narrow range so that a small change in δ is as effective, on the average, as a large change in altering the placement of the gross structure as observed on a scale of residual nuclear excitation. (5) The angular distributions can still be formulated in terms of single nucleon orbitals, with a definite mixture of terms in each part of the spectrum.

The basis of the first three statements is that the density of single nucleon levels in the non-spherical potential, which is the function (of excitation) displaying the gross structure described, varies slowly with δ at a fixed energy relative to the spherical well levels. Levels lost to a given excitation interval through a change in δ are roughly balanced by intrusions, since the divergence of levels [†] with increasing δ is roughly symmetrical about the spherical well positions, almost linear with δ and at a rate not initially very sensitive to l. Hence peaks in single nucleon level density tend to persist near the degenerate spherical well positions, as δ is increased, the closer ones (those within a shell) merging but the gaps between different shell concentrations remaining sparsely populated even after having been traversed many times. Hence the areas of greatest level density in the deformed well correspond to clustering in the spherical well, over a broad range of δ. Further, since the population number of the active nucleon affects only the lowest single nucleon level contributing to the density function, that function is independent of the population number (for fixed δ) except near the nuclear ground state.

[†] In the distorted oscillator potential [4]) the perturbation of a single nucleon level from its position in the isotropic potential is proportional to an odd polynomial in δ and the mean square radial variable. Dependence on deformation is implicit in the second factor as well as explicit in the first. Since the deformations relevant to actual nuclei of intermediate mass are small relative to unity, the polynomial is approximated by its first term and the radial factor by its value for harmonic oscillator eigenfunctions. In this approximation the energy shift is proportional to δ, the proportionality factor depending only on the oscillator number. The latter is the same for all levels originating within a given shell and for intermediate nuclei varies by only 15 % – 20 % from one shell to the next.

The position of the nuclear ground state relative to the gross structure pattern depends on the population number of the added nucleon both directly and indirectly, through the deformation parameter which varies with it. The resulting displacement of the pattern from one nucleus to the next is rapid, but limited in magnitude by the crossing of levels. When the Fermi level for a particular nucleon number is crossed by another level, the latter becomes the Fermi level and reverses the sense of the variation with δ. Further, half of the time a rise in the ground level due to an increase in nucleon numbers is opposed by an energy depression resulting from the consequent deformation change.

Finally, while the single nucleon orbital angular momentum is not a constant of motion in the Nilsson eigenstates, the eigenfunction expansion coefficients identify relative frequencies of occurrence of the various l values contained in each state [†]. A direct interaction involving one Nilsson eigenstate may be expected to behave as a composite of processes involving pure l values with these frequencies. Similarly, the various $l_{\min}$ values entering the angular distribution of a direct reaction linking one eigenstate to another should have weights predictable by appropriate summation of products of the frequency coefficients, so that weights for the various possible $l_{\min}$ values can be computed for each portion of a gross structure spectrum. In some cases a single $l_{\min}$ dominates a given part of the gross structure as if the well were undeformed; in others, up to three or four, of mixed parities, are equi-probable. Each inter-shell gap occasions a substantial change in the pattern of contributing $l_{\min}$ values, and hence in the angular distribution.

3. Illustrations

The figures illustrate effects discussed for the nuclei ${}_{44}\mathrm{Ru}_{59}^{103}$, ${}_{48}\mathrm{Cd}_{67}^{115}$ and ${}_{50}\mathrm{Sn}_{71}^{121}$. These were chosen since they are the products of three of the (n, p) reactions studied experimentally [1]), but only fig. 3 is specific to the reaction by which the nucleus is formed.

In fig. 1 the density of single neutron levels in the deformed well is plotted as a function of excitation on a scale [††] fixed relative to spherical well positions.

[†] Actually, l is an effective quantum number to the extent of 80 % –90 % for most eigenstates, under reasonable deformations.

[††] To use the Nilsson level diagram for quantitative predictions it is necessary to adjust the energy scale for the mass region under study. The adjustment has been made [7]) by reference to a number of spherical-well level positions deduced from reaction Q-values. The resulting scale factor, approximately [illegible] the numerical estimate of ref. [4]), is internally consistent to good accuracy and in reasonable agreement with the representation of Cohen and Price [5]) for the same mass region.

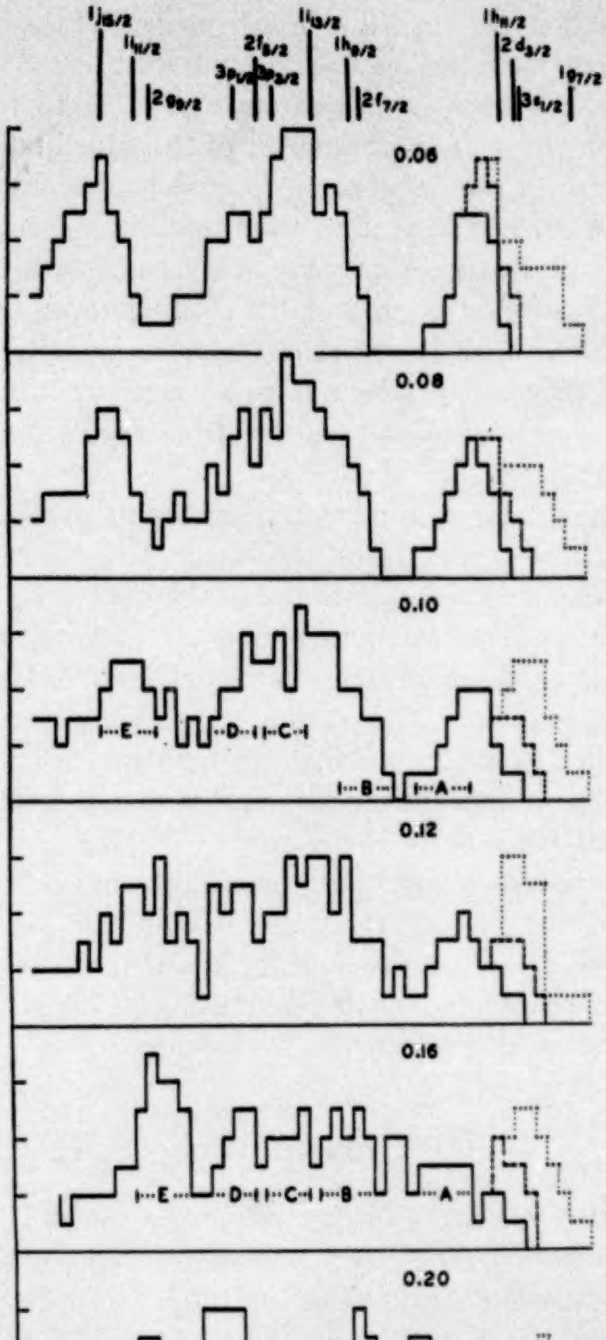

Fig. 1. Single neutron level density in a deformed well. The abscissa is the excitation energy (MeV) on a scale fixed relative to the degenerate level positions in a spherical well, indicated at the top of the diagram. The origin is arbitrarily set at the $1g_{7/2}$ level. The ordinate is the number of levels within the excitation range 0.6 MeV; scale unit = 2 levels. Each histogram is labelled with the deformation (δ of ref. [4])), all values being positive. At low lexcitations the solid line refers to 71, the dashed line to 67 and the dotted line to 59 neutrons; elsewhere, the same histogram applies to each neutron number. Energy groups (A ⋯ E) are those for which angular distribution components are displayed in fig. 3(Ru^{103}, 59 neutrons, $\delta = +0.20$; Cd^{115}, 67 neutrons, $\delta = +0.16$; Sn^{121}, 71 neutrons, $\delta = +0.10$).

This function will affect a low resolution (n, p) or (d, p) spectrum as a modulating factor and may in fact largely determine the shape of the spectrum, since the remaining factor (neutron strength function averaged not only over many nuclear levels but also over contributions from several different types of single neutron levels) is unlikely to vary rapidly. The density plotted is the number of single neutron levels falling within an energy interval of 0.6 MeV, representing the combined effects of beam inhomogeneity and detector channel width in a spectrum determination. The value 0.6 MeV is the one appropriate to the experimental study which was made. Use of a histrogram interval smaller than the energy resolution, resulting in a redundant presentation, conforms to common experimental practice.

The minima at 3 and 7 MeV bound the set of levels of the sixth shell, and correspond to neutron numbers 82 and 126. The first is still visible at $\delta = +0.14$ but is obscured thereafter by an intruding group; the second does not close before $\delta = +0.20$. These gaps, and in fact all of the gross structure above 1–2 MeV, are independent of variations in neutron population so long as the core is not affected. Structure within the central mass changes more rapidly with deformation.

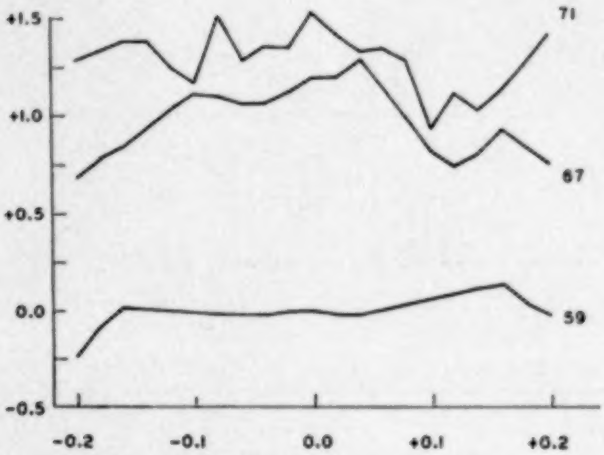

Fig. 2. Fermi level position as a function of deformation (δ) for neutron numbers as labelled. The ordinate is the position of the single neutron level occupied in the ground state by the last neutron, on the energy scale of fig. 1.

Shifts, relative to a conventional excitation scale, of the gross structures from neighbouring nuclei are expressed in the varying starting points of fig. 1. As noted in the general discussion, they are erratic and never very large. These shifts are displayed explicitly in fig. 2, showing the position of the Fermi level for each of three neutron numbers as a function of deformation. The variation in the absolute position of each level is rather small as result of the crossing phenomenon, and the variation in spacing often smaller still as a result of roughly parallel trends. For the nuclei considered explicitly, calculated shifts of gross structure between successive reaction spectra vary within ±0.2 MeV for any combination of deformation parameters within ±50 % of the nominal values [6]). Thus the gross structure shift can in most cases be predicted with fair accuracy from even a crude value of δ.

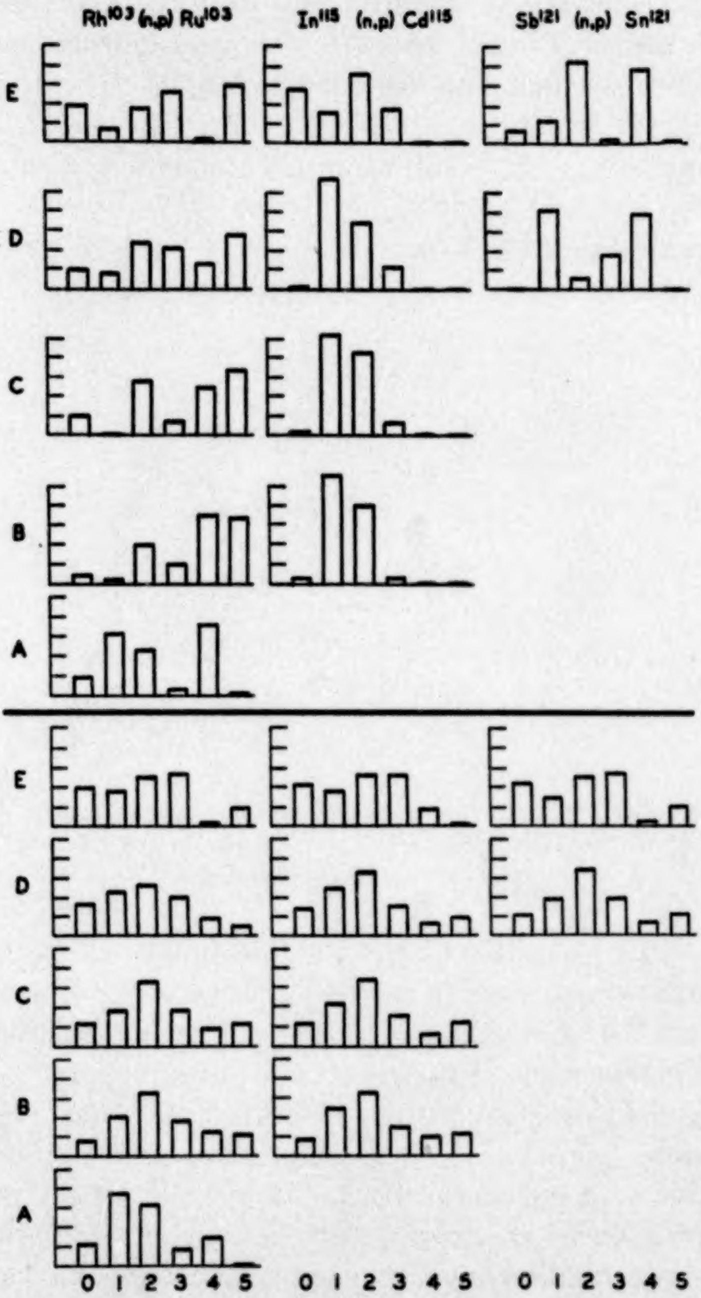

Fig. 3. Angular distribution components. The abscissa is $l_{\min} = |l_n - l_p|$. The ordinate is the relative frequency of occurrence of the possible $l_{\min}$ values in each gross structure group, normalized to unit sum for each distribution for the reaction at the head of each column and the energy group at the left of each row (defined in fig. 1). Scale unit = 10 %. In the upper half of the figure, only the unpaired target proton contributes; below, contributions are included from all protons in the fourth shell.

Fig. 3 shows the relative weights with which the various possible direct interaction forms should enter the angular distributions of different parts of the spectra of three illustrative (n, p) reactions[†]. The ordinates for each group constitute a normalized set of frequencies of occurrence of the various l_{min}, in the set of all possible combinations of single proton level (target) and single neutron level (product) consistent with the definition of the energy group (fig. 1). In the upper half of the figure, only the proton unpaired in the target is assumed to participate. In the lower half, contributions with equal *a priori* probabilities are included of all protons in the same shell (or, for the antimony target, the shell preceding). Suppression of contributions by the more tightly bound protons[††] should come about only gradually, through shielding by the outer ones, and at the excitations represented by the strong gross structure there is no energetic bar to such contributions. In all cases illustrated the next several protons after the unpaired one contribute virtually the same distribution of l_{min} values.

The eigenfunction parameters tabulated by Nilsson[4]), identified as $A_{l\Lambda}$, are wave function coefficients with arbitrary normalization. Hence, in a particular state (reference number N) at a definite deformation, the probability of occurrence of the single nucleon orbital angular momentum l is $\alpha(l, N) = \sum_{\Lambda} A^2_{l\Lambda}/\sum_{l\Lambda} A^2_{l\Lambda}$. Each ordinate in fig. 3 is $\sum \alpha(l_{\mathrm{p}}, N_{\mathrm{p}})\alpha(l_{\mathrm{n}}, N_{\mathrm{n}})$; the summation is fourfold, extended over all of the product neutron states (N_{n}) which fall within the energy group being described, over the states of all target protons (N_{p}) which are assumed to contribute, and over all combinations of l_{p} and l_{n} which are consistent with the condition $|l_{\mathrm{n}}-l_{\mathrm{p}}| = l_{\mathrm{min}}$. (The parity condition is automatically satisfied by this form of the combination rule.) In an alternative computation (not shown), each summand contained as a third weighting factor that fraction of the yield from the neutron state (N_{n}), uniformly dispersed by experimental resolution over 0.6 MeV, which would fall within the energy group. This computation, discriminating against marginal contributions. introduced no significant change in fig. 3. Of the 66 ordinates (upper half of figure) only two were changed by more than 30 % of the values shown and half changed by 10 % or less; the effect on the lower half of fig. 3 was even smaller.

In spite of the latitude of allowed values generated by core deformation, fig. 3 shows a definite predominance of specific l_{min} terms in the gross structure angular distributions, nor is sensitivity of the distributions to the target nucleus lost so long as a unique proton state is involved. Considering contributions from all protons in the unfilled shell, we naturally suppress any reference to specific nuclei and find the same pattern of weights, reduced in structure, for neighbouring reactions. Even in this extremely homogenized situation, however, the $l_{\min}$ distribution is not uniform. Exhibiting a maximum at $l_{\min} = 2$ (for groups B, C and D) the many-proton distribution still reflects the elementary character of the (n, p) process in this region: the substitution of a sixth shell neutron for a fourth shell proton, a process involving a change of 2 in oscillator number and no change in parity.

[†] Deformation parameters have been taken from the table of Okamoto [6]), and are identified in fig. 1 (caption).

[††] Contributions from "deeper" protons are to different parts of the spectrum. In view of the relatively close packing of single particle levels near the top of a shell, however, and of the broad definition of energy groups in the gross structure, several protons are capable of contributing to the same group. The lower half of fig. 3 sets an upper limit to the effect of such contributions.

A strong parity preference might be anticipated for each energy group in fig. 3, especially in the upper half, inasmuch as the single particle levels comprising an oscillator shell are parity-pure except for the one intruding member of the lowest spin-orbit doublet arising in the shell above. However, parities are seen to be well mixed in all cases. The reason for this mixing is that the off-parity intruder, having a higher angular momentum j than any levels in the shell entered, has a degeneracy comparable to all of theirs combined and so makes an anomalously strong contribution to the local single particle level density in the deformed potential. Mixed parity is thus a systematic property of the gross structure and not peculiar to the illustrative nuclei.

Marked changes in the distribution of $l_{\min}$ values occur only between groups E and D and between B and A, and so are associated with the major minima in the gross structure. This is the more remarkable in that, at the deformations involved in fig. 3, the corresponding gaps in the single particle level scheme have been traversed by numerous single levels; in fact, the minima themselves are barely visible in the gross structure spectrum at these deformations (fig. 1). Even the strong homogenizing infleunce of many proton contributions fails to suppress the effect entirely.

4. Conclusion

The major gap between product levels of the fifth and sixth oscillator shells, around 3 MeV in fig. 1, has been observed in (d, p) studies with low resolution [7]) and, more recently, with resolution sufficient to show the real single neutron levels simultaneously [5]). Weaker evidence for the same gap is found in the (n, p) spectra [1]), in which the low-excitation terminus occurs at the predicted position of the minimum rather than at the ground state. No significant yield is observed, however, corresponding to single neutron levels below the 82 neutron gap. The same neutron-induced spectra show a marked and systematic dip at higher excitation, correctly placed to represent the 126 neutron gap (7 MeV in fig. 1). This part of the spectra also coincides with open intervals in the known (n, d) product levels. however, and the (n, d) procces is definitely dominant at lower excitations. The significance of the observed high-excitation minimum is therefore not clear.

Although the single particle gross structure of direct reactions is drastically altered by core deformation among intermediate nuclei, its properties are distinctive. For an experimental study one has a number of features by which to identify and check this structure: the occurrence of the major inter-shell gaps, their separation and reproducibility in reactions on neighbouring nuclei; the "fine structure" within each concentration of yield correponding to single nucleon levels of a single shell, predictable if the deformation is known; the few values of l_{min} expected to dominate the angular distribution in each portion of the spectrum; and the energy shifts required to achieve coincidence among the structures appearing in the spectra of neighbouring nuclei. It is conceivable that the sensitivity of these shifts to deformation might in some cases be utilized to determine distortion parameters.

References

1) R. A. Peck, Jr., Phys. Rev. **133** (1961) 1738
2) A. M. Lane and R. G. Thomas, Revs. Modern Phys. **30** (1958) 257 (section XI.5)
3) Schiffer, Lee and Zeidman, Phys. Rev. **110** (1958) 1216, **115** (1959) 427;
Cohen, Mead, Price, Quisenberry and Martz, Phys. Rev. **118** (1960) 499
4) S. G. Nilsson, Mat. Fys. Medd. Dan. Vid. Selsk. **29**, no. 16 (1955)
5) B. L. Cohen and R. E. Price, Nuclear Physics **17** (1960) 129
6) K. Okamoto, Phys. Rev. **110** (1958) 143
7) R. A. Peck, Jr. and J. Lowe, Phys. Rev. **114** (1959) 847, appendix

2.B

Nuclear Physics **27** (1961) 606—611; © *North-Holland Publishing Co., Amsterdam*

Not to be reproduced by photoprint or microfilm without written permission from the publisher

POLARISATION OF PROTONS ELASTICALLY SCATTERED BY Li^7 NEAR THE 441 keV RESONANCE

J. R. ROOK [†]

Department of Theoretical Physics, University of Manchester

Received 17 April 1961

Abstract: It is shown that the polarisation effects in the elastic scattering of 441 keV protons by Li^7 depends on the ratio of the contributions of the two channel spins. The magnitude of this ratio is given by measurements on the $Li^7(p, \gamma)Be^8$ process but the sign is not determined. The polarisation effects depend on this sign, being large if it is negative and small if it is positive. A shell model calculation indicates that a fit to the energy levels of Li^8 is obtained only if the sign is positive and, together with the value of the channel spin mixing ratio, identifies the value of the intermediate coupling parameter for Be^8 which is not well determined from the energy levels. It is concluded that the polarisation effects in this process are probably less than 5 %.

1. Introduction

A detector of polarised $\frac{1}{2}$ MeV protons would be of some use in the calibration of polarised proton sources. It was considered that the elastic scattering of protons by Li^7 near the 441 keV resonance could serve this purpose, but it is shown in this paper that this is probably not the case.

It is well known [1]) that there are no polarisation effects involving protons if there is only one reaction matrix element (e.g. near a resonance). The 441 keV resonance has angular momentum and parity $J^\pi = 1^+$ so that there are two allowed values of the channel spin, i.e. 1 and 2. The Breit-Wigner forms [2]) for the reaction matrix elements corresponding to these two channel spins have no phase difference between them, so that in this case also there are no polarisation effects from resonance scattering alone. However, it has been shown [3]) that large polarisation effects can arise from the interference between resonance and potential scattering. We give in sect. 2 the formulae for the polarisation arising from the $Li^7(p, p)Li^7$ process and show that it depends on the magnitude and sign of the ratio of the square roots of the reduced widths for the two channel spins. We write this ratio, in the notation of ref. [2]), as $g(2)/g(1)$ and denote it by R. The value of R^2 has been given by Neuert [4]) from measurements on the $Li^7(p, \gamma)Be^8$ process as $R^2 = 4.1 \pm 0.1$. Our calculations show that if R is negative the polarisation effects are large (≈ 40 %) while if this quantity is positive these effects are small (≈ 5 %). The sign of

---

[†] Now at the Clarendon Laboratory, Oxford

R has not been measured and can, indeed, only be determined by some kind of polarisation measurement. We calculate in sect. 3 the sign of R using the shell model wavefunctions of Soper [5]). The intermediate coupling parameter a/K for Li^7 is given in ref. [5]) as 1.5 but that for Be^8 is obtained with a value of a/K between 1 and 2. Our calculations indicate that a value of a/K for Be^8 of 1.8 agrees with the measurements of ref. [4]) and that the sign of R for this value of a/K is positive. Thus we conclude that the polarisation effects are probably small.

2. Formulae for the Polarization

We use the techniques described in ref. [3]) for the calculation of the polarisation and adhere to the notation used there. In particular we denote by $W_0(\theta)$ the angular distribution observed when no polarisation measurements are made, and by $W_1(\theta)$, the addition to $W_0(\theta)$ when the outgoing beam is measured using detectors whose polarisation sensitivity is described by a vector $\mathbf{P}^{\mathrm{d}}$, defined as in ref. [1])†. The quantity $W_0(\theta)$ is the sum of three terms representing the potential and resonance scattering and the interference between the two. The effect of potential scattering other than Coulomb is very small in this process and is neglected. We thus write

$$W_0(\theta) = W_{\text{res.}}(\theta)+W_{\text{Coul.}}(\theta)+W_{\text{Coul.res.}}(\theta). \tag{1}$$

The quantity $W_{\text{Coul.}}(\theta)$ is given by

$$W_{\text{Coul.}}(\theta) = Z^2 \operatorname{cosec}^4 \tfrac{1}{2}\theta, \tag{2}$$

where $Z = 3e^2/2Mv$, the quantities e, M and v being the electronic charge, the reduced proton mass and the relative velocity of the proton and Li^7 nucleus.

The resonance term is given by

$$W_{\text{res}} = \frac{3\lambda\!\!\!^{-2}}{32}\left\{1+\frac{1}{2}\,\frac{1-\frac{1}{5}R^2}{1+R^2}\,P_2\,(\cos\theta)\right\}\frac{\Gamma^2}{(E-E_0)^2+\frac{1}{4}\Gamma^2}, \tag{3}$$

where $\lambda\!\!\!^{-}$ is the reduced wavelength of the proton in the centre-of-mass system and R is the ratio defined above. The quantity E_0 is the resonance energy, Γ represents the total width of the resonance and E is the bombarding energy.

The interference term is given by

$$W_{\text{Coul.res.}}(\theta) = \frac{3\lambda\!\!\!^{-}Z}{8}\,\frac{\Gamma \operatorname{cosec}^2 \frac{1}{2}\theta P_1(\cos\theta)}{\{(E-E_0)^2+\frac{1}{4}\Gamma^2\}^{\frac{1}{2}}}\sin(2\eta \log \sin \tfrac{1}{2}\theta+2\phi+\beta), \tag{4}$$

---

† If instead the initial beam is polarised exactly the same expression is obtained for $W_1(\theta)$ but $\mathbf{P}^{\mathrm{d}}$ now refers to the polarisation of the initial beam.

where the quantities η, ϕ and β are given by the equations

$$\eta = \frac{3e^2}{\hbar v}, \qquad e^{2i\phi} = \frac{1+i\eta}{1-i\eta}, \qquad \tan\beta = \frac{2(E-E_0)}{\Gamma}.$$

It is observed, as expected, that the sign of R does not appear in the formulae, indicating the absence of channel spin mixing.

The polarisation term is given by

$$W_1(\theta) = \frac{3\lambda Z}{32}\mathbf{P}^D\cdot\mathbf{n}P_1{}^1(\cos\theta)\,\frac{\Gamma\operatorname{cosec}^2\frac{1}{2}\theta}{\{(E-E_0)^2+\frac{1}{4}\Gamma^2\}^{\frac{1}{2}}} \times \frac{1+2\sqrt{5}R-3R^2}{1+R^2}\cos(2\eta\log\sin\tfrac{1}{2}\theta+2\phi+\beta), \tag{5}$$

where $\mathbf{n}$ represents the normal to the reaction, i.e. $\mathbf{n} = \mathbf{k}_1\times\mathbf{k}_2/|\mathbf{k}_1\times\mathbf{k}_2|$, the vectors $\mathbf{k}_1$ and $\mathbf{k}_2$ being propagation vectors for the initial and final radiations. The outgoing polarisation $\mathbf{P}(\theta)$ is given by

$$\mathbf{P}(\theta) = \frac{W_1(\theta)}{W_0(\theta)}\mathbf{n}. \tag{6}$$

In fig. 1 we show the angular dependence of the polarisation for several values of R while in fig. 2 we show an energy dependence of $P(\theta)$, for $\theta = 80°$

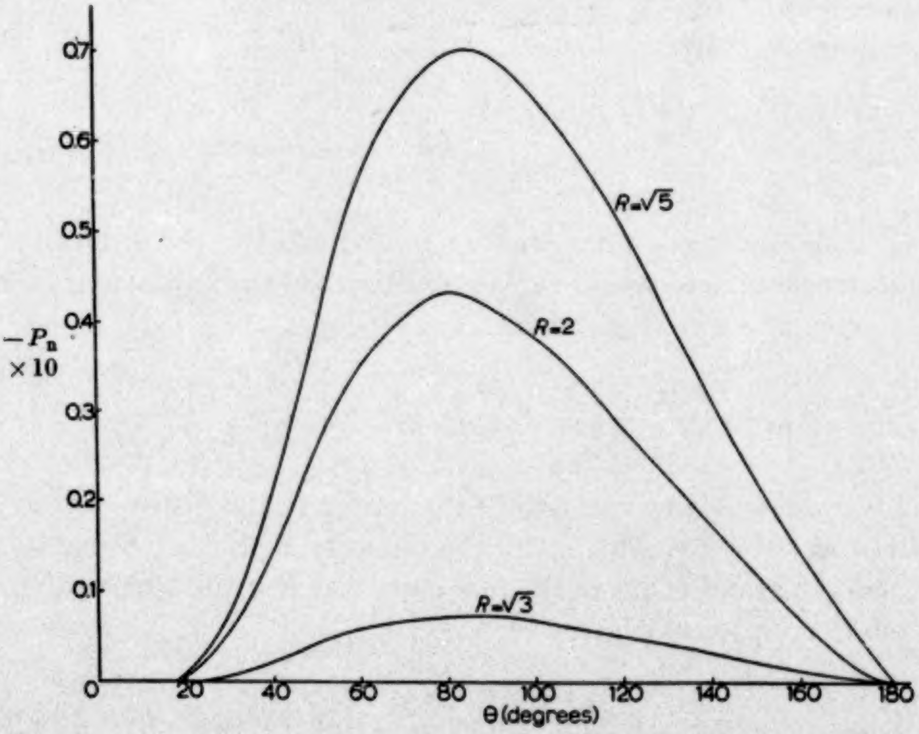

Fig. 1. Polarisation in the direction of the negative normal ($-\mathbf{n}$) of the outgoing protons from the $Li^7(p, p)Li^7$ process, as a function of the centre-of-mass angle (θ) at a proton energy $E_p = 441$ keV for indicated values of the channel-spin mixing ratio R. The sign of R is taken to be positive in accordance with the shell model calculations.

and $R = -2$. We can see from eq. (5) that the value of $P(\theta)$ is sensitive to the sign of R being large if it is negative.

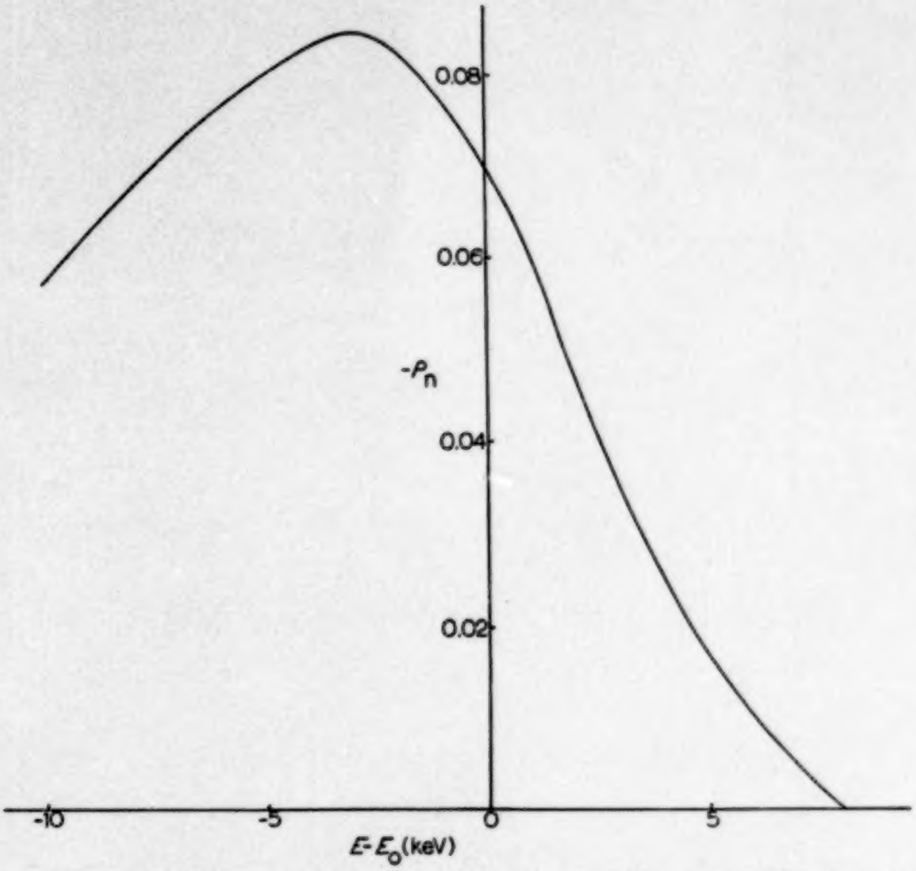

Fig. 2. Energy variation of the proton polarisation at $\theta = 80°$ for a channel spin mixing ratio $R = \sqrt{5}$. The width of the resonance Γ is taken to be 12 keV.

3. Shell Model Calculation of R

A formula for the reduced nucleon width in terms of the shell model wavefunction of the target nucleus and compound state has been given by Lane [6]). (See for this section also ref. [4])). Soper [5]) has successfully applied the shell model to the p shell nuclei. The value of the intermediate coupling parameter (a/K) for Li^7 is determined in ref. [5]) to be 1.5 but that for Be^8 is only determined, for the energy levels of Li^8, to lie between 1 and 2. We describe the states in L–S coupling in terms of the spin S and isospin T and in terms of the representation of the permutation group to which the wavefunctions belong. Thus a general L–S coupled wavefunction is represented by ${}^{2T+1,\,2S+1}L[ij\ldots]$.

The symbol in square brackets denotes the particular permutation group representation [4]). Near the L–S limit the ground state of Li^7 is almost a pure ${}^{22}\mathrm{P}[3]$ state while the particular state in Be^8 corresponding to the 441 keV resonance is approximately

$$|J\rangle = a|{}^{33}\mathrm{P}[31]\rangle + b|{}^{31}\mathrm{P}[31]\rangle. \tag{7}$$

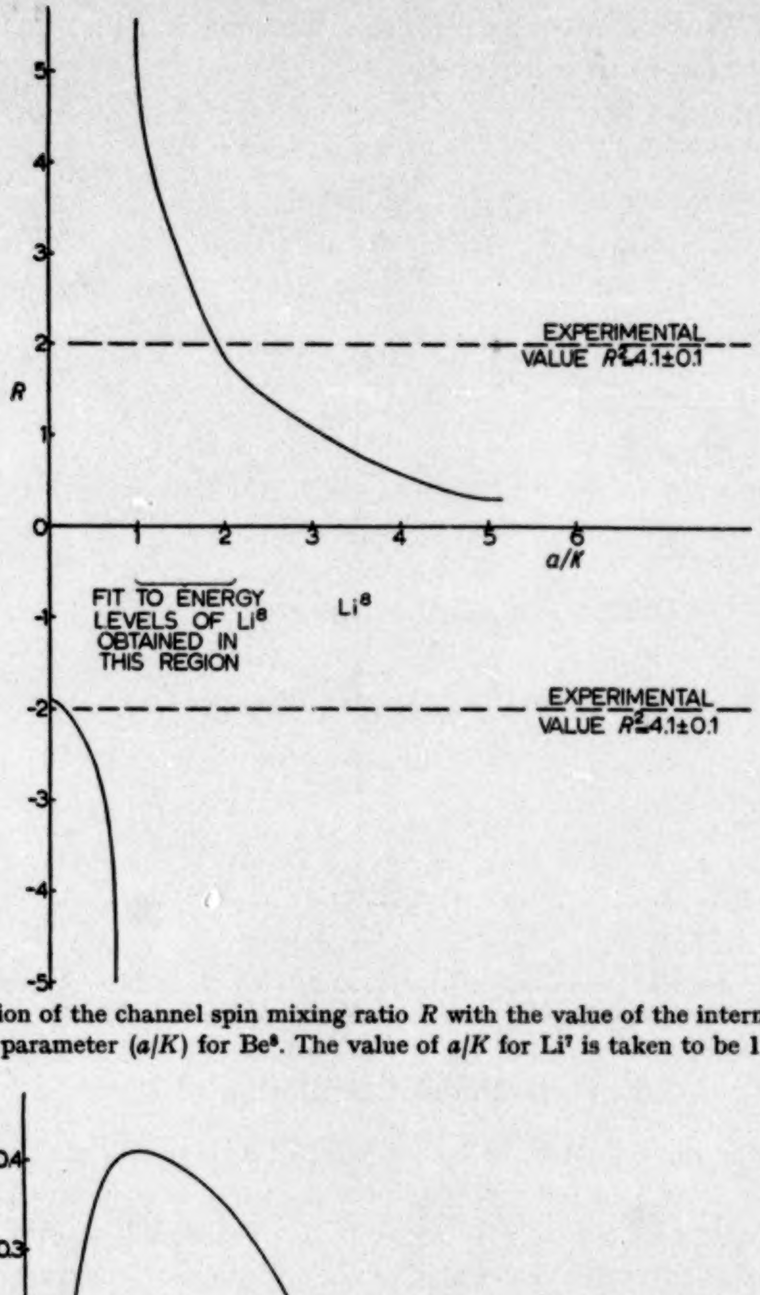

Fig. 3. Variation of the channel spin mixing ratio R with the value of the intermediate coupling parameter (a/K) for Be^8. The value of a/K for Li^7 is taken to be 1.5.

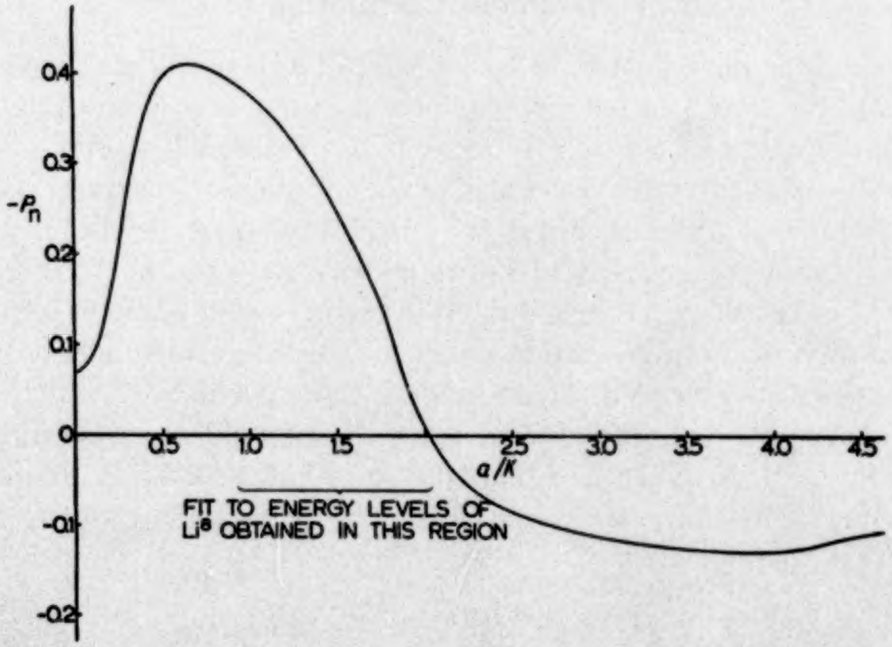

Fig. 4. Variation of the proton polarisation at $\theta = 80°$ with the intermediate coupling parameter (a/K) for Be^8 at a proton energy $E_p = 441$ keV. The value of the intermediate coupling parameter in Li^7 is taken to be 1.5.

In this approximation R is given by

$$R = -\frac{\sqrt{5}}{1+\frac{1}{2}\sqrt{2}\, b/a}. \tag{8}$$

Thus at the L–S limit, $R = -\sqrt{5}$ and, since b/a is negative, R becomes large and changes sign as the intermediate coupling parameter for Be^8 increases. The result of a calculation using all the component wavefunctions is given in fig. 3.

We see that the experimental result of Neuert for R^2 does not give a unique value for a/K, viz. it could be 0.1 or 1.8. A fit to the energy levels can however, only be obtained with the latter value. Hence it appears that the sign of R is positive and the polarisation effects small. In fig. 4 we show the variation with a/K of the polarisation at $E_{\mathrm{p}} = 441$ keV and $\theta = 80°$.

I am indebted to Dr. J. M. Soper for providing details of the shell model wavefunctions and to Dr. L. J. B. Goldfarb for advice during the course of the work.

References

1) S. Devons and L. J. B. Goldfarb, Hand. Phys. **42** (Springer-Verlag, Berlin, 1958)
2) J. M. Blatt and L. C. Biedenharn, Rev. Mod. Phys. **24** (1952) 258
3) L. J. B. Goldfarb and J. R. Rook, Nuclear Physics **12** (1959) 494
4) H. Neuert and T. Retz-Schmidt, Z. Naturforsch. **13** (1959) 829
5) J. M. Soper, Phil. Mag. **8** (1957) 1219
6) A. M. Lane, Proc. Phys. Soc. **66** (1953) 977
7) H. A. Jahn and H. van Wieringen, Proc. Roy. Soc. **209** (1951) 502

1.E.3

Nuclear Physics **27** (1961) 612—619; © *North-Holland Publishing Co., Amsterdam*

Not to be reproduced by photoprint or microfilm without written permission from the publisher

LIFETIME AND *g*-FACTOR OF THE FIRST EXCITED STATE IN $\mathbf{Fe^{56}}$

F. R. METZGER

Bartol Research Foundation of the Franklin Institute, Swarthmore, Pennsylvania †

Received 15 May 1961

Abstract: With the gamma rays from a gaseous source of Co^{56}, resonance scattering from the first excited state of Fe^{56} has been observed. From a study of the self-absorption of the resonance radiation, a width $\Gamma = (6.2 \pm 1.0) \times 10^{-5}$ eV was obtained. Making use of the large magnetic field at the position of the iron nuclei, the rotation of the very anisotropic pattern was observed when the iron scatterer was placed in an external field perpendicular to the plane of scattering. The measured precession angle corresponds to a *g*-factor of $+0.53 \pm 0.16$.

1. Introduction

In the past few years the nuclear *g*-factors of a considerable number of excited states have been determined from measurements of the precession in an external magnetic field. The precession was measured by observing the gamma rays deexciting the level which had been populated either by cascade gamma rays or by Coulomb excitation. Several of these experiments ¹) were carried out with 2+ states in rotational nuclei, the lifetimes of which are conveniently $\approx 10^{-9}$ sec.

As one moves away from the region of the rotational nuclei, the energies of the 2+ levels increase rapidly and the lifetimes become so short that the precession in a practical magnetic field can no longer be measured using the anisotropy of a 4-2-0 gamma-gamma cascade. The situation is somewhat more favourable if resonance scattering is used since the anisotropy for the 0-2-0 spin sequence, which then applies, is 17 times larger than the anisotropy for the 4-2-0 sequence. If this large anisotropy for the 0-2-0 sequence is combined with a large magnetic field, it becomes feasible to study levels with lifetimes as short as 10^{-11} seconds.

For iron, the strength ²) and direction ³) of the internal field are known, and the numerical values make a magnetic moment experiment appear feasible for the first excited state in Fe^{56}. In the case of the first excited state of Fe^{58}, the low abundance (0.31 %) is a strong deterrent, in the case of Fe^{54} there does not exist a suitable radioisotope feeding the 2+ level. For Fe^{56}, the problem of finding a suitable source of resonant 845-keV gamma rays is easily

---

† This research was supported by the United States Office of Naval Research. Reproduction in whole or in part is permitted for any purpose of the United States Government.

solved. The decay energies in both the Mn^{56} and Co^{56} decays are sufficient to provide adequate compensation for the gamma ray recoil energy losses in the emission and absorption processes if gaseous sources are used; in addition, both isotopes are readily available. Co^{56} was chosen because of its more convenient half life and because previous experiments with gaseous $CoCl_2$ sources [4]) had been successful.

For small precession angles (in the case of Fe^{56} one expects angles of the order of one degree), the main effect of the magnetic field, when averaged over the lifetime of the excited state, is a rotation of the zero-field radiation pattern by an angle

$$\Delta\phi = \omega\tau, \tag{1}$$

where

$$\omega = g\mu_{\text{NM}}H/\hbar \tag{2}$$

is the Larmor frequency and τ is the mean life of the level. In eq. (2) g is the nuclear g-factor, μ_{NM} the nuclear magneton defined as $e\hbar/2Mc$, where M is the proton mass, H is the magnetic field at the nucleus and $\hbar$ Planck's constant divided by 2π.

For the 845-keV state in Fe^{56}, the mean life τ had been measured by Coulomb excitation techniques [5–9]). The results of refs. [5–7]) agreed very well (B(E2) ≈ 0.10), but differed appreciably from those of refs. [8, 9]) (B(E2)≈0.06). Under these circumstances it was decided to carry out an independent measurement of τ using resonance fluorescence techniques. The considerable error quoted for the lifetime reported here should not be taken as an indication of the difficulties involved in such a measurement, but rather as a consequence of the desire to spend as large a fraction of the useful source life for the statistically less favourable determination of the precession angle. It does not appear difficult to reduce the error in τ by a factor of three, i.e., to 5 %, if circumstances should demand it.

For the determination of the g-factor it would, in principle, be sufficient to measure the change in the resonance counting rate caused by the reversal of the direction of magnetization for a single scattering angle, the most favourable angle being approximately 144°. However, since the counting rate changes were rather small and since the non-resonant counting rate depended also on the direction of the magnetic field, it was decided to measure at several angles and to ascertain that the change in the resonance counting rate depended on the scattering angle in the expected manner.

2. Source Preparation

Armco iron was bombarded in the MIT cyclotron with 600 μA · hr of 15-MeV deuterons. After the bombardment, the target was dissolved in HCl, 0.2 mg of Co carrier and H_2O_2 added. After evaporation to dryness, the activity was taken up in 9*M* HCl and put on an ion exchange column. The column, 2 cm in diameter and 20 cm long, consisted of Dowex 1-X 10 anion exchange resin (200—400 mesh) which had been conditioned with concentrated HCl. The Co activity was eluted with 4*M* HCl. Two more elutions were carried out with smaller columns, 0.8 cm in diameter and 7 cm long. After this procedure, the amount of iron present in the Co fraction was negligible. The solution was then transferred to a quartz vacuum system and evaporated to dryness. The water of crystallization was driven out by heating, the anhydrous $CoCl_2$ was distilled into a quartz ampoule of approximately 2 cm^3 volume, and the ampoule sealed off. All the $CoCl_2$ in the ampoule was expected to be in the vapour phase for temperatures exceeding 870° C. Ordinarily, the ampoule was kept at 950° C. The consequent resonance scattering experiments indicated that the number of resonant gamma rays emitted by this source decreased more rapidly than expected for the 77-day half life of Co^{56}. Diffusion into the walls or decomposition of $CoCl_2$ reduced the number of resonant gamma rays on the average by 0.5 % for every hour the source was kept at 950°C. In order to avoid large uncertainties due to this "decay" correction, the scattering angles were cyclically alternated.

3. Lifetime of the 845-keV Level

The necessity to use a molecular vapour rather than a monatomic gas as the source material made it impossible to obtain a reliable value for the lifetime of the 845-keV state in Fe^{56} from a simple resonance scattering experiment. Even with a monatomic gas some uncertainty would have remained because of the lack of knowledge of the β-γ, γ-γ and β-ν angular correlations for the various decay paths leading from Co^{56} to the 845-keV state, and the limited accuracy of the complicated decay scheme. Under these circumstances, a self absorption experiment was indicated since it involves the measurement of a ratio of counting rates and does not depend on the knowledge of the absolute number of resonant gamma rays emitted by the source [4, 10]).

The experimental arrangement used for the self absorption experiment is shown in fig. 1. The average path length in the iron absorber was 1.44 cm. A comparison absorber of nickel was used after it had been closely matched to the iron absorber with respect to the electronic attenuation of the 845-keV radiation. The self absorption in the iron absorber was determined as 7.9±1.3%. In first approximation, this absorption *A* may be written as

$$A = \frac{nd\,(g_2/g_1)\lambda^2\Gamma}{4[\pi(\Delta_a^2+\Delta_s^2)]^{\frac{1}{2}}}, \tag{3}$$

where

$$\Delta_\nu^2 = 2kT_\nu E_\gamma^2/Mc^2. \tag{4}$$

Here n is the number of Fe^{56} nuclei per cm^3 of the absorber, d is the average path length in the absorber and g_2 and g_1 are the statistical weights of excited state and ground state, respectively. The wave length of the gamma rays of energy E_γ is denoted by λ, the width of the 845-keV level by Γ; Δ_a and Δ_s are the Doppler widths of absorber and scatterer, respectively, k is Boltzmann's constant, T the effective temperature, M the mass of the Fe nucleus and c the velocity of light. Two Doppler widths were introduced because, due to the proximity of the oven (see fig. 1), the absorber was at a temperature (340°K) which was considerably higher than the temperature of the scatterer (300°K). Using the accepted value $\theta = 420°$ for the Debye temperature of Fe, Lamb's correction for crystalline binding [11]) leads to effective temperatures $T_a = 366°K$ and $T_s = 329°K$. The corresponding Doppler widths are $\Delta_a = 0.93$ eV and $\Delta_s = 0.88$ eV, respectively. With these values and $(g_2/g_1) = 5$, $\lambda^2 = 2.15\times10^{-20}$ cm^2 and $n = 7.8\times10^{22}$, eq. (1) takes on the form $A = 1.32\times10^3\times\Gamma_{eV}$. For an absorption of 7.9 %, one thus finds $\Gamma = 6\times10^{-5}$ eV. A rigorous calculation taking also into account the self absorption in the scatterer led to $\Gamma = (6.2\pm1.0)\times10^{-5}$ eV, corresponding to a mean life $\tau = 1.06\times10^{-11}$ sec.

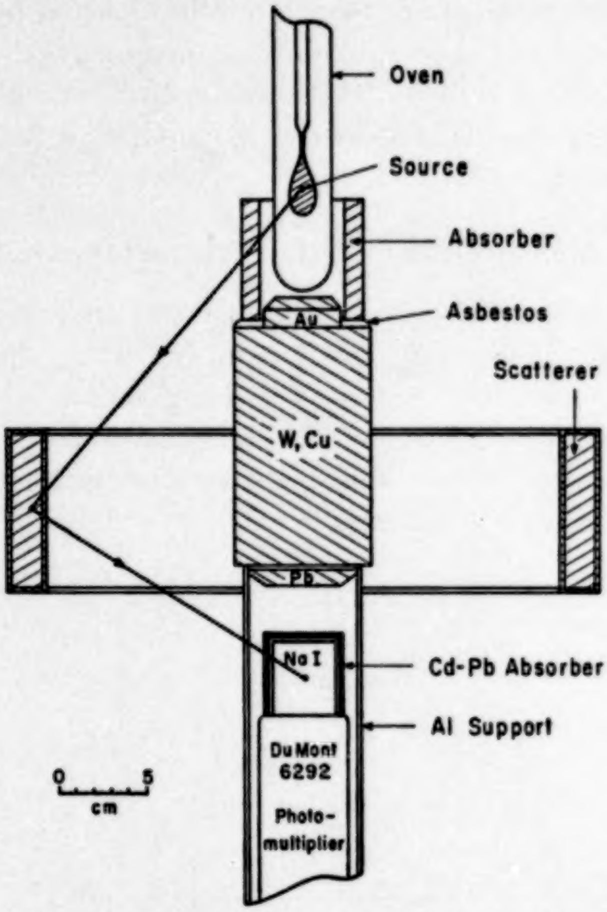

Fig. 1. Experimental arrangement used for the self absorption experiment.

It might be mentioned here that an evaluation of the scattering experiment on the basis of the value $N(E_r) = 1.40 \times 10^{-2}\ N$, calculated from the presently accepted decay scheme assuming isotropic correlations and monatomic Co gas, led to a width $\Gamma = 4.7 \times 10^{-5}$ eV. A comparison with the self absorption value for Γ shows that, for the actual source, the number of resonant gamma rays $N(E_r)$ was 32 % smaller than it would be for a source of monatomic Co vapour with isotropic correlations in all cascades leading to the 845-keV state.

Our value for the mean life of the 845-keV state corresponds to a B(E2) of 0.088; it lies somewhat closer to the results reported by refs. 5-7)]. Very recently, another lifetime determination has been carried out 12]) using the resonance fluorescence technique. In this case Mn^{56} was used as the source of the resonance radiation. The value for Γ found, $\Gamma = (7.3 \pm 2.5) \times 10^{-5}$ eV, agrees with our result.

4. Measurement of the Precession Angle

For the measurement of the precession angle $\Delta\phi$ an experimental arrangement similar to that shown in fig. 1 was used. Naturally, the absorbers in the incident beam were removed and the relative positions of source, scatterer and detector were changed in order to obtain scattering angles of 91°, 114°, 126° and 142°. The detector was shielded from stray magnetic fields by three layers of high permeability material.

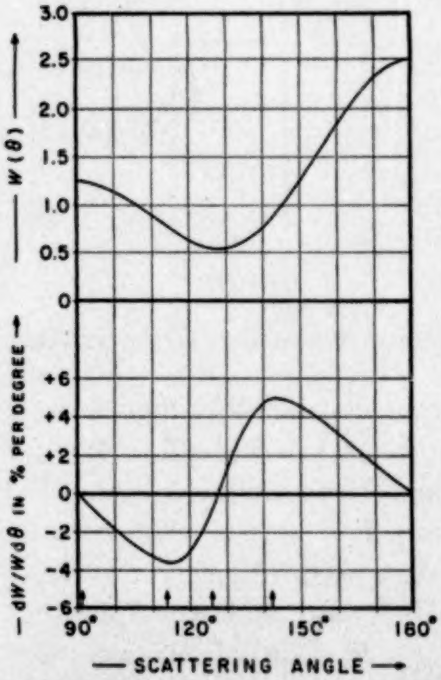

Fig. 2. Angular distribution of the resonance radiation expected for the spin sequence 0-2-0 (top). Sensitivity of the resonance counting rate to a rotation of the 0-2-0 angular distribution pattern (bottom). The arrows indicate the four experimental angles.

The top curve in fig. 2 represents the angular distribution of the resonance radiation expected for a spin sequence 0-2-0. An analysis of the resonance counting rates in the *g*-factor experiments showed that the actual angular distribution agreed accurately with the expectation. This is illustrated in table 1 where the resonance counting rates for the different scattering angles are compared with the counting rates expected for the actual geometries if the distribution $W(\theta) = 1.25-3.75 \cos^2 \theta + 5 \cos^4 \theta$, typical for a 0-2-0 spin sequence, is assumed. In judging the agreement, it should be kept in mind that the differential cross section changes by a factor of 0.44 as one goes from 90° to 126° and by a factor of 1.5 going from 126° to 142°. The lower curve in fig. 2 depicts the angular dependence of the sensitivity for the detection of a small rotation of the 0-2-0 radiation pattern. A value of 4.9 % per degree rotation is reached at a scattering angle of $\approx$ 144°. The arrows indicate the angles used in the actual experiments.

TABLE 1

Resonance scattering from Fe^{56} check of the angular distribution

Scattering angle	Counting rate		Ratio obs/exp
	observed	expected [a])	
91.0	256	264	0.97
113.6	241	241	1.00
126.0	159	156	1.02
142.0 I	84	84	1.00
142.0 II	131	129	1.02

[a]) Assuming $W(\theta) = 1.25-3.75 \cos^2\theta + 5 \cos^4\theta$

Since preliminary runs indicated a change in counting rate upon reversal of the field even in the absence of resonance scattering, i.e., for a cold Co^{56} source, readings had to be taken for both field directions with the cold source and with the source at $\approx$ 950°C. The cold source effect, which did not exhibit a change of sign for the four angles studied, was attributed to the magnetic deflection of the secondary electrons created in the iron scatterer by the higher energy gamma rays of Co^{56}. For one choice of the field direction these electrons and the accompanying bremsstrahlung would be deflected towards the γ-detector, for the other choice of the field direction they would be deflected away from the γ-detector. The sign of the effect agreed with the assumption that electrons were responsible. The magnitude of the effect was reasonable in view of the fact that bremsstrahlung from the higher energy secondary electrons represented the largest portion of the counting rate observed with the cold source.

After applying the corrections for the cold source effects, the experimental counting rate changes of the resonance scattering upon reversal of the direction of the magnetic field had the values indicated by the points in fig. 3. The dashed line in this figure represents the best fit, with the angle of rotation $\Delta\phi$ as parameter, of a curve of the shape given in fig. 2, modified by the finite angular resolution of the experimental apparatus, to the experimental points. The value for $\Delta\phi$ found from this comparison was $2\Delta\phi = 0.73 \pm 0.16$ degrees.

A measurement of the magnetic flux for the magnetizing current used in the experiment showed that the iron of the scatterer was not fully saturated, the indication being that the measured rotation was only 75±10 % of the saturation rotation. The corrected precession angle is therefore, $2\Delta\phi_{\text{corr}} = 0.97 \pm 0.23$ degrees.

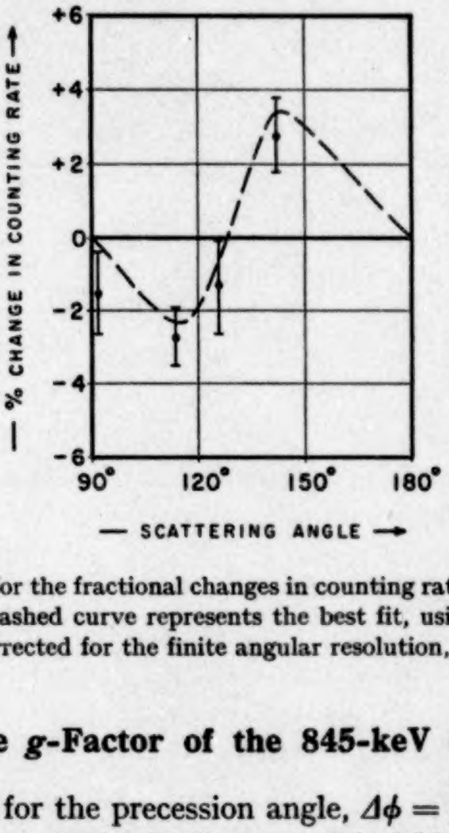

Fig. 3. Experimental values for the fractional changes in counting rate upon reversal of the direction of magnetization. The dashed curve represents the best fit, using $\Delta\phi$ as parameter, of the sensitivity curve of fig. 2, corrected for the finite angular resolution, to the experimental points.

5. The *g*-Factor of the 845-keV State

Combining the value for the precession angle, $\Delta\phi = 0.485$ degrees with the value for the mean life, $\tau = 1.06 \times 10^{-11}$ sec, eq. (1) yields the Larmor precession frequency

$$\omega = (8.0 \pm 2.3) \times 10^{8}\ \text{sec}^{-1}.$$

With $\mu_{\text{NM}} = 5.05 \times 10^{-24}$ erg · G^{-1}, $H_{\text{eff}} = 3.17 \times 10^{5}$ G, $\hbar = 1.05 \times 10^{-27}$ erg · sec and $\omega = (8 \pm 2.3) \times 10^{8}\ \text{sec}^{-1}$, eq. (2) then gives for the *g*-factor of the first excited state in Fe^{56}

$$g = +0.53 \pm 0.16.$$

The magnetic moment of the 2+ first excited state in Fe^{56} is then

$$\mu = (1.06 \pm 0.32)\mu_{\text{NM}}.$$

No theoretical estimates exist for the magnetic moment of this particular excited state.

The author wishes to thank Mrs. E. K. Sheppard for her help with the chemical treatment of the target. He is indebted to Mr. J. B. Bulkley of the MIT Radioactivity Center for arranging the cyclotron bombardments and to Mr. E. White for his efforts to improve the bombardment conditions and for carrying out the actual cyclotron bombardments.

References

1) G. Goldring and R. P. Scharenberg, Phys. Rev. **110** (1958) 701;
K. Sugimoto, J. Phys. Soc. Japan **13** (1958) 240;
P. Debrunner, W. Kündig, J. Sunier and P. Scherrer, Helv. Phys. Acta **31** (1958) 326;
E. Bodenstedt, E. Matthias, H. J. Körner, E. Gerdau, F. Frisius and D. Hovestadt, Nuclear Physics **15** (1960) 239;
P. Debrunner and W. Kündig, Helv. Phys. Acta **33** (1960) 395;
G. Manning and J. Rogers, Nuclear Physiscs **19** (1960) 675;
E. Bodenstedt, H. J. Körner, C. Günther and J. Radeloff, Nuclear Physics **22** (1961) 145;
R. Stiening and M. Deutsch, Phys. Rev. **121** (1961) 1484
2) S. S. Hanna, J. Heberle, C. Littlejohn, G. J. Perlow, R. S. Preston and D. H. Vincent, Phys. Rev. Lett. **4** (1960) 177
3) S. S. Hanna, J. Heberle, G. J. Perlow, R. S. Preston and D. H. Vincent, Phys. Rev. Lett. **4** (1960) 513
4) F. R. Metzger, Phys. Rev. **103** (1956) 983
5) G. M. Temmer and N. P. Heydenburg, Phys. Rev. **104** (1956) 967
6) H. E. Gove and C. Broude, Progress Report, Physics Division, Atomic Energy of Canada Limited, AECL No. 1069
7) B. M. Adams, D. Eccleshall and M. J. L. Yates, Proc. Second Conf. on reactions between complex nuclei ed. by A. Zucker, K. D. Halbert and F. T. Howard (John Wiley and Sons, Inc., New York, 1960) p. 95
8) D. G. Alkhazov, A. P. Grinberg, K. I. Erokhina and I. Kh. Lemberg, Izv. Akad. Nauk. SSSR (Ser. Fiz.) **23** (1959) 223
9) D. S. Andreyev, A. P. Grinberg, K. I. Erokhina and I. Kh. Lemberg, Nuclear Physics **19** (1960) 400
10) F. R. Metzger, Progress in nuclear physics, Vol. 7, ed. by O. R. Frisch (Pergamon Press, New York, 1959);
F. R. Metzger, Phys. Rev. **110** (1958) 123
11) W. E. Lamb, Phys. Rev. **55** (1939) 190
12) W. H. Kelly and G. B. Beard, Nuclear Physics (to be published)

2.L

Nuclear Physics **27** (1961) 620—631; © *North-Holland Publishing Co., Amsterdam*

Not to be reproduced by photoprint or microfilm without written permission from the publisher

DISTORTED WAVE EXPANSION FOR SCATTERING PROBLEMS

P. SWAN

Department of Physics, University of Melbourne, Australia

Received 17 April 1961

Abstract: The properties of a distorted wave method for the scattering wave function $\psi_l(r)$ and phase-shift δ_l are examined. For $|\delta_l| < \frac{1}{2}\pi$, $\tan^{(1)} \delta_l$ reduces to a series whose leading term is the first Born approximation for $\tan \delta_l$, whereas at low energies an approximate form of the shape-independent formula is obtained. For weak potentials ($|\delta_l(k)| \leqq \pi$ for all k), the method is valid for all k, but for strong potentials the assured range of validity is $|\delta_l| < \frac{1}{2}\pi$, provided the energy is sufficiently high. The overall accuracy is 2—3 % for δ_l, using non-singular potentials. Potentials singular at $r = 0$ may give rather lower accuracy.

Higher approximations in the form of series expansions for $\psi_l^{(n)}(r)$ and $\tan \delta_l^{(n)}$ are developed, which reduce in the limit $n \to \infty$ to the corresponding Born series, convergent for $|\delta_l| < \frac{1}{2}\pi$. However, the rate of convergence for small n is much better than for the Born expansions, particularly for potential strengths near the radius of convergence. The expansions are also convergent for weak potentials when $\pi \geqq |\delta_l| > \frac{1}{2}\pi$, whereas the Born series are not.

It is concluded that $\psi_l^{(1)}(r)$ and $\tan^{(1)} \delta_l$ are approximate summations of the corresponding Born series for $|\delta_l| < \frac{1}{2}\pi$, and therefore include contributions from the Born expansions of all orders. The summations for $\psi_l^{(n)}(r)$ and $\tan \delta_l^{(n)}$ are also valid for weak potentials for $\pi \geqq |\delta_l| \geqq \frac{1}{2}\pi$, having the character of Born expansions in inverse powers. The method is illustrated on zero energy neutron-proton scattering.

1. Introduction

A distorted wave method, giving simple analytical expressions for the elastic scattering wave function $\psi_l(r)$ and phase-shift δ_l, has been applied to a number of nuclear collision problems [1, 2, 3]. It takes as basis the trial wave function

$$\psi_l^{(0)}(r) = \mathscr{J}_l(kr)\cos \delta_l - g_l(r)\mathscr{N}_l(kr)\sin \delta_l, \tag{1}$$

where $\mathscr{J}_l(kr)$ and $\mathscr{N}_l(kr)$ are the regular and irregular plane wave solutions for the wave equation with zero potential. They are related to the spherical Bessel and Neumann functions by the relations

$$\begin{aligned} \mathscr{J}_l(x) &= xj_l(x) = (\tfrac{1}{2}\pi x)^{\frac{1}{2}} J_{l+\frac{1}{2}}(x), \\ \mathscr{N}_l(x) &= xn_l(x) = (\tfrac{1}{2}\pi x)^{\frac{1}{2}} N_{l+\frac{1}{2}}(x), \end{aligned} \tag{2}$$

where the definitions of $j_l(x)$ and $n_l(x)$ are those given by Schiff [4].

In eq. (7), $g_l(r)$ is a form factor, which must satisfy the boundary conditions

$$g_l(r \to 0) \approx r^{2l+1}, \qquad 1 - g_l(r \to \infty) \sim U(r) \to 0, \tag{3}$$

where $U(r) = (2\mu/\hbar^2)V(r)$ is the interaction potential. Results are practically independent of the detailed form of $g_l(r)$, provided conditions (3) are satisfied [1, 2, 3].

Comparison of (1) with the asymptotic wave function

$$\psi_l(r) \xrightarrow[r\to\infty]{} \mathscr{J}_l(kr)\cos\delta_l - \mathscr{N}_l(kr)\sin\delta_l \tag{4}$$

shows that $\psi_l^{(0)}(r)$ itself gives no information about the phase-shift δ_l. However, it may in effect be iterated to give a value by substitution in the integral equation for the phase-shift [5]):

$$\sin\delta_l = -\frac{\lambda}{k}\int_0^\infty U(r)\mathscr{J}_l(kr)\psi_l(r)\mathrm{d}r, \tag{5}$$

where the parameter λ is a measure of the strength of the interaction $\lambda U(r)$. This leads to

$$\tan\delta_l^{(1)} = \lambda B_{1l}/(1-\lambda B_{2l}), \tag{6}$$

where

$$B_{1l} = -\frac{1}{k}\int_0^\infty U(r)\mathscr{J}_l^2(kr)\mathrm{d}r, \tag{7}$$

$$B_{2l} = \frac{1}{k}\int_0^\infty g_l(r)U(r)\mathscr{J}_l(kr)\mathscr{N}_l(kr)\mathrm{d}r. \tag{8}$$

Here, B_{1l} is the first Born approximation integral, and B_{2l} an integral measuring the distortion of the wave function due to $U(r)$, and introducing a strong interference effect in δ_l; $B_{2l}(k)$ is a function which initially decreases from a maximum value $B_{2l}(0)$ and oscillates with diminishing amplitude thereafter.

That (6) corresponds to an order of approximation one higher than (1) may be seen by the following argument. The wave equation and its associated boundary conditions on $\psi_l(r)$ may be expressed in the equivalent integral equation form [6])

$$\psi_l(r) = \mathscr{J}_l(kr)\cos\delta_l - \lambda\int_0^\infty \mathrm{d}r' G_l(r,r')U(r')\psi_l(r'), \tag{9}$$

the Green's function $G_l(r, r')$ being given by

$$G_l(r,r') = -\frac{1}{k}\mathscr{J}_l(kr_<)\mathscr{N}_l(kr_>), \tag{10}$$

where $r_<$ and $r_>$ are the smaller and larger of r, r' respectively. We next define the integrals

$$B_{1l}(r) = -\frac{1}{k}\int_0^r \mathrm{d}r' U(r')\mathscr{J}_l^2(kr'), \tag{11}$$

$$B_{2l}(r) = \frac{1}{k}\int_0^r \mathrm{d}r' g_l(r')U(r')\mathscr{J}_l(kr')\mathscr{N}_l(kr'), \tag{12}$$

$$B_{3l}(r) = \frac{1}{k}\int_r^\infty \mathrm{d}r' U(r')\mathscr{J}_l(kr')\mathscr{N}_l(kr'), \tag{13}$$

$$B_{4l}(r) = -\frac{1}{k}\int_r^\infty \mathrm{d}r' g_l(r')U(r')\mathscr{N}_l^2(kr'). \tag{14}$$

Substitution of (1) for $\psi_l^{(0)}(r)$ in the right hand side of (9) gives

$$\psi_l^{(1)}(r) = \mathscr{J}_l(kr)[\{1+\lambda B_{3l}(r)\}\cos\delta_l+\lambda B_{4l}(r)\sin\delta_l]-\mathscr{N}_l(kr)[\lambda B_{1l}(r)\cos\delta_l + \lambda B_{2l}(r)\sin\delta_l]. \tag{15}$$

From the definitions (11)—(14) and (6), (7), we have

$$B_{1l}(\infty) = B_{1l}, \qquad B_{2l}(\infty) = B_{2l}, \qquad B_{3l}(\infty) = B_{4l}(\infty) = 0,$$

so that the asymptotic form of (15) for large r is

$$\psi_l^{(1)}(r \to \infty) = \mathscr{J}_l(kr)\cos\delta_l - \mathscr{N}_l(kr)[\lambda B_{1l}\cos\delta_l + \lambda B_{2l}\sin\delta_l]. \tag{16}$$

On equating the coefficient of $-\mathscr{N}_l(kr)$ to $\sin\delta_l$ (c.f. (4)), we get eq. (6) for $\tan\delta_l^{(1)}$.

Equation (6) for $\tan\delta_l^{(1)}$ has been extensively tested for a number of potential well shapes and l values in the range $0 \leqq \delta_l \leqq \pi$, giving an overall accuracy of about 2—3 %, dependent on the care with which the form factor $g_l(r)$ is chosen [1, 2, 3]). Potentials singular at $r = 0$ may give somewhat lower accuracy [3]). It is preferable, although not necessary, to choose an arbitrary parameter inside $g_l(r)$ so as to give the correct zero-energy scattering length a. The latter may itself be estimated easily and accurately for the potential in question by using a recent variational procedure [7]).

At low energies, $k^2 \lesssim 1$, eq. (6) reduces to an approximate form of the shape-independent formula [2]):

$$k\cot\delta_0^{(1)} = A + Bk^2 + \mathrm{O}(k^4), \tag{17}$$

where $A \approx -1/a$, $B \approx \frac{1}{2}r_0$, r_0 being the effective range of the interaction. A choice of the parameter inside $g_l\,(r)$ to make $A = -1/a$ thus normalizes the method at zero energy.

2. Limits of Validity for the tan $\delta_l^{(1)}$ Approximation

Provided $|\lambda B_{2l}| < 1$, the expression (6) may be expanded in the series

$$\tan\delta_l^{(1)} = \lambda B_{1l} \sum_{n=0}^{\infty} \lambda^n B_{2l}^n, \tag{18}$$

which for sufficiently high energy, $k^2 \gg |\lambda U(r)|$, reduces to the first Born approximation for tan δ_l:

$$\tan\delta_l \approx \lambda B_{1l} \qquad (k^2 \to \infty). \tag{19}$$

However, interactions singular at the origin, such as the Yukawa potential, do not satisfy the necessary condition $k^2 \gg |\lambda U(r)|$ for r sufficiently small, which accounts for the poor accuracy obtained for the Born approximation both for $\tan\delta_l$ and for the scattering amplitude $f(\theta)$ with this type of potential. The accuracy of (6) is also affected to a lesser degree [3]).

Eq. (18), although much simpler, bears a sufficient resemblance to the Born expansion of tan δ_l to suggest that (6) is a good approximation to the Born series, illustrated strikingly by the example in sect. 4. The known accuracy of (6) supports this hypothesis. In sect. 3 we show that an alternative expansion for $\psi_l(r)$ using (1) as initial function to iterate the integral equation (9), reduces in the limit $n \to \infty$ to the Born series, provided $|\delta_l| < \frac{1}{2}\pi$, the latter being also the condition for convergence of the Born expansion. Convergence conditions for Born expansions have been dealt with by a number of authors [8-12]), both for partial wave and full wave expansions.

The condition $|\lambda B_{2l}| < 1$ necessary for the validity of the series (18) for tan $\delta_l^{(1)}$ corresponds to $|\delta_l^{(1)}| < \frac{1}{2}\pi$, provided we assume $\delta_l^{(1)}$ is in the range $0 \leqq |\delta_l^{(1)}| \leqq \pi$ (all k), so that $B_{2l}(k)$ has one zero only. That (1), (6) and (15) are invalid for $|\delta_l^{(1)}| \geqq \pi$ $(k \neq 0)$, follows from the following arguments:

1) The trial wave function (1) for $\psi_l^{(0)}(r)$ is non-degenerate only within the region $-\pi < \delta_l^{(1)} < \pi$. Thus if $|\delta_l| \geqq \pi (k \neq 0)$, there is no reason why iteration of (1) in (9) should lead to a convergent expansion, since the initial function is a very bad choice. Physically this corresponds to the 'inside' wave function being a distorted 'outside' wave function, whereas for $|\delta_l| > \pi$, the potential is so strong that the correct 'inside' wave function has a quite different character, coupled with a large wave number. The function $\psi_l^{(0)}(r)$ cannot describe the case of strong distortion even approximately, as the 'inside' wave function is dependent largely on the potential and very little on δ_l, except at sufficiently high energies

2) The method breaks down for $|\delta_l| = \pi$ $(k \neq 0)$, as tan $\delta_l^{(1)} = 0$ contradicts $B_{1l} \neq 0$ in (6). However, $|\delta_l| = \pi$ $(k = 0)$ is acceptable as in this case $B_{1l} \equiv 0$.

Two-body interactions may be conveniently divided into two main classes:

1) The weak potentials, for which $|\delta_l(k)| < \pi$ $(k \neq 0)$, $\delta_l(0) = 0$ or π [13]). Examples are the n–p interaction and the equivalent two-body interactions between the very light nuclei, such as the n–α system. Our formula (6) for tan $\delta_l^{(1)}$ should always be valid in these cases.

2) The strong potentials, for which $|\delta_l(k)| \geqq \pi$ $(k_{1l} \leqq k \leqq k_{2l})$, where $k_{1l} = 0$ for attractive potentials which do not change sign, and $k_{1l} \neq 0$ for repulsive potentials, as $\delta_l(0) = 0$ [13]). Eq. (6) is clearly invalid for $k_{1l} \leqq k \leqq k_{2l}$ in both cases, and also in the latter case for $0 \leqq k < k_{1l}$, although δ_l may be small, as the 'inside' wave function cannot be represented by the weakly distorted function (1).

Examples include the optical model potentials for interactions between all but the lightest nuclei, where we have by Levinson's theorem

$$\delta_l(0) - \delta_l(\infty) = n\pi, \tag{20}$$

n being the number of composite bound states with non-zero binding energy.

It is usual to define $\delta_l(\infty) = 0$, giving $\delta_l(0) = n\pi$. These potentials may be very strong compared to the n–p interaction, the optical potential between a neutron and the nucleus $A = 125$ giving $n = 4$ for $l = 0$. Simple arguments based on a square well of depth U_0 and width b show that the minimum interaction strength $U_0\, b^2$ required for $n = 4$ is 49 times that needed for $n = 1$ $(l = 0)$.

The same arguments show that eq. (6) must fail for strong potentials for $|\delta_l| = \pi-\varepsilon_l$, $\varepsilon_l \ll 1$, as tan $\delta_l^{(1)}$ small contradicts B_{1l} large. On the other hand, eq. (6) must be valid under Born approximation conditions, $k^2 \gg \overline{|U(r)|}$, so that δ_l is small. An intermediate region exists for which eq. (6) but not the Born appproximation is valid, defined by $\delta_l(k)$ decreasing monotonically from either $\frac{1}{2}\pi$ or a maximum value $\delta_l(k_m)$ towards zero, whichever is the smaller. In the former case, this requires $|\lambda B_{2l}| < 1$. However, $\lambda B_{2l}(k)$ is a function of energy oscillating with decreasing amplitude, so that $\lambda B_{2l}(k)-1$ may have a number of zeros say at $k = k_1, k_2, \ldots, k_n$. The modified condition becomes

$$|\lambda B_{2l}(k > k_n)| < 1.$$

In the intermediate region eq. (6) is valid in the sense that it is an approximation to the Born series (cf. sect. 3). However, for l sufficiently large, $\delta_l(k)$ may be small for all k, although neither the first Born approximation nor eq. (6) are valid except at high energies. The Born and distorted wave series of sect. 3 are valid for all k, but may be very slowly convergent for small k. Kohn [9]) has noted that the convergence of Born series for $\psi_l(r)$ and tan $\delta_l(k)$ improves with increasing l, so that if eq. (6) is valid for $l = 0$ for $k^2 > k'^2$, the same condition should suffice to make (6) valid for all $l \geqq 1$.

Many-body interactions may be classified similarly, although the size of δ_l is often dependent on symmetry considerations rather than the strength of the potential. In these cases, δ_l satisfies the theorem

$$\delta_l(0)-\delta_l(\infty) = (n+m)\pi, \tag{21}$$

where n is the number of composite bound states of non-zero binding energy and m is the number of states excluded by the Pauli principle [14]). Taking $\delta_l(\infty) = 0$, we see that $\delta_l(0)$ and hence $\delta_l(k)$ can have large values even although the potential is weak in the sense that $n = 0$. Thus electron scattering by the rare gases He, Ne, A, Kr and Xe gives $\delta_0(0) = \pi, 2\pi, 3\pi, 4\pi, 5\pi$ respectively, although the inert character of the gases shows that $n = 0$ in each case, corresponding to the non-existence of negative ions. Instead we have $m = 1, 2, 3, 4$ and 5 corresponding to the number of full electron shells (excluded states).

Examples for which $|\delta_l(k)| > \pi$ are treated exactly as if they were strong potentials in category 2) above. The tan $\delta_l^{(1)}$ formula (6) may be used safely only if $|B_{2l}(k > k_n| < 1$, where B_{2l} has the modified form given in sect. 4

of an earlier paper[2]). However, the weak potential cases where $|\delta_l(k)| \leqq \pi$ (all k) obey the conditions in category 1) above, so that the tan $\delta_l^{(1)}$ formula (6) is valid over the whole range $|\delta_l(k)| \leqq \pi$ (all k).

3. Series Expansions for $\psi_l(r)$ and tan δ_l

The usual Born expansion of $\psi_l(r)$ and tan δ_l, as exemplified in the work of Kohn[9]), is based on an asymptotic wave function normalised to $1/\cos\delta_l$ at $r \to \infty$, rather than the unit amplitude of (4). Thus sin δ_l changes to tan δ_l in the left hand side of the integral equation (5) for δ_l and cos δ_l is deleted in the integral equation (9) for $\psi_l(r)$. Iteration of the initial trial function $\mathscr{J}_l(kr)$ leads to the Born series for $\psi_l\ (r)$ and tan δ_l, convergent for $|\delta_l| < \frac{1}{2}\pi$.

The necessary initial assumptions are that $V(r)$ is sectionally continuous, $\lim_{r\to 0} rV(r)$ is finite and $\lim_{r\to\infty} r^{2+\varepsilon}\, V(r) = 0, \varepsilon > 0$.

An alternative but equivalent procedure is to retain the unit asymptotic amplitude for $\psi_l(r)$ as in (4), with integral equations (5) and (9) unchanged. The initial trial function is then $\mathscr{J}_l(kr)\cos\delta_l$, leading to the Born expansions as before. In particular, the first Born approximation is

$$\tan\delta_l^{(1)} = B_{1l}.$$

It is worth noting that with this normalization, if we take δ_l as small and use an initial trial function $\mathscr{J}_l(kr)$, we obtain for the first Born approximation[5])

$$\sin\delta_l^{(1)} = B_{1l}.$$

There is no contradiction between the two cases for δ_l small, but in the latter case, iteration of the initial function leads to an inconvenient transcendental equation for the nth order approximation of the type

$$\sin\delta_l^{(n)} = \sum_{m=1}^{n-1} \lambda^m S_l^{(m)} \cos\delta_l^{(n)} + \lambda^n S_l^{(n)},$$

where the $S_l^{(m)}$ are series summations. The coefficient of cos $\delta_l^{(n)}$ is in fact the Born series for tan $\delta_l^{(n-1)}$, so that in the limit $n \to \infty$ and for $|\delta_l| < \frac{1}{2}\pi$ (condition for convergence), we have $\lambda^n S_l^{(n)} \to 0$, leaving the Born series for tan $\delta_l^{(n)}$. However, from (5), $\mathscr{J}_l(kr)\cos\delta_l$ is clearly a better initial function to use than $\mathscr{J}_l(kr)$ for δ_l not small, so it can be surmised that results for $\delta_l^{(n)}$ are appreciably better for the former choice for n small.

It is evident that a series expansion for $\psi_l(r)$ can be constructed in the same way as the Born series, but using the distorted wave (1) as initial function in iterating (6). As (1) is a much better trial function than $\mathscr{J}_l(kr)\cos\delta_l$, we may expect greatly improved results, at least for low n values. We define the following multiple integrals for $m \geqq 1$:

$$B_{1\alpha_1\alpha_2\ldots\alpha_m l}(r) = -\frac{1}{k}\int_0^r \mathrm{d}r' B_{\alpha_1\alpha_2\ldots\alpha_m l}(r')U(r')\mathscr{J}_l^2(kr'), \tag{22}$$

$$B_{2\alpha_1\alpha_2\ldots\alpha_m l}(r) = \frac{1}{k}\int_0^r \mathrm{d}r' B_{\alpha_1\alpha_2\ldots\alpha_m l}(r')U(r')\mathscr{J}_l(kr')\mathscr{N}_l(kr'), \tag{23}$$

$$B_{3\alpha_1\alpha_2\ldots\alpha_m l}(r) = \frac{1}{k}\int_r^\infty \mathrm{d}r' B_{\alpha_1\alpha_2\ldots\alpha_m l}(r')U(r')\mathscr{J}_l(kr')\mathscr{N}_l(kr'), \tag{24}$$

$$B_{4\alpha_1\alpha_2\ldots\alpha_m l}(r) = -\frac{1}{k}\int_r^\infty \mathrm{d}r' B_{\alpha_1\alpha_2\ldots\alpha_m l}(r')U(r')\mathscr{N}_l^2(kr'), \tag{25}$$

where $\alpha_\nu (\nu = 1, 2, \ldots, m)$ may have any of the values 1, 2, 3 or 4. Eqs. (11)—(14) and (22)—(25) completely specify the expansion for $\psi_l^{(n)}(r)$, while that for $\tan \delta_l^{(n)}$ is covered by defining

$$B_{1\alpha_1\alpha_2\ldots\alpha_m l}(\infty) = B_{1\alpha_1\alpha_2\ldots\alpha_m l}, \qquad B_{2\alpha_1\alpha_2\ldots\alpha_m l}(\infty) = B_{2\alpha_1\alpha_2\ldots\alpha_m l},$$
$$B_{3\alpha_1\alpha_2\ldots\alpha_m l}(\infty) = B_{4\alpha_1\alpha_2\ldots\alpha_m l}(\infty) = 0.$$

It is worth noting that (22)—(25) are functions of the form factor $g_l(r)$ only if the last index number α_m has the value 2 or 4. Expressions for the first few $\psi_l^{(n)}(r)$ and $\tan \delta_l^{(n)}$ are listed below:

$$\psi_l^{(0)}(r) = \mathscr{J}_l(kr)\cos \delta_l - g_l(r)\mathscr{N}_l(kr)\sin \delta_l, \tag{26}$$

$$\begin{aligned}\psi_l^{(1)}(r) = {} & [\{1+\lambda B_{3l}(r)\}\cos \delta_l + \lambda B_{4l}(r)\sin \delta_l]\mathscr{J}_l(kr) - [\lambda B_{1l}(r)\cos \delta_l \\ & + \lambda B_{2l}(r)\sin \delta_l]\mathscr{N}_l(kr),\end{aligned} \tag{27}$$

$$\begin{aligned}\psi_l^{(2)}(r) = {} & [\{1+\lambda B_{3l}(r)+\lambda^2(B_{33l}(r)+B_{41l}(r))\}\cos \delta_l + \lambda^2\{B_{42l}(r) \\ & + B_{34l}(r)\}\sin \delta_l]\mathscr{J}_l(kr) \\ & -[\{\lambda B_{1l}(r)+\lambda^2(B_{13l}(r)+B_{21l}(r))\}\cos \delta_l + \lambda^2\{B_{22l}(r) \\ & + B_{14l}(r)\}\sin \delta_l]\mathscr{N}_l(kr),\end{aligned} \tag{28}$$

$$\begin{aligned}\psi_l^{(3)}(r) = {} & [\{1+\lambda B_{3l}(r)+\lambda^2(B_{33l}(r)+B_{41l}(r))+\lambda^3(B_{133l}(r)+B_{341l}(r)+B_{413l}(r) \\ & + B_{421l}(r))\}\cos \delta_l \\ & + \lambda^3\{B_{422l}(r)+B_{342l}(r)+B_{414l}(r)+B_{334l}(r)\}\sin \delta_l]\mathscr{J}_l(kr) \\ & -[\{\lambda B_{1l}(r)+\lambda^2(B_{13l}(r)+B_{21l}(r))+\lambda^3(B_{133l}(r)+B_{141l}(r)+B_{213l}(r) \\ & + B_{221l}(r))\}\cos \delta_l + \lambda^3\{B_{222l}(r)+B_{142l}(r)+B_{214l}(r) \\ & + B_{134l}(r)\}\sin \delta_l]\mathscr{N}_l(kr),\end{aligned} \tag{29}$$

$$\tan \delta_l^{(1)} = \lambda B_{1l}/(1-\lambda B_{2l}), \tag{30}$$

$$\tan \delta_l^{(2)} = [\lambda B_{1l}+\lambda^2(B_{13l}+B_{21l})]/[1-\lambda^2(B_{22l}+B_{14l})], \tag{31}$$

$$\tan\delta_l^{(3)} = [\lambda B_{1l}+\lambda^2(B_{13l}+B_{21l})+\lambda^3(B_{133l}+B_{141l}+B_{213l} \\ +B_{221l})]/[1-\lambda^3(B_{222l}+B_{142l}+B_{214l}+B_{134l})], \quad (32)$$

$$\tan\delta_l^{(4)} = [\lambda B_{1l}+\lambda^2(B_{13l}+B_{21l})+\lambda^3(B_{133l}+B_{141l}+B_{213l}+B_{221l})+\lambda^4(B_{1333l} \\ +B_{1341l}+B_{1413l}+B_{1421l} \\ +B_{2133l}+B_{2141l}+B_{2213l}+B_{2221l})]/[1-\lambda^4(B_{2222l}+B_{1422l}+B_{2142l} \\ +B_{1342l}+B_{2134l}+B_{2214l}+B_{1334l}+B_{1414l})]. \quad (33)$$

It is evident that $\psi_l^{(n)}(r)$ reduces to the corresponding Born series if the coefficients of $\sin\delta_l$ in eqs. (26)—(29) are equated to zero, and that the terms additional to the Born expansion are of order λ^n only. Similarly $\tan\delta_l^{(n)}$ as exemplified by eqs. (30)—(33) reduces to the Born expansion for $\tan\delta_l^{(n)}$ if the λ^n terms in the denominator are equated to zero.

By induction we can write for the general case ($n \geqq 1$),

$$\psi_l^{(n)}(r) = [\{1+\sum_1^{2^{m-1}} E(p_\mu, p_\nu)\sum_{m=1}^{n}\lambda^m B_{p_0p_1\dots p_ml}(r)\}\cos\delta_l+\{\lambda^n\sum_1^{2^{n-1}}E(q_\mu,q_\nu)B_{q_0q_1\dots q_nl}(r)\}\sin\delta_l]\mathscr{J}_l(kr) \\ -[\{\sum_1^{2^{m-1}}E(\alpha_\mu,\alpha_\nu)\sum_{m=1}^{n}\lambda^m B_{\alpha_0\alpha_1\dots\alpha_ml}(r)\}\cos\delta_l+\{\lambda^n\sum_1^{2^{n-1}}E(\beta_\mu,\beta_\nu)B_{\beta_0\beta_1\dots\beta_nl}(r)\}\sin\delta_l]\mathscr{N}_l(kr), \quad (34)$$

where $\sum_1^N E(p_\mu, p_\nu)$ denotes a summation over N terms, each differing from its neighbour by an unspecified number of exchanges of the suffices p_μ, p_ν.

From eq. (34), the asymptotic wave function is

$$\psi_l^{(n)}(r\to\infty) = \mathscr{J}_l(kr)\cos\delta_l-[\{\sum_1^{2^{m-1}}E(\alpha_\mu,\alpha_\nu)\sum_{m=1}^{n}\lambda^m B_{\alpha_0\alpha_1\dots\alpha_ml}\}\cos\delta_l \\ +\{\lambda^n\sum_1^{2^{n-1}}E(\beta_\mu,\beta_\nu)B_{\beta_0\beta_1\dots\beta_nl}\}\sin\delta_l]\mathscr{N}_l(kr). \quad (35)$$

On equating the coefficient of $-\mathscr{N}_l(kr)$ to $\sin\delta_l$, we obtain

$$\tan\delta_l^{(n)} = [\sum_1^{2^{m-1}}E(\alpha_\mu,\alpha_\nu)\sum_{m=1}^{n}\lambda^m B_{\alpha_0\alpha_1\dots\alpha_ml}]/[1-\lambda^n\sum_1^{2^{n-1}}E(\beta_\mu,\beta_\nu)B_{\beta_0\beta_1\dots\beta_nl}]. \quad (36)$$

Conditions for the convergence of the Born series as given by the $\cos\delta_l$ terms in (34), have been studied by Kohn [9]), leading to radii of convergence $\lambda_{\max}(k)$. However, for our purpose, it is sufficient that $|\delta_l| < \frac{1}{2}\pi$. Then the extra terms in (34), coefficient $\lambda^n\sin\delta_l$, must approach zero as $n\to\infty$, giving us the Born series:

$$\lim_{n\to\infty}\psi_l^{(n)}(r) = [\{1+\sum_1^{2^{m-1}}E(p_\mu,p_\nu)\sum_{m=1}^{n}\lambda^m B_{p_0p_1\dots p_ml}(r)\}\mathscr{J}_l(kr) \\ -\{\sum_1^{2^{m-1}}E(\alpha_\mu,\alpha_\nu)\sum_{m=1}^{n}\lambda^m B_{\alpha_0\alpha_1\dots\alpha_ml}(r)\}\mathscr{N}_l(kr)]\cos\delta_l, \quad (37)$$

$$\lim_{n\to\infty} \psi_l^{(n)}(r\to\infty) = [\mathscr{J}_l(kr) - \{\sum_1^{2^{m-1}} E(\alpha_\mu, \alpha_\nu) \sum_{m=1}^{n} \lambda^m B_{\alpha_0\alpha_1\ldots\alpha_m l}\}\mathscr{N}_l(kr)]\cos\delta_l, \tag{38}$$

$$\lim_{n\to\infty} \tan\delta_l^{(n)} = \sum_1^{2^{m-1}} E(\alpha_\mu, \alpha_\nu) \sum_{m=1}^{n} \lambda^m B_{\alpha_0\alpha_1\ldots\alpha_m l}. \tag{39}$$

The extra terms, coefficient $\lambda^n \sin\delta_l$, are of the same order of magnitude as the λ^n terms in the Born series, which must vanish for $n\to\infty$. Their magnitude, and that of the Born terms in (36), may be estimated if we use the known fact that (6) is a good approximation for $\tan\delta_l$ for $|\delta_l| < \frac{1}{2}\pi$, at least for weak potentials. The case of strong potentials requires the additional proviso of sufficiently high energy. We mayrewrite (6) in the alternative form for $|B_{2l}| < 1$,

$$\tan\delta_l \approx \tan\delta_l^{(1)} = \lambda B_{1l} \sum_{m=0}^{n-1} (\lambda B_{2l})^m / [1-(\lambda B_{2l})^n]. \tag{40}$$

As $\tan\delta_l^{(1)}$ is already a good approximation, with error of order 2 %, we have

$$\tan\delta_l^{(1)} \approx \tan\delta_l^{(n)} \approx \lambda B_{1l} \sum_{m=0}^{n-1} (\lambda B_{2l})^m / [1-\lambda^n B_{2l}^n]. \tag{41}$$

Comparison of (41) with (36) gives us

$$\sum_1^{2^{m-1}} E(\alpha_\mu, \alpha_\nu) B_{\alpha_0\alpha_1\ldots\alpha_m l} \approx B_{1l} B_{2l}^{m-1} \qquad (m = 1, 2, \ldots, n), \tag{42}$$

$$\sum_1^{2^{n-1}} E(\beta_\mu, \beta_\nu) B_{\beta_0\beta_1\ldots\beta_m l} \approx B_{2l}^n. \tag{43}$$

These relations are verified for n–p scattering in sect. 4.

The case of $\pi \geqq |\delta_l| \geqq \frac{1}{2}\pi$ is of particular interest, as it is known that the Born series for $\psi_l(r)$ and $\tan\delta_l$ are divergent in this region. Nevertheless we shall show that expansions (35) and (36) for $\psi_l^{(n)}(r\to\infty)$ and $\tan\delta_l^{(n)}$ are convergent for the weak potentials of sect. 2 ($|\delta_l| \leqq \pi$ for all k). The former case involves the finite difference between two divergent series and the latter the finite ratio of two divergent series. The result does not apply to strong potentials, where $|\delta_l|$ can exceed π.

A rigorous proof is not attempted here.

For weak potentials, $\pi \geqq |\delta_l| \geqq \frac{1}{2}\pi$ corresponds to $|\lambda B_{2l}| \geqq 1$. It is interesting to note that the scattering system has one bound composite state in this case. Eq. (6) for $\tan\delta_l^{(1)}$ is then known to be a good approximation, which we proceed to expand in the form

$$\tan\delta_l \approx \tan\delta_l^{(1)} = \frac{-\lambda B_{1l} \sum_{m=1}^{n-1} (\lambda B_{2l})^m}{(\lambda B_{2l})^n - 1} \approx \tan\delta_l^{(n)}, \tag{44}$$

equivalent to the series in inverse powers

$$\tan \delta_l^{(1)} = -\frac{\lambda B_{1l}}{\lambda B_{2l}} \sum_{m=1}^{n-1} (\lambda B_{2l})^{-m}/[1-(\lambda B_{2l})^{-n}] \approx \tan \delta_l^{(n)}, \tag{45}$$

which is convergent for $n \to \infty$, provided $|\lambda B_{2l}| > 1$. If $|\lambda B_{2l}| = 1$, then we get $\tan \frac{1}{2}\pi = \infty/0 = \infty$ as required, the one point at which a pole in the $\tan \delta_l$ series is obtained (but necessarily so).

Equating terms in (36) and (44), we again find the approximate relations (42) and (43) hold, these leading in turn to the convergence of $\psi_l^{(n)}(r \to \infty)$ in (35). It is worth noting that the convergence of (36) in fact follows, independent of the above, provided only we assume

$$\lim_{n\to\infty} \{\sum_{1}^{2^{n-1}} E(\alpha_\mu, \alpha_\nu) B_{\alpha_0\alpha_1\ldots\alpha_n l}\}/\{\sum_{1}^{2^{n-1}} E(\beta_\mu, \beta_\nu) B_{\beta_0\beta_1\ldots\beta_n l}\} = R_l(k), \tag{46}$$

where R_l is some number independent of n.

The terms in the denominator of (46) involve a first integration over the form factor $g_l(r)$, but apart from this, only differ from the numerator terms in the order in which the successive integrations are carried out, and these are summed over 2^{n-1} permutations.

From (42) and (43), we see

$$R_l(k) \approx B_{1l}/B_{2l}. \tag{47}$$

4. Application to Neutron-Proton Scattering

Relations (42) and (43) hold with surprising accuracy, illustrated in the following example of neutral particle scattering at zero energy ($l = 0$) by a square well potential

$$U(r) = \begin{cases} -U_0 & (r < b), \\ 0 & (r \geqq b). \end{cases}$$

We take as form factor [2])

$$g_0(r) = \begin{cases} (3r/2b - r^3/2b^3) & (r < b), \\ 1 & (r \geqq b), \end{cases}$$

obtaining the values

$$B_{10} = \tfrac{1}{3}\lambda U_0 b^3 k, \qquad B_{20} = \tfrac{2}{5}\lambda U_0 b^2,$$

so that $\delta_0^{(1)}(0)$ is $\frac{1}{2}\pi$ for $\lambda U_0 b^2 = 2.5$. The correct value for zero binding energy, corresponding to $\delta_0^{(1)}(0) = \frac{1}{2}\pi$ by Levinson's theorem [13]), is actually $U_0 b^2 = \frac{1}{4}\pi^2 = 2.4674\ldots$, indicating an error of order 2 %. Defining the zero-energy scattering length as

$$a = \lim_{k\to 0}\left(-\frac{\tan\delta_0(k)}{k}\right),$$

we evaluate eqs. (30)—(32) to find

$$a^{(1)} = -\tfrac{1}{3}\lambda U_0 b^3/[1-0.4\lambda U_0\, b^2], \tag{48}$$

$$a^{(2)} = -\tfrac{1}{3}\lambda U_0 b^3[1+0.4\lambda U_0 b^2]/[1-0.1619(\lambda U_0\, b^2)^2], \tag{49}$$

$$a^{(3)} = -\tfrac{1}{3}\lambda U_0 b^3[1+0.4\lambda U_0 b^2+0.1619(\lambda U_0 b^2)^2]/[1-0.06561(\lambda U_0\, b^2)^3]. \tag{50}$$

The agreement between eqs. (36), (42), (43) and (48)—(50) is excellent, considered as an approximation.

A numerical application of eqs. (48)—(50) is ^{1}S n–p scattering at zero energy. Using the parameters [2])

$$\lambda U_0 = 0.3390\times 10^{26}, \qquad b = 2.5860\ \text{fm},$$

we find results for $a^{(n)}$ and the corresponding Born values $a_B{}^{(n)}$, given in table 1. Note that as $B_{20} = 0.4\ U_0\, b^2 = 0.90681$, the convergence of the Born series should be slow, as is indeed found.

TABLE 1

Zero-energy scattering lengths for ^{1}S n-p scattering (in fm). Square well, $\lambda U_0 = 0.3390\times 10^{26}$, $b = 2.5860$ fm.

	$a^{(1)}$	$a^{(2)}$	$a^{(3)}$
Series (44)—(46)	−20.97	−22.19	−22.72
Born series	− 1.954	− 3.726	− 5.352
Correct value	−23.69	−23.69	−23.69

The initial value $a^{(1)}$ is already quite good, while $a^{(2)}$ and $a^{(3)}$ show rapid convergence to the correct value. On the other hand, $a_B{}^{(1)}$ is very poor and $a_B{}^{(2)}$ and $a_B{}^{(3)}$ therefore converge slowly. Asymptotically, of course, $a^{(n)}$ and $a_B{}^{(n)}$ will converge at the same rate ($n \to \infty$), but for n small there is no comparison between the two methods.

TABLE 2

Zero- energy scattering lengths for ^{3}S n-p scattering (in fm). Square well, $\lambda U_0 = 0.87704\times 10^{26}$, $b = 2.0048$ fm.

	$a^{(1)}$	$a^{(2)}$	$a^{(3)}$
Series (48)—(50)	5.745	5.611	5.559
Born series	−2.355	−5.676	−10.416
Correct value	5.38	5.38	5.38

^{3}S n–p scattering at zero energy involves the zero-energy phase $\delta_0(0) = \pi$, corresponding to the singlet bound state of the deuteron and $0.4\, U_0 b^2 = 1.4100$. Table 2 lists values of $a^{(n)}$ obtained via eqs. (44)—(46) and the Born series. The series expansions (48)—(50) again show rapid convergence of $a^{(n)}$, but the Born values $a_B{}^{(n)}$ have the wrong sign and diverge rapidly with n, as expected.

References

1) P. Swan, Nature **187** (1960) 585
2) P. Swan, Nuclear Physics **18** (1960) 245
3) P. Swan, Nuclear Physics **21** (1960) 233
4) L. I. Schiff, Quantum Mechanics (McGraw-Hill, New York, 1949)
5) N. F. Mott and H. S. W. Massey, The theory of atomic collisions (Oxford University Press, 1949) 2nd ed.
6) J. M. Blatt and J. D. Jackson, Phys. Rev. **76** (1949) 18
7) L. Spruch and L. Rosenberg, Phys. Rev. **116** (1959) 1034;
L. Spruch and L. Rosenberg, Phys. Rev. **117** (1960) 1095;
L. Spruch and L. Rosenberg, Nuclear Physics **17** (1960) 30;
L. Rosenberg, L. Spruch and T. F. O'Malley, Phys. Rev. **119** (1960) 164;
L. Rosenberg and L. Spruch, Phys. Rev. **120** (1960) 474;
8) R. Jost and A. Pais, Phys. Rev. **82** (1951) 840
9) W. Kohn, Rev. Mod. Phys. **26** (1954) 292
10) T. Kikuta, Prog. Theor. Phys. **12** (1954) 225, 234
11) Ch. Zemach and A. Klein, Nuovo Cim. **10** (1958) 1078
12) H. Davies, Nuclear Physics **14** (1959—60) 465
13) N. Levinson, Mat. Fys. Medd., Dan. Vid. Selsk. **25**, No. 9 (1949)
14) P. Swan, Proc. Roy. Soc. **228** (1955) 10;
K. B. Mather and P. Swan, Nuclear scattering (Cambridge University Press, 1958) Appendix B

1.D.2:
1.E.4

Nuclear Physics **27** (1961) 632—647; © *North-Holland Publishing Co , Amsterdam*
Not to be reproduced by photoprint or microfilm without written permission from the publisher

MEASUREMENTS OF E1 TRANSITION PROBABILITIES IN SEVERAL DEFORMED ODD-MASS NUCLEI AS A STUDY OF SINGLE PARTICLE MOTION[†]

U. HAUSER[††],
California Institute of Technology, Pasadena, California, USA
K. RUNGE and G. KNISSEL
Zweites Physikalisches Institut der Universität Heidelberg, Heidelberg, Germany

Received 9 May 1961

Abstract: Lifetime measurements of nuclear states in the rare earth region have been performed by delayed fast-slow coincidence experiments. Results: (1) 321 keV $\frac{9}{2}+$ individual particle state of Hf^{177}, $t_{\frac{1}{2}} = (6.3 \pm 0.5) \times 10^{-10}$ sec; corresponding to three E1 transitions with hindrance factors $> 10^5$. (2) 113 keV $\frac{9}{2}-$ rotational state of Hf^{177}, $t_{\frac{1}{2}} = (5.2 \pm 0.4) \times 10^{-10}$ sec. (3) 396 keV $\frac{9}{2}-$ individual particle state of Lu^{175}, $t_{\frac{1}{2}} = (3.1 \pm 0.3) \times 10^{-9}$ sec; corresponding to three E1 transitions with hindrance factors of $\approx 10^6$. (4) 113 keV $\frac{9}{2}+$ rotational state of Lu^{175}, $t_{\frac{1}{2}} \leqq 1.5 \times 10^{-10}$ sec.

The E1 transition probabilities obtained, together with those of Lu^{177}, 147 keV (de Waard; McGowan) and Ta^{181}, 6.25 keV (Hauser) are analyzed in terms of the strong coupling model. (a) The single particle wave function of the rotational levels of the $K = \frac{7}{2}-$ ground state band in Hf^{177} is perturbed, presumably by interaction with a $K = \frac{9}{2}-$ state. (b) The five E1 matrix elements for the $K = \frac{9}{2}- \rightarrow K' = \frac{7}{2}+$ transitions in Lu^{175}, Lu^{177} and Ta^{181} are equal within a factor < 3. From this one can infer that the considerable changes of the nuclear core features are of no significant influence on the single particle wave functions of the initial and of the final states. (c) The transition probabilities deduced from configuration mixtures for the individual particle states in a Nilsson-potential are two orders of magnitude greater than the experimental values. Reducing the configuration mixture, as e.g. recently derived by Lemmer and Green from a non-local nucleon-nuclear interaction, will improve the agreement considerably.

1. Introduction

In recent years many experiments were performed to study the properties of the deformed odd-mass nuclei and their analysis proved the success of the Bohr-Mottelson [1, 2]) model.

A low-lying individual particle state of spin $I = K$ is described by several partial wave functions (N, l, j) whose projection of the total angular momentum j on the nuclear axis of symmetry equals K. The partial wave functions are of the same parity and their amplitudes depend on the deformation parameter

---

[†] This work is supported in part by Deutsches Bundesministerium für Atomkernenergie, Badisch Württembergisches Wirtschaftsministerium and the U. S. Atomic Energy Commission.

[††] On leave from Zweites Physikalisches Institut der Universität Heidelberg, Heidelberg, Germany.

δ, which has to be determined from the quadrupole moment or from the E2 transition probabilities between the collective rotational levels of the individual particle state. Apart from higher order effects the intrinsic structure is unchanged by a collective excitation mode, i.e. the configuration mixture is identical within the rotational levels. The partial wave functions correspond to pure shell model states (N, l, j) with $I = j$ in the limit of zero deformation.

The work of several authors which calculated individual particle states in different analytically simple, spheroidal potentials has been discussed and treated in detail by Villars [1]) and Moszkowski [2]). The most extensive and successful calculations were done by Nilsson [3]) who considered the individual particle motion in a spheroidal harmonic oscillator potential with $\mathbf{l} \cdot \mathbf{s}$-coupling and a l^2-term which represents a square well approximation. The coupling parameters, in magnitude determined by the shell model limit, are adjusted in the different shells to reproduce the empirical level sequence in the best way. Mottelson and Nilsson [4]) recently pusblished an elaborate analysis of the properties of the low-lying states of deformed nuclei on the basis of the "unified theory".

Very recently the problem of single particle motion in a spheroidal potential according to the Bohr-Mottelson picture was approached by Lemmer and Green [5]) in a different way. They calculated the non-analytical solutions for a phenomenological potential which is velocity dependent, non-local, has a diffuse boundary and includes a spin-orbit term. The necessary constants concerning well depth, non-locality distance, surface diffuseness and spin-orbit coupling are so chosen that the differential cross sections for elastic and inelastic neutron scattering in the mass range $A = 20$ to $A = 210$ were reproduced sufficiently well by an optical model calculation with a spherical potential. As to be expected the obtained level scheme in a spheroidal potential is practically identical with Nilsson's. There are, however, essential differences. There is much less configurational mixing, and the amplitudes of the partial wave functions are less sensitive to deformation changes.

The calculated magnetic moments are dependent on the intrinsic nuclear structure through the *intensities* of the predicted partial wave functions *and* on the collective motion through the gyromagnetic factor g_R. In Mottelson and Nilsson's [4]) and in Lemmer and Green's [5]) calculations there is only a rough agreement with the experimental results. It may be argued that this is partially due to the improper knowledge of the g_R-factor. Bernstein and de Boer [6]) summarizing the results of the rare earth nuclei reported significant variations of g_R as a function of Z and N. On the other hand their statements are derived from the measurements of g-factors and M1 transition probabilities of rotational bands assuming unchanged configurational mixture. Intensity ratios of γ-transitions from an individual particle state decaying to a rotational band, however, indicate that this assumption is not always valid.

A very sensitive test on the validity of the unified theory and the associated configuration mixture of the individual particle levels is provided by measurements of electromagnetic transition probabilities between individual particle levels because they depend on the ***amplitudes and phases*** of the partial wave functions of the two states and are independent of the collective motion. E1 transitions, which occur in general extremely hindered when compared with the single particle estimate, are especially sensitive and suited. Initial and final states cannot mix with each other because they have different parity. The transitions proceed in the view of the model via the small amplitude wave-functions which may be of minor influence on the g_K-factor of the intrinsic motion. E1 transitions between nuclear states of high spin are the simplest[†] to consider because the number of available orbits (N, l, j) contributing to a state is limited by the postulate $j_z = K$.

Two cases are of special interest to study the question whether the electromagnetic transitions also quantitatively can be explained within the framework of the present theory, whether a more realistic potential in the single particle model has to be taken into account, and whether the influence of residual interactions still can be neglected:

a) The decay of an individual particle state to the different levels of a rotational band. The absolute transition probabilities to these levels reflect the variations of their intrinsic structure which partly may be due to the spin dependent interaction with other excited states. The transitions $I = \frac{9}{2} \xrightarrow{\mathrm{E1}} I' = \frac{7}{2}, \frac{9}{2}, \frac{11}{2}$ in the neutron nucleus Hf^{177} and in the proton nucleus Lu^{175} represent such cases[††].

b) The neighbouring proton nuclei ${}_{71}\mathrm{Lu}^{175}$, ${}_{71}\mathrm{Lu}^{177}$, ${}_{73}\mathrm{Ta}^{179}$ and ${}_{73}\mathrm{Ta}^{181}$ have the same ground state spin $\frac{7}{2}+$ and are expected to be described by an almost identical configuration mixture. All the senuclei have a $\frac{9}{2}-$ excited state whose distance to the ground state decreases considerably with increasing mass number and which decays by E1 radiation to the ground state. Again it is expected in the single particle model that the configuration mixture of the excited states is almost identical. A measurement of the E1 transition probabilities between these states is a sensitive test on the influence of the added protons and neutrons on the particle motion in both states.

In sect. 2 we report experiments measuring the lifetime of the 321 keV $\frac{9}{2}+$ state of Hf^{177} which results in the determination of three E1 transition probabilities to the rotational band of the $\frac{7}{2}-$ ground state. The lifetime of the 396 keV $\frac{9}{2}-$ state of Lu^{175} decaying to the three members of the rotational band of the $\frac{7}{2}^+$ ground state is also measured and found to be in good agreement with a previous measurement reported by Vartapetian 9). Further, the lifetime of the 113 keV $\frac{9}{2}^-$ rotational state of Hf^{177} is determined. For the lifetime of the 113 keV $\frac{9}{2}^+$ rotational state of Lu^{175} an upper limit is given.

[†] Strominger and Rasmussen 7) have analyzed transition probabilities of several E1 transitions occurring in the mass region $A \approx 235$ by Nilsson's wave functions. The interpretation of the analysis is complicated by the great number of partial wave functions per nuclear state (5 or more).

[††] The level scheme of Lu^{175} has been considered under the aspects of the unified theory by Chase and Wilets 8) who also estimate the E1 hindrance in Lu^{175} and Hf^{177}.

In sect. 3 we analyze the E1 transition probabilities of Hf^{177} and Lu^{175} in terms of the strong coupling model. The E1 transition probabilities of Lu^{175} are further compared with those of Lu^{177} measured by de Waard 10) and McGowan 11) and of Ta^{181} measured by Hauser 12).

2. Experimental

2.1. PROCEDURE AND RESULTS

The delayed coincidence experiments are done with a Bell-type fast-slow coincidence apparatus. The coincidence rate is measured as a function of the delay between the "fast" signals under the condition that the "slow" signals correspond to the right energy.

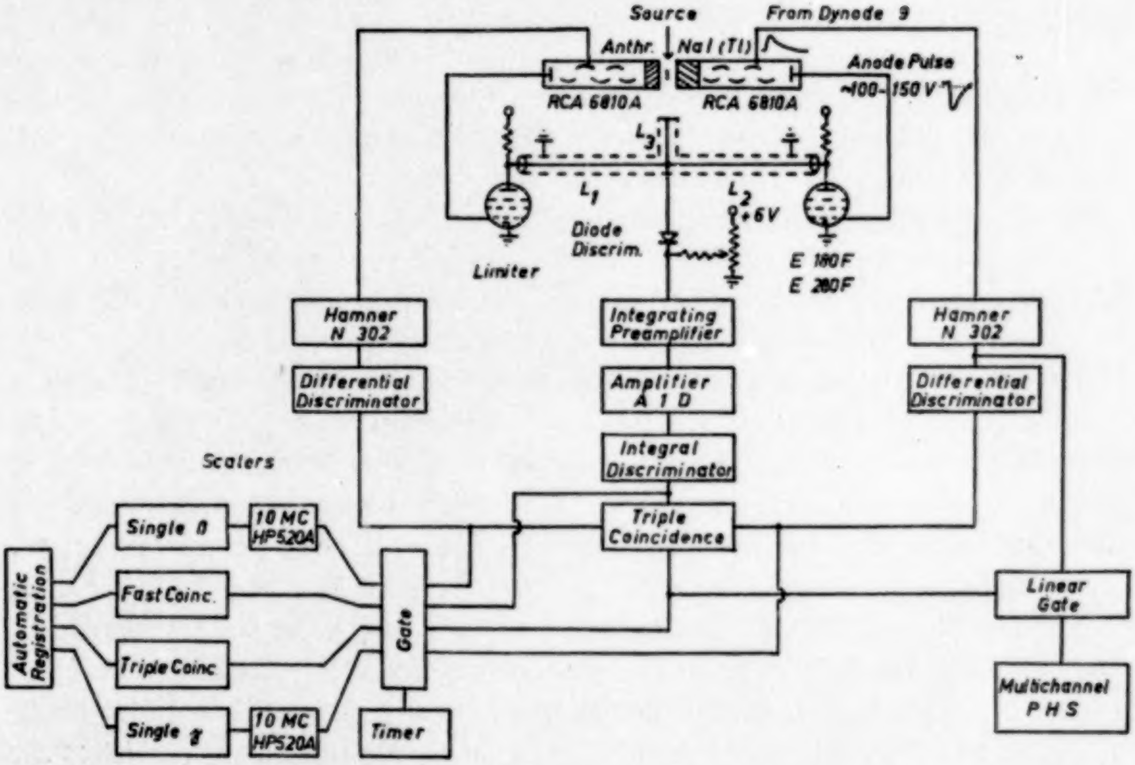
Source
From Dynode 9
Anthr.
NaI (Tl)
Anode Pulse
~100-150 V
RCA 6810A
RCA 6810A
L_3
L_1
L_2
+6V
Diode Discrim.
Limiter
E 180F
E 280F
Hamner N 302
Integrating Preamplifier
Hamner N 302
Differential Discriminator
Amplifier A 1 D
Differential Discriminator
Integral Discriminator
Scalers
Single β
10 MC HP520A
Triple Coincidence
Automatic Registration
Fast Coinc.
Gate
Linear Gate
Triple Coinc.
Single γ
10 MC HP520A
Timer
Multichannel PHS

Fig. 1. Schematic diagram of the experimental arrangement.

Fig. 1 shows schematically the experimental arrangement including important details. Because the apparatus has been described in an earlier paper 13) in some detail only a few features have to be mentioned which are essential for the life-time measurements.

The γ-detectors are 3.8 cm × 5 cm Harshaw NaI(Tl) crystals covered with

0.1 cm brass to absorb β-rays. The β-detector is 3.8 cm × 0.4 cm anthracene crystal covered by a 2.2 mg/cm^2 aluminium light reflector. The crystals are mounted directly on the photocathodes of RCA 6810A 14-stage photomultipliers.

The negative anode pulses of the photomultiplier of about 150 V amplitude are fed directly to the grid of the limiter pentodes (E180F or E280F) of very high transconductance, their cut-off voltage being only about 1.3 V. The resulting cut-off time is very small when compared to the long decay time of the NaI scintillators.

With this apparatus we achieve an optimum time resolution of $\tau_0 = 1.2 \times 10^{-9}$ sec. The coincidence loss at this resolution time is less than 10 % even with NaI crystals measuring (γ, γ)-coincidences at energies above 100 keV. For obtaining this result the two photomultiplier grids must be set carefully for maximum electron collection and minimum time jitter. Furthermore, there is an optimum setting of the fast coincidence diode bias which depends on the chosen resolution time and which determines the ratio of actual to random coincidences.

Because the β- and γ-spectra under investigation are of complicated structure the coincident spectra of both channels are checked during a run at regular time intervals by displaying them on a multichannel analyzer whose gate is initiated by the triple coincidence signal.

In the following we report lifetime measurements in the decay $\mathrm{Lu}^{177} \xrightarrow{\beta} \mathrm{Hf}^{177}$ and in the decay $\mathrm{Yb}^{175} \xrightarrow{\beta} \mathrm{Lu}^{175}$. The resolution time used is 1.5×10^{-9} sec and 3.5×10^{-9} sec, respectively. Because of several experimental difficulties in case of Hf^{177} the procedures are described in some detail.

The $\mathrm{Lu_2O_3}$ sources produced in the reactor of Harwell, England, with a specific activity of about 10 mCur/mg are deposited on a collodium film and covered by a second one. The films are supported by a thin aluminium ring of 3.8 cm inner diameter. The source diameter is about 0.5 cm, its thickness about 0.01 mg/cm^2. A source is placed directly between the two crystal detectors.

The decay scheme of $\mathrm{Lu}^{177} \xrightarrow{\beta} \mathrm{Hf}^{177}$ is shown in fig. 2(a). The 321 keV $\frac{9}{2}^+$ state is populated by the 176 keV β-radiation and decays by the 208 keV γ-radiation to the 113 keV $\frac{9}{2}^-$ state. For the lifetime measurements of the 321 keV state these two radiations are used. The 208 keV ray, however, is succeeded by the strongly K and L converted 113 keV transition ($\alpha_K = 0.75$, $K : L_I : L_{II} : L_{III} = 1.3 : 0.2 : 1.2 : 1.0$). This means that intense conversion electrons of about 50 keV and 100 keV are superposed on the β-spectrum and that they are coincident with the 208 keV γ-ray. Therefore at a negative delay of the γ-signal we measure (γ, e^-)-coincidences due to the 113 keV level, while at a positive delay the lifetime of the 321 keV level will be measured by (β, γ)-coincidences. Fig. 3 shows the coincident electron counter spectra displayed on the gated multichannel analyzer at two different signal delay times, namely $\pm 4 \times 10^{-9}$ sec from the centre of symmetry.

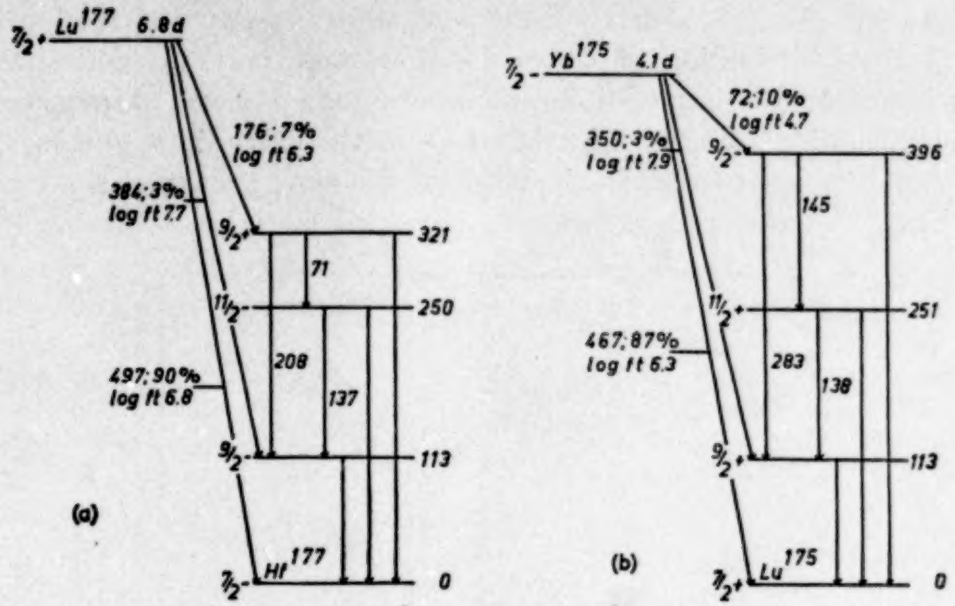
7/2+ Lu177 6.8d
176; 7% log ft 6.3
384; 3% log ft 7.7
9/2+ 321
71
11/2- 250
208
137
497; 90% log ft 6.8
9/2- 113
(a)
7/2- Hf177 0
7/2- Yb175 4.1d
72; 10% log ft 4.7
350; 3% log ft 7.9
9/2- 396
145
11/2+ 251
467; 87% log ft 6.3
283
138
9/2+ 113
(b)
7/2+ Lu175 0

Fig. 2. Level schemes of the decays Lu^{177} $\xrightarrow{\beta}$ Hf^{177} and Yb^{175} $\xrightarrow{\beta}$ Lu^{175}. The energies are given in keV.

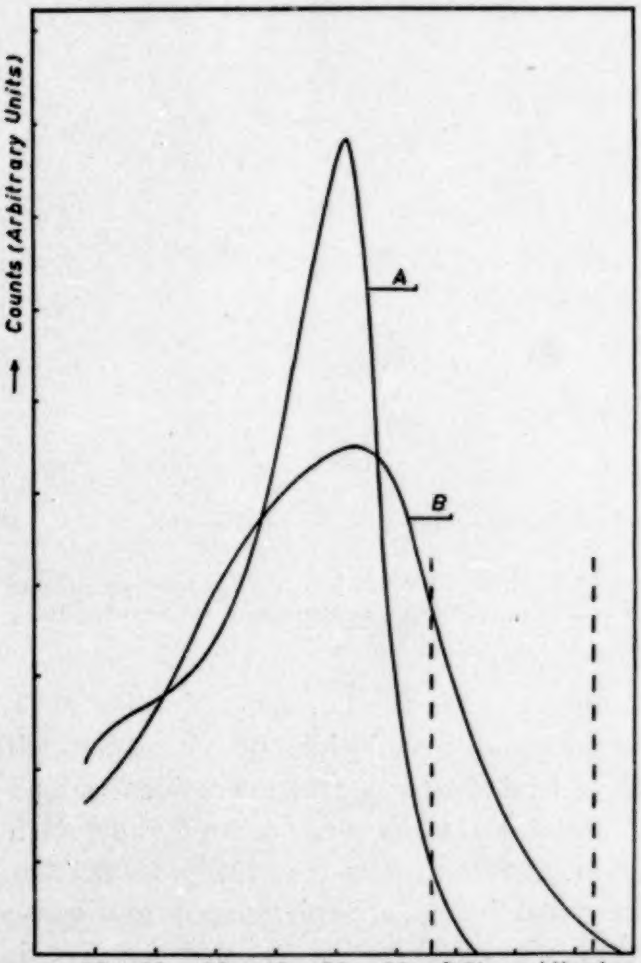

Fig. 3. Electron spectrum which is coincident with the 208 keV γ-ray of Hf^{177}. Curve A corresponds to the conversion electron spectrum of the 113 keV transition measured at a delay of the β-signal of -4×10^{-9} sec. Curve B corresponds to the 179 keV β-group measured at a delay of the β-signal of $+4\times10^{-9}$ sec. The dashed lines indicate the setting of the differential discriminator for the lifetime determination of the 321 keV level.

Curve A corresponds to a delay of the β-signal of -4×10^{-9} sec and shows a predominant contribution of conversion electrons, curve B corresponding to a delay of 4×10^{-9} sec exhibits the almost pure 179 keV β-spectrum. To avoid contributions of conversion electrons in the delayed (β, γ)-coincidence experiment the differential discriminator of the slow β-channel is set to the high energy end of the β-spectrum as indicated in fig. 3.

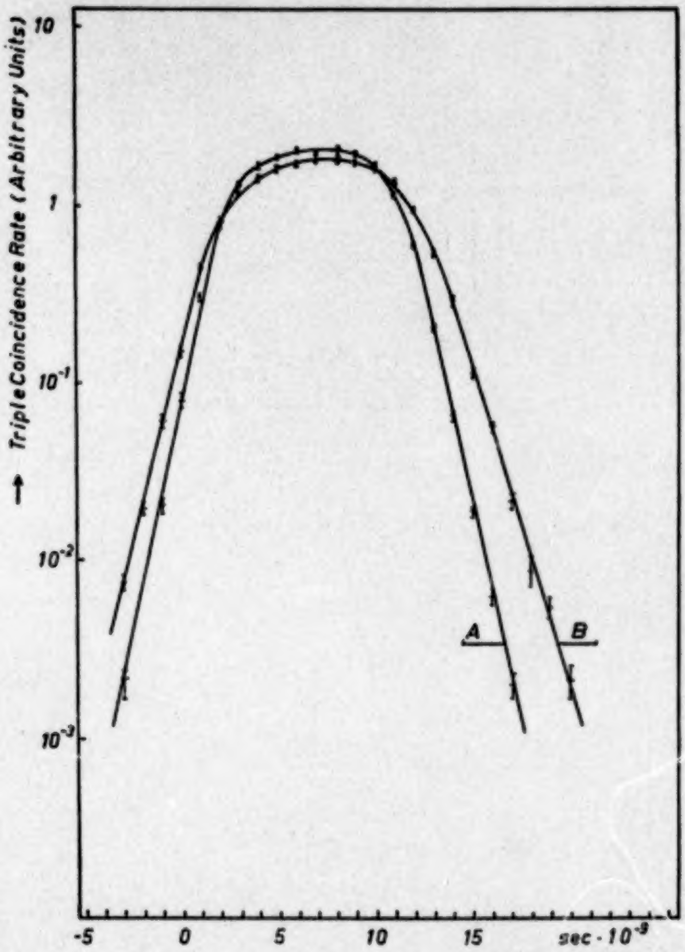

Fig. 4. Measurement of the lifetime of the 321 keV level of Hf^{177} by delayed (β, γ)-coincidences. Curve A is measured with Au^{198} as a prompt source, curve B with a Lu^{177} source.

Fig. 4 shows the result of the lifetime determination of the 321 keV level. Curve A represents the prompt resolution curve measured with a Au^{198} source where the β- and γ-discriminator settings are identical as with the Lu^{177} source. This means that the 411 keV γ-ray of Au^{198} is detected at the Compton tail by the γ-detector. Curve B shows the Lu^{177} result. The left part of the curve is due to the remaining (γ, e^-)-coincidences and corresponds to a half life of the 113 keV level of Hf^{177} of $\approx 5\times10^{-10}$ sec. The intensity drop at the right side is measured carefully for three orders of magnitude to avoid any contribution of conversion electrons. The curves are corrected for the lifetime of the source, the damping of the delay cables and the random coincidences. The evaluation is done by folding the delayed coincidence curve with the prompt one according to the method of Newton[14]). For the 321 keV level of Hf^{177} we obtain a half life

$$t_{\frac{1}{2}} = (6.3 \pm 0.5) \times 10^{-10} \text{ sec.}$$

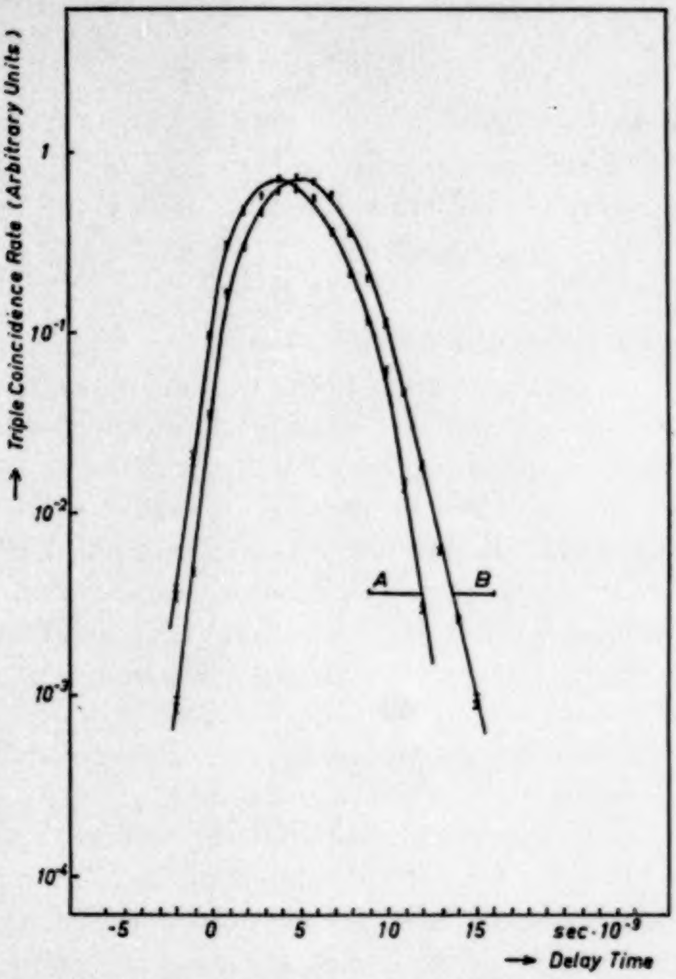

Fig. 5. Measurement of the lifetime of the 113 keV level of Hf^{177} by delayed (γ, γ)-coincidences. Curve A is measured with Co^{60} as a prompt source, curve B with a Lu^{177} source.

The half life of the 113 keV state of Hf^{177} is measured by (γ, γ)-coincidences between the 208 keV and the 113 keV γ-rays. The result is shown in fig. 5. The prompt source is Co^{60}, again measured with unchanged discriminators. The result is

$$t_{\frac{1}{2}} = (5.2 \pm 0.4) \times 10^{-10} \text{ sec}$$

for the 113 keV level of Hf^{177}.

The Yb_2O_3 sources are produced in the reactor of Harwell, England, with a specific activity of about 1 mCur/mg. Only fresh sources are used to avoid the increasing percentage of the decay $Yb^{169} \xrightarrow{E.C.} Tm^{169}$. The decay scheme $Yb^{175} \xrightarrow{\beta} Lu^{175}$ is shown in fig. 2b. There is a 72 keV β-transition of 10 % to the 396 keV $\frac{9}{2}-$ state of Lu^{175} which decays in 60 % by a direct cross over transition to the ground state of Lu^{175}. These two radiations are used for the (β, γ)-coincidence experiment. The aluminium light reflector of the β-counter is reduced to a thickness of 1 mg/cm^2. The measurements result in a half life of

$$t_{\frac{1}{2}} = (3.1 \pm 0.3) \times 10^{-9} \text{ sec}$$

for the 396 keV level of Lu^{175}.

Delayed (γ, γ)-coincidences between the 283 keV and the 113 keV γ-rays to determine the lifetime of the 113 keV level of Lu^{175} result only in an upper limit of

$$t_{\frac{1}{2}} \leqq 1.5 \times 10^{-10} \text{ sec.}$$

2.2. COMPARISON WITH PREVIOUS RESULTS

Recently Blaugrund, Dar and Goldring [15]) modulated by a microwave pulsing system the protons, which Coulomb-excite collective states, and the conversion electrons, which are produced from these states. From the phase shifts they determined half lives in the region of 10^{-11} to 10^{-10} sec. One of the three cases reported is the 113 keV rotational state of Lu^{175}. They report $t_{\frac{1}{2}} = (1.01 \pm 0.07) \times 10^{-10}$ sec which is below the upper limit given by us. The 113 keV rotational level of Hf^{177} was not within the range of their experimental arrangement; however, they give a lower limit $t_{\frac{1}{2}} \geqq 4.2 \times 10)^{-10}$ sec which is also in good agreement with our result.

There is, however, some disagreement with the result of $t_{\frac{1}{2}} = (4.2 \pm 0.6) \times 10^{-10}$ sec reported by Berlovich [16]) for the 113 keV level of Hf^{177}. This was obtained by a (β, γ)-coincidence experiment between the 384 keV β-group of 3 % intensity and the 113 keV γ-ray. The evaluation of the measurement was done with a self comparison method using the centroid shift of the delayed coincidence curve. Unfortunately no experimental details and curves are reported.

The half life of the 396 keV state of Lu^{175} has been measured in a previous experiment by Vartapetian [9]), $t_{\frac{1}{2}} = (3.4 \pm 0.3) \times 10^{-9}$ sec, which is in agreement with our result within the assigned errors.

3. Analysis of E1 Transitions and Discussion

Table 1 summarizes the experimental results concerning E1 transitions together with other data as conversion coefficients, mixing ratios etc. necessary for the analysis †. The experimental data of the 147 keV transition [10, 11]) in Lu^{177} and of the 6.25 keV transition [12]) in Ta^{181} are also added.

† The principal ideas of describing a single particle motion in a spheroidal potential have been outlined in sect. 1. We shall not define the details and notations usually used in the theory but refer to the original and review papers [1-4]).

TABLE 1

Experimental results concerning E1 transitions

Nucleus	Transition energy [17]) (keV)	Half life $t_{\frac{1}{2}}$ (sec)	M2 admixture (%)	Total conversion coeff.	Relativ γ-ray intensities	E1 transition probability T(E1) (sec^{-1})	G^2_{E1} (exp)
Hf^{177}	321 208 71	6.3×10^{-10} [a])		0.2 [b]) 0.05 [b]) 1.0 [b])	3 [b]) 220 [b]) 2 [b])	1.4×10^{7} 9.7×10^{6} 9.3×10^{6}	1.1×10^{-7} 1.3×10^{-4} 2.9×10^{-4}
Lu^{175}	396 283 145	3.1×10^{-9} [a])	20 [c]) 4 [c])	0.075 [c]) 0.034 [c]) 0.12 [c])	100 [c]) 62 [c]) 5.9 [c])	1.1×10^{8} 6.2×10^{7} 5.7×10^{6}	4.5×10^{-7} 3.2×10^{-6} 2.2×10^{-5}
Lu^{177}	147	1.2×10^{-7} [d])	10 [d,e])	0.4 [d,e])		4.3×10^{6}	3.5×10^{-7}
Ta^{181}	6.25	6.8×10^{-6} [g])		44 [f])		2.3×10^{3}	2.4×10^{-6}

[a]) present results

[b]) P. Marmier and F. Boehm, Phys. Rev. **97** (1955) 103

[c]) E. N. Hatch, F. Boehm, P. Marmier and J. W. M. DuMond, Phys. Rev. **104** (1956) 745

[d]) See ref. [10])

[e]) J. P. Mize, M. E. Bunker and J. W. Starner, Phys. Rev. **103** (1956) 182

[f]) A. H. Muir and F. Boehm, Bull. Am. Phys. Soc. **4** (1959) 367, Phys. Rev. (in press)

[g]) See ref. [12])

In the strong coupling model the E1 transition probability (except for $K=\frac{1}{2}\pm\rightarrow K'=\frac{1}{2}\mp$) is given by

$$T(\mathrm{E}1) = \left\{\frac{16\pi}{9}\frac{1}{\hbar}\left(\frac{\omega}{c}\right)^3\left[e^2\left(1-\frac{Z}{A}\right)^2\frac{\hbar}{M\omega_0}\frac{3}{4\pi}\langle I\,1KK'-K|I1I'K'\rangle^2\right]\right\}G^2_{\mathrm{E}1}\ \mathrm{sec}^{-1}. \quad (1)$$

The quantity

$$G_{\mathrm{E}1} = \sum_{l'l}\langle N'l'|r|Nl\rangle\sqrt{\frac{2l+1}{2l'+1}}\,\langle l1\,0\,0|l\,1\,l'\,0\rangle\sum_{\Lambda'\Lambda\,\Sigma'\Sigma}\delta_{\Sigma'\Sigma}a'_{l'\Lambda'}a_{l\Lambda}\langle l1\Lambda K'-K|l1l'\Lambda'\rangle \quad (2)$$

represents the transition matrix element, the $a_{l\Lambda}$ being the amplitudes of the partial wave functions of initial and final state and Λ the projection of the orbital momentum l on the nuclear symmetry axis (Λ obeys with the spin quantum number Σ the condition $\Lambda+\Sigma=K=\Omega$), while $B(\mathrm{E}1)=[\quad]G^2_{\mathrm{E}1}$ is the reduced transition probability.

In order to compare the transition probabilities of the different nuclei in a perspicuous way we have divided the experimental results by the expression between brackets $\{\ldots\}$ of eq. (1) so that they can be simply confronted with the squares of the matrix elements $G^2_{\mathrm{E}1}$ which are independent of Z, A, the

TABLE 2

Amplitudes of partial wave functions

K	Nucleus	Level energy and spin	Classification		Shell model state	Amplitudes of configuration mixture				δ	$3\hbar^2/\mathscr{J}$ (keV)
			M. & N. [4])	L. & G. [5])		M. & N.		L. & G.			
						$\delta = 0.2$	$\delta = 0.3$	$\delta = 0.2$	$\delta = 0.3$		
$\frac{9}{2}-$			$\frac{9}{2}-[505]$ No. 25	No. 18, $\frac{9}{2}-$	$1h_{\frac{11}{2}}$ $1h_{\frac{9}{2}}$	$+0.2244$ -0.9744	$+0.1981$ -0.9801	0.064 0.998	0.090 0.996		
$\frac{9}{2}+$	Hf^{177}	321; $\frac{9}{2}+$	$\frac{9}{2}+[624]$ No. 49	No. 19, $\frac{9}{2}+$	$1i_{\frac{13}{2}}$ $1i_{\frac{11}{2}}$ $2g_{\frac{9}{2}}$	0.9423 0.3128 0.1188	0.9479 0.2805 0.1507		≈ 1		
$\frac{7}{2}-$	Hf^{177}	0; $\frac{7}{2}-$ 113; $\frac{9}{2}-$ 251; $\frac{11}{2}-$	$\frac{7}{2}-[514]$ No. 41	No. 17, $\frac{7}{2}-$	$1h_{\frac{11}{2}}$ $1h_{\frac{9}{2}}$ $2f_{\frac{7}{2}}$	-0.321 $+0.941$ -0.111	-0.279 $+0.953$ -0.117	0.051 0.991 0.120	0.075 0.991 0.113	0.27	76
$\frac{5}{2}+$	Lu^{175} Lu^{177} Ta^{179} Ta^{181}	349; $\frac{5}{2}+$ 433; $\frac{7}{2}+$ 482; $\frac{5}{2}+$	$\frac{5}{2}+[402]$ No. 31	No. 13, $\frac{5}{2}+$	$1g_{\frac{9}{2}}$ $1g_{\frac{7}{2}}$ $2d_{\frac{5}{2}}$	-0.228 $+0.137$ $+0.964$	-0.257 $+0.119$ $+0.959$	-0.184 -0.044 $+0.982$	-0.240 -0.062 $+0.969$		
$\frac{9}{2}-$	Lu^{175} Lu^{177} Ta^{179} Ta^{181}	396; $\frac{9}{2}-$ 147; $\frac{9}{2}-$ 30; $\frac{9}{2}-$ 6.25; $\frac{9}{2}-$	$\frac{9}{2}-[514]$ No. 32	No. 14, $\frac{9}{2}-$	$1h_{\frac{11}{2}}$ $1h_{\frac{9}{2}}$	0.9745 0.2241	0.9802 0.1979				
$\frac{7}{2}+$	Lu^{175} Lu^{177} Ta^{179} Ta^{181}	0; $\frac{7}{2}+$ 113; $\frac{9}{2}+$ 251; $\frac{11}{2}+$ 0; $\frac{7}{2}+$ 119; $\frac{9}{2}+$ 0; $\frac{7}{2}+$ 0; $\frac{7}{2}+$ 136; $\frac{9}{2}+$ 301; $\frac{11}{2}+$	$\frac{7}{2}+[404]$ No. 25	No. 12, $\frac{7}{2}+$	$1g_{\frac{9}{2}}$ $1g_{\frac{7}{2}}$	-0.2352 $+0.9719$	-0.2037 $+0.9790$	0.093 0.996	0.128 0.992	0.28 0.26 0.23	76 79 91

oscillator level spacing $\hbar\omega_0$ and the vector coupling coefficients which contain the spin I' of the final state. All E1 transitions under consideration proceed from $I = \frac{9}{2}$ to $I' = \frac{7}{2}, \frac{9}{2}, \frac{11}{2}$ or $K = \frac{9}{2}$ to $K' = \frac{7}{2}$, i.e., they are K-allowed, however asymptotically forbidden through the selection rules of the asymptotic quantum numbers.

While the radial parts of the matrix elements $\langle N'l' |r| Nl \rangle$ can be calculated analytically for the harmonic oscillator potential chosen by Nilsson [3]) this is not the case for the "bathtub" potential of Lemmer and Green [5]). Unfortunately these authors have not computed numerically the radial parts of electric dipole matrix elements. Further, the amplitudes and phases of the partial wave functions describing a single particle state in this non-local potential are calculated only for the even parity states of protons with $50 \leqq Z \leqq 82$ and the odd parity states of neutrons with $82 \leqq N \leqq 126$. Therefore a quantitative comparison of the experimental results can only be made with the harmonic oscillator potential, although one still can draw some conclusions concerning the behaviour of single particle states in the non-local potential.

Table 2 lists the amplitudes of the partial wave functions of the nuclear states under consideration according to Nilsson [3, 4]) (normalized to $\sum a_{l\Lambda}^2 = 1$) and Lemmer and Green [5]) † and shows the considerable difference of amplitudes for the two potentials. The actual deformations of the states have to be derived from E2 transition probabilities or quadrupole moments, but nothing is known for the excited states. From other nuclei of the rare earth region it is known experimentally that the deformation is practically constant in different intrinsic states [4]). We have therefore assumed for the numerical calculations that the deformation of initial and final states is identical. On the other hand changes of δ up to 10 % do not alter the results decisively.

Fig. 6 shows the normalized transition probabilities for the three neutron transitions in Hf^{177} and fig. 7 those for the proton nuclei. The theoretical values are also inserted †† as a function of the deformation parameter δ. Especially the neutron transitions demonstrate the strong influence of admixtures of wave functions of small amplitudes and of their phases †††. Not taking into account the transition modes $2g_{\frac{9}{2}} \rightarrow 1h_{\frac{11}{2}}$ and $2g_{\frac{9}{2}} \rightarrow 2f_{\frac{7}{2}}$ but only $1i_{\frac{13}{2}} \rightarrow 1h_{\frac{11}{2}}$ and $1i_{\frac{11}{2}} \rightarrow 1h_{\frac{9}{2}}$ results in a transition probability which is two orders of

---

† We thank Dr. A. E. S. Green for furnishing us with the tables of computed amplitudes of the normalized eigenfunctions. The configuration mixture of the $\frac{9}{2}+$ state of Hf^{177} has not been calculated, however, it has been estimated roughly in order to obtain the g_K-factor of the Hf^{179} ground state.

†† The G_{E1}^2 shown in figs. 6 and 7 are calculated as a function of Nilsson's deformation parameter η, which is related to δ by $\delta = \kappa\eta$. The δ-abscissa is drawn for $\kappa = 0.05$, which is the spin-orbit coupling parameter for the $N = 5$ and 6 shell; for the $N = 4$ shell it has the value 0.0613 (ref. [3])).

††† We have not applied the small effective charge correction [4]) for the neutron transitions.

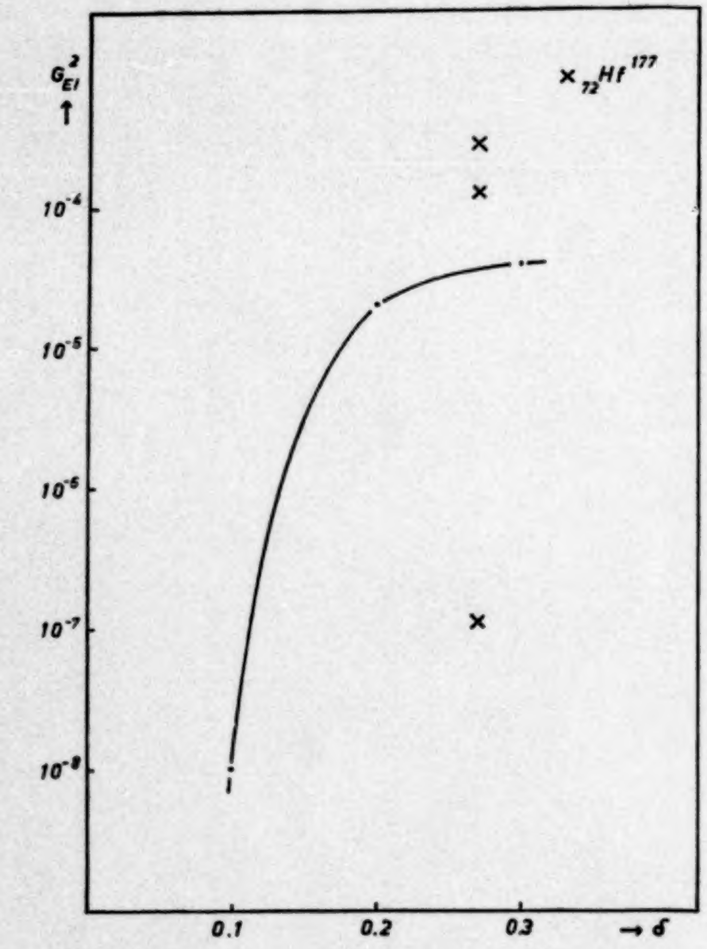

Fig. 6. Normalized experimental transition probabilities G^2_{E1} for the neutron E1 transitions in Hf^{177}. For comparison the theoretical predictions derived from a spheroidal harmonic oscillator potential are inserted as a function of the nuclear deformation parameter δ.

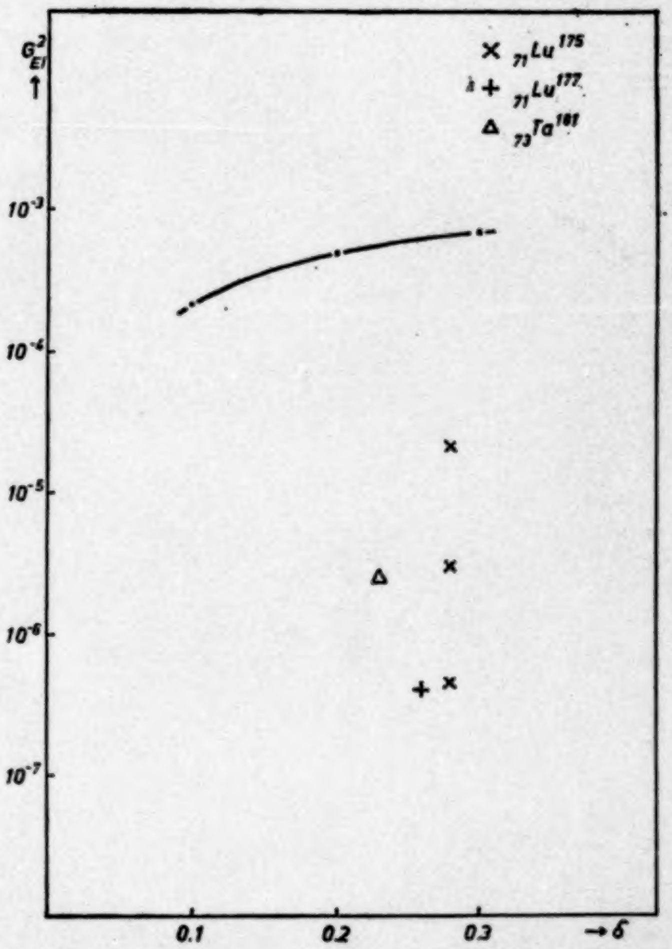

Fig. 7. Normalized experimental transition probabilities G^2_{E1} for the proton E1 transitions in Lu^{175}, Lu^{177} and Ta^{181}. For comparison the theoretical predictions derived from a harmonic oscillator potential are inserted.

magnitude greater than those given in fig. 6. For the proton transitions there are only two transition modes.

In general we note that the experimental hindrance of all the groundstate transitions is at least a factor 100 greater than predicted from the configuration mixture in a spheroidal harmonic oscillator potential and it is obvious that these deviations are neither due to a wrongly chosen deformation parameter nor to the neglect of a difference in deformation between initial and final states. Further, we notice that the transition probability to the rotational levels of the lower state increases with increasing level energy and spin. This is however, only a factor 7 in the proton transitions and a factor 2 in the neutron case, which means a variation of the matrix element by a factor of 2 to 3 and can be considered as a higher order effect.

While the small variations of the transition probabilities in Lu^{175} confirm the constancy of the intrinsic structure of a rotational band, the differences between the $\frac{9}{2}+ \rightarrow \frac{7}{2}-$ and the $\frac{9}{2}+ \rightarrow \frac{9}{2}-$, $\frac{11}{2}-$ transitions by a factor of 1000 in Hf^{177} reflects a change of the structure within the ground state band[†]. Such a change of the intrinsic structure is expected to be caused by interaction with another state of $I = K = \frac{9}{2}-$, for which the perturbed wave function is given by

$$\psi = \psi_0 + \frac{\langle 0\,|H'|\,n\rangle}{E_n - E_0}\,\psi_n. \tag{3}$$

However, no low-lying $\frac{9}{2}-$ individual particle state of Hf^{177} is known at present or can be expected from the predicted level scheme [3–5]).

The 113 keV $\frac{9}{2}-$ rotational state of Hf^{177} decays predominantly by E2 radiation. The M1 admixture is about 5 %, its actual intensity cannot be determined from the present experimental data without great error, neither from the conversion and angular correlation results, as Arns and Wiedenbeck [18]) have pointed out, nor from Coulomb excitation data [17]). Therefore our measurement of the lifetime of this state gives little information on the g_K- and g_R-factors of the ground state band. In addition, at least three independent measurements of the magnetic properties are necessary to be sure that the observed variation of the intrinsic structure is of minor influence on the inherent g-factors.

[†] It is interesting to note that for Lu^{175} as well as Hf^{177} (and also Ta^{181}) the ratio of the rotational energies is in excellent agreement with the predicted formula $I_{K+2}/I_{K+1} = 2+(1/K+1) = 2.22$ for $K = \frac{7}{2}$.

An additional check (however much less sensitive than that from E1 transitions) on a change of the intrinsic structure of the Hf^{177} ground state band is given by the ratios of the reduced M1 and E2 transitions within the band, i.e. $I(\mathrm{E2})_{250\,\mathrm{keV}}(\frac{11}{2} \rightarrow \frac{7}{2}) : I(\mathrm{E2})_{137\,\mathrm{keV}}(\frac{11}{2} \rightarrow \frac{9}{2})$, which are determined in an undisturbed band only by the quadratic ratios of the vector coupling coefficients involved. Because of the great experimental limits of error and the different results obtained in Coulomb excitation [17]) possible deviations in Hf^{177} cannot be definitely stated at present.

A comparison of the energy spacing of the ground state bands between Yb^{174} and Lu^{175} shows no significant change of the moment of inertia in Lu^{175} due to the addition of the odd proton. A similar comparison in the case of Hf^{176} and Hf^{177} shows a 17 % increase of the moment of inertia in Hf^{177} due to the addition of the odd neutron. This may be of importance when considering the perturbation of the Hf^{177} ground state band as a result of Coriolis mixing with another rotational band of $K = \frac{9}{2}-$ (see also our discussion below connected with the proton transitions).

Additional information on the intrinsic structure of the rotational bands of Lu^{175} and Hf^{177} could be gained from the ft-values of the β-decays ${}^{105}\mathrm{Yb}^{175} \rightarrow {}_{71}\mathrm{Lu}^{175}(K = \frac{7}{2}- \rightarrow K = \frac{7}{2}+)$ and ${}_{71}\mathrm{Lu}^{177} \rightarrow {}^{106}\mathrm{Hf}^{177}(K = \frac{7}{2}+ \rightarrow K = \frac{7}{2}-)$ which are expected to be "mirror transitions" between the same intrinsic particle wave functions ($N = 105 \longleftrightarrow Z = 71$). However, sufficiently accurate experimental information is lacking at present.

Fig. 7 shows the normalized E1 transition probabilities for the proton nuclei. Their over-all constancy at an absolute retardation of about 10^6 is very remarkable. Although the nuclear properties do change considerably as a function of Z and N, which is indicated by the decrease of the $\frac{9}{2}^-$ level energy, the decrease of the intrinsic quadrupole moment or deformation parameter and that of the nuclear moment of inertia with increasing mass number, there seems to be no significant change of the single particle wave functions of both levels, ground state and excited state. The different residual interactions of Lu^{177} and Ta^{181} caused by the addition of a proton and a neutron pair hardly affect the single particle properties at all. It seems rather improbable that each of the two partial wave functions in each of the two states vary in all three nuclei in such a way that an almost constant electric dipole matrix element is resulting [†].

There is a close-lying $I = K = \frac{5}{2}^+$ state (349 keV in Lu^{175}, 482 keV in Ta^{181} and not known at present for Lu^{177} and Ta^{179}) whose rotational states ($I = \frac{7}{2}^+$ at 433 keV in Lu^{175}) could mix with the $K = \frac{7}{2}^+$ groundstate band by rotational-particle interaction (Coriolis term) analogue to W^{183} which was calculated by Christy [19]) and Kerman [20]). From the estimated change of the denominator of eq. (3) by about 20 to 30 % from Lu^{175} to Ta^{181} we can conclude that the perturbation H' must be rather small.

In addition the proton transitions demonstrate that transitions between the always purer states (especially for higher angular momenta) of the non-local potential [5]) are predicted to be more hindered than those of the local potential [3,4]) in accordance with the experimental results. If we approximate in eq. (2) the radial part of the matrix element for the non-local interaction by the local one we can estimate from the decrease in configuration mixture that the transition probabilities will be smaller [††] by a factor of at least 10 to 100.

We may state in summary that it has been shown that in these nuclei the odd nucleon motion seems to be determined predominantly by the collective potential of the nuclear core, and that neither rather drastic changes of the intrinsic core features nor changes of the residual interactions caused by filling of neighbouring orbits are of significant influence on the odd particle wave functions. On the other hand better and rather accurate wave functions presumably based on a realistic nucleon-nuclear potential are necessary for a better agreement with the experimental data and for further information on the interactions between odd particle states and higher bound and continuous states.

[†] For these transitions eq. (2) is of the simple form $G_{E1} \approx (ka_1a'_2-a_2a'_1) \approx$ const., with $\Sigma a^2 = \Sigma a'^2 = 1$, $a_1, a'_1 \approx 1$ and $k \approx 1$.

[††] With such pure states the observed small differences in the proton transition probabilities can already result from less than a 1 % change of the intensity of the predominant wave function.

We are indebted to Professor O. Haxel for his interest and support. It is a pleasure to thank in particular Professor F. Boehm, California Institute of Technology, Pasadena, for stimulation and support during a stay at this laboratory in 1959 and for his further interest in this investigation. We thank Dr. E. N. Hatch, Dr. J. D. Rogers and Dr. H. A. Weidenmüller for interesting discussions and H. C. Weber for experimental help. Financial support has been granted by the Bundesministerium für Atomkernenergie and the Badisch-Württembergisches Wirtschaftsministerium and is gratefully acknowledged.

References

1) F. Villars, Annual Review of Nuclear Sciences, Vol. 7 (Annual Review Inc., Stanford 1957)
2) S. A. Moszkowski, Handbuch der Physik, Vol. **39** (Springer-Verlag, Berlin, 1957)
3) S. G. Nilsson, Mat. Fys. Medd. Dan. Vid. Selsk. **29** no. 16 (1955)
4) B. R. Mottelson and S. G. Nilsson, Mat. Fys. Skr. Dan. Vid. Selsk. **1** no. 8 (1959)
5) R. H. Lemmer and A. E. S. Green, Phys. Rev. **119** (1960) 1043
6) E. M. Bernstein and J. de Boer, Nuclear Physics (in press)
7) D. Strominger and J. O. Rasmussen, Nuclear Physics **3** (1957) 197
8) D. Chase and L. Wilets, Phys. Rev. **101** (1956) 1038
9) H. Vartapetian, Compt. Rend. **244** (1957) 65
10) H. de Waard, Phil. Mag. **46** (1955) 445
11) F. K. McGowan, Phys. Rev. **76** (1949) 1730, ORNL-952 (1951)
12) U. Hauser, Nuclear Physics (in press)
13) F. Boehm and U. Hauser, Nuclear Physics **14** (1959) 615
14) T. D. Newton, Phys. Rev. **78** (1950) 490
15) A. E. Blaugrund, Y. Dar and G. Goldring, Phys. Rev. **120** (1960) 1328
16) E. Berlovich, Izvest. Akad. Nauk SSSR, Ser. Fiz. **20** (1956) 1438
17) Nuclear Data Sheets, National Academy of Sciences, Washington D.C.
18) R. G. Arns and M. L. Wiedenbeck, Phys. Rev. **111** (1958) 1631
19) R. F. Christy, Phys. Rev. **96** (1954) 858
20) A. Kerman, Mat. Fys. Medd. Dan. Vid. Selsk. **30**, no. 15 (1955)

2.J

Nuclear Physics **27** (1961) 648—664; © *North-Holland Publishing Co., Amsterdam*

Not to be reproduced by photoprint or microfilm without written permission from the publisher

TWO-PROTON RADIOACTIVITY

V. I. GOLDANSKY

P. N. Lebedev Physical Institute, Academy of Sciences of the USSR, Moscow, USSR

Received 24 December 1960

Abstract: Basic information is presented on two-proton radioactivity, a new and unique kind of nuclear radioactive decay which was predicted previously.

The paper enumerates the 2p-radioactive nuclei and the optimum conditions of producing them in reactions with the participation of He^3 or heavy multi-charged ions, with the indication of the number of evaporated neutrons and the thresholds of these reactions. Estimates are made of the cross-sections for the production of 2p-radioactive nuclei, which reach 0.1 to 1 mb.

Under consideration are the energy and angular correlations of the two emitted protons depending on the nature of their interaction within the nucleus and outside it.

The interpretation of the triple fission of nuclei with the emission of long-range alpha-particles is suggested by analogy with certain properties of two-proton decay.

1. Introduction

As we have pointed out earlier [1]), a new and rather peculiar kind of radioactive decay — the two-proton radioactivity — should be observed for a number of neutron-deficient isotopes of even light elements. This kind of radioactivity is by no means a rare exception but rather a general property of light nuclei with an even number of protons close to the proton-instability limit. The origin of two-proton radioactivity can be traced to the pairing of protons in a nucleus, owing to which it proves to be easier to eject from the nucleus a pair of protons at once than to break them apart (see fig. 1). With a negative binding energy of the odd $(2m+1)$-th-proton ($B_{p_{\text{odd}}} < 0$), the binding energy of the subsequent $(2m+2)$-th even proton proves to be larger by the pairing energy $E_{\text{pairing}} \approx 1$—2 MeV:

$$B_{p_{\text{even}}} = E_{\text{pairing}} + B_{p_{\text{odd}}} = E_{\text{pairing}} - |B_{p_{\text{odd}}}|$$

(with this definition we somewhat underestimate the pairing energy, for we neglect the change in nuclear Coulomb energy as an extra proton is added). If even B_p proves to be positive, the emission of the $(2m+2)$th proton alone is impossible energetically, whereas the emission of a pair of protons occurs with the release of energy $|E_{pp}| = |B_{p_{\text{odd}}}| - B_{p_{\text{even}}}$ ($E_{pp} < 0$ being the negative two-proton binding energy).

Just like beta decay, two-proton radioactivity is a problem of three bodies.

After the conversion there are two protons and a recoil nucleus. But the inevitable penetration of the two emitted protons through the Coulomb potential barrier leads to strong energy correlation between them, as was mentioned in ref. [1]). The experimental detection and investigation of two-proton radioactivity seems to be desirable not only because the phenomenon is new, but primarily because the investigation of the correlation of the protons emitted can yield certain information on the nature of their interaction within and outside the nucleus. The present paper considers the basic characteristics of the energy and angular correlations of protons in two-proton decay, and presents certain data and estimates regarding the prospects of experimental investigation of two-proton radioactivity.

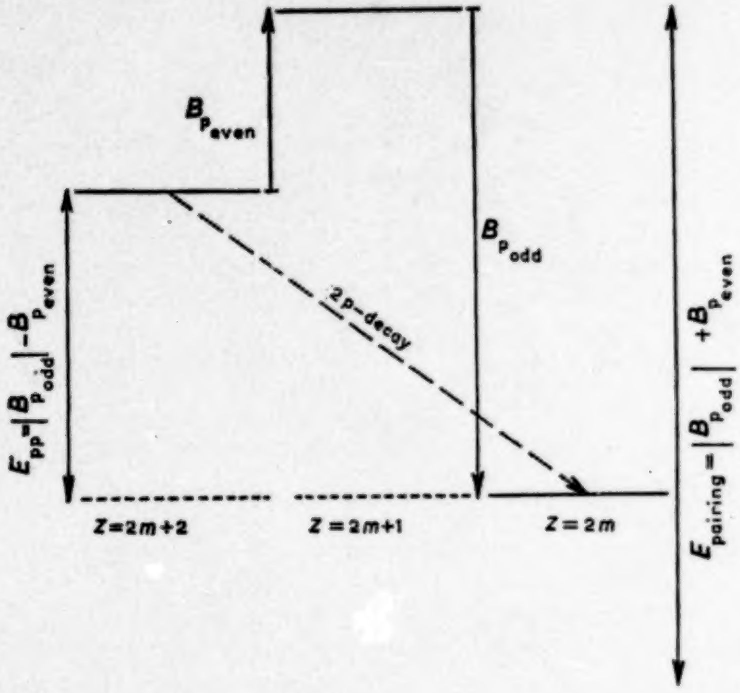
$B_{p_{\text{even}}}$
$B_{p_{\text{odd}}}$
2p-decay
$E_{pp}=|B_{p_{\text{odd}}}|-B_{p_{\text{even}}}$
$E_{\text{pairing}}=|B_{p_{\text{odd}}}|+B_{p_{\text{even}}}$
$Z=2m+2$
$Z=2m+1$
$Z=2m$

Fig. 1

2. Two-Proton Radioactive Nuclei

To estimate proton binding energy in neutron-deficient nuclei and to list the nuclei belonging to the two-proton-radioactive class we can make use of ref. [1]) and the tables of nuclear masses computed by Cameron [2]). In his calculations Cameron employed and improved version of the Weizsäcker-Fermi formula, taking the shell structure of nuclei into account to a certain extent. It is noteworthy that in the region where the calculations of ref. [1]) and ref. [2]) overlap, the stability limit obtained by Cameron for neutron-deficient nuclei almost coincides with that obtained in ref. [1]) on the basis of isobaric invariance.

Table 1

2p-radioactive nuclei

Nucleus	$M—A$ (MeV)	E_{pp} (MeV)	E_{pairing} (MeV)
${}_{4}\mathrm{Be}_{2}^{6}$	20.3	1.5	2,1
${}_{10}\mathrm{Ne}_{6}^{16}$	27.7—29 g)	0.5—1.8 g)	4.1—2.8 g)
${}_{12}\mathrm{Mg}_{5}^{17}$			
${}_{12}\mathrm{Mg}_{6}^{18}$			
${}_{14}\mathrm{Si}_{7}^{21}$			
${}_{14}\mathrm{Si}_{8}^{22}$			
${}_{16}\mathrm{S}_{8}^{24}$			
${}_{16}\mathrm{S}_{9}^{25}$			
${}_{18}\mathrm{Ar}_{10}^{28}$			
${}_{18}\mathrm{Ar}_{11}^{29}$ a)	40.6	(4.1)	1.8
${}_{18}\mathrm{Ar}_{12}^{30}$ b)	25.1	1.4	1.8
${}_{20}\mathrm{Ca}_{13}^{33}$ a)	33.8	(2.4)	2.3
${}_{20}\mathrm{Ca}_{14}^{34}$ c)	19.0	(−0.1)	2.3
${}_{22}\mathrm{Ti}_{15}^{37}$ d)	28.2	2.7	2.7
${}_{22}\mathrm{Ti}_{16}^{38}$	21 g) 15.5	0.1 g) 0.4	1.3 g)
${}_{24}\mathrm{Cr}_{17}^{41}$ e)	24.6	1.8	2.3
${}_{24}\mathrm{Cr}_{18}^{42}$ c, e)	<18 g) 12.3	0.6 g) (−0.3)	0.6—0.8 g) 2.3
${}_{26}\mathrm{Fe}_{17}^{43}$			
${}_{26}\mathrm{Fe}_{18}^{44}$ a)	30.4	(2.9)	2.0
${}_{26}\mathrm{Fe}_{19}^{45}$	20.9	1.0	2.0
${}_{28}\mathrm{Ni}_{18}^{46}$			
${}_{28}\mathrm{Ni}_{19}^{47}$			
$({}_{28}\mathrm{Ni}_{20}^{48})$ f)	25.8 g) 27.3	(−0.3) g) (2.9)	2.5 g) 1.7
${}_{28}\mathrm{Ni}_{21}^{49}$ b)	18.2 g) 18.9	(−1.3) g) 1.1	1.7 g) 1.7

For 2p-active nuclei $B_{p_{\text{even}}} > 0$, $B_{p_{\text{odd}}} < 0$, but

$$|B_{p_{\text{odd}}}| > B_{p_{\text{even}}} \begin{cases} E_{pp} = |B_{p_{\text{odd}}}| - B_{p_{\text{even}}}, \\ E_{\text{pairing}} = |B_{p_{\text{odd}}}| + B_{p_{\text{even}}}, \end{cases}$$

i.e., the relation $E_{\text{pairing}} \geqq E_{pp}$ should always hold, and all exceptions are due only to the fact that proton binding energies are sometimes taken from other sources than that from which the very fact of 2p-radioactivity of the given nucleus follows.

Table 1 (continued)

2p-radioactive nuclei

Nucleus	$M-A$ (MeV)	E_{pp} (MeV)	$E_{pairing}$ (MeV)
$_{30}Zn^{53}_{23}$ a)	16.2 g) 19.4	1.1 g) (3.7)	1.9 g) 1.0
$_{30}Zn^{54}_{24}$ a)	5.3 g) 7.6	0.2 g) (2.0)	1.6 g) 1.0
$_{30}Zn^{55}_{25}$ b)	−2.4 g) −0.6	(−1.3 g) 0.4	1.1 g) 0.9
$_{32}Ge^{58}_{26}$ a)	3.9 g) 7.0	1.1 g) (2.5)	2.1 g) 1.5
$_{32}Ge^{59}_{27}$	−3.5 g) −1.4	0 g) 0.9	2 g) 1.5
$_{34}Se^{62}_{28}$ a)	3.2 g) 6.4	1.2 g) (2.9)	2.6 g) 2.1
$_{34}Se^{63}_{29}$ b)	−3.3 g) −0.6	(−0.1 g) 1.4	1.7 g) 2.1
$_{36}Kr^{66}_{30}$ a)	4.9 g) 8.7	1.4 g) (2.7)	2.8 g) 2.0
$_{36}Kr^{67}_{31}$	1.9	1.3	2.0
$_{36}Kr^{68}_{32}$ c)	−6.9	(−0.1)	2.0
$_{38}Sr^{71}_{33}$	4.6	1.6	1.8
$_{38}Sr^{72}_{34}$	−4.2	0.2	1.8
$_{40}Zr^{76}_{36}$	−1.4	0.8	1.5
$_{42}Mo^{80}_{38}$	1.0	0.9	1.4
$_{44}Ru^{84}_{40}$	3.5	1.4	1.7
$_{44}Ru^{85}_{41}$	−2.5	0.2	1.7
$_{46}Pd^{88}_{42}$	6.1	2.0	2.0
$_{46}Pd^{89}_{43}$	−0.1	0.8	2.0
$_{48}Cd^{93}_{45}$	1.9	1.5	2.1
$_{48}Cd^{94}_{46}$	−7.1	0.4	2.1
$_{50}Sn^{97}_{47}$	3.6	1.6	2.3
$_{50}Sn^{98}_{48}$	−5.6	0.6	2.3
($_{52}Te^{105}_{53}$)	−16.9	1.6 $E_\alpha = 4.2$	1.7
($_{52}Te^{106}_{54}$)	−22.2	0.7 $E_\alpha = 4.3$	1.7

a) These are the 2p-radioactive nuclei, according to ref. 1), which are proton-unstable according to ref. 2).

b) Proton-stable nuclei according to ref. 1).

c) Proton-stable nuclei (though close to 2p-instability) according to ref. 2). (Cr^{42} is proton-unstable 1)).

d) The proton stability is questionable.

e) Proton-unstable nuclei according to ref. 1).

f) This is a nucleus 2p-stable according to ref. 1) but proton-unstable according to ref. 2).

g) Ref. 1)

Table 1 lists over forty 2p-radioactive nuclei related to this class on the basis of our [1]) and/or Cameron's [2]) values of nuclear masses. The table also contains the mass defects, proton-pair binding energies and proton pairing energies for these nuclei.

The spread of two-proton radioactivity is limited to the region of light nuclei up to tin ($Z = 50$) since in heavier nuclei it is alpha instability that first arises as neutron deficiency increases.

3. Energy Correlation of Emitted Protons

The energy correlation of the two protons emitted by 2p-radioactive nuclei arises as a direct consequence of the tunnel passage of protons through the Coulomb potential barrier and is characterized by the predominance of such cases when the decay energy is equally divided between the protons.

The decrease in the probability of the passage through the barrier $W_{\text{bar}}(E)$ when the proton energy decreases by a certain fraction κ indeed proves always to be larger than the increase of this probability for the same increase (by κE) of proton energy, i.e.

$$\frac{W_{\text{bar}}(E)}{W_{\text{bar}}(E-\kappa E)} > \frac{W_{\text{bar}}(E+\kappa E)}{W_{\text{bar}}(E)}. \tag{1}$$

As a result, the equal distribution of energy between the two protons proves to be the most probable in their simultaneous emission.

It can easily be shown that without the Coulomb barrier the energy correlation pattern would be quite different. Let us indeed represent the total energy of the two-proton radioactive decay E_{pp} (further on we shall drop the subscripts pp) as a sum of the kinetic energy of the centre of gravity of a proton-proton pair $E-\varepsilon = \frac{1}{2}q^2/2m$ (where m is the proton mass and q the translation momentum) and the energy of the relative motion of the protons in the centre-of-gravity system (CGS) ε (for each proton the energy in CGS being equal to $\frac{1}{2}\varepsilon = p^2/2m$, where p is the momentum). We shall neglect the energy of the recoil nucleus, putting $A \gg 1$. If the emission angle of one of the protons in CGS is equal to θ, then the energy of each proton in the laboratory system can be determined by the relations

$$\begin{aligned} \varepsilon_1 &= \tfrac{1}{2}E+\kappa E = \tfrac{1}{2}E\left[1+2\sqrt{\frac{\varepsilon}{E}\left(1-\frac{\varepsilon}{E}\right)}\cos\theta\right], \\ \varepsilon_2 &= \tfrac{1}{2}E-\kappa E = \tfrac{1}{2}E\left[1-2\sqrt{\frac{\varepsilon}{E}\left(1-\frac{\varepsilon}{E}\right)}\cos\theta\right]. \end{aligned} \tag{2}$$

The difference of these energies is

$$\varepsilon_1 - \varepsilon_2 = 2\kappa E = 2E\sqrt{\frac{\varepsilon}{E}\left(1-\frac{\varepsilon}{E}\right)}\cos\theta. \tag{3}$$

The proton energy correlation can be described by the correlation parameter $\kappa = |\varepsilon_i/E - \frac{1}{2}|$. Each on the following possibilities (see fig. 2) corresponds to the equality of the energies of two protons in the laboratory system, i.e. $\kappa = 0$:

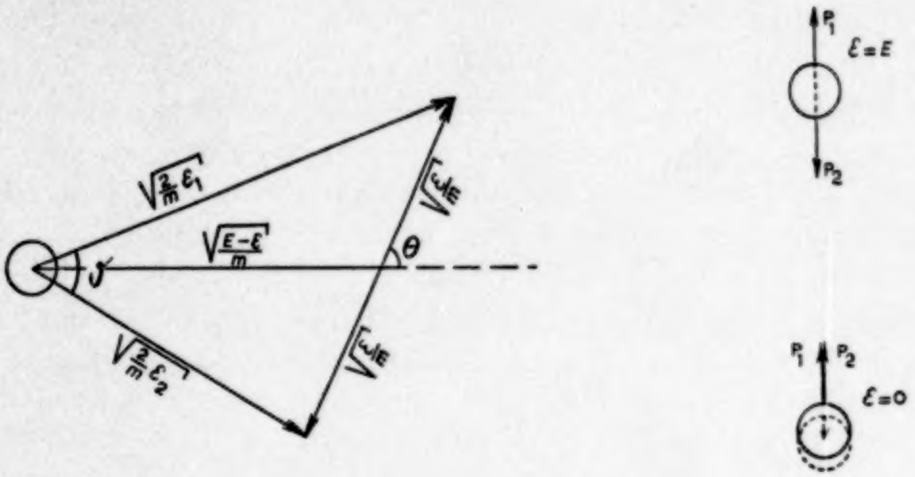
$\sqrt{\frac{2}{m}\varepsilon_1}$
$\sqrt{\frac{E-\varepsilon}{m}}$
$\sqrt{\frac{\varepsilon}{m}}$
θ
ϑ
$\sqrt{\frac{2}{m}\varepsilon_2}$
$\sqrt{\frac{\varepsilon}{m}}$
p_1
$\varepsilon = E$
p_2
p_1
p_2
$\varepsilon = 0$

Fig. 2

(1) $\varepsilon = 0$, i.e. a proton pair is released from a nucleus as a single whole, as a diproton, at the maximum energy of nuclear recoil, equal to $(2/A)E$.

(2) $\varepsilon = E$, i.e. the centre of gravity of a proton pair coincides with the nucleus and the protons fly out in opposite directions, the nuclear recoil energy being equal to zero.

(3) $\cos\theta = 0$, i.e. $\theta = \frac{1}{2}\pi$ (regardless of the value of ε). The condition $\varepsilon = \frac{1}{2}E$ corresponds to the largest energy difference of the two protons in the laboratory system, while $\kappa = \kappa_{\max} = \frac{1}{2}\cos\theta$, so that

$$\varepsilon_1 = \tfrac{1}{2}E(1+\cos\theta), \qquad \varepsilon_2 = \tfrac{1}{2}E(1-\cos\theta); \tag{4}$$

for $\theta = 0$, we get $\varepsilon_1 = E$ and $\varepsilon_2 = 0$. If there is no interaction of the emitted protons (between each other or with the recoil nucleus) in the final state, their energy spectrum in CGS is determined by the relation

$$f(\varepsilon)\mathrm{d}\varepsilon \propto p^2\mathrm{d}p\int q^2\,\mathrm{d}q\,\delta\left(E-\frac{p^2}{m}-\frac{q^2}{4m}\right) \propto \sqrt{\varepsilon}(E-\varepsilon)\mathrm{d}\varepsilon. \tag{5}$$

Since $\kappa = \sqrt{(\varepsilon/E)(1-\varepsilon/E)}\cos\theta$, and since for isotropy of emission in CGS the averaging over angles yields $\bar{\kappa} = \frac{1}{2}\kappa_{\max} = \frac{1}{2}\sqrt{(\varepsilon/E)(1-\varepsilon/E)}$, it is easy from relation (5) to obtain the distribution function for the averaged parameter $\bar{\kappa}$, describing the deviation from equality of the energies of two protons:

$$f(\bar{\kappa})\mathrm{d}\bar{\kappa} \propto \frac{[\varepsilon(E-\varepsilon)]^{\frac{3}{2}}}{\sqrt{\varepsilon}(E-2\varepsilon)}\,\mathrm{d}\bar{\kappa} \propto \frac{\bar{\kappa}^3}{\sqrt{\varepsilon}\sqrt{1-16\bar{\kappa}^2}}\,\mathrm{d}\bar{\kappa}. \tag{6}$$

It is obvious that this simple consideration leads us to the predominance of the largest possible values of $\bar{\kappa}$, close to $\frac{1}{4}$, i.e. the largest possible differences in the laboratory energies of two protons. It ought to be borne in mind, however, that owing to the Coulomb interaction between the protons and the residual nucleus the isotropy of the fly-out of a proton pair in CGS must shift in favour of angles θ close to $\frac{1}{2}\pi$ at the expense of small ($\theta \approx 0$) and large ($\theta \approx \pi$) angles, which will lead to a certain decrease of $\bar{\kappa}$, i.e. the rapprochement of the energies of two protons. But even if this is taken into account, the general conclusion on the predomination of $\bar{\kappa}$ close to $\frac{1}{2}\kappa_{\max}$ nevertheless remains valid.

Yet the energy correlation pattern radically changes owing to the presence of the Coulomb potential barrier through which the emitted protons pass. In a close-to-barrier case ($x = E/V_{\text{coul.}} = ER/2(Z-2)e^2 \ll 1$) the product of the two exponents of barrier permeability, if the energy is divided equally between the two protons, with $\frac{1}{2}E$ for each ($\kappa = 0$), is equal to

$$W_{\mathrm{p}}(0) = \exp\left\{-\frac{2}{\hbar}\,\frac{2\pi(Z-2)\,e^2\sqrt{m}}{\sqrt{E}}\right\} = W_{\mathrm{pp}}, \tag{7}$$

i.e. proves the same as the barrier permeability exponent W_{pp} for a doubly-charged particle of mass $2m$.

If, on the other hand, the energies of the protons are $\frac{1}{2}E \pm \kappa E$, the product of the two barrier permeability exponents for the protons is equal to

$$\begin{aligned} W_{\mathrm{p}}(\kappa) &= \exp\left\{-\frac{2}{\hbar}\,\frac{\pi(Z-2)\,e^2\sqrt{m}}{\sqrt{E}}\left[\frac{1}{\sqrt{1+2\kappa}} + \frac{1}{\sqrt{1-2\kappa}}\right]\right\} \\ &= W_{\mathrm{p}}(0)\exp\left\{-\frac{6\pi(Z-2)e^2\sqrt{m}}{\hbar\sqrt{E}}\,\kappa^2\right\}, \end{aligned} \tag{8}$$

the latter relation being obtained in the approximation $2\kappa \ll 1$.

Thus, owing to the influence of the Coulomb potential barrier, in the approximation $x \ll 1$ and $2\kappa \ll 1$ there is a rather simple Gaussian relation $W_{\mathrm{p}}(\kappa) \approx W_{\mathrm{p}}(0)\mathrm{e}^{-\alpha\kappa^2}$, in which the coefficient α describes the degree of barrier energy correlation of the protons. In the general case, without using the approximation of sub-barrier energies ($x \ll 1$), we obtain instead of relations (5) and (6)

$$W_{\mathrm{p}}(0) = \exp\left\{-\frac{4\sqrt{2m(Z-2)e^2R}}{\hbar}\,[x^{-\frac{1}{2}}\arccos x^{\frac{1}{2}} - (1-x)^{\frac{1}{2}}]\right\} = W_{\mathrm{pp}} \tag{9}$$

and

$$W_{\mathrm{p}}(\kappa) = W_{\mathrm{p}}(0) \exp\left\{-\frac{2\sqrt{2m(Z-2)e^2R}}{\hbar}\left[\frac{3 \arccos x^{\frac{1}{2}}}{x^{\frac{1}{2}}} + \frac{3-x}{(1-x)^{\frac{1}{2}}}\right]\kappa^2\right\}. \quad (10)$$

All the above formulae for energy correlation have been obtained without taking account of the mutual Coulomb and nuclear interaction of the emitted protons. If, however, the exponential part of the probability of penetration through the barrier is the same in two extreme cases — for a diproton as a whole (mass $2m$, charge 2 and energy E) and for two independent protons with the same energy (m, 1 and $\frac{1}{2}E$) — it can be supposed that the circumstances described, as well as the need of taking account of the pair correlations of the emitted protons in the initial nucleus affect only the pre-exponential factors, the evaluation of which lies beyond the scope of the present paper.

In concluding this section it is necessary to note that the type of energy correlation of the emitted protons must be rather sensitive to the form of the Coulomb potential barrier. The diffuse edge of the nuclear potential, as well as the possibility of energy exchange between the protons when one of them is in the nucleus and the other is outside it, but inside the Coulomb barrier represented by the "tail" of the wave function), lead to an increase of the barrier permeability, i.e. a decrease of the barrier energy correlation coefficient α compared with the value

$$\alpha_{\max} = \frac{2\sqrt{2m(Z-2)e^2R}}{\hbar}\left[\frac{3 \arccos x^{\frac{1}{2}}}{x^{\frac{1}{2}}} + \frac{3-x}{(1-x)^{\frac{1}{2}}}\right],$$

determined by eq. (10). One of the major experimental problems in investigating two-proton radioactivity is therefore the establishment of the distribution function of the energy correlation parameter $\kappa = |\varepsilon_i/E-\frac{1}{2}|$, and, if this distribution is Gaussian, the determination of the corresponding exponent.

4. Angular Correlation of Emitted Protons

The predominance, conditioned by the Coulomb barrier, of the cases when the energies of the protons emitted in 2p-radioactive decay are approximately equal, corresponds, as is clear from relations (2), to the predominance of the variants $\varepsilon = 0$ or $\varepsilon = E$. If $\varepsilon \approx E$, the protons are emitted at a large angle, close to 180° (their centre-of-gravity system practically coinciding with the laboratory system) and cease to interact between themselves immediately outside the nucleus. Thus there arises a typical problem of three bodies, and the angular distribution in the region $\varepsilon > \frac{1}{2}E$ must be characterised by isotropy, somewhat shifted, as has already been mentioned, towards the angles $\theta \approx \frac{1}{2}\pi$ on account of the Coulomb interaction of the protons with the nucleus.

In the case $\varepsilon \approx 0$, however, when both protons are emitted from the nucleus simultaneously, the distribution over the angles ϑ between their directions in the laboratory system proves to be essentially dependent on the interactions of the protons in the final state †.

The form of this distribution can be studied with the aid of the method evolved by Migdal ³) for nuclear reactions with the production of pairs of slow nucleons (nn, pp, np). Let us first neglect the Coulomb interaction of the emitted protons with each other. Then the problem becomes similar to the case, considered by Migdal, of the production of a neutron pair, the only difference arising from the taking into account of the permeability of the Coulomb potential barrier for the emitted protons.

The probability of 2p-decay for the given values ε and θ is

$$w(E-\varepsilon,\, \varepsilon)\mathrm{d}\varepsilon\mathrm{d}\Omega \propto \frac{a}{\sqrt{\varepsilon(E-\varepsilon)}}\,|\psi_{E-\varepsilon}(R)|^2|\psi_\varepsilon(2p)|^2\mathrm{d}\varepsilon\mathrm{d}\Omega, \tag{11}$$

where $\mathrm{d}\Omega = 2\pi \sin\theta\, \mathrm{d}\theta$ is an element of solid angle, a a certain constant and $\psi_{E-\varepsilon}(R)$ the value of the Coulomb function corresponding to a proton pair of energy $E-\varepsilon$ at the nuclear radius R (the protons being assumed to be emitted with zero orbital momentum).

For the sub-barrier case

$$\frac{1}{\sqrt{E-\varepsilon}}\,|\psi_{E-\varepsilon}(R)|^2 \propto \exp\left\{-\frac{2\pi 2(Z-2)e^2\sqrt{m}}{\hbar\sqrt{E-\varepsilon}}\right\}, \tag{12}$$

and if the Coulomb interaction of the protons is neglected we have

$$\frac{1}{\sqrt{\varepsilon}}\,|\psi_\varepsilon(2p)|^2\mathrm{d}\varepsilon\mathrm{d}\Omega \approx \frac{\sqrt{\varepsilon}}{\varepsilon+\varepsilon_0}\,\mathrm{d}\varepsilon \sin\theta\, \mathrm{d}\theta, \tag{13}$$

where ε_0 is the energy of the virtual (singlet) level of nucleon-nucleon interaction; the emission of a proton pair in CGS being assumed to be isotropic. Thus,

$$w(E-\varepsilon,\, \varepsilon)\mathrm{d}\varepsilon\mathrm{d}\Omega \propto \frac{\sqrt{\varepsilon}}{(\varepsilon+\varepsilon_0)\sqrt{E-\varepsilon}}\exp\left\{-\frac{4\pi(Z-2)e^2\sqrt{m}}{\hbar\sqrt{E-\varepsilon}}\right\}\mathrm{d}\varepsilon \sin\theta\mathrm{d}\theta. \tag{14}$$

Since $\mathrm{tg}\,\vartheta = \delta \sin\theta$, where $\delta = 2\sqrt{\varepsilon(E-\varepsilon)}/(E-2\varepsilon)$, expression (14) can be transformed into

$$w(E-\varepsilon,\, \varepsilon)\mathrm{d}\varepsilon\mathrm{d}\Omega \propto f(\varepsilon)\mathrm{d}\varepsilon\,\frac{\mathrm{tg}\,\vartheta}{\cos^2\vartheta}\,\frac{1}{\delta\sqrt{\delta^2-\mathrm{tg}^2\vartheta}}\,\mathrm{d}\vartheta, \tag{15}$$

where

$$f(\varepsilon) = \frac{\sqrt{\varepsilon}}{(\varepsilon+\varepsilon_0)\sqrt{E-\varepsilon}}\exp\left\{-\frac{4\pi(Z-2)e^2\sqrt{m}}{\hbar\sqrt{E-\varepsilon}}\right\}. \tag{16}$$

---

† Here we do not discuss the possible influence of the energy and angular correlation of protons inside the nucleus on the corresponding correlations in their emission.

The case of the interaction of the emitted protons under consideration corresponds to the region $\varepsilon < \frac{1}{2}E$, i.e. $\vartheta < 90°$, while $\mathrm{tg}\,\vartheta_{\max} = \delta$. The presence of the Coulomb potential barrier further contributes to the predominance of small ε, i.e. of angles $\vartheta < 1$. Therefore expression (15) can be written in approximate terms as

$$w(E-\varepsilon, \varepsilon)\mathrm{d}\varepsilon\mathrm{d}\Omega \propto f(\varepsilon)\mathrm{d}\varepsilon \frac{\vartheta\mathrm{d}\vartheta}{\delta\sqrt{\delta^2-\vartheta^2}} \approx \frac{f(\varepsilon)\mathrm{d}\varepsilon\mathrm{d}\Omega_{\mathrm{lab}}}{\delta\sqrt{\delta^2-\vartheta^2}}, \tag{17}$$

where $\delta \approx 2\sqrt{\varepsilon/E}$ and $\mathrm{d}\Omega_{\mathrm{lab}} \approx 2\pi\vartheta\mathrm{d}\vartheta$ is an element of solid angle in the laboratory system. To obtain the required angular distribution $\mathrm{d}w(\vartheta)/\mathrm{d}\Omega_{\mathrm{lab}} = \Phi(\vartheta)$ we integrate over energies and obtain

$$\Phi(\vartheta) \approx \exp\left\{\frac{3}{4}\frac{A}{\sqrt{E}}\frac{\varepsilon_0}{E}\frac{\gamma}{E}\right\} \frac{1-\mathrm{erf}\sqrt{a(\varepsilon_0+\gamma)}}{\sqrt{\varepsilon_0+\gamma}}, \tag{18}$$

where

$$\gamma = \tfrac{1}{4}E\vartheta^2, \qquad a = \frac{A}{2(E-\gamma)^{\frac{3}{2}}}, \qquad A = \frac{4\pi(Z-2)e^2\sqrt{m}}{\hbar}.$$

The difference due to taking into account barrier permeability, from Migdal's formula for two neutrons, reduces itself to factors close to unity (despite the fact that $A/\sqrt{E} \gg 1$; and even the exponential factor is close to unity because $\varepsilon_0/E < 1$ and $\gamma/E \ll 1$).

Consequently the shape of distribution over small angles ϑ between the directions of the two 2p-decay protons in the given approximation is described by a relation close to that obtained in ref. [3]) for two neutrons:

$$\Phi(\vartheta) \propto \frac{1}{\sqrt{\varepsilon_0/E + (\frac{1}{2}\vartheta)^2}}, \tag{19}$$

so that the half-width of distribution corresponds to $\vartheta = 2\sqrt{3\varepsilon_0/E}$ or $\vartheta \approx \sqrt{1/E(\mathrm{MeV})}$ if $\varepsilon_0 \lessapprox 100$ keV. The Coulomb interaction between the emitted protons is bound to lead to a certain spread of the distribution over ϑ. Since the barrier does not lead to an appreciable change of angular distribution, as we have seen above, it is possible to make a direct use of the following numerical result obtained by Migdal for the production of slow-proton pairs and based on the data on the pp-scattering at low energies:

$\Phi(\gamma = \frac{1}{4}E\vartheta^2)$	1.00	0.82	0.59	0.40	0.34	0.31
γ (MeV)	0	1	2	3	4	5

In this case the half-width of the distribution over ϑ corresponds to $\vartheta = \sqrt{3/E(\mathrm{MeV})}$, i.e. it is appreciably larger than when neglecting the Coulomb interaction of the protons emitted.

5. Experimental Prospects of Production of 2p-Radioactive Nuclei in Reactions Involving He^3 or Multi-Charged Heavy Ions.

The two-proton-radioactive nuclei listed in table 1 can in principle be obtained with any incident particles of sufficiently high energy. Thus, for example, the nuclei of Ne^{16} can be produced in the reaction $Ne^{20}(\gamma, 4n)\,Ne^{16}$ for γ-quantum energies exceeding 63 MeV, or in the reaction $F^{19}(p, 4n)Ne^{16}$ for proton energies exceeding 53 MeV. Yet the probabilities of these processes prove to be rather small, for at energies of order of scores and hundreds of MeV most of the excitation energy is as a rule carried away by one or two nucleons as a result of direct interaction and before the formation of the intermediate nucleus.

Therefore, the most realistic method of obtaining two-proton radioactive nuclei of atomic number Z is, as was already pointed out in ref. [1]), to bombard the lightest isotopes of the element (Z—2) by He^3 nuclei or the lightest isotopes of the element (Z—Z_1) by multi-charged ions of the element Z_1.

Table 2 lists certain characteristics of the reactions of He^3 and multi-charged ions leading to the production of 2p-radioactive nuclei with $Z = 10$ to 50. Indicated also are the number of neutrons to be emitted by a compound nucleus for the 2p-instability to appear, as well as the reaction thresholds calculated using the data of table 1. Consideration is given to He^3 nuclei and the ions of nine elements from boron to nickel as possible incident particles. The mass number of the target nucleus was assumed to be the lowest of the values of A for the stable isotopes of a given element. In table 2, not all squares for each incident ion are filled, but only those for which the use of a given ion corresponds to the minimum or next-to-minimum number of neutrons to be emitted by a compound nucleus for the production of 2p-radioactive nuclei (the reactions with evaporation of a still larger number of neutrons being far less probable).

Table 3 lists more comprehensive data on certain reactions of the production of 2p-radioactive nuclei, largely those reactions which demand the evaporation of a relatively small number of neutrons. It is clear from table 3 that the cross sections of these reactions can come up to 1 mb. The cross sections listed in table 3 were calculated on the basis of the statistical theory of nuclear reactions with the aid of the relation

$$\sigma_{\max} = \sigma_c \prod_{i=0}^{m-1} \left(\frac{\Gamma_n}{\Gamma_n+\Gamma_p}\right)_i P(E, x), \tag{20}$$

similar to that used by Tarantin [4]) for evaluating the cross sections of the reactions of multi-charged ions with heavy nuclei with evaporation of neutrons, as well as that used in the recent investigation of Karnaukhov and Tarantin [5]) for evaluating the cross sections of the production of proton-unstable isotopes.

In eq. (20) $\sigma_c = \pi(R_1+R_2)^2$ is the geometric cross section for the interaction

TABLE 2

Conditions of obtaining 2p-radioactive nuclei (numbers of evaporated neutrons and threshold in MeV)

Atomic number of 2p-active product / The nucleus-projectile	10	12	14	16	18	20	22	24	26	28	30	32	34	36	38	40	42	44	46	48	50
${}_2He^3$	3 45	5.6	5.6	6.7	5.6.7 74 100 ?	5.6 70 95	5.6 70 92	7.8 91 113	8.9 114 133	8.9 117 134	6.7.8 81 98 120										
${}_5B^{10}$	4 83	6.7						7.8 98 125													
${}_6C^{12}$		6.7	6.7	7.8	6.7.8 118 153 ?	6.7 113 146	6.7 108 137	6.7 105 132	7.8 129 152			7.8 95 112	7.8 118 136			4 156 *)					
${}_8O^{16}$				7.8	6.7.8 137 181 ?	6.7 127 166	6.7 124 157	6.7 119 150	7.8 143 169	7.8 141 164		7.8 122 145	7.8 128 147	6.7.8 110 132 151							
${}_{10}Ne^{20}$					6.7.8 171 234 ?	6.7 143 190	6.7 135 174	6.7 132 167	7.8 158 187	7.8 153 179	5.6.7 98 123 153	7.8 128 152	7.8 133 154	6.7.8 116 140 161	6.7 121 144						
${}_{12}Mg^{24}$					6.7.8 236 306 ?	6.7 190 250	6.7 162 209	6.7 152 194	7.8 185 218	7.8 177 206	5.6.7 113 140 174	5.6 112 139	7.8 145 169	6.7.8 124 150 172	6.7 133 158	6 136					
${}_{16}S^{32}$							6.7 288 366	6.7 238 300	7.8 253 300	7.8 234 275	5.6.7 152 187 231	5.6 147 181	5.6 146 176	4.5.6 119 150 177	6.7 157 186	6 165	6 172	5.6 154 176			
${}_{18}Ar^{36}$								6.7 315 390	7.8 322 380	7.8 276 322	5.6.7 170 210 260	5.6 167 206	5.6 164 198	4.5.6. 131 165 196	4.5 137 169	6 177	6 183	5.6 166 189	5.6 169 193	6.7 172 199	
${}_{26}Fe^{54}$												7.8 520 610	7.8 430 500	6.7.8 314 376 434	6.7 300 358	6 297	6 290	5.6 250 284	5.6 247 280	6.7 248 286	6.7 250 287
${}_{28}Ni^{58}$													7.8 570 660	6.7.8 400 480 547	6.7 388 446	6 334	6 330	5.6 280 320	5.6 272 310	4.5 226 270	6.7 267 323

*) Here, the projectile is ${}_{20}Ca^{40}$

TABLE 3

Examples of the formation of 2p-radioactive nuclei

Reaction	V_p Coul (MeV)	ΣB_n (MeV)	ΣB_p (MeV)	E_{Thr} (MeV)	$E_{\sigma_{\max}}$ (MeV)	$\left(\frac{\Gamma_p}{\Gamma_n}\right)_{\text{Av.}}$	σ_c(b)	$\sigma_{\max}$(μb)
$O^{16}(He^3, 3n)Ne^{16}$	2.5	46	12	45	66	20	1	100
$B^{10}(B^{10}, 4n)Ne^{16}$		63	25	65	113	11.5	1.5	50
$Ar^{36}(He^3, 5n)Ca^{34}$	4.1	76.3	23.6	70	102	9.7	1.6	8
$Ar^{36}(He^3, 6n)Ca^{33}$		99.4	24.8	95	134	18.2		0.02
$Ca^{40}(Ne^{20}, 5n)Zn^{55}$	5.6	76.9	13.5	98	143	12.5	2.7	4
$Ca^{40}(Ne^{20}, 6n)Zn^{54}$		93.5	13.8	123	177	15.4		0.09
$Ca^{40}(Ne^{20}, 7n)Zn^{53}$		113.7	13.2	153	216	19.5		0.001
$Ar^{36}(Mg^{24}, 5n)Zn^{55}$		76.9	13.5	113	164	12.5	2.6	4
$Ar^{36}(Mg^{24}, 6n)Zn^{54}$		93.5	13.8	140	200	15.4		0.09
$Ar^{36}(Mg^{24}, 7n)Zn^{53}$		113.7	13.2	174	244	19.5		0.001
$Fe^{54}(Ne^{20}, 6n)Kr^{68}$	6.6	81.9	20.5	116	166	4.1	3	100
$Fe^{54}(Ne^{20}, 7n)Kr^{67}$		99.1	21.6	140	198	5.4		4
$Fe^{54}(Ne^{20}, 8n)Kr^{66}$		114.3	22	161	227	6.3		0.2
$Ca^{40}(S^{32}, 4n)Kr^{68}$		56.6	11	119	163	6	3.1	1000
$Ca^{40}(S^{32}, 5n)Kr^{67}$		73.8	12.1	150	205	8.2		40
$Ca^{40}(S^{32}, 6n)Kr^{66}$		89	12.5	177	242	9.3		2
$Ar^{36}(Ar^{36}, 4n)Kr^{68}$		56.6	11	131	179	6	3.1	1000
$Ar^{36}(Ar^{36}, 5n)Kr^{67}$		73.8	12.1	166	226	8.2		40
$Ar^{36}(Ar^{36}, 6n)Kr^{66}$		89	12.5	196	268	9.3		2
$Ca^{40}(Ca^{40}, 4n)Zr^{76}$	7.0	58.9	7.6	156	204	8.7	3.3	200
$Ni^{58}(Ar^{36}, 5n)Pd^{89}$	7.8	76.5	10.8	169	218	7.7	3.6	40
$Ni^{58}(Ar^{36}, 6n)Pd^{88}$		91.1	11.4	193	252	8.1		4
$Ca^{40}(Ni^{58}, 4n)Cd^{94}$	8.0	60.4	8.6	226	284	6.8	3.7	500
$Ca^{40}(Ni^{58}, 5n)Cd^{93}$		77.8	9.5	270	344	8.4		30

of nuclei of radii R_1 and R_2, Γ_n and Γ_p are the neutron and proton partial widths of nuclear levels, i is the index characterising the compound nucleus ($i = 0$) and the nuclei produced after the emission of 1, 2, 3, . . ., $(m-1)$ neutrons and $P(E, x)$ is a quantity of the order of several tenths characterizing the probability for the excitation of the compound nucleus to disappear after the evaporation of m neutrons [6]). We neglect the probability of emission of α-particles since $\Gamma_\alpha \ll \Gamma_p + \Gamma_n$. According to the statistical model the ratio of partial widths is

$$\frac{\Gamma_p}{\Gamma_n} \approx \frac{Z}{N} \exp\left\{\frac{B_n - B_p - 0.9\,V_p}{T}\right\}, \tag{21}$$

where B_n and B_p are the binding energies of a neutron and a proton, V_p is the Coulomb potential barrier for a proton and T is the temperature of the nucleus. The values B_n and B_p at all stages of the evaporation of neutrons were taken from ref. [1]) or ref. [2]), the quantities $\bar{B}_n = \Sigma B_n/m$ and $\bar{B}_p = \Sigma B_p/m$, averaged over the emission of m neutrons, being used instead of B_n and B_p, to simplify the calculations. The values of V_p, ΣB_n and ΣB_p as well as σ_c are listed in table 3.

The temperature T was also averaged over all stages of neutron evaporation. Besides, in our case $Z \approx N$. Then instead of the ratio of (21) we obtain the averaged ratios of partial widths

$$\left(\frac{\Gamma_p}{\Gamma_n}\right)_{Av} \approx \exp\left\{\frac{\frac{1}{m}\Sigma B_n - \frac{1}{m}\Sigma B_p - 0.9V_p}{T}\right\}, \tag{22}$$

which is listed in table 3, as well as the values

$$\left(\frac{\Gamma_n}{\Gamma_n+\Gamma_p}\right)_{Av} = \bar{G}_n = \left[1-\left(\frac{\Gamma_p}{\Gamma_n}\right)_{Av}\right]^{-1},$$

that are necessary for using formula (20).

In the final analysis the maximum cross section σ_{max} of the reaction considered $A_1\,(A_2,\,mn)\,A$, obtained for the energy of the incident particles $E_{\sigma_{max}}$, equal to $E_{thresh}+[(A_1+A_2)/A_1]\;2Tm$, (see table 3), is determined in the form

$$\sigma_{max} \approx \pi(R_1+R_2)^2(\bar{G}_n)^m. \tag{23}$$

The most uncertain quantity in the calculation under discussion is the averaged temperature of the nucleus T. The quantities σ_{max} obtained are rather sensitive to the choice of T since if the assumed temperature T_{ass} does not equal the true temperature T, then (as long as $(\Gamma_p/\Gamma_n)_{Av} \ll 1$) we have

$$\sigma_{max} \approx (\sigma_{max})_{calcul}(\bar{G}_n)^{m\left(\frac{T_{ass}}{T}-1\right)},$$

i.e. if the assumed temperature is overestimated, the calculated cross sections will prove to be overestimated as well.

Using different variants of the statistical theory and extrapolating the temperature values, determined by the data on the evaporation reactions of several neutrons by heavy nuclei [4]), the nuclei listed in table 3, we obtain $T = 3$ MeV as a reasonable estimate. It is this value that was used in the calculations, the results of which are represented in table 3. It is not impossible that for the lightest of the listed 2p-radioactive nuclei (Ne^{16}, Ca and Zn isotopes) the values of T and, accordingly, the cross sections σ_{max} are also underestimated.

The estimates of the cross-sections of the production of 2p-radioactive nuclei (up to 1mb) warrant optimistic conclusions as to the possibility of observing this phenomenon before long. In this connection it should be noted once again [1]) that the most rational method of observing two-proton radioactivity is probably the introduction of incident nuclei into nuclear photoemulsions and various chambers. The observation of sub-barrier proton pairs with definite total energy $\varepsilon_1+\varepsilon_2 = E$ and their energy and angular correlation will make it possible not only to detect the two-proton radioactivity itself even with the smallest half-lives † but also to check the basic assumptions of the theory of this phenomenon. The study of the energy correlation of the emitted protons is especially stimulating in this respect.

It is also essential to emphasize once again the desirability of detecting the emission of correlated neutron pairs (delayed neutron pairs among fission fragments, for example) a phenomenon kindred to two-proton radioactivity, with subsequent investigation of the nature of their energy and angular correlation.

6. Some Remarks on Three-Particle Nuclear Fission

On the boundary of the proton stability of neutron-deficient nuclei there arises, apart from two-proton radioactivity, a well-pronounced phenomenon of proton radioactive decay. The emission of single protons is characteristic of nuclei of elements with odd Z as well as of those of elements with even Z which possess even larger neutron deficiency than 2p-radioactive nuclei. The abundance of possible p-radioactive isotopes may give rise to decay chains with proton emission similar, for example, to α-decay chains in radioactive families.

Suppose, for example, that two consecutive proton emission events are energetically possible,

$$\mathrm{A} \xrightarrow{\mathrm{p}} \mathrm{B} \xrightarrow{\mathrm{p}} \mathrm{C},$$

i.e. both the odd $(2m+1)$th proton in the nucleus B and the even $(2m+2)$th proton in the nucleus A possess negative binding energies. It is clear that the direct two-proton decay

$$\mathrm{A} \xrightarrow{\mathrm{pp}} \mathrm{C}$$

is also possible energetically and the possibility of this decay increases the width of the initial state of the nucleus A and shortens its life. In general, the production in radioactive decay of an active product capable of further transformations increases the probability of the decay of the initial unstable nucleus. The case of two-proton emission is interesting in that at sufficiently high energies of the emission of the second "odd" proton $(|B_{\mathrm{p}_{\mathrm{odd}}}| > 7|B_{\mathrm{p}_{\mathrm{even}}}|)$, the simultaneous emission predominates, though two consecutive decays are also energetically possible. It seems probable that a similar circumstance can essentially affect the characteristics of nuclear fission, in particular increase the partial width of the fission of excited nuclei and shorten the lives of nuclei undergoing spontaneous fission. If indeed in fission there may arise fragments with lives short with respect to the α-decay, i.e. emitting long-range α-particles (from the ground state or excited states), this is bound to lead to a higher probability of the fission of the initial nucleus.

---

† See *Note added in proof* at the end of this paper.

Furthermore, just like the emission of a proton pair proves to be more probable under the conditions described above than the consecutive emission of two protons and indeed begins to predominate, so too the triple fission with the emission of two fragments and a long-range α-particle can predominate over the decay in two consecutive stages, fission and α-decay of a fragment (fig. 3).

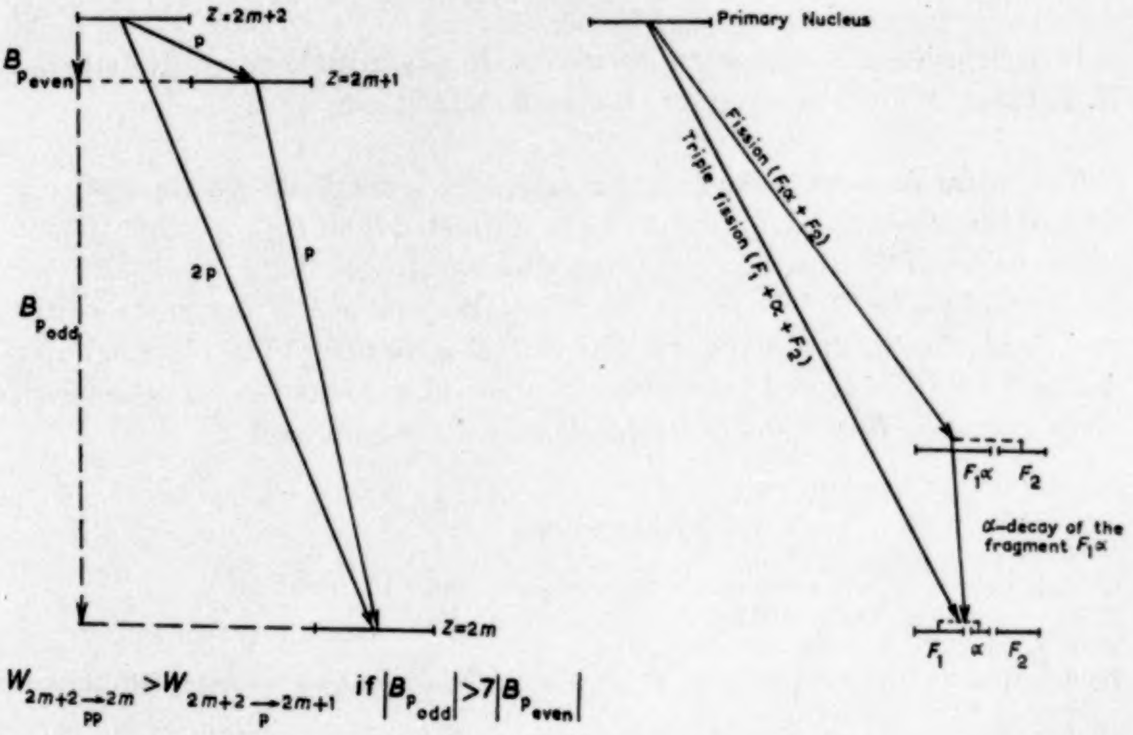
Z=2m+2
p
$B_{p_{even}}$
Z=2m+1
2p
p
$B_{p_{odd}}$
Z=2m
$W_{2m+2 \xrightarrow[pp]{} 2m} > W_{2m+2 \xrightarrow[p]{} 2m+1}$ if $|B_{p_{odd}}| > 7|B_{p_{even}}|$
Primary Nucleus
Fission ($F_1\alpha + F_2$)
Triple fission ($F_1 + \alpha + F_2$)
$F_1\alpha$
F_2
α-decay of the fragment $F_1\alpha$
F_1
α
F_2

Fig. 3

Thus triple fission must be precisely the fission into two fragments with the emission of a long-range α-particle, which is known to correspond to the actual character of this fission. In a recent survey on triple fission 7) it is pointed out that the principal objection against the otherwise attractive hypothesis of the emission of long-range α-particles by fragments is the form of the angular distribution of these particles, with respect to the direction of the fragments, determined by the Coulomb interaction with both fragments. It is clear that in the case of the combination, through the above-mentioned cause, of the consecutive events of the fission and α-decay of a fragment into a single triple fission event, the form of the angular distribution of α-particles will be precisely such as is observed in experiment.

On the basis of the above considerations it can also be concluded that the spontaneous fission is bound to be especially probable when α-active nuclei appear among the fragments. This spontaneous fission must also occur chiefly as a three-particle kind. In this connection mention should be made of the possibility of shortening the spontaneous fission halflives of the isotopes of element no. 102 since in their fission there may appear fragments with magic $Z = 50$ and alpha-active fragments with $Z = Z_{\text{mag}} + 2 = 52$. It seems worthwhile to undertake the analysis of the problem of the spontaneous fission of elements $Z > 102$ from the viewpoint of possible production of α-active fragments, the shortening of fission half-lives and the predominance of triple fission events with emission of α-particles.

In conclusion the author expresses his deep gratitude to A. I. Baz and N. I. Tarantin for their interest in his work and stimulating discussions.

Note added in proof: Like $E_{\text{pp}} \leqq E_{\text{pairing}}$, the lower limits on the 2p-decay lives of the nuclei listed in table 1 can be estimated from E_{pairing} values. These lowest values of the lives increase systematically with Z so that $(T_{\frac{1}{2}})_{2\text{p}} \geqq 10^{-21}$ sec for Ne^{16}, $(T_{\frac{1}{2}})_{2\text{p}} \geqq 10^{-3}$ sec for Sn^{97} and Sn^{98}. Because of this circumstance the probability for the 2p-decays of nuclei with $Z \approx 40$ to 50 to be observed may diminish appreciably and the number of observable 2p-active isotopes for each given even Z in this region (see table 1) may decrease to unity.

References

1) V. I. Goldansky, JETP **39** (1960) 497; Nuclear Physics **19** (1960) 482
2) A. G. Cameron, AECL-CRP-690 (1957)
3) A. B. Migdal, JETP **28** (1955) 3
4) N. I. Tarantin, JETP **38** (1960) 250; Thesis, Nuclear Physics Research Institute of the Moscow State University (1960)
5) V. A. Karnaukhov and N. I. Tarantin, JETP **39** (1960) 1106
6) J. D. Jackson, Can. J. Phys. **34** (1956) 767
7) N. A. Perfilov, Yu. F. Romanov and Z. I. Solovyova, Uspekhi Fiz. Nauk **71** (1960) 471

1.E.1:
2.L

Nuclear Physics **27** (1961) 665—672; © *North-Holland Publishing Co., Amsterdam*

Not to be reproduced by photoprint or microfilm without written permission from the publisher

LEVEL STRUCTURE OF A^{40}

JACOB BENVENISTE, REX BOOTH and ARTHUR C. MITCHELL
Lawrence Radiation Laboratory, University of California, Livermore, California

Received 9 May 1961

Abstract: The energy spectrum of inelastically scattered protons leading to excited levels in A^{40} has been measured at bombarding energies of 7.32 and 9.39 MeV using the Livermore variable-energy cyclotron. The argon target was contained in a 7 cm diameter gas cell with mylar window extending uninterruptedly for about 300° except for the region within 15° of the beam line. The protons were observed in a "particle-namer" detector incorporating a gas proportional counter and p-n junction solid-state detector. Twenty-one levels were observed up to an excitation energy of 6.65 MeV.

In the course of studying proton interactions with A^{40}, it quickly became clear that more structure was observed in the spectrum of inelastically scattered protons than was expected from the published information [1]) on the level structure of this nucleus. The bulk of this information is well summarized in the review article of Endt and Braams [2]). It serves to show that the excitation energy of the first level is rather well established at 1.462 MeV by charged particle inelastic scattering observations as well as de-excitation γ-ray measurements; however, observations of the higher states are few. Heitler *et al.* [1]) working with inelastically scattered protons and Helm [1]) with 187-MeV electrons, report a level at 2.4 MeV. Morinaga [1]) observed γ-rays following decay of Cl^{40} and assigned to A^{40} levels at 1.46, 4.2 and 6.0 MeV. Finally Van Heerden and Prowse [1]) observed the spectrum of inelastically scattered protons in nuclear plates. They found levels at 1.48, 2.22, (2.66), 3.12, 3.80 (? doublet), (4.40), 4.50 and 4.98 MeV. The following report describes the observation and measurement of 21 levels up to an excitation energy of 6.65 MeV. Measurements were made at 5 angles for each of 2 bombarding energies to assure ourselves freedom from some systematic errors.

After emerging from the cyclotron, the proton beam is deflected, focused, and passed through 0.3 cm collimators and antiscattering diaphragms just ahead of the scattering chamber. The scattering chamber is 101 cm in diameter. Within the chamber is a remotely rotatable table to which the detector may be quickly and accurately mounted. Careful calibration and measurements of right-left scattering cross sections insure that the table position read-out at a digital voltmeter in the control room is precise to ±0.10°.

The bombarding energy is measured by scattering a portion of the incident beam 90° through a variable absorber into a double proportional counter. An anticoincidence arrangement permits a differential range measurement of the scattered beam. For our two sets of observations the beam energy was measured to be 9.39 MeV and 7.32 MeV, respectively, with a precision about equal to that of the range-energy data.

Back of the proportional counters is a NaI crystal and photomultiplier tube. After the range has been measured only enough absorber is left in to allow about 1.5 MeV to be deposited in the crystal. Pulses from the photomultiplier tube, after suitable amplification, are fed into a "continuous energy monitor", a device which measures the average height of input pulses and yields a continuously visible meter reading. Sensitivity checks show that in the course of a run the incident energy is constant within ±0.15 %.

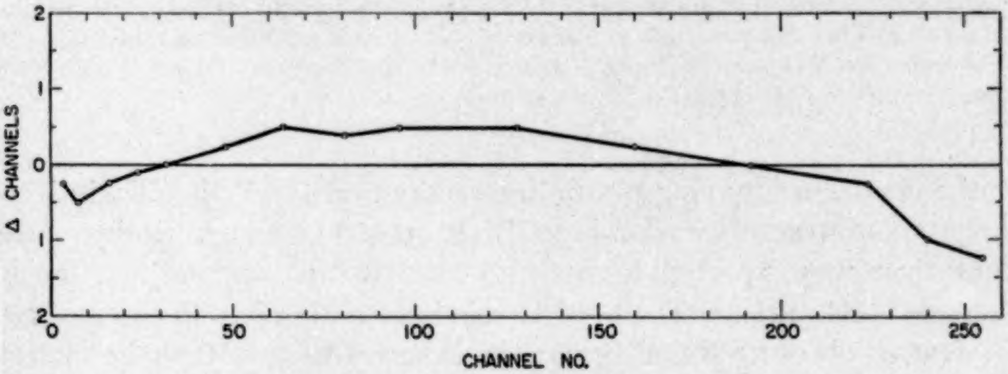

Fig. 1. Linearity of response of electronic system.

The detector is made up of a lithium-drifted p-n junction detector preceded by a gas proportional counter with offset centre wire. Together with a pulse-multiplier network this assembly constitutes a "particle-namer" in that the multiplied output is a pulse whose size is characteristic of the type of particle detected. This pulse is used to gate the input to the multichannel analyzer where the spectrum of protons seen by the solid-state detector is recorded. Previous measurements [3]) of the response of this detector to protons as high as 13 MeV showed it to be quite linear.

The response of the electronic system (linear amplifier to pulse analyzer) was measured by introducing "tail pulses" at the input to the linear amplifier The tail-pulser forms pulses by means of a switch which in one position charges up a capacitance to a voltage determined by a setting on a potentiometer, and in the other position discharges the capacitance through a resistance (RC $\approx$ 20 μsec). The linearity of the pulser potentiometer (Helipot) was measured with a precision voltmeter and found to be true within 0.1 %.

Rather than note the channel into which a given size pulse fell, more precise alignment was achieved by measuring the size of the pulse required to fall accurately between channels and comparing this size with that required for

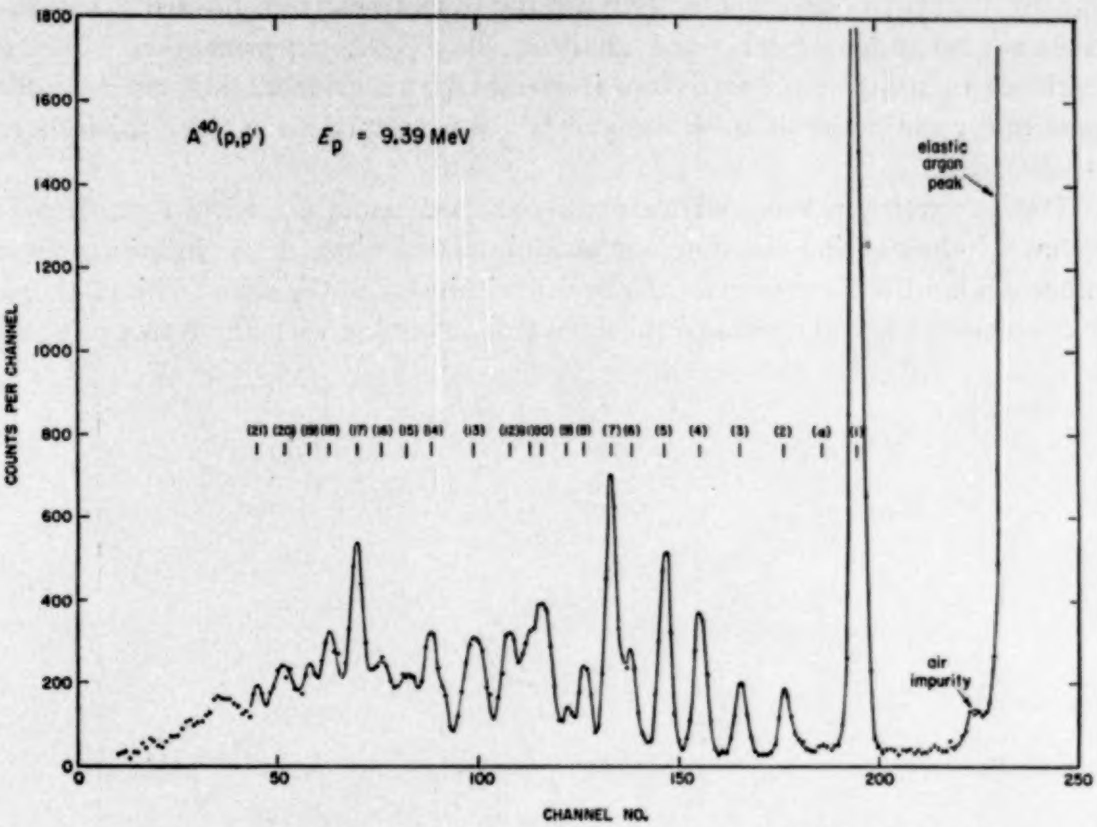

Fig. 2a. Spectrum of inelastically scattered protons at 60° with $E_p = 9.39$ MeV.

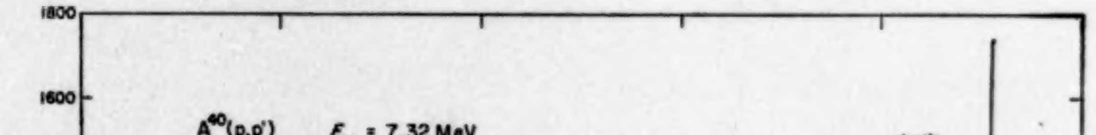

Fig. 2b. Spectrum of inelastically scattered protons at 60° with $E_p = 7.32$ MeV.

perfectly linear response. Fig. 1 shows the deviations from linearity over the 256-channel range of the pulse analyzer. For those experimenters with experience in using these analyzers it should be mentioned that considerable care and certain circuit modifications [4]) are necessary to achieve this degree of linearity.

The gas cell is a 7 cm diameter disc-shaped container with a continuous mylar window giving the detector an unimpeded view of the interior over a range of about 300°, except for the region within 15° of the beam. This chamber was evacuated and flushed several times prior to filling with argon to a pressure of about $\frac{1}{2}$ atm. The spectrum of scattered protons was then observed at 30°, 60°, 90° 120° and 150°. Typical spectra appear in fig. 2(a) and (b). The locations of the groups associated with levels in argon are identified by numbers corresponding to those appearing in table 1. It should be mentioned that some of these groups appear more prominently at other angles or at other energies. For example, (9), while still a relatively weak group, appears clearly in the 7.32-MeV data, although it might be considered doubtful from the 9.39-MeV observations.

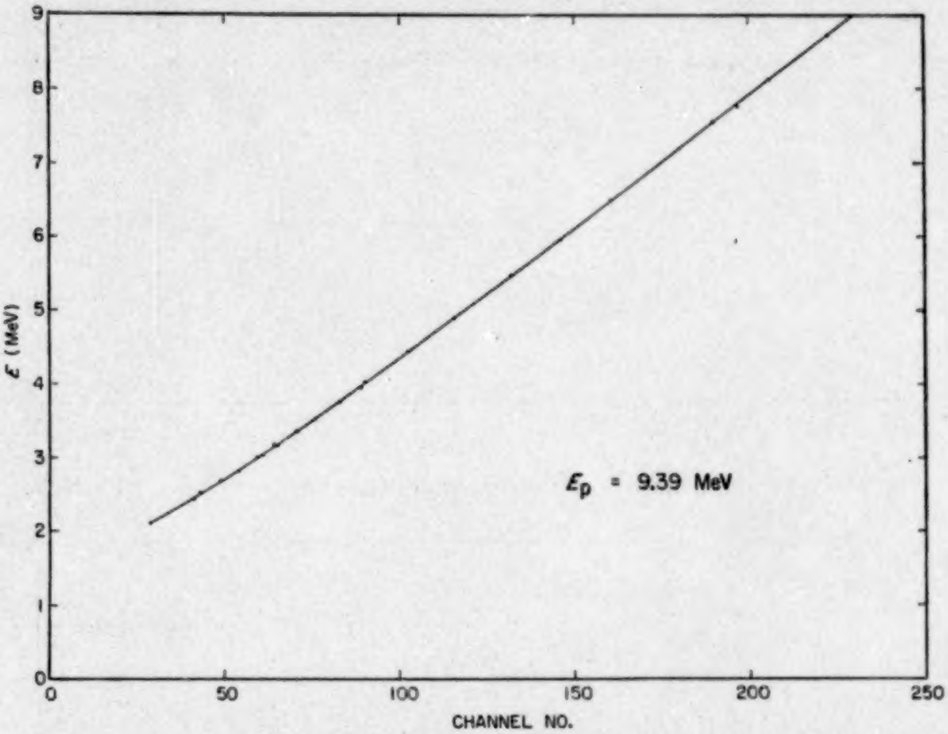

Fig. 3. Calibration curve constructed from observations on protons scattered from air; $E_p = 9.39$ MeV.

For the calibration runs, the gas cell was filled with air to a pressure of about $\frac{1}{2}$ atm and the spectrum of scattered protons was observed at 60°, 90° and 120°. The energies of the scattered particles leading to the well-known final states in N^{14} and O^{16} were calculated from the kinematics of the reaction.

These were plotted *versus* the pulse-height response of the solid-state detector to yield the calibration curve of fig. 3. This curve is not linear because the scattered particle loses energy in the gas, mylar window and proportional counter on its way to the solid-state detector. Thus the pulse height is not proportional to the energy of the scattered proton.

The excitation energies for the several argon states were determined by use of the relation [5]) for the energy E of the scattered particle in the laboratory system

$$\sqrt{E} = v + \sqrt{v^2 + \omega},$$

where

$$v = \frac{\sqrt{E_1}}{1+A} \cos \theta_{\text{lab}}, \quad \omega = \frac{AQ + E_1(A-1)}{1+A},$$

E_1 being the bombarding energy in lab system and A the mass number of target nucleus. The energy E is determined from the calibration curve by noting the channel into which the peak falls. At each angle v is calculated and a value for ω is derived from

$$\omega = E - 2v\sqrt{E}.$$

Thus an independent measurement of Q is obtained at each angle of observation.

It has been pointed out that use of the calibration curve to determine the energy of the scattered particle is tantamount to comparing the excitation energies of the argon levels with the well-known states in nitrogen and oxygen. However, direct comparison is not quite proper, for a small correction must be made due to the difference in the rate of energy loss of protons in argon and in air. This means that, first of all, the bombarding energy at the centre of the gas cell is different for the two cases by an amount

$$\Delta E_{\text{B}} = \left(\frac{\mathrm{d}E}{\mathrm{d}x}\right)_{\text{A}} \Delta X_{\text{A}} - \left(\frac{\mathrm{d}E}{\mathrm{d}x}\right)_{\text{air}} \Delta X_{\text{air}},$$

where $\mathrm{d}E/\mathrm{d}x$ is evaluated in each case at the bombarding energy, and second, for a given energy at the detector, the scattered particle energy will be different by

$$\Delta E = \left(\frac{\mathrm{d}E}{\mathrm{d}x}\right)_{\text{A}, E} \Delta X_{\text{A}} - \left(\frac{\mathrm{d}E}{\mathrm{d}x}\right)_{\text{air}, E} \Delta X_{\text{air}},$$

where $(\mathrm{d}E/\mathrm{d}x)_{\text{A}, E}$ means the rate of energy loss in argon evaluated at the energy of the scattered particle. This was obtained by interpolation from Sternheimer's [6]) values for carbon, aluminium, copper and lead. The values for $(\mathrm{d}E/\mathrm{d}x)_{\text{air}}$ were taken from the same article.

Although an attempt was made to minimize the correction ΔE by proper selection of the ratio of argon and air pressures, we were not completely successful. The corrections finally applied to the measured Q-values ranged from 3 to 22 keV for the 9.39-MeV data and from 3 to 13 keV for the 7.32-MeV data.

Contributions to the uncertainty in the Q-value measurements come from the following sources:

(1) An error in the measurement of the bombarding energy. Due to our method of comparing the excitation energies in argon with those in nitrogen and oxygen, this contribution is relatively weak. Even if we grant an error of 100 keV in the measurement of the bombarding energy, the error contributed to the Q-value measurements is only about 4 keV.

TABLE 1

Excitation energies of argon levels

Level no.	9.39 MeV	7.32 MeV
1	1.453±0.014	1.453±0.018
(a)	(1.85)	(1.85)
2	2.125±0.014	2.100±0.018
3	2.527±0.014	2.517±0.018
4	2.910±0.014	2.879±0.022
5	3.217±0.016	3.219±0.020
6	3.562±0.024	3.528±0.022
7	3.709±0.016	3.69 ±0.02
8	3.934±0.016	3.92 ±0.024
9		4.07 ±0.02
10	4.297±0.024	4.29 ±0.03
11	4.426±0.024	4.41 ±0.04
12	4.595±0.024	4.58 ±0.03
13 (doublet?)	4.884±0.024	4.84 ±0.03
14	5.298±0.024	
15	5.530±0.024	
16	5.695±0.033	
17	5.901±0.024	
18	6.129±0.024	
19	6.270±0.033	
20	6.475±0.042	
21	6.650±0.024	

(2) An error in the construction of the calibration curve. The precision of this construction appears to be good to $\pm\frac{1}{4}$ channel. This is the equivalent of ± 9 keV for $E_p = 9.39$ MeV and ± 7 keV for $E_p = 7.32$ MeV. A similar error of $\frac{1}{4}$ to $\frac{1}{2}$ channel arises from locating the centre of proton groups in the spectrum of scattered particles from argon.

(3) The uncertainty in the Q-values of the N^{14} levels. Above the first level we take, for the uncertainty, the average value 8 keV.

(4) In the case of the 7.32-MeV data, a gain-shift of $1\frac{1}{2}$ channels at channel 220 (and correspondingly less at lower channels) was noted. The proper correction was made; however, we incorporated an additional uncertainty of 15 keV into the *Q*-values derived from this data.

The final values of the excitation energies obtained for the argon levels appear in table 1. Except for the levels above 6.129 MeV, each of these numbers represents the average of three to five separate observations, depending on the number of angles at which the group was prominent enough for a measurement.

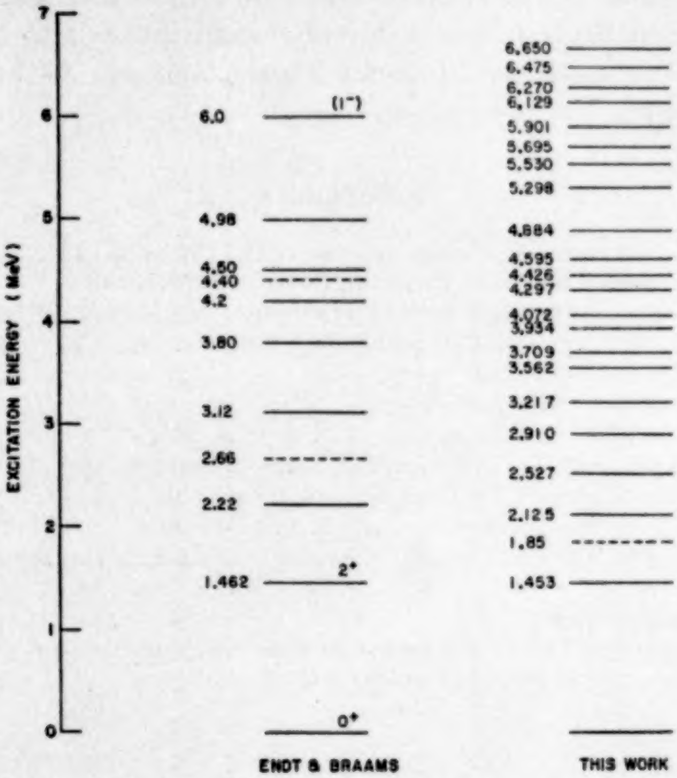
7
6
5
4
3
2
1
0
EXCITATION ENERGY (MeV)
6.0
(1⁻)
4.98
4.50
4.40
4.2
3.80
3.12
2.66
2.22
1.462
2⁺
0⁺
ENDT & BRAAMS
6.650
6.475
6.270
6.129
5.901
5.695
5.530
5.298
4.884
4.595
4.426
4.297
4.072
3.934
3.709
3.562
3.217
2.910
2.527
2.125
1.85
1.453
THIS WORK

Fig. 4. Energy levels of A^{40}.

For the higher levels only one or two determinations were made, so that some reservations may be held in these cases. The uncertainties associated with the excitation energy measurements were derived from the contributions noted above combined as the square root of the sum of the squares.

The energy level diagram of fig. 4 summarizes the data and graphically compares it with the information appearing in the compilation of Endt and Braams. The first level agrees within the stated precision with the generally accepted value. The other states, however, when identifiable with previously observed levels, appear to be at least 100 keV lower than their counterparts. It has caused us some concern that this difference is larger than the combination of quoted uncertainties; however, we find no remedy in an analysis of our observations. Group (13) at 4.88 MeV is clearly too wide to be a single level. It should be considered as at least a doublet until it is investigated with higher resolution equipment. The very weak group (a) was at first ignored as being too uncertain an indication of a level. However, subsequent analysis of 7.32- and 9.39-MeV spectra plus some unreported 8.11-MeV data, gave consistent indication of a level at 1.85 MeV. We are now inclined to credit this observation as genuine.

The authors wish to express their sincere gratitude to Curt L. Rowe for his invaluable contributions to the creation of the gas cell, and to Doris Hine, Joanna Phifer and Brenda Masluk for their contributions to the preparation of this report. This work was performed under auspices of the U. S. Atomic Energy Commission.

References

1) H. Heitler, A. N. May and C. F. Powell, Proc. Roy. Soc. **190** (1947) 180;
R. W. Pringle, S. Standil and K. I. Roulston, Phys. Rev. **77** (1950) 841;
P. R. Bell and J. M. Cassidy, Phys. Rev. **77** (1950) 409, **79** (1950) 173;
R. G. Freemantle, D. J. Prowse, A. Hossain and J. Rotblatt, Phys. Rev. **96** (1954) 1270;
R. H. Helm, Phys. Rev. **104** (1956) 1466;
H. Morinaga, Phys. Rev. **103** (1956) 504;
I. J. Van Heerden and D. J. Prowse, Phil. Mag. **1** (1956) 967;
L. Seidlitz, E. Bleuler and D. J. Tendam, Phys. Rev. **110** (1958) 682;
H. Tyren and Th. A. J. Maris, Nuclear Physics **6** (1958) 446
2) P. M. Endt and C. M. Braams, Rev. Mod. Phys. **29** (1957) 683
3) J. Benveniste, R. Booth and A. Mitchell, Lawrence Radiation Laboratory report UCRL-6441 (1961)
4) R. Booth, to be published
5) R. D. Evans, The atomic nucleus (McGraw-Hill Book Co., New York, 1955) p. 410
6) R. M. Sternheimer, Phys. Rev. **115** (1959) 137

1.E.1:
4.E

Nuclear Physics **27** (1961) 673—680; © *North-Holland Publishing Co., Amsterdam*

Not to be reproduced by photoprint or microfilm without written permission from the publisher

LOW LYING STATES OF Th^{229}

TORKILD ANDERSEN †, K. MAACK BISGÅRD and P. GREGERS HANSEN ††
The Physical Institute, University of Aarhus, Denmark

Received 25 April 1961

Abstract: The decay of 1.6×10^5y U^{233} has been studied by means of a six gap beta-ray spectrometer, a xenon filled proportional counter and scintillation spectrometers.

Internal conversion electrons having energies below 100 keV were measured. The mixing ratios for the 42 keV and the 55 keV transitions agree with the assumed rotational character of the 42 keV and 97 keV states. Results concerning the 163 keV state indicate that this state is also a member of the ground state rotational band.

1. Introduction

Because of the low specific activity of U^{233} ($T_{\frac{1}{2}} = 1.6 \times 10^5$ y) the conversion-electron spectrum from transitions following the α-decay of this isotope has not until recently been studied by means of any high or medium resolution method. Energies of some Th^{229} levels have been determined by means of α- and γ-spectroscopy [1]) and results so obtained are supported by nuclear emulsion work as regards the low energy transitions [2]). The existence of a rotational band based on the ground state was in this way shown.

In view of the poor statistics and resolution in range measurements or grain counting in nuclear emulsions it was decided to study the internal conversion-electron spectrum in a beta-spectrometer utilizing the relatively high transmission of the six gap spectrometer [3]). Meanwhile results from a study mainly based upon a toroidal, ironfree spectrometer have been published by Tret'yakov *et al.* [4]). By selection of electrons which are coincident with α-particles from the decay of U^{233} Tret'yakov *et al.* have lowered the background effectively and a number of previously unknown levels and transitions are reported. Such a method was not used in the present investigation which deals mainly with the lowest transitions. The results are in good agreement with those of Tret'yakov *et al.* but because of an improved resolution the conversion-electron spectrum is more detailed in its limited range of energy.

2. Experimental Method

The source material, supplied by the United States Atomic Energy Commission, had the following composition as to weight: U^{233} 98.06 %, U^{232} 0.0034 %, U^{234} 1.74 %, U^{236} 0.21 %.

---

† Permanent address: The Institute of Chemistry, University of Aarhus

†† Permanent address: Danish Atomic Energy Commission, Risø pr. Roskilde, Denmark

A main problem is the preparation of sufficiently pure and uniform sources. Even small amounts as to weight of the 4n series result in dominating lines from the decay of U^{232} and Bi^{212} (58 keV and 239 keV transitions, respectively). The separation of U from Th, Bi and Pb was carried out by anion-exchange. Dowex 1×10 was applied on cloride form. After equilibrating with 6*N* HCl there is no absorption of Th to the anion-exchanger [5]) and the separation of U from Pb and Bi is accomplished by a 0.4 *N* HCl elution. The purified U was accumulated on sheets of platinum (thickness about 20 mg/cm^2) by electroplating [6]) and the chemical purification tested by the disappearance of the Th F-line. The active areas were circular with diameters of 14 mm and 8 mm, their mean thickness being about 100 μg/cm^2. By means of an adjustable diaphragm placed on the source holder different parts of the active area could be used and in this way resolution and transmission were changed within certain limits. The activities ranged from about 0.2 μCur to about 1 μCur. Some measurements were performed with two sources placed back to back and utilizing all six gaps. As one of the sources was more homogenous than the other ones some runs were made with three gaps only.

The γ-ray spectrum was studied by means of a xenon filled proportional counter and a 7.6 $\times$ 7.6 cm sodium iodide crystal spectrometer in connection with a RCL 256-channel pulse-height analyzer, vacuum tube model. A fast-slow coincidence circuit and the multi-channel analyzer were used for γ-γ and e-γ measurements.

3. Results

The region from 15 keV to 100 keV was scanned for conversion lines. The intensities of transitions corresponding to energies above 100 keV are of the order of 0.01 % or less per α-decay and the present geometry and activity did not allow sufficient statistics to be obtained. Among 14 lines measured, 12 conversion lines belonging to the 42 keV, 55 keV and 97 keV transitions were clearly established. Further some indications for the 29 keV transitions reported by Tret'yakov *et al.* are present, whereas the existence of a 71 keV transition reported by the same authors cannot be confirmed by the present data. Our energy values are between 1 and 2 keV lower than those found by Tret'yakov *et al.*, who have made accurate energy determinations by calibration with known lines from three different isotopes. As the differences can be explained by the source thicknesses an energy notation close to that used by Tret'yakov *et al.* is adopted.

In table 1 are listed conversion line intensities together with those of Tret'yakov *et al.* In lack of direct comparison with the α-decay rate all values are normalized relatively to the 42 L_{II} intensity found by Tret'yakov *et al.*

Table 2 contains experimental values of relative conversion coefficients for the three transitions mentioned above together with some theoretical values [7])

TABLE 1

Conversion line intensities

Transition energy (keV)	Shell				
	L_I	L_{II}	L_{III}	M	N
29				6 (5.7)	1.4 (3.3)
42	90 (49)	100 (100)	86 (92)	$\gtrsim$86 (85)	24 (25)
55	9 (13)	10			
97	0.8 (5.3)	4.0	3.4 (3.8)	2.2 (2.5)	0.6 (0.6)

The 42 L_{II} intensity has been used for normalization of the intensities relative to those of Tret'yakov *et al.* The 42 M line coincides in part with the 55 L_{III} line. All experimental values are corrected for variations in crystal efficiency. The results of Tret'yakov *et al.* are given in parenthesis.

TABLE 2

Conversion ratios and multipolarities

Transition energy (keV)	Conversion ratio	Experimental values	Theoretical values		Multipolarity
			M1	E2	
42	$\frac{L_I+L_{II}}{L_{III}}$	2.2±0.1	160	1.05	(86±2)% M1 (14±2)% E2
	$\frac{L_I}{L_{II}}$	0.9±0.1	13	0.03	
	$\frac{L}{M}$	3			
55	$\frac{L_I}{L_{II}}$	0.9±01.	12	0.04	(85±5)% M1 (15±5)% E2
97	$\frac{L_I+L_{II}}{L_{III}}$	1.4±0.1	200	1.4	E2
	$\frac{L_I}{L_{II}}$	0.2±0.1	10	0.05	
	$\frac{L}{M}$	3.7			

and the multipolarities according to our results. The assignments made by Albouy [2]) and by Tret'yakov *et al.* are also given. According to the present data the ratio L_I/L_{II} for the 97 keV transition is larger than expected. It has been confirmed during a repeated measurement.

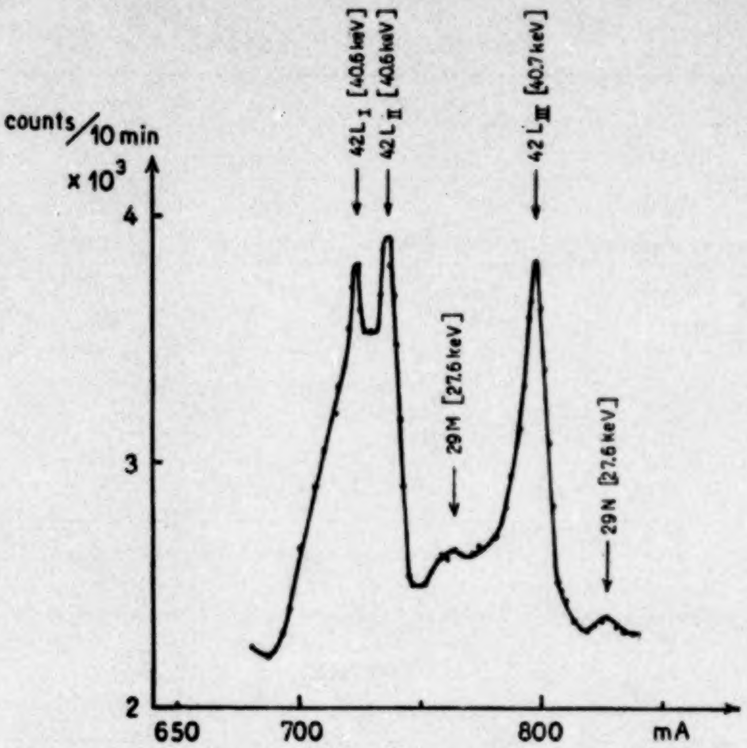

Fig. 1. Part of the conversion-electron spectrum showing the L_I, L_{II} and L_{III} lines together with the two weak lines which are assigned to a 29 keV transition by Tret'yakov *et al.* The energy notation of Tret'yakov *et al.* is used. Transition energies found in the present investigation are given in parenthesis. The binding energies 20.46 keV (L_I) 19.69 keV (L_{II}), 16.30 keV (L_{III}), 5.18 keV (M) and 1.32 keV (N), respectively, are used. No efforts were done to obtain a precise absolute energy calibration.

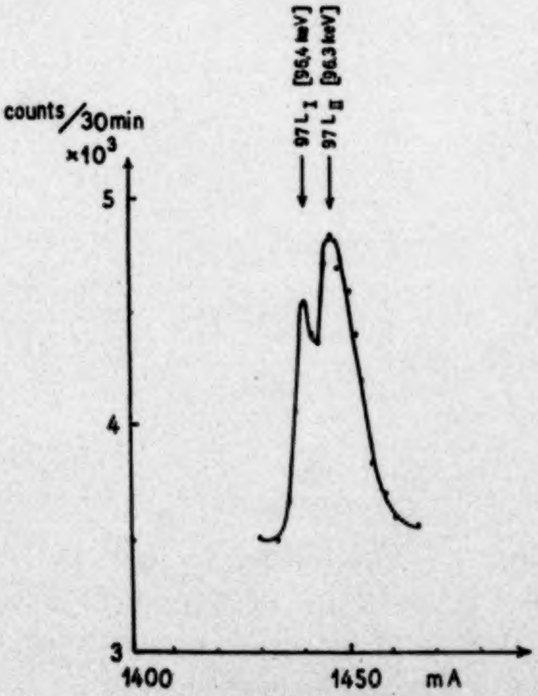

Fig. 2. Part of the conversion-electron spectrum showing the 97 L_I and 97 L_{II} lines. The present energy values are given in parenthesis. The binding energies 20.46 keV (L_I) and 19.69 keV (L_{II}), respectively, are used. No absolute energy calibrations were made.

The three *L* conversion lines belonging to the 42 keV transition are shown on fig. 1. It appears from the curve that the existence of M and N conversion lines from a 29 keV transition is not ruled out.

In view of the large ratio of the L_I to the L_{II} conversion groups belonging to the 97 keV transition the corresponding curve is also shown (fig. 2).

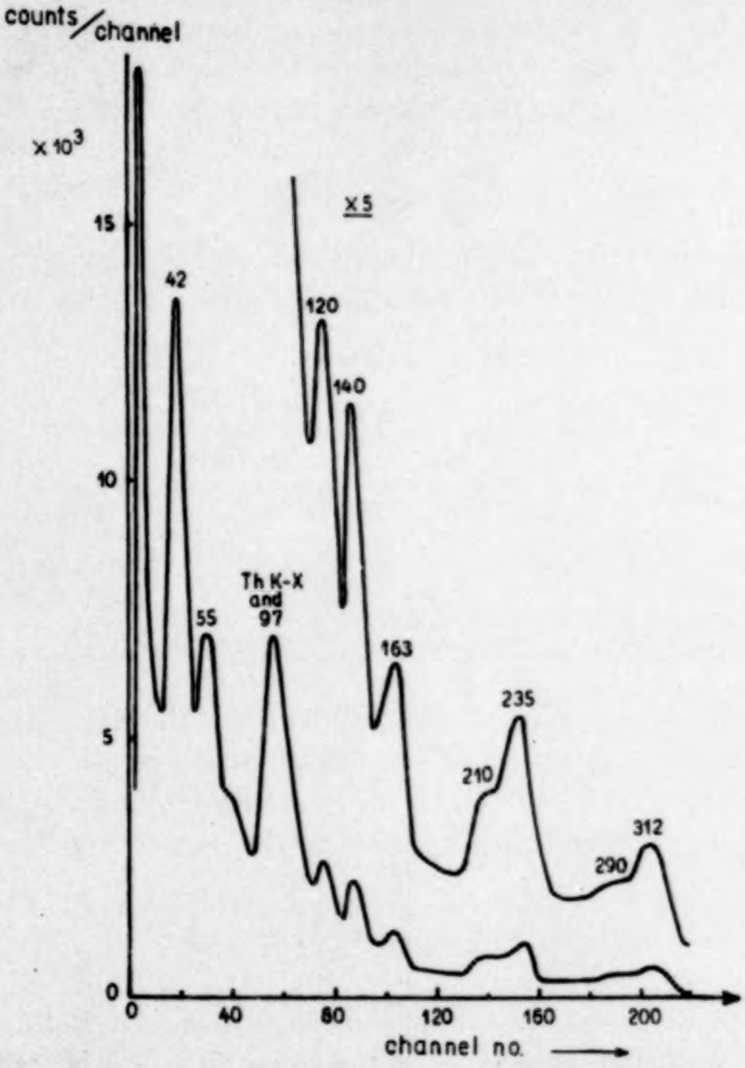

Fig. 3. U^{233} gamma-ray spectrum. Gamma lines corresponding to the 71 keV transition tentatively proposed by Tret'yakov *et al.* and a possible 66 keV transition will be coinciding with the group seen on the high energy flank of the 55 keV gamma line.

On fig. 3 the total γ-scintillation spectrum is shown. Transitions corresponding to the following energies are present (relative peak intensities are given in parenthesis): 42 (100), 55 (15), 97 (66), 121 (4), 140 (4), 163 (3), 210 (2.5), 235 (5), 290 (1.5) and 312 (3). The last group consists of unresolved lines. By means of data from a spectrum taken with a xenon filled proportional counter the intensity of the 55 keV group is corrected for contributions from the 58 keV transition belonging to the U^{232} decay. X-rays are included in the relative intensity of the 97 keV group.

Measurements of γ-γ coincidences howed that the 42 keV line is coincident with a 55 keV and a 121 keV transition, whereas the latter did not show coincidences with the 55 keV line, in agreement with the previously proposed level scheme.

As a result of e-γ measurements coincidences between the 42 keV L-electrons and 55 keV and 121 keV gamma lines were confirmed, but because of poor statistics any quantitative relations can hardly be deduced.

4. Remarks

The mixture of M1 and E2 in the 42 keV transition as determined from L_I+L_{II}/L_{III} and L_I/L_{II} conversion ratios are given in table 3 together with

TABLE 3

Multipolarities

Transition energy (keV)	Assignments		
	Albouy [2])	Tret'yakov *et al.* [4])	Present results
42	M1+E2	80% M1+20% E2	86% M1+14% E2
55	M1+E2	M1+E2	85% M1+15% E2
97	E2	E2	E2

results found by Tret'yakov *et al.* and by Albouy. The mixing ratio δ_1^2 which gives the ratio of E2 to M1 quanta in the transition can be expressed by the intrinsic quadrupole moment Q_0 and the gyromagnetic ratios g_K and g_R associated with the intrinsic and the rotational motion respectively [8]):

$$\delta_1^2 = \frac{T_1(\text{E2})}{T_1(\text{M1})} = \frac{3}{20}\,\frac{1}{I+2}\left(\frac{E_1}{\hbar c}\right)^2\left(\frac{M_0 c}{\hbar}\right)\,\frac{Q_0^2}{(g_K-g_R)^2},$$

where $I = K \neq \frac{1}{2}$ denotes the total angular momentum of the ground state and E_1 is the transition energy. M_0 is the mass of the proton. Our results lead to a value of δ_1^2 equal to 0.16. On the basis of α-decay probabilities the ground state of Th^{229} is assigned [9]) the same Nilsson level $\frac{5}{2}+[633]$ as that of U^{233}. Neither the electric quadrupole moment nor the magnetic moment is known, but the large admixture of E2 agree with the proposed collective nature of the transition. An admixture of 30 % E2 resp. 24 % E2 is found by Albridge *et al.*[10]) and in this laboratory for the corresponding transition in the ground state rotational band of U^{233}.

If the corresponding expression for the 55 keV transition from the second to the first excited state ($K+2 \rightarrow K+1$) is used together with the energy sequence for odd A rotational states

$$E_{\mathscr{I}} = \frac{\hbar^2}{2\mathscr{I}}\,[I(I+1)-K(K+1)], \qquad K \neq \tfrac{1}{2},$$

then the relative mixing ratios can be expressed as

$$\left(\frac{\delta_1}{\delta_{21}}\right)^2 = \left(\frac{K+1}{K+2}\right)^2 \frac{(K+1)(K+3)}{K(K+2)}.$$

It leads to a value of 1.04 for $K = \frac{5}{2}$ in agreement with the experimental value of 0.9 ± 0.3 which follows from $\delta_1^2 = 0.16 \pm 0.02$ and $\delta_{21}^2 = 0.18 \pm 0.06$ (see table 3). A check on the spin assignment for the ground state cannot be obtained in this way as the corresponding ratios for $K = \frac{3}{2}$ and $K = \frac{7}{2}$ amount to 1.10 and 1.02, respectively.

Similarly the E2 parts of the relative gamma transition probabilities of the cascade to cross-over decay from the second rotational state can be expressed as

$$\frac{T_2(\mathrm{E2})}{T_{21}(E2)} = \frac{1}{2}\left(\frac{E_2}{E_{21}}\right)^5 \frac{(2K+1)(K+3)}{K^2(2K+3)}.$$

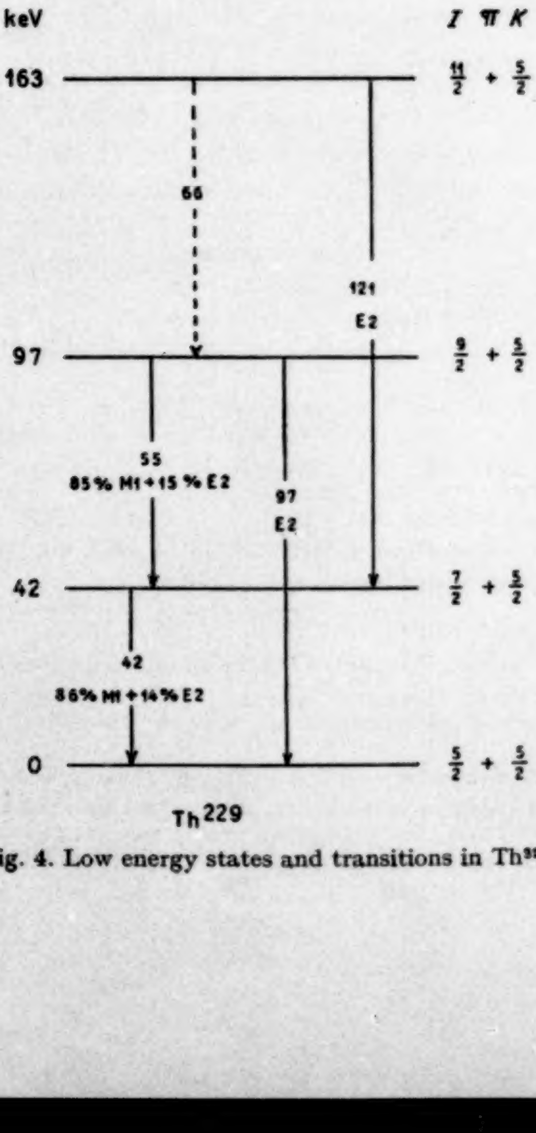

Fig. 4. Low energy states and transitions in Th^{229}.

By means of the energy relations for rotational states this ratio takes the value

$$\frac{T_2(\mathrm{E2})}{T_{21}(\mathrm{E2})} = \tfrac{1}{2}\left(\frac{2K+3}{K+2}\right)^5 \frac{(2K+1)(K+3)}{K^2(2K+3)} = 5.86 \text{ for } K = \tfrac{5}{2}.$$

The mixing ratio for the 55 keV transition together with the relative intensities of the 55 keV L and 97 keV L groups lead to an experimental value equal to 6 ± 2. According to theory the corresponding values for $K = \frac{3}{2}$ and $K = \frac{7}{2}$ are 9.87 and 4.21, respectively.

If the previously observed 163 keV level is also a member of the ground state rotational band, the 121 keV gamma line observed in the single gamma spectrum and also seen in coincidence with the 42 keV transition is expected to be pure E2. On this assumption the relative conversion electron intensities for the 42, 55 and 121 keV transitions can be derived using our gamma intensities. A good agreement is in this way obtained with our relative conversion intensities and with those of Tret'yakov *et al.* which include also the 121 keV L lines.

From the values of $T_{31}(\mathrm{E2})$: $T_{32}(\mathrm{E2})$ and of $\delta_{32}^2 : \delta_{21}^2$ it follows that the gamma intensity of the 66 keV transition (163 → 97) is expected to be about 50 % of the 121 keV gamma intensity. The deduced intensities of the corresponding electron groups are on the limit of what could be observed in this investigation. The relevant part of the level scheme is shown on fig. 4.

Our thanks are due to Mr. Poul Dahl and Mr. Knud Olesen, who have provided us with most of the electronic equipment and been advisers in questions related to its performance. We are also indebted to Mr. P. Ambrosius-Olesen and Mr. E. Christensen for very valuable assistance in the solution of technical problems.

References

1) M. Studier, PPR-CD-3793 (1947);
C. A. Prohaska, UCRL 1395 (1951);
D. West, J. K. Dawson and C. J. Mandleberg, Phil. Mag. **43** (1952) 875;
F. Asaro, UCRL 2180 (1953);
L. L. Gol'din, G. I. Novika and E. F. Tret'yakov, Phys. Rev. **103** (1956) 1004;
B. S. Dzehelepov, R. B. Ivanov, V. G. Nedovesov and B. P. Shishin, Izvest. Akad. Nauk. SSSR, Ser. Fiz. **23** (1959) 782 [Columbia Tech. Trans. p. 785]
2) K. Maack Bisgård, Proc. Phys. Soc. **65** (1952) 677;
G. Albouy, Ann. Phys. **1** (1956) 116
3) O. B. Nielsen and O. Kofoed Hansen, Mat. Fys. Medd. Dan. Vid. Selsk. **29** No. 6 (1955);
K. Maack Bisgård, Preliminary report, sept. 1960
4) E. F. Tret'yakov, M. P. Anikina, L. L. Gol'din, G. I. Novikova and N. I. Pirogova, JETP (Soviet Physics) **37** (1960) 656
5) K. A. Kraus and F. Nelson, Proc. Int. Conf. on the peaceful uses of atomic energy (United Nations) **7** (1956) 113
6) B. Cohen and D. E. Hull, Analytical chemistry of the Manhattan project (N.N.E.S. VIII-I (1950) 526
7) M. E. Rose, Internal conversion coefficients (North-Holland Publ. Co., Amsterdam, 1958)
8) Aage Bohr and Ben R. Mottelson, Mat. Fys. Medd. Dan. Vid. Selsk. **27**, No. 16 (1953)
9) F. S. Stephens, Frank Asaro and I. Perlman, Phys. Rev. **113** (1959) 212
10) R. G. Albridge, I. M. Hollander, C. I. Gallagher and I. M. Hamilton, UCRL-9438, oct. 1960

3.B

Nuclear Physics **27** (1961) 681—687; © *North-Holland Publishing Co., Amsterdam*

Not to be reproduced by photoprint or microfilm without written permission from the publisher

THE K-CONVERSION COEFFICIENT OF THE 368 keV E2 TRANSITION IN ^{200}Hg

W. H. G. LEWIN, B. VAN NOOIJEN and A. H. WAPSTRA

Laboratorium voor Technische Fysika, Delft, Holland

Received 4 May 1961

Abstract: The K-conversion coefficient of the 368 keV E2 transition in ^{200}Hg has been determined by means of K-conversion electron-gamma coincidence measurements. The result $\alpha_K =$ $= 0.0395 \pm 0.0008$ is in excellent agreement with the theoretical values computed by Rose and by Sliv and Band.

1. Introduction

The effect of nuclear structure on conversion coefficients [1-3]) is expected to be rather small for E2 transitions, and negligible for unhindered ones.

Yet McGowan and Stelson [4]) found that the conversion coefficients of ground state E2 transitions in ^{166}Er, ^{170}Yb and ^{176}Hf are 15 to 25 % higher than the theoretical values [1,2]), whereas the Amsterdam group [5,6]) reported that those in ^{194}Pt, ^{196}Pt and ^{198}Hg are 10 to 30 % lower.

Indications for a systematic variation in the deviation from the theoretical values have been discussed by Subba Rao [7]).

The dependability of some of these results is, however, made somewhat doubtful by the fact that in the case of the 412 keV gamma ray in ^{198}Hg, the method of comparison of internal and external conversion of the same gamma ray [6,8,9]) gives consistently results lower by more than 10 % than the method of comparing the internal conversion line with the ^{198}Au beta spectrum feeding the corresponding level [5]) in ^{198}Hg.

It is therefore useful to apply an independent method of measuring conversion coefficients. Such a method can be the measurement of coincidences between conversion electrons selected in a beta ray spectrometer and other radiations preceding these conversion electrons. The present article describes such a measurement on ^{200}Tl.

2. Method of Measurements

The method which has been applied may best be elucidated on basis of the decay scheme [10,11]) of ^{200}Tl (see fig. 1).

The current through the β-spectrometer is adjusted to the top of the 285 keV K-conversion line of the 368 keV gamma transition; the channel of a gamma scintillation spectrometer is set to accept gamma rays in the 1200 keV region. Then, one has

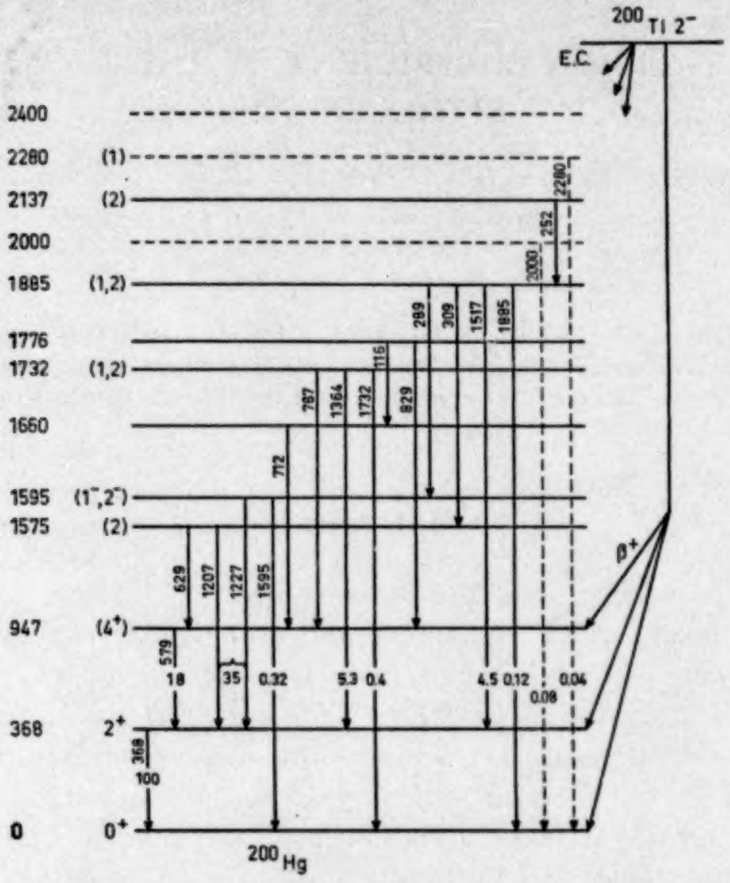

^{200}Tl 2$^-$
E.C.
2400
2280 (1)
2137 (2)
2000
1885 (1,2)
1776
1732 (1,2)
1660
1595 (1$^-$,2$^-$)
1575 (2)
947 (4$^+$)
368 2$^+$
0 0$^+$
2280
252
2000
289
309
1517
1885
116
787
1364
1732
829
712
629
1207
1227
1595
579
18
35
0.32
5.3
0.4
4.5
0.12
0.08
0.04
368
100
β^+
^{200}Hg

Fig. 1. Decay scheme of ^{200}Tl. Energies and relative intensities of the gamma rays are indicated in the figure.

$$\frac{N_{\gamma e}}{N_\gamma} = CT\,\frac{\alpha_K}{1+\alpha_T}\,, \tag{1}$$

where $N_{\gamma e}$ is the coincidence counting rate, N_γ the gamma ray counting rate corrected for the influence of non-coincident gamma rays, α_K the K-conversion coefficient of the 368 keV transition, α_T the total conversion coefficient, and T the transmission of the beta spectrometer (top counting rate in a single conversion line divided by the total number of conversion electrons of this energy emitted by the source). The factor C is a correction factor, nearly equal to one, taking care of the influence of the detection efficiency of the anthracene counter of the beta spectrometer, the coincidence efficiency and, if necessary, the directional correlation between the conversion electrons and gamma quanta.

In the above equation, α_T is related to α_K by $\alpha_T = \alpha_K\{1+(L+M+\ldots)/K\}$ so that the ratio of the conversion line intensities in this formula also has to be determined.

The quantity *CT* is inversely proportional to the relative half-width *R* (resolution) of the spectrum lines (see sect. 3.2). The proportionality constant *CTR* can be determined experimentally by measuring beta-gamma coincidences between the 412 keV gamma rays and the electrons of the preceding 966 keV beta transition [5]) in the decay of ^{198}Au. One finds

$$\frac{N_{\beta\gamma}}{N_\gamma} = 0.989 \text{ a } CTR\, f(\eta)\eta, \tag{2}$$

in which $N_{\beta\gamma}$ is the coincidence counting rate, N_γ the gamma ray counting rate, *R* the resolution of the beta spectrometer (relative half-width), *a* a form factor (ratio of the area of a conversion line and that of a rectangle with the same height and a width equal to the half-width), $f(\eta)$ the momentum distribution of the beta rays normalised in such a way that $\int f(\eta)d\eta = 1$, and 0.989 the fraction of the 412 keV gamma rays preceded by the 966 keV beta transition.

The constant *C* in eqs. (1) and (2) is not necessarily the same since it is dependent on the energy; the influence of this dependence is, however, made negligible if the beta spectrometer in the ^{198}Au experiment is again set at the energy of 285 keV of the conversion electrons in the ^{200}Tl experiment. The choice of this low energy in combination with the large solid angles used in the present experiments also makes the influence of the weak beta-gamma directional correlation in ^{198}Au (ref. [12])) negligible. As shown below the directional correlation in ^{200}Tl is isotropic too, in sufficient approximation.

3. Measurements

3.1. INSTRUMENTAL

The beta-gamma coincidence equipment used in the present experiments [13]) consists of a long lens beta ray spectrometer with an anthracene scintillation detector behind the ring focus.

A NaI(Tl) scintillation spectrometer for detection of gamma rays can be placed near the source at angles of 90° and 180° with respect to the axis of the beta spectrometer, in order to investigate a possible directional correlation.

Coincidences in the two detectors are registered with a fast-slow coincidence arrangement with a resolution time of $2\tau = 0.09$ μsec; this was sufficient to make the number of accidental coincidences less than 10 % of the true ones in all experiments.

3.2. MEASUREMENTS ON ^{198}Au

Sources of this material prepared by neutron irradiation of gold were obtained from Messrs. Philips Duphar. Spectrometer sources with different diameters were used in order to check the dependence of CT on the resolution R. The resulting values of CTR are constant within the limits of error (2 %).

Using for the momentum distribution function of the beta particles the shape factor g, as found by Wapstra[5,14]), an average value of $CTR = (452 \pm 4) \times 10^{-6}$ is obtained. If an allowed shape had been assumed, this value would have been $(461 \pm 4) \times 10^{-6}$ and consequently the resulting conversion coefficient for the 368 keV transition in ^{200}Hg 2 % lower (see sect. 2).

Special care was taken to ascertain that the coincidence counting rate in the above experiment was not unduly influenced by scattering. For this purpose, the Fermi plot of single particles was measured with the gamma ray detector in the 180° position (where it may cause a considerable amount of scattering) and in the 90° position; the difference at 285 keV was only 10 %, and the points found in the 90° position coincided quite accurately with the forbidden Fermi plot through points of higher energy.

Moreover, the coincidence experiment was repeated at electron-energies of 500 keV. The measurements at this point gave the same result as given above indicating that the influence of scattering on CTR is negligible.

3.3. MEASUREMENTS ON ^{200}Tl

Carrier free ^{200}Tl sources were prepared in the I.K.O. synchro-cyclotron in Amsterdam by the reaction ^{200}Hg(d, 2n)^{200}Tl. The activity was separated chemically and converted into chloride.

The first measurements were carried out with sources which were obtained by evaporating drops of solution onto zapon films rendered conductive by vacuum-deposited aluminium. Later measurements were performed with sources made by vacuum-evaporation of the ^{200}Tl activity onto 6 μm aluminium backings. Extremely thin sources have been used in order to avoid scattering of the electrons in the sources.

In the measurements with these sources, the beta spectrometer current was adjusted to the top of the K-conversion line of the 368 keV transition. The setting of the scintillation spectrometer is shown in fig. 2; analysis of this spectrum shows that (4.8 ± 0.5)% of the pulses accepted in the gamma ray channel are due to gamma rays not feeding the 368 keV level.

In order to investigate whether the coincidence counting rate may have been influenced by possible long low energy tails to electron lines, coincidence measurements were made on L-conversion electrons of the 368 keV transition at a setting of 320 keV. It is not possible to use a current setting just before the 285 keV K-conversion peak due to the presence of other ^{200}Tl conversion lines[10]). The amount of coincidences found was, however, negligible.

It is also possible that gamma rays reach the beta ray detector by scattering in the beta spectrometer and thus contribute to the coincidence counting rate.

Therefore, the latter was measured with a spectrometer current equal to zero. The resulting coincidence rate was negligible (≈ 1 ‰).

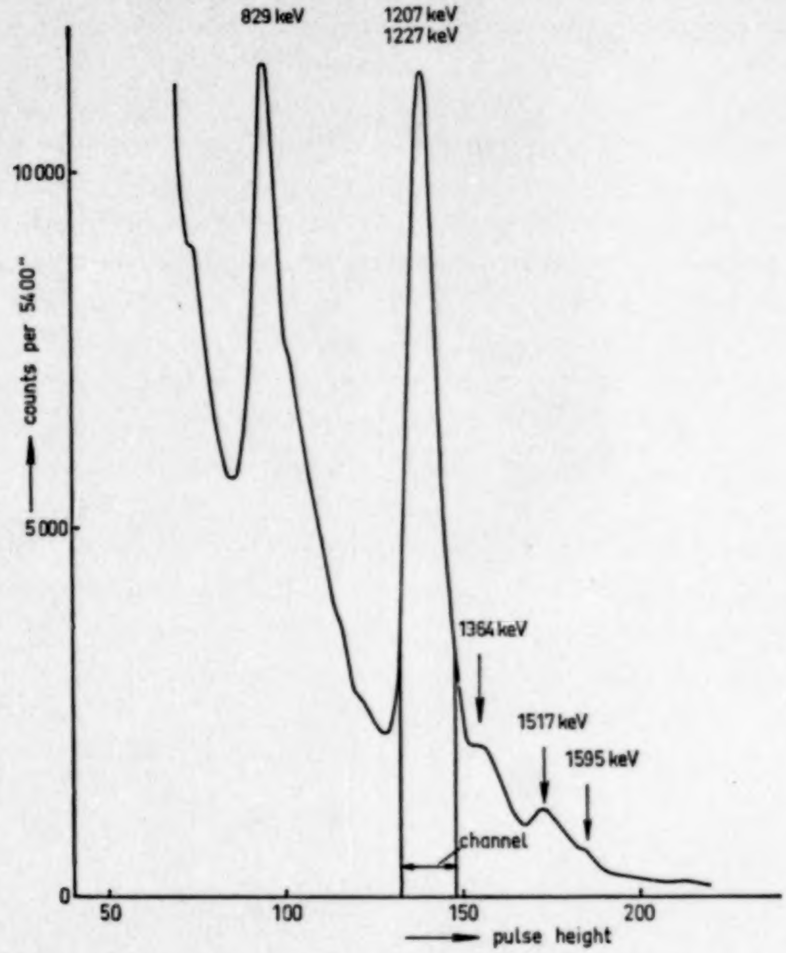

Fig. 2. Single gamma ray spectrum of ^{200}Tl (high energy part).

The results of the ^{200}Tl measurements are summarized in table 1. The first column shows the quantities $N_{\gamma e}/N_\gamma$ after applying the corrections discussed in sect. 3.

TABLE 1

Results of the ^{200}Tl measurements

$10^6 N_{\gamma e}/N_\gamma$	$10^2 R$	$10^7 A$	ϑ
422±18	3.86±0.07	163±8	90°
453±12	3.69±0.07	167±6	90°
500±10	3.38±0.05	169±5	180°
450± 9	3.67±0.05	165±4	180°
477±10	3.70±0.07	176±6	180°
	average value	168±3	

The sources used had different diameters; column 2 gives the resolution *R* for the 285 keV K-conversion line.

Column 3 contains the quantities $A = N_{\gamma e}R/N_{\gamma}$. The values mentioned in this column indeed agree with the assumption that CTR is a constant. They also show that the relative counting rates at 90° and 180° are equal within the errors of the measurements:

$$\frac{A\ (180^\circ)}{A\ (90^\circ)} = 1.03 \pm 0.03.$$

Evidently the gamma-electron directional correlation is either isotropic or weak. We therefore felt justified in taking for $N_{\gamma e}R/N_{\gamma}$ an average value of the results at both positions.

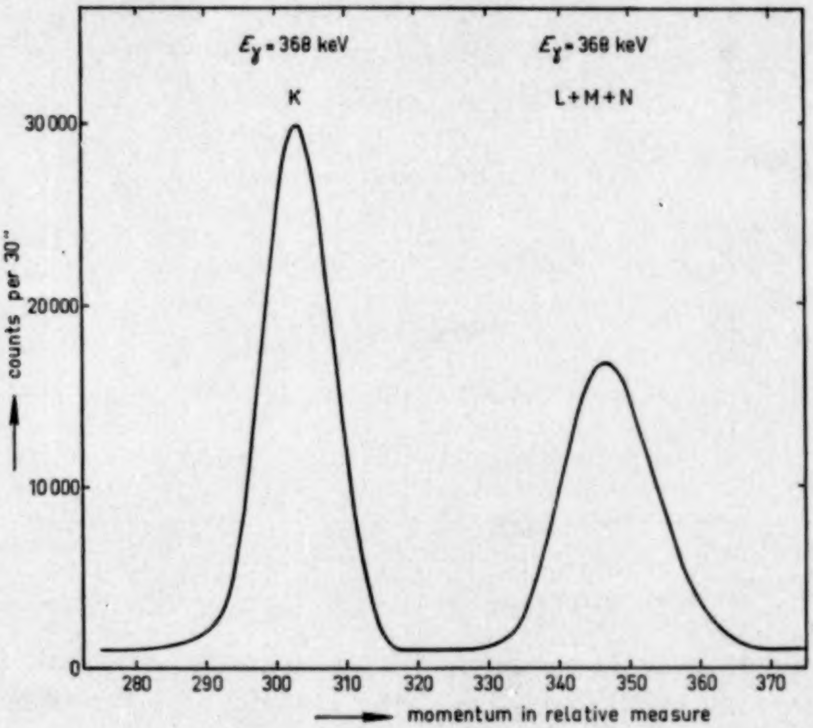

Fig. 3. Internal conversion lines of the 368 keV transition in ^{200}Hg.

Fig. 3 shows the K and the L+M+ ... conversion lines of the 368 keV transition. The K/(L+M+ ...) ratio is 1.815±0.05. This value is in good agreement with the theoretical value 1.82±0.05. The latter has been derived from Rose's tables.

The screening effect in the M-shell has been neglected by Rose. A correction factor [15]) of 0.60 has been applied for α_M to take this effect into account. A value of 0.0009 has been adopted [15]) for α_N.

The internal K-conversion coefficient of the 368 keV transition may now be computed using eq. (1). The result is $\alpha_K = 0.0395 \pm 0.0008$.

4. Conclusion

The experimental result $\alpha_K = 0.0395 \pm 0.0008$ is in perfect agreement with the theoretical values. Rose's tables give $\alpha_K = 0.0391$, according to Sliv and Band $\alpha_K = 0.0396$.

Recently Van Nooijen *et al.*^{16}) measured α_K by a different method. Their value $\alpha_K = 0.040 \pm 0.003$ covers the present result.

After our measurements had been completed, Petterson *et al.*^{17}) published their result of the measurement of the K-conversion coefficient of the 412 keV E2 transition in ^{198}Hg. They report a value for α_K which is also in excellent agreement with theory.

The authors are indebted to Mr. Dalenberg for the chemical separations and to the crew of the I.K.O synchro-cyclotron in Amsterdam for the irradiations.

References

1) M. E. Rose, Internal conversion coefficients (North-Holland Publ. Co., Amsterdam, 1958)
2) L. A. Sliv and I. M. Band, Coefficients of internal conversion of gamma radiation (USSR Academy of Sciences, Moscow, Leningrad, 1956)
3) G. J. Nijgh and A. H. Wapstra, Nuclear Physics **9** (1958) 545
4) F. K. McGowan and P. H. Stelson, Phys. Rev. **107** (1957) 1764
5) A. H. Wapstra, G. J. Nijgh, N. Salomons-Grobben and L. Th. M. Ornstein, Nuclear Physics **9** (1958) 538
6) C. de Vries, E. J. Bleeker and N. Salomons-Grobben, Nuclear Physics **18** (1960) 454
7) B. N. Subba Rao, Nuovo Cim. **17** (1960) 189
8) S. Hultberg, private communication
9) J. H. Hamilton, W. F. Frey and S. Hultberg, Bull. Amer. Phys. Soc. **5** (1960) 449
10) C. J. Herrlander and T. R. Gerholm, Nuclear Physics **3** (1957) 161
11) R. K. Gupta, R. K. Girgis and R. van Lieshout, Nuclear Physics **14** (1959) 597
12) R. M. Steffen, Phys. Rev. **118** (1960) 763
13) B. van Nooijen, J. Konijn, A. Heyligers, J. F. van der Brugge and A. H. Wapstra, Physica **23** (1957) 753
14) A. H. Wapstra, Nuclear Physics **9** (1958) 519
15) C. de Vries, Thesis, University of Amsterdam (1960)
16) B. van Nooijen, H. van Krugten, W. J. Wiesehahn and A. H. Wapstra, to be published in Nuclear Physics
17) B. G. Petterson, J. E. Thun and F. R. Gerholm, Nuclear Physics **24** (1961) 243

10.B Nuclear Physics 27 (1961) 688; © North-Holland Publishing Co., Amsterdam

NEWS ITEM

CERN THEORETICAL CONFERENCE

(5—10 June 1961)

The 1961 International Conference on Theoretical Aspects of Very High Energy Nuclear Phenomena gathered at CERN 100 physicists from all parts of the world.

Prof. D. A. Blokhintsev, Director of the Dubna Joint Institute stated that "the Conference proved most useful in many fields, but particularly in 'pionization' (multiple pion production). This is one field where one could see how theoretical predictions are verified by experiments made with large particle accelerators."

Prof. T. D. Lee, now at CERN on leave from the Institute of Advanced Study, Princeton, suggested during the conference: "At very high energies and for a number of processes, one can expect, at least, that dynamical effects of mass differences between elementary particles can be neglected. Therefore, it would be easier to find out whether there exists any further symmetry which might be hidden at low energy".

Reporting discussions about the need for new, more powerful accelerators, Prof. R. E. Marshak, of Rochester University, said: "This conference opened a series of others where physicists try to come to some conclusion on how interesting physics could be performed with accelerators of higher energies than those at present in operation in the world. Such new machines would accelerate particles to kinetic energies of several hundreds of GeV, would cost up to 500 million dollars and would be a major undertaking for technical man-power."

Prof. L. Van Hove, Head of CERN's Theory Division, said in his concluding address as Chairman of the Conference: "In the field of weak and strong interactions, laboratories must strive for a great variety of high energy experiments. Very good accuracy, especially for the detection of rare nuclear events, is required. This calls for high intensity accelerators. As an example of qualitative questions put forward again at the conference, one can mention two fundamental problems in the field of weak interactions: (1) Are there one or two types of neutrinos? (2) Is there an intermediate boson of rather low mass?"

10.A Nuclear Physics 27 (1961) 689; © North-Holland Publishing Co., Amsterdam

NEWS ITEM

NUCLEAR COMPILATIONS

Physicists who are presently compiling information in a particular area of nuclear physics or who are planning to undertake such projects are urged to contact the Subcommittee of Nuclear Constants of the United States National Academy of Sciences-National Research Council. The Subcommittee is concerned with the need to encourage adequate coverage of areas where compilations would be useful and to supply co-ordination to prevent duplication of effort by separate groups. The Subcommittee offers its services as a co-ordination centre to perform the following functions:

(a) To endeavour to find sources of financial assistance in cases in which publications may be delayed by lack of funds to meet secretarial or drafting expenses in preparing the manuscript, or to cover costs of publication or printing of reprints. It is hoped such assistance may be available whether or not the recipient is resident in the United States.

(b) At the request of the compiler, to provide advice concerning the content or scope of a proposed compilation and to make suggestions concerning format and mode of publication.

Past efforts of the Subcommittee have encouraged a number of compilation projects, several of them involving direct participation by committee members themselves, e.g. a collection of publications concerning mass differences in Reviews of Modern Physics **26**, No. 4 (1954) and **29**, No. 4 (1957). Other projects for which the Subcommittee has given encouragement are the preparation of "A Directory to Nuclear Data Tabulations" by Gibbs and Way, and "Accelerator Energy Calibrations" by J. B. Marion, Reviews of Modern Physics **33** (1961) 139.

Examples of compilations of nuclear information which would clearly be of great value if they were available today are: lifetimes of nuclear states, γ-ray partial widths, γ-ray multipole mixing ratios and phases, double stripping data; elastic scattering phase shifts, and scattering and reaction data for ions heavier than He^4.

Active or prospective compilers in these or other areas are urged to contact subcommittee members J. B. Marion, University of Maryland, College Park, Maryland or G. A. Bartholomew, Atomic Energy of Canada Limited, Chalk River, Ontario, Canada.

10.D *Nuclear Physics* **27** (1961) 690—693; © *North-Holland Publishing Co., Amsterdam*

BOOK REVIEWS

SILVAN S. SCHWEBER, *An introduction to relativistic field theory* (Rowe, Peterson and Co., Evanston, Illinois, 1961. xiv-905 p. $13.75.)

An attempt at revising the first part of the two-volume work *Mesons and Fields* by Bethe, de Hoffmann and Schweber has led to the present treatise, which most happily supersedes the previous (not very successful) presentation of the principles of quantum field theory. The author has adopted a broad textbook style of exposition, which distinguishes the present work from others by its outstanding suitability for a first introduction into the subject and the acquisition of a working knowledge of the mathematical techniques (there is a large number of exercises and suggestions for further reading). At the same time, the treatment is by no means superficial; on the contrary the author goes very thoroughly into the many obscurities which beset the subject and leaves the student in no doubt about their serious character. The scope of the book is rather wide; it includes the less shaky part of π-meson theory, as well as the recent developments of an "axiomatic" formulation and of dispersion relations; it leaves out those problems which are usually classified under the concept of "elementary particles". It is understandable that in spite of his thoroughness the author could not treat every aspect of the many problems in the same detail, and one may differ from him in the appreciation of the relative importance of such aspects: thus, I feel that Caianiello's work deserves more than a bare quotation, whereas I do not share the confidence, expressed in Prof. Bethe's curiously optimistic preface, in the axiomatic formulation to which the author devotes much space (axioms have a dangerous propensity to acting as strait-jackets).

However, this may be, one must be deeply grateful to the author for having, with admirable care and devotion, as well as insight and fine critical judgment, drawn such a full picture of our slowly progressing enquiry into some of the most fundamental laws of nature.

L. R.

MARY A. EMERY and SERGE A. EMERY, *Scientific Russian guide* (McGraw-Hill Book Co., London, 1961. vii-191 p. 35s)

This is a collection of 40 articles, extracted from contemporary Russian textbooks and magazines, each (except the last four) fully accented and followed by questions and lists of words (generously including such trivialities as "teleskop- telescope"). At the end, there is a glossary, in which all these words appear again, so that the utility of the individual lists is questionable. The book is too summary to be suitable for self-study; it can only serve as a basis for oral tuition.

L. R.

Consistent set of Q-Values (1960 Nuclear Data Tables, Parts I, II) (National Academy of Sciences, Washington 1960. xvi-214 p. $1.50; xii-456 p. $2.75)

These two-volume tables are a most valuable addition to the series edited by Miss K. Way (see this journal **12** (1959) 20). They present a consistent set of Q-values for all possible reactions, computed by Koenig, Mattauch and Wapstra (together with Everling for the first volume) on the basis of critically selected experimental data. As is now becoming usual, the tables are directly printed by the computer; they are very legible and clearly disposed.

L. R.

OEEC, ***Second annual report on Halden reactor project*** (OEEC, Paris, 1961. iii-151 p.)

The Halden (Norway) Boiling Heavy Water Reactor, which first went critical in June 1959 and achieved boiling for the first time in October 1960, is at present the only one of its type to have reached this stage.

The Project's First Report, which was a short technical document covering the preliminary period of joint operation, was submitted to the ENEA Steering Committee in November 1959. The Report now published covers not only the technical progress achieved during the period under review (1st November 1959 to 31st December 1960) but also gives a full detailed description of the reactor installation and the general administration of the Project.

The Report is in six sections, of which the first (Introduction and Organisation) surveys briefly the historical background of the Project, its structure and objectives, and a number of administrative details, including staff organisation, contracts policy, arrangements covering information and patents resulting from the experimental work, and finance. The other sections cover the reactor design and construction, fuel, reactor operation, safety organisation and the research programme. There is also a list of reports published by the Project.

Fact sheets on U. S. nuclear power projects (Electric Companies Public Information Program, New York, 1961. xii-456 p.)

Summary information (published in stencil form) on characteristics, history of construction and other practical data about various industrial reactors in the U.S.

L. R.

Infra-red physics (Pergamon Press, London, 1961. £ 7 per annum)

This is a new international research journal specalized in the physics of infra-red radiation. The publisher's statement accompanying the review copy of the first issue is here reproduced:

"This new journal is being established as an international forum for the publication of scientific papers devoted to infrared physics and its applications. It is concerned with infrared theory, experiment, and instrumentation as applied to infrared detection and transmission and to problems of atmospheric, meteorological, geophysical, astrophysical and space research. Except as they pertain directly to infrared studies of planetary and stellar atmospheres, papers on molecular spectroscopy or spectrochemical analysis are considered outside the scope of Infrared Physics. The journal will contain research papers, specially invited critical surveys, quickly published research notes and book reviews. The language preferred is English, but papers will be published occasionally in French and German. Manuscripts for editorial consideration should be sent to the member of the Board of Editors most conveniently located."

The production is of the usual high standard of the Pergamon Press.

L. R.

Nuclear propulsion, Bibliographical series No. 3 (International Atomic Energy Agency, Vienna, 1961. 227 p. 42Sch)

This book contains abstracts of some 1500 papers on aspects of nuclear propulsion under the five main headings: general aspects of nuclear propulsion, nuclear propulsion for aircraft, nuclear propulsion for rockets, nuclear propulsion for marine vessels and nuclear propulsion for other transportation.

The introduction is given in four languages. The abstracts are in English or Russian, the index of authors uses the Western alphabet only.

By far the largest section is that on nuclear ships. This section is broken down in five subsections: General problems, economic aspects, design and construction of nuclear ships, reactor and equipment for nuclear ships and safety.

Quite a useful bibliography.

O. Kofoed-Hansen

M. **Lois Marckworth** (Compiler), *Dissertations in physics. An indexed bibliography* 1861—1959 (Stanford University Press, Stanford, 1961. xi—283. $ 10.00)

This bulky volume contains an indexed bibliography of all doctoral theses accepted by American universities from 1861 (when the first doctor's degree in physics was awarded at Yale University) to 1959, by which date they reached a total of more than 8600. The theses are first listed alphabetically by authors' names, each entry giving, besides a running number, the title, the University and also the channel through which a copy may be procured. Then comes an index of a novel type, called "permutation subject index": it is entirely worked out by a machine, which scans the titles and compares each word with a list of words to be *excluded* from the index; the other words, regarded as "key-words", are classified alphabetically, each followed by the complete title in which it occurs and the corresponding running number. The helpfulness of the resulting index is therefore strongly dependent on the adequacy of the titles (a point about which authors are notoriously casual). Apart from this unavoidable uncertainly, however, it presents the user looking for a definite topic with a task likely to be as ticklish as that of spotting the telephone number of his friend Smith in the London directory. One has the impression that, to play safe, the compiler has been rather too timid in composing the list of excluded words: it is very doubtful, for instance, whether anybody will ever care to go through 3 columns of "positive" or 10 columns of "scattering". The trouble is, of course, that the significant units of communication are not in most cases single words, but combinations of words, the sorting out of which is no simple task for a machine. Still this experiment in indexing is a most instructive and creditable one.

L. R.

M. H. **Hausner**, *Powder metallurgy in nuclear reactor construction*, Review Series No. 11 (International Atomic Energy Agency, Vienna, 1961. 72 p. 21 s.)

This booklet appear in the IAEA series of reviews, which are intended to help specialists to keep in touch with the field of nuclear energy, and to be a tool for educational activities. The authors are chosen among the specialists of the member states, in the present case USA.

The booklet gives a short survey of the powder metallurgy of nuclear metals (U, Th, Be, Zr), alloys and ceramics. Basic chapters deal with characteristics of powder and consolidated materials and fabrication of powders.

The booklet can be recommended as an introduction to the field of powder metallurgy in nuclear engineering, but cannot be regarded as a reference source for those working in this field, owing to the restricted number of references to other publications.

Niels Hansen

Regulations for the safe transport of radioactive materials, Safety Series No. 6 (International Atomic Energy Agency, Vienna, 1961. 72 p. 31.50 Sch)

This little booklet contains lots of information for anybody interested in shipments of nuclear material. The content of the booklet can hardly be disputed. The qualifications of the eminent specialists who have participated in the preparation of these regulations should be a guarantee for the authoritative value of the booklet.

However, one may ask how does somebody who wants to ship two megacuries of spent fuel go about it. I guess that he will have some suspicion that there may be limitations on the total one-unit shipment, and accordingly consult section 6. He then finds that radioisotopes are classified in three groups and that Table IV of Annex I will aid in the classification. He finds that he has activity of all three kinds. He also finds in 6.2.1 that his shipment belongs to the category of large shipments and he is referred to subsection 6.2.3 if his shipment is not exempt as in section 13. He finds that section 13 is not his business, but it has cross references to a dozen other sections or subsections, so that he is not completely certain. Subsection 6.2.3. sends him off to section 16 where he might have started originally because this section is headed "Large Radioactive Sources". Having investigated another dozen subsections he winds up with 16.2.5 dealing with irradiated nuclear fuel. He then finds that he has to wait until his fuel has cooled down and probably by this time he personally is also cooled down — or may be the contrary. The book contains no real subject index, but only a list of contents. Apart from this, it has a list of definitions for the purpose of these regulations. This list defines the following items: Competent authority, fissile materials, gamma and/or X-radiation, maximum credible accident, radiation units, radioactive materials, and vehicles. The definition of vehicles says: Vehicles shall include railroad cars (waggons).

I think this gives a sufficient impression of the book. In the introduction the following promise is made: "In connection with the regulations, further scientific information and practical guidance relating to certain aspects of the problem of the transport of radioactive materials will be published in separate volumes of this Safety Series beginning with No. 7". So while the spent fuel is cooling down there is still hope for our friend with the two megacuries.

O. Kofoed Hansen

H. C. Corben and P. Stehle, *Classical mechanics* (John Wiley and Son, New York, 1960. xi-389 p. 96 s.)

It is difficult to innovate in the most classical of all classical subjects. In the present textbook, which is clearly and competently written without the traditional emphasis on mathematical developments, a fresh note is given by illustrations taken from such modern topics as rocket motion and Rutherford scattering. Multiply-periodic systems are only granted one section, and the mechanics of continuous media one chapter. On the other hand, there is a chapter on special relativity and another devoted to the orbits of particles in high energy accelerators, for the inclusion of which I see little point: the authors themselves declare their discussion of relativity insufficient as an introduction into the subject, and the last chapter has more the character of a sketchy survey article than of a didactic exposition. Likewise, the appendices have no clear relation to the subject of the book. There is a good selection of exercises, and general references to books or survey articles at the end of each chapter.

L. R.

R. E. Marshak and E. C. G. Sudarshan, *Elementary particle physics* (Interscience Publishers, New York, 1961. viii-231 p. $ 2.50 paperbound, $ 4.50 clothbound.)

Another exposition of our present views on the so-called elementary particles, following the familiar pattern of transformation properties and conservation laws, which is becoming almost stereotyped — a symptom of the formidable difficulties which are in the way of further progress. The distinguished authors have skilfully condensed within the compass of a handy tract a very substantial and well-balanced account of the theoretical methods which have so far been successful in reducing the experimental data to some provisional order. They have thus achieved a clear and concise presentation which provides quite a stimulating introduction to the subject.

L. R.

S. Flügge (Editor), *Handbuch der Physik XLVI/1: Cosmic rays* (Springer-Verlag, Berlin, 1961. xvi-333 p. 98 DM.)

The present volume of the Encyclopedia is particularly satisfying because its content is homogeneous and well-ordered. It opens with a survey by P. Morrison of the origin of cosmic rays: this is a brilliant essay, remarkable by its methodical rigour and masterly handling of the observational evidence. It is followed by a series of excellent articles reviewing in succession the geomagnetic effects (M. S. Vallarta), the evidence from stratospheric flights (E. C. Ray), the penetrating showers (K. Sitte), the extensive showers (G. Cocconi) and the hard component of μ-mesons in the atmosphere (G. N. Fowler and A. W. Wolfendale). Each article is followed, as usual, by a bibliography listing the more extended publications (ordinary papers are quoted in footnotes): in some cases, the authors had the good idea of adding comments about the books or articles quoted, thus making the list to what it ought to be: a guide for the inexperienced reader desirous of pursuing the study of some particular problem.

L R.

AUTHOR INDEX

Albridge, R. G., J. M. Hollander, V. J. Gallagher and J. H. Hamilton, The energy levels of U^{233} 529

Albridge, R. G. and J. M. Hollander, The K- and L-auger spectrum of uranium 554

Allcock, G. R., A space-time model of isospace 204

Amar, V., and M. Pauri, On the $K^+ + n \to K^\circ + p$ scattering amplitude poles. 52

Andersen, Torkild, K. Maack Bisgård and P. gregers Hansen, Low lying states of Th^{229} 673

Badrinathan, C., *see* Kondaiah

Balashov, V. V., V. G. Shevchenko and N. P. Yudin, Two-body forces and the giant resonance in photonuclear reactions 323

Balashov, V. V. and V. N. Fetisov, Role of nucleon clusters in deep photodisintegration of light nuclei 337

Balian, Roger, Claude Bloch et Cyrano de Dominicis, Formulation de la mécanique statistique en termes de nombres d'occupation (II) . 294

Bass, R., *see* Davis

Beard, G. B., *see* Kelly

Benveniste, Jacob, Rex Booth and Arthur C. Mitchell, Level structure of A^{40}. 665

Bird, L., P. Christmas, A. E. Taylor and E. Wood, De-polarization parameter in p-p scattering at 143 MeV 586

Bisgård, K. Maack, *see* Andersen

Blin-Stoyle, R. J. and Herman Feshbach, Effects of parity nonconserving internucleon potentials on the photoeffect in H^2 and H^3 395

Bloch, Claude, *see* Balian

Bonch-Osmolovskaya, N. A., B. S. Dzelepov, O. E. Kraft and Wang Young-Yu, Decay chain $Er^{158} \xrightarrow[E]{2.5h} Ho^{158} \xrightarrow[E,\beta^+]{37\text{ min}} Dy^{158}_{stab}$ 581

Bonner, T. W., *see* Davis

Booth, Rex, *see* Benveniste

Borello, O., S. Costa and F. Ferrero, The E. C./β^+ ratio in Pr^{139} . . 25

Bradley, G. E., *see* Pipkin

Budzanowski, A., R. W. Clifft and B. Hird, Inelastic proton scattering asymmetries at 8.9 MeV. 193

Carter-Waschek, C., and B. Linder, An isomeric state of Y^{90} . . 415

Chaban, A. A., *see* Davydov

Christmas, P., *see* Bird

Clegg, A. B., and G. R. Satchler, Gamma-rays from inelastic scattering of high-energy nucleons 431
Clifft, R. W., *see* Budzanowski
Costa, S., *see* Borello
Cunninghame, J. G., G. P. Kitt and E. R. Rae, The ratio of asymmetric to symmetric fission in p-wave neutron fission of U^{235}. 154
Davis, E. A., F. Gabbard, T. W. Bonner and R. Bass, The disintegration of B^{10} and F^{19} by fast neutrons 448
Davydov, A. S., V. S. Rostovsky and A. A. Chaban, The shape of the atomic nucleus and zero spin excited states 134
De Dominicis, Cyrano, *see* Balian
Dietzsch, O., Y. Hama, E. W. Hamburger and F. C. Zawislak, Study of the O^{16}(d, n)F^{17} reaction 103
Dzelepov, B. S., *see* Bonch-Osmolovskaya
El-Nesr, M. S. and R. Othaz, A study of beta-gamma directional correlation in the decay of Au^{199} 507
Evans, J. E., Polarization in C^{12}(p, p) scattering from 5 to 10.5 MeV 41
Fabre de la, Ripelle, Michel, Le mouvement collectif dans la résonance géante photonucléaire (I) Énergie de résonance pour les noyaux sphériques et déboublement pour les noyaux déformés 561
Ferguson, J. M., Isomeric level in Y^{90} 344
Ferguson, J. M., *see* Hurley
Ferrero, F., *see* Borello
Feshbach, Herman, *see* Blin-Stoyle
Fetisov, V. N., *see* Balashov
Fossan, D. B., *see* Wilson
Friedländer, E. M., and M. E. Mayer, An estimation of the spectrum of true multiplicities in antinucleon annihilations 418
Gabbard, F., *see* Davis
Gallagher, C. J., *see* Albridge
Goldansky, V. I., Two-proton radioactivity. 648
Goldfarb, L. J. B., *see* Rook
Green, H. S., Proton-proton scattering at relativistic energies 405
Hama, Y., *see* Dietzsch
Hamburger, E. W., *see* Dietzsch
Hamilton, J. H., *see* Albridge
Hamilton, W. D. and B. S. Sood, The resonant scattering of gamma rays in ^{177}Hf 66
Hansen, P. G., O. J. Jensen and K. Wilsky, Decay of Er^{172} and Tm^{172} 516
Hansen, P. Gregers, *see* Andersen
Hauser, U., K. Runge and G. Knissel, Measurements of El transition probabilities in several deformed odd-mass nuclei as a study of single

particle motion 632
Hird, B., *see* Budzanowski
Ho, Grace P., and Edwin L. Iloff, The relative deuteron/proton yield from 45 MeV bremsstrahlung irradiation of copper 234
Hollander, J. M., *see* Albridge
Hurley, J. P. and J. M. Ferguson, Measurements of K conversion coefficient of 279 keV gamma radiation in Tl^{203} 75
Iloff, Edwin L., *see* Ho
Isaev, P. S., and M. V. Sewerynski, Scattering of π-mesons on K-mesons at low energies 148
Jensen, O. J., *see* Hansen
Jhingan, M. L., *see* Kondaiah
Kelly, W. H. and G. B. Beard, Nuclear resonance fluorescence measurements on the 845 keV level in Fe^{56} 188
Kembhavi, V. K., Reduced matrix elements in nuclear shell theory . . . 38
Kitt, G. P., *see* Cuninghame
Knissel, G., *see* Hauser
Kobayashi, S., *see* Matsuda
Kondaiah, E., M. L. Jhingan and C. Badrinathan, Surface direct interaction of 14 MeV neutrons with fluorine 166
Kraft, O. E., *see* Bonch-Osmolovskaya
Lewin, W. H. G., B. van Nooijen and A. H. Wapstra, The K-conversion coefficient of the 368 keV E2 transition in ^{200}Hg 681
Linder, B., *see* Carter-Waschek
Maris, Th. A. J., An interpretation of the isobaric spin space 46
Markov, M. A. and I. M. Zheleznykh, On high energy neutrino physics in cosmic rays 385
Matsuda, K., Y. Nagahara, Y. Oda, N. Yamamuro and S. Kobayashi, The elastic and inelastic scattering of protons by magnesium in the energy range from 7.3 MeV to 15.9 MeV 1
Mayer, M. E., *see* Friedländer
Metzger, F. R., Lifetime and g-factor of the first excited state in Fe^{56} . . 612
Meyer, V., H. Müller, H. H. Staub and R. Zurmühle, The γ-radiation of the $Li^7(p, \gamma)$ resonance at 441.3 keV 284
Mitchell, Arthur C., *see* Benveniste
Müller, H., *see* Meyer
Nagahara, Y., *see* Matsuda
Nordhagen, Rolf, The spin and parity of the 648 keV resonance in $Mg^{26}(p, \gamma)Al^{27}$ 112
Oda, Y., *see* Matsuda
Othaz, R., *see* El-Nesr
Pauri, M., *see* Amar

Peck, Jr., R. A., Gross structure in reactions of deformed nuclei . . . 596

Pinkston, W. T. and G. R. Satchler, Collective effects in inelastic scattering from nuclei . . . 270

Pipkin, F. M., G. E. Bradley and R. E. Simpson, Beta decay matrix elements in As^{76} . . . 353

Rae, E. R., *see* Cuninghame

Rao, B. N. Subba, Angular correlation studies of the 358 keV → 81 keV cascade in Cs^{133} . . . 28

Reiner, A. S., Electric monopole transitions in collective nuclei . . . 115

Rikmenspoel, R., *see* Van Patter

Rook, J. R., Polarisation of protons elastically scattered by Li^{7} near the 441 keV resonance . . . 606

Rook, J. R. and L. J. B. Goldfarb, The use of polarised deuterons to study the D+D reactions . . . 79

Rostovsky, V. S., *see* Davydov

Runge, K., *see* Hauser

Rustgi, M. L., Alpha-deuteron model of the Li^{6} nucleus and the Be^{9}(Li^{6}, α)B^{11} reaction . . . 58

Satchler, G. R., *see* Clegg

Satchler, G. R., *see* Pinkston

Scott, H. D., The application of distorted wave Born approximation calculations to the analysis of some (d, p) angular distributions . . . 490

Sewerynski, M. V., *see* Isaev

Shevchenko, V. G., *see* Balashov

Simpson, R. E., *see* Pipkin

Smirnov, Yu. F., Talmi transformations for particles with different masses . . . 177

Sokolik, H., Interpretation of isobaric multiplets in terms of the space-time reflection group . . . 94

Sood, B. S., *see* Hamilton

Staub, H. H., *see* Meyer

Strutinski, V. M., Dependence of the angular distribution of fission fragments on the target nuclear spin . . . 348

Swan, P., Distorted wave expansion for scattering problems . . . 620

Taylor, A. E., *see* Bird

Tolstov, K. D., On the mechanism of interaction of fast protons with nuclei . . . 144

Trehan, P. N., *see* Van Patter

Umezawa, M., Pairings in the shell model (III) . . . 248

Van Nooijen, B., *see* Lewin

Van Patter, D. M., R. Rikmenspoel and P. N. Trehan, The $(p, p'\gamma)$ reaction in even isotopes of Zn, Ge and Se . . . 467

WALTER, R. L., *see* WILSON
WAPSTRA, A. H., *see* LEWIN
WILSKY, K., *see* HANSEN
WILSON, W. E., R. L. WALTER and D. B. FOSSAN, Differential cross sections for the T(p, n) He^3 reaction 421
WOOD, E., *see* BIRD
YAMAMURO, N., *see* MATSUDA
YOUNG-YU, WANG, *see* BONCH.-OSMOLOVSKAYA
YUDIN, N. P., *see* BALASHOV
ZAWISLAK, F. C., *see* DIETZSCH
ZHELEZNYKH, I. M., *see* MARKOV
ZURMÜHLE, R., *see* MEYER

SUBJECT INDEX

1. Nuclear structure

1.B *Two- and three-body problems*

Effects of parity non-conserving internucleon potentials on the photoeffect in H^2 and H^3, R. J. Blin-Stoyle and Herman Feshbach 395
Proton-proton scattering at relativistic energies, H. S. Green 405
Differential cross sections for the $T(p, n)He^3$ reaction, W. E. Wilson, R. L. Walter and D. B. Fossan 421
De-polarization parameter in p–p scattering at 143 MeV, L. Bird, P. Christmas, A. E. Taylor and E. Wood 586

1.C *Many-Particle systems*

Pairings in the shell model (III), M. Umezawa 248
Formulation de la mécanique statistique en termes de nombres d'occupation (II), Roger Balian, Claude Bloch et Cyrano de Dominicis 294

1.D *Nuclear models*

1.D.1 *Shell model*

Reduced matrix elements in nuclear shell theory, V. K. Kembhavi . . 38
Talmi transformations for particles with different masses, Yu. F. Smirnov 177
Pairings in the shell model (III), M. Umezawa 248
Isomeric level in Y^{90}, J. M. Ferguson 344

1.D.2 *Collective model*

The resonant scattering of gamma rays in ^{177}Hf, W. D. Hamilton and B. S. Sood 66
Electric monopole transitions in collective nuclei, A. S. Reiner 115
The shape of the atomic nucleus and zero spin excited states, A. S. Davydov, V. S. Rostovsky and A. A. Chaban 134
Measurements of E1 transition probabilities in several deformed odd-mass nuclei as a study of single particle motion, U. Hauser, K. Runge and G. Knissel 632

1.D.3 *Other models*

The γ-radiation of the $Li^7(p, \gamma)$ resonance at 441.3 keV, V. Meyer, H. Müller, H. H. Staub and R. Zurmühle 284

1.D.4 *Relationship between different models*

Le mouvement collectif dans la résonance géante photonucléaire (I) Énergie de résonance pour les noyaux sphériques et déboublement pour les noyaux déformés, Michel Fabre de la Ripelle 561

1.E *Properties of nuclei*

1.E.1 *Energy levels*

The spin and parity of the 648 keV resonance in $Mg^{26}(p, \gamma)Al^{27}$, Rolf Nordhagen 112

An isomeric state of Y^{90}, C. Carter-Waschek and B. Linder 415
Decay of Er^{172} and Tm ^{172}, P. G. Hansen, O. J. Jensen and K. Wilsky 516
The energie levels of U^{233}, R. G. Albridge, J. M. Hollander, C. J. Gallagher and J. H. Hamilton. 529
Level structure of A^{40}, Jacob Benveniste, Rex Booth and Arthur C. Mitchell. 665
Low lying states of Th^{229}, Torkild Andersen, K. Maack Bisgård and P. Gregers Hansen 673

1.E.3 *Electric and magnetic moments*

Lifetime and *g*-factor of the first excited state in Fe^{56}, F. R. Metzger . 612

1.E.4 *Transition probabilities; Cross sections*

The resonant scattering of gamma rays in ^{177}Hf, W. D. Hamilton and B. S. Sood 66
Electric monopole transitions in collective nuclei, A. S. Reiner . . . 115
Nuclear resonance fluorescence measurements on the 845 keV level in Fe^{56}, W. H. Kelly and G. B. Beard 188
The (p, $p'\gamma$) reaction in even isotopes of Zn, Ge and Se, D. M. Van Patter, R. Rikmenspoel and P. N. Trehan 467
Measurements of E1 transition probabilities in several deformed odd-mass nuclei as a study of single particle motion, U. Hauser, K. Runge and G. Knissel. 632

2. Nuclear Reactions

2.A *General properties*

2.A.1 *Cross-sections, energy relations*

The disintegration of B^{10} and F^{19} by fast neutrons, E. A. Davis, F. Gabbard, T. W. Bonner and R. Bass 448

2.B *Angular distributions; Correlations; Polarization*

Angular correlation studies of the 358 keV → 81 keV cascade in Cs^{133}, B. N. Subba Rao 28
Polarization in C^{12} (p, p) scattering from 5 to 10.5 MeV, J. E. Evans 41
The use of polarised deuterons to study the D+ D reactions, J. R. Rook and L. J. B. Goldfarb 79
The γ-radiation of the $Li^7(p, \gamma)$ resonance at 441.3 keV, V. Meyer, H. Müller, H. H. Staub and R. Zurmühle 284
Differential cross sections for the $T(p, n)He^3$ reaction, W. E. Wilson, R. L. Walter and D. B. Fossan 421
Polarisation of protons elastically scattered by Li^7 near the 441 keV resonance, J. R. Rook 606

2.E *Optical model*

Polarization in C^{12} (p, p) scattering from 5 to 10.5 MeV, J. E. Evans 41
Inelastic proton scattering asymmetries at 8.9 MeV, A. Budzanowski, R. W. Clifft and B. Hird 193

2.F *Coulomb excitation*

Surface direct interaction of 14 MeV neutrons with fluorine, E. Kondaiah, M. L. Jhingan and C. Badrinathan 166

Collective effects in inelastic scattering from nuclei, W. T. Pinkston and G. R. Satchler 270
Gamma-rays from inelastic scattering of high-energy nucleons, A. B. Clegg and G. R. Satchler 431
Gross structure in reactions of deformed nuclei, R. A. Peck, Jr., ... 596

2.G *Stripping and pick-up*

Alpha-deuteron model of the Li^6 nucleus and the Be^9(Li^6, α)B^{11} reaction, M. L. Rustgi 58
Study of the O^{16} (d, n)F^{17} reaction, O. Dietzsch, Y. Hama, E. W Hamburger and F. C. Zawislak. 103
The application of distorted wave Born approximation calculations to the analysis of some (d, p) angular distributions, H. D. Scott 490

2.I *Photonuclear processes*

The E. C./β^+ ratio in Pr^{139}, O. Borello, S. Costa and F. Ferrero 25
The relative deuteron/proton yield from 45 MeV bremsstrahlung irradiation of copper, Grace P. Ho and Edwin L. Iloff 234
Two-body forces and the giant resonance in photo-nuclear reactions, V. V. Balashov, V. G. Shevchenko and N. P. Yudin 323
Role of nucleon clusters in deep photodisintegration of light nuclei, V. V. Balashov and V. N. Fetisov 337
Le mouvement collectif dans la résonance géante photonucléaire. (I) Énergie de résonance pour les noyaux sphériques et dédoublement pour les noyaux déformés, Michel Fabre de la Ripelle 561

2.J *Fission and spallation*

The ratio of asymmetric to symmetric fission in p-wave neutron fission of U^{235}, J. G. Cuninghame, G. P. Kitt and E. R. Rae 154
Dependence of the angular distribution of fission fragments on the target nuclear spin, V. M. Strutinski. 348
Two-proton radioactivity, V. I. Goldansky 648

2.L *Scattering processes (except two-nucleon system and meson scattering)*

The elastic and inelastic scattering of protons by magnesium in the energy range from 7.3 MeV to 15.9 MeV, K. Matsuda, Y. Nagahara, Y. Oda, N. Yamamuro and S. Kobayashi 1
Polarization in C^{12} (p, p) scattering from 5 to 10.5 MeV, J. E. Evans 41
Inelastic proton scattering asymmetries at 8.9 MeV, A. Budzanowski, R. W. Clifft and B. Hird 193
Collective effects in inelastic scattering from nuclei, W. T. Pinkston and G. R. Satchler 270
Gamma-rays from inelastic scattering of high-energy nucleons, A. B. Clegg and G. R. Satchler. 431
Distorted wave expansion for scattering problems, P. Swan 620
Level structure of A^{40}, Jacob Benveniste, Rex Booth and Arthur C. Mitchell 665

3. Electromagnetic Radiation

3.A *Gamma radiation*

The resonant scattering of gamma rays in ^{177}Hf, W. D. Hamilton and B. S. Sood 66

The spin and parity of the 648 keV resonance in $Mg^{26}(p, \gamma)Al^{27}$, Rolf Nordhagen . . . 112
Nuclear resonance fluorescence measurements on the 845 keV level in Fe^{56}, W. H. Kelly and G. B. Beard . . . 188
Collective effects in inelastic scattering from nuclei, W. T. Pinkston and G. R. Satchler . . . 270
Isomeric level in Y^{90}, J. M. Ferguson . . . 344
An isomeric state of Y^{90}, C. Carter-Waschek and B. Linder . . . 415
The (p, p′γ) reaction in even isotopes of Zn, Ge and Se, D. M. Van Patter, R. Rikmenspoel and P. N. Theran . . . 467

3.B *Internal conversion*

Angular correlation studies of the 358 → 81 keV cascade in Cs^{133}, B. N. Subba Rao . . . 28
Measurement of K conversion coefficient of 279 keV gamma radiation in Tl^{203}, J. P. Hurley and J. M. Ferguson . . . 75
The K-conversion coefficient of the 368 keV E2 transition in ^{200}Hg, W. H. G. Lewin, B. Van Nooijen and A. H. Wapstra . . . 681

3.C *Extranuclear effects*

The K- and L-Auger spectrum of uranium, R. G. Albridge and J. M. Hollander 554

4. Beta Decay; Parity

4.C *Evaluation of matrix elements*

Beta decay matrix elements in As^{76} ,F. M. Pipkin, G. E. Bradley and R. E. Simpson . . . 353

4.D *K-capture*

The E.C./β^+ ratio in Pr^{139}, O. Borello, S. Costa and F. Ferrero . . . 25

4.E *Analysis of data*

A study of beta-gamma directional correlation in the decay of Au^{199}, M. S. El-Nesr and R. Othaz . . . 507
Decay of Er^{172} and Tm^{172}, P. G. Hansen, O. J. Jensen and K. Wilsky . . . 516
The energy levels of U^{233}, R. G. Albridge, J. M. Hollander, C. J. Gallagher and J. H. Hamilton . . . 529
Decay chain $Er^{158} \xrightarrow[E]{2.5h} Ho^{158} \xrightarrow[E,\,\beta^+]{27\ min} Dy^{158}_{stab}$, N. A. Bonch-Osmolovskaya, B. S. Dzelepov, O. E. Kraft and Wang Young-Yu . . . 581
Low lying states of Th^{229}, Torkild Andersen, K. Maack Bisgård and P. Gregers Hansen . . . 673

6. Instruments and Methods

6.D *Tables and computation aids*

Reduced matrix elements in nuclear shell theory, V. K. Kembhavi . . . 38

7. Quantum Field Theory

7.A *General*

Scattering of π-mesons on K-mesons at low energies, P. S. Isaev and M. V. Sewerynski . . . 148

7.C *π-meson field (scattering and nuclear forces)*

On the mechanism of interaction of fast protons with nuclei, K. D. Tolstov . 144
Proton-proton scattering at relativistic energies, H. S. Green . . . 405
An estimation of the spectrum of true multiplicities in antinucleon annihilations, E. M. Friedländer and M. E. Mayer . . . 418

8. Elementary Particles

8.B *Theory: interactions, transformation properties*

An interpretation of the isobaric spin space, Th. A. J. Maris . . . 46
On the $K^+ + n \rightarrow K^0 + p$ scattering amplitude poles, V. Amar and M. Pauri 52
Interpretation of isobaric multiplets in terms of the space-time reflection group, H. Sokolik . . . 94
A space-time model of isospace, G. R. Allcock . . . 204
On high energy neutrino physics in cosmic rays, M. A. Markov and I. M. Zheleznykh . . . 385
Effects of parity non-conserving internucleon potentials on the photoeffect in H^2 and H^3, R. J. Blin-Stoyle and Herman Feshbach . . . 395

9. Cosmic Radiation

9.A *General*

On high energy neutrino physics in cosmic rays, M. A. Markov and I. M. Zheleznykh . . . 385

10. News Items

10.A *News items*

Nuclear compilations . . . 689

10.B *Reports on conferences and congresses*

CERN Theoretical Conference (5—10 June 1961). . . . 688

10.D *Book Reviews*

Silvan S. Schweber, An introduction to relativistic field theory (L. R.) . . 690
Mary A. Emery and Serge A. Emery, Scientific Russian guide (L. R) . . . 690
Consistent set of Q-values (L. R.) . . . 690
OEEC, Second annual report on Halden reactor project . . . 691
Fact sheets on U. S. nuclear power projects (L. R.) . . . 691
Infra-red physics (L. R.) . . . 691
Nuclear propulsion (O. Kofoed-Hansen) . . . 691

M. Lois Marckworth (Compiler), Dissertations in physics. An indexed bibliography 1861—1959 (L. R.) 692
M. H. Hausner, Powder metallurgy in nuclear reactor construction (Niels Hansen) 692
Regulations for the safe transport of radioactive materials (O. Kofoed-Hansen) 692
H. C. Corben and P. Stehle, Classical mechanics (L. R.) 693
R. E. Marshak and E. C. G. Sudarshan, Elementary particle physics (L. R) 693
S. Flügge (Editor), Handbuch der Physik XLVI/1: Cosmic rays (L. R) . . . 693

10.E *Erratum*

E. Arbman, S. Bjørnholm and O. B. Nielsen, Levels in Th^{228} in the electron capture decay of Pa^{228}, Nuclear Physics **21** (1960) 406 352

NORTH-HOLLAND BOOKS

Just out

Elements of Hamiltonian Mechanics

by D. TER HAAR
University Reader in Theoretical Physics
and Fellow of Magdalen College, Oxford

CONTENTS:

1. Newtonian mechanics
2. The Lagrangian equations of motion
3. Small vibrations
4. Dynamics of rigid bodies
5. The canonical equations of motion
6. Hamilton-Jacobi theory
7. Perturbation theory
8. Continuous systems

Bibliography - Problems

This book is based upon a course of lectures given to final year undergraduates and first year graduate students at Oxford University. The emphasis and the selection of subject matter differs in a number of points from those in existing modern textbooks. The main differences are in the way constraints are introduced by freezing in of degrees of freedom, and in the discussion of classical perturbation theory.

6x9" 196 pp. Gld. 20.— (40s.)

NORTH-HOLLAND PUBLISHING COMPANY
P. O. BOX 103 - AMSTERDAM
Distributor for U.S.A.: Interscience Publishers, Inc. — New York

NORTH-HOLLAND BOOKS

N·H
P C

QUANTUM MECHANICS

Just out

VOL. I

by ALBERT MESSIAH (Centre d'Etudes Nucléaires de Saclay)

translated from the French by G. M. Temmer (Florida State University, Tallahassee)

6×9" 520 pp. Gld. 50.- (100s.)

CONTENTS VOL. I. *The formalism and its interpretation.* Origins of the Quantum Theory. Matter waves and the Schrödinger equation. One dimensional quantum systems. Statistical interpretation of the wave-corpuscle duality and uncertainty relations. The development of the formalism of Wave Mechanics and its interpretation. Classical approximation and WKB method. The general formalism of Quantum Theory: A) Mathematical framework. B) Description of physical phenomena. — *Simple systems.* Solution of the Schrödinger equation by separation of variables. Central force field. Scattering problems. Central force field and the method of phase shifts. Coulomb interaction. Harmonic oscillator. — *Appendices:* «δ function» and distributions. Special functions and related formulae.

". . . . the reviewer would like to recommend the book to students taking a beginner's course in quantum mechanics, to teachers for broadening the scope of such courses, and also to research workers in understanding the principles and methods of quantum mechanics and for acquiring the necessary knowledge for an understanding of the advanced parts of the field."

(PHYSICS TODAY on the original French Edition)

VOLUME II
in preparation

Ask your bookseller or

NORTH-HOLLAND PUBLISHING COMPANY

P.O. BOX 103—AMSTERDAM

Distributor for U.S.A.: Interscience Publishers, Inc. — New York